# Purification of *Bacillus amyloliquefaciens* lipopeptides for postharvest disease control

by

Sebenzile Mazibuko

Thesis presented in partial fulfilment
of the requirements for the Degree

of
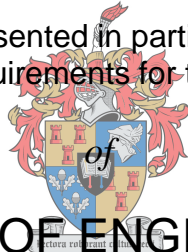
MASTER OF ENGINEERING
(PROCESS ENGINEERING)

in the Faculty of Engineering
at Stellenbosch University

Supervisor
Prof. K.G. Clarke

Co-Supervisor
Dr. R.W.M. Pott

March 2018

Declaration

By submitting this thesis electronically, I declare that the entirety of the work contained therein is my own, original work, that I am the sole author thereof (save to the extent explicitly otherwise stated), that reproduction and publication thereof by Stellenbosch University will not infringe any third party rights and that I have not previously in its entirety or in part submitted it for obtaining any qualification.

i

Abstract

South Africa is the largest exporter of fresh fruit (by volume) in the southern hemisphere and as such, the quality of fruit must be maintained throughout the global supply chain. Several fungal pathogens contribute to significant fruit loss and wastage due to disease during postharvest storage. The use of chemical fungicides as a postharvest disease control strategy has become limiting due to negative environmental concerns (toxicity, non-specificity and non-biodegradability) while the efficient use of bacterial cells/spores as biocontrol agents is restrictive as the viability is dependent on suitable postharvest environments. An alternative and novel biocontrol strategy proposed in this study is to use antifungal lipopeptides, namely fengycin and iturin, produced by *Bacillus amyloliquefaciens* DSM 23117, as second-generation biocontrol agents for postharvest disease control. However, to be sufficiently effective, concentration and purification of the lipopeptides is necessary due to the low yields produced and the presence of metabolic products such as lipid and protein impurities that are not desired in the final product. The aim of the study was to develop an appropriate downstream concentration and purification programme for antifungal lipopeptides using acid precipitation, solvent extraction and macroporous adsorption as downstream unit operations.

To concentrate the lipopeptides, while effecting some degree of purification, acid precipitation studies were conducted by acidification of the cell-free supernatant to pH values 1 – 4 to determine the effect of pH on the recovery and purity of fengycin and iturin. Reverse-phase high performance liquid chromatography (RP-HPLC) quantification of acid precipitate showed high recoveries of 78% and 62% for fengycin and iturin respectively at pH 2 with an optimal fengycin purity of 64% obtained at pH 3. Acid precipitation of the cell-free supernatant at pH 3 would be suitable as the initial concentration step, due to the percentage purity of fengycin and iturin.

To improve the purity of fengycin and iturin above that obtained from acid precipitation, solvent extraction was the next unit operation in the purification programme. Organic solvents of varying polarity indices were screened for their efficiency in extracting fengycin and iturin. Following screening experiments, a three-stage methanol extraction and a three-stage diethyl ether-methanol extraction were conducted to further improve the purity. Lipopeptides in solvent extracts were quantified by thin layer chromatography (TLC) which showed methanol to be the best solvent which extracted 100% of lipopeptides with a purity of 74% for fengycin. A final purity of 89% and 16% for fengycin and surfactin respectively was obtained after the 3-stage methanol extraction, while final purities of 74% and 13% were obtained for fengycin and surfactin respectively, with the diethyl ether-methanol extraction. The extraction efficiency of fengycin by the organic solvents was found to be related the functional groups of the solvents, in addition to the polarity.

Further analysis of the lipopeptide solvent extract by liquid chromatography electrospray ionisation mass spectroscopy (LC-ESI-MS) was conducted to identify the two bands that appeared on the plate when the solvent extracts were analysed by TLC, and which were assumed to be fengycin. LC-ESI-MS indicated inconclusive results and it could not be confirmed with certainty that both bands were indeed fengycin.

Adsorption was the final unit operation used to improve the purity of fengycin and iturin. Batch adsorption experiments were designed through a central composite design (CCD) to elucidate the optimal adsorption conditions for fengycin and iturin on a polymeric macroporous resin HP-20. Batch adsorption experiments showed the lipopeptide to resin (LP/R) ratio and pH to be significant ($\alpha = 0.05$) parameters in the adsorption of fengycin with an optimal LP/R of 0.5 and optimal pH of 10. Although the LP/R ratio and temperature were found to be equally significant ($\alpha = 0.05$) in the adsorption of iturin, no optimal conditions could be deduced as the LP/R ratio ranges may have existed outside the experimental region and thus further optimisation studies for iturin are required.

To better understand the mechanism of fengycin and iturin adsorption, adsorption kinetics and adsorption isotherm studies were conducted, and the experimental adsorption data modelled through pseudo-kinetic-order rate models and the Langmuir and Freundlich isotherm models. Equilibrium times of 22 h and 24 h were obtained for fengycin and iturin respectively, at the optimal fengycin adsorption conditions. The experimental data was individually fitted to the pseudo-first-order rate model and pseudo-second-order rate model to determine whether the rate limiting step of fengycin and iturin adsorption could be explained by physisorption or chemisorption. Neither of the pseudo-order rate models could explain the kinetics of antifungal LP adsorption on HP-20 due to poor fit, suggesting that the kinetic data obtained in this study is inconclusive and further experimental work is required.

After the kinetics of fengycin and iturin was studied, adsorption isotherms were conducted to determine the saturation concentration of fengycin and iturin at a constant temperature of 43°C and pH 10. A saturation concentration of 3 g/L and adsorption percentage of 76.5 ± 0.37% was obtained for fengycin while 0.5 g/L was determined to be the saturation concentration of iturin, with a % adsorption of 54.5 ± 3.99%. The experimental data was individually fitted to the Langmuir and Freundlich isotherm models to determine which model best represented the data and thus characterised the adsorption behaviour of the lipopeptides. As with the adsorption kinetic modelling, neither of the isotherm models could explain the adsorption mechanism of fengycin and iturin on HP-20, implying that other isotherm models such as the Redlich–Peterson model may be used in further experimental work to explain the adsorptive behaviour of the antifungal lipopeptides.

To determine the effectiveness of the partially purified lipopeptides and purified lipopeptide mixtures, *in vitro* efficacy studies were conducted on six common fungal phytopathogens that cause diseases of fruit during postharvest storage. The fungal phytopathogens were grown separately on PDA plates containing the cell-free supernatant, resolubilised acid precipitate, methanol extract and diethyl ether-methanol extract. The growth inhibition was determined after a 5-day incubation period. 12 g/L fengycin resolubilised acid precipitate was the most effective treatment with fungal growth inhibition ranging between 30 – 100%, depending on the target phytopathogen. It was discovered that *A. brassicicola* was the most susceptible phytopathogen to all the treatments used while *A. sclerotiorum* was found to be the most resistant phytopathogen of the six phytopathogens studied. It was concluded that the effectiveness of the lipopeptides in fungal growth inhibition was the lipopeptide concentration and phytopathogen species dependent.

It can be concluded from this study that an effective purification programme for fengycin and iturin would entail acid precipitation at pH 3, followed by a 3-stage extraction procedure involving methanol as the solvent, a programme which would potentially produce purities of 89% and 17% for fengycin and iturin respectively, with recoveries of 100% and 53% for fengycin and iturin respectively. To date, no study has systematically investigated existing downstream unit operations for the development of an appropriate concentration and purification programme for fengycin and iturin lipopeptides produced by *B. amyloliquefaciens*.

Recommendations for further work include the following. While the optimal batch equilibrium adsorption conditions of 3 g/L fengycin at pH 10 and 43°C would ensure maximum fengycin adsorption on HP-20, further optimisation studies for iturin adsorption are required. Refinement in the adsorption kinetic and isotherm modelling studies is also required to elucidate the mechanism of fengycin adsorption.

Samevatting

Suid-Afrika is die grootste uitvoerder van vars vrugte (per volume basis) in die Suidelike Halfrond en as gevolg hiervan moet die gehalte van vrugte regdeur die globale aanbod ketting gehandhaaf word. Verskeie swam patogene dra by tot aansienlike vrugte verlies en vermorsing as gevolg van siektes gedurende na-oes berging. Die gebruik van chemiese swamdoders as 'n na-oes siekte beheer strategie word beperk as gevolg van negatiewe omgewings bekommernisse (onder andere toksisiteit en nie-bioafbreekbaarheid) terwyl die doeltreffende gebruik van bakteriële selle/spore 'n beperkende lewensvatbaarheid toon en grootliks afhanklik is van die geskikte na-oes omgewing. 'n Alternatiewe en nuwe strategie word voorgestel in hierdie studie aanrakend swamdodende lipopeptiedes, naamlik fengycin en iturin, geproduseer deur Bacillus amyloliquefaciens DSM 23117, as 'n tweede generasie bio-beheer agent vir na-oes siekte beheer. Om egter voldoende doeltreffendheid te toon, is die suiwering van lipopeptiedes nodig as gevolg van die lae opbrengste geproduseer en die teenwoordigheid van metaboliese produkte soos lipied- en proteïen onsuiwerhede wat nie in die finale produk verlang word nie. Die doel van hierdie studie was die ontwikkeling van 'n toepaslike stroomaf konsentrasie en suiwerings program vir swamdodende lipopeptiedes deur gebruik te maak van suur neerslag, ekstraksie metodes en makro poreuse adsorpsie as stroomaf eenheid bedrywighede.

Om die swamdodende lipopetides te konsentreer, terwyl ook 'n mate van suiwering aan te bring, was suur neerslag studies uitgevoer op die sel-vrye oplossing tussen pH waardes van 1 tot 4 om sodoende die suiwerheid van fengycin en iturin te bepaal. Suur neerslag omkeerbare-fase hoëverhittingvloeistofchromatografie het 'n hoë opbrengs van 78% en 62% vir fengycin en iturin onderskeidelik getoon by 'n pH waarde van 2 en 'n optimale fengycin suiwerheid van 64% by pH 3 bekom. Sel-vrye suur neerslag by pH 3 is dus geskik vir die aanvanklike konsentrasie stap, as gevolg van die persentasie suiwerheid van fengycin en iturin bereik.

Die suiwerheid van fengycin en iturin, bo wat reeds verkry is weens suur neerslagvorming, was verbeter deur gebruik te maak van ekstraksie metodes as die volgende eenheid bewerking in die suiwerings program. Organiese oplosmiddels van wisselende polariteit indekse was ondersoek vir hul doeltreffendheid in fengycin en iturin ekstraksie. Na aanleiding van die ondersoek was 'n drie-fase metanol ekstraksie en 'n drie-fase diëtieleter-metanol ekstraksie uitgevoer om verder die suiwerheid te verhoog. Die swamdodende lipopeptiede uittreksel was gekwantifiseer deur middel van dun laag Chromatografie en het getoon dat metanol die beste oplosmiddel is met 'n 100% ekstraksie en 'n 74% fengycin suiwerheid. 'n Finale suiwerheid van 89% en 16% vir fengycin en surfactin is onderskeidelik verkry na die drie-fase ekstraksie met metanol terwyl diëtieleter-metanol 'n finale suiwerheid van 74%

en 13% onderskeidelik verkry het vir fengycin en surfactin. Tydens die studie was doeltreffende ekstraksie van fengycin gekoppel aan die oplosmiddel funksionele groepe, benewens die polariteit.

'n Verdere ondersoek van die swamdodende lipopeptiede ekstraksie metodes deur middel van vloeibare Chromatografie elektro-sproei ionisasie massa spektroskopie was ingespan om die twee plaat bande te identifiseer wat of die bord verskyn het tydens die dun laag Chromatografie metode. Dit was aanvaar dat die plaat bande fengycin voorstel. Weens onvoldoende resultate was dit nie moontlik of vas te stel of beide plaat bande fengycin was nie.

Adsorpsie was die laaste eenheid bewerking gebruik om die suiwerheid van fengycin en iturin te verbeter. Enkellading adsorpsie eksperimente was opgestel deur middel van 'n sentrale saamgestelde ontwerp om sodoende die optimale voorwaardes uit te lig vir fengycin en iturin polimeriese makro poreuse HP-20 hars adsorpsie. Enkellading adsorpsie eksperimente het getoon dat die lipopeptiede tot hars verhouding en pH belangrike ($\alpha = 0.05$) parameters vir fengycin adsorpsie is met 'n optimale fengycin lipopeptiede tot hars verhouding van 0.5 en 'n optimale pH waarde van 10. Alhoewel die lipopeptiede tot hars verhouding en temperatuur ewe belangrik was vir iturin adsorpsie kon geen optimale toestande vasgestel word nie weens die moontlikheid dat die lipopeptiede tot hars verhouding buite die eksperimentele streek lê, dus is verdere optimalisering studies vir iturin nodig.

Om die fengycin en iturin adsorpsie begrip te verbeter, was adsorpsie kinetika en adsorpsie isoterm studies uitgevoer om sodoende die eksperimentele adsorpsie data deur middel van pseudo-orde kinetika en Langmuir en Freudlich modelle voor te stel. Ewewig tye van 22 h en 24 h was behaal vir fengycin en iturin onderskeidelik, by die optimale fengycin adsorpsie toestande. Die eksperimentele data was toegepas met beide 'n pseudo-eerste-orde reaksie model en pseudo-tweede-orde reaksie model om te bepaal of die beperkende stap vir fengycin en iturin adsorpsie verduidelik kon word deur fisiesoprsie of chemisorpsie. Nie een van die modelle kon die kinetika van die swamdodende lipopeptiede HP-20 adsorpsie verduidelik nie as gevolg van die swak model passing. Hierdie is 'n moontlike aanduiding dat die resultate onvoldoende is en dat verdere eksperimentele werk vereis word.

Na die kinetika ondersoek ten opsigte van fengycin en iturin, is 'n adsorpsie isoterm ondersoek uitgevoer om die versadigde konsentrasie van fengycin en iturin by 'n konstante temperatuur van 43° C en pH waarde van 10 te evalueer. 'n Versadiging konsentrasie van 3 g/L en adsorpsie persentasie van 76.5 ± 0.37% was vir fengycin verkry terwyl 0.5 g/L verkry was vir iturin met 'n % adsorpsie van 54.5 ± 3.99%. Die eksperimentele data was toegepas met Langmuir en Freudlich isoterm modelle om te bepaal watter model die beste die swamdodende lipopeptied data verteenwoordig. Soos met die

adsorpsie kinetika modellering, kon nie een van die isoterm modelle die adsorpsie meganisme van fengycin en iturin op HP-20 verduidelik nie wat impliseer dat ander isoterm modelle soos die Redlich – verdor model of die Dubinin-Radushkevich model gebruik kan word in verdere eksperimentele werk om die adsorpsie gedrag van die swamdodende lipopeptiedes te benader.

Om die doeltreffendheid van die gedeeltelik gesuiwerde swamdodende lipopeptiedes asook die gesuiwerde lipopeptiede mengsel te bepaal, was *in vitro* effektiwiteit studies uitgevoer op 6 algemene fitopatogene wat na-oes berging siektes veroorsaak. Die swam fitopatogene was gegroei op afsonderlike PDA bakkies wat die sel-vrye oplossing, suur neerslag presipitaat, metanol ekstraksie en diëtieleter-metanol ekstraksie bevat. Groei vertraging was na 'n vyf dae inkubasie tydperk bepaal. Die mees effektiewe behandeling was die suur neerslag presipitaat wat groei vertraag het tussen 30-100%, afhangende van die teiken fitopatogeen. Die studie het uitgelig dat *A. brassicicola* was die mees vatbare fitopatogeen vir al die toegepaste behandelinge terwyl *A. sclerotiorum* die mees weerstandige van die ses ondersoekte fitopatogene was. Die gevolgtrekking was dat die effektiwiteit van die swamdodende lipopeptiedes vir groei vertraging afhanklik is van die lipopeptiede konsentrasie en tipe fitopatogeen.

Die studie het bepaal dat 'n effektiewe program vir fengycin en iturin suiwering behels suur neerslag by 'n pH waarde van 3, gevolg deur 'n drie-fase ekstraksie metode waarby metanol as die oplosmiddel gebruik was om sodoende 89% en 17% fengycin en iturin suiwerheid onderskeidelik te behaal met 'n 100% en 53% fengycin en iturin opbrengs onderskeidelik. Hierdie studie is die eerste van sy soort en behels 'n stelselmatige ondersoek van bestaande stroomaf eenheid bedrywighede vir die ontwikkeling van 'n toepaslike konsentrasie en suiwering program vir fengycin en iturin swamdodende lipopeptiedes geproduseer deur *B. amyloliquefaciens*.

Aanbevelings vir verdere ondersoeke sluit die volgende in. Die optimale ewewig voorwaardes van 3 g/L fengycin by 'n pH waarde van 10 en temperatuur van 43°C sal maksimum fengycin HP-20 adsorpsie verseker, alhoewel verder optimaliserings studies benodig word vir iturin adsorpsie. Verdere verfyning van kinetika en isoterm modellering studies word ook vereis om die fengycin adsorpsie meganisme uit te lig.

Acknowledgements

Nomenclature

Q_e	Adsorption capacity at equilibrium
Q_t	Adsorption capacity at time t
°C	Degrees Celsius
μm	Micrometre
$CaCl_2.2H_2O$	Dihydrate calcium chloride
CCD	Central composite design
$FeSO_4.7H_2O$	Heptahydrate ferrous sulphate
g	Gram
g/L	Gram per litre
h	Hour
HMW	High Molecular Weight
KH_2PO_4	Potassium dihydrogen phosphate
$KNaC_4H_4O_6.4H_2O$	Sodium potassium tartrate
L	Litre
LC-ESI-MS	Liquid Chromatography Electrospray Ionisation Mass Spectroscopy
LLE	Liquid-Liquid Extraction
LMW	Low Molecular Weight
LP	Lipopeptide
LP/R	Lipopeptide to resin ratio
LPs	Lipopeptides
mg	Milligram
$MgSO_4.7H_2O$	Heptahydrate magnesium sulphate
min	Minute
mL	Millilitre
mM	Millimolar
$MnSO_4.H_2O$	Monohydrate manganese sulphate
Na_2HPO_4	Disodium hydrogen phosphate
NH_4NO_3	Ammonium nitrate
PFO	Pseudo-first-order
PSO	Pseudo-second-order
RP-HPLC	Reverse-Phase High Performance Liquid Chromatography
rpm	Revolutions per minute
RSM	Response surface methodology
t	Time
TLC	Thin Layer Chromatography
x g	x gravity

Table of contents

List of figures

List of tables

Chapter 1

Introduction

1.1. The South African deciduous fruit industry

The climatic conditions of South Africa make it an ideal area for growing a variety of fruit (Van Dyk and Maspero, 2004). The difference in temperature, moisture and soil features across the country influences the distribution of plants (Bond *et al.*, 2003; Van Dyk and Maspero, 2004). This distribution can be illustrated through studying the deciduous fruit industry of South Africa.

The deciduous fruit industry of South Africa is concerned with the production and global exportation of large volumes of fruit on an annual basis (Greef *et al.*, 2007). South Africa has been reported as the largest exporter of fresh fruit (by volume) in the southern hemisphere (Forum, 2016). The fruit types of interest in this industry include: (1) pome fruit (apples and pears), (2) stone fruit (plums, nectarines, peaches and apricot) and (3) table grapes (used for consumption and not for wine production) (Van Dyk and Maspero, 2004; Greef *et al.*, 2007). The distribution of deciduous fruit growing regions can be seen across the country as illustrated in Figure 1-1, with the largest being the Western Cape province.
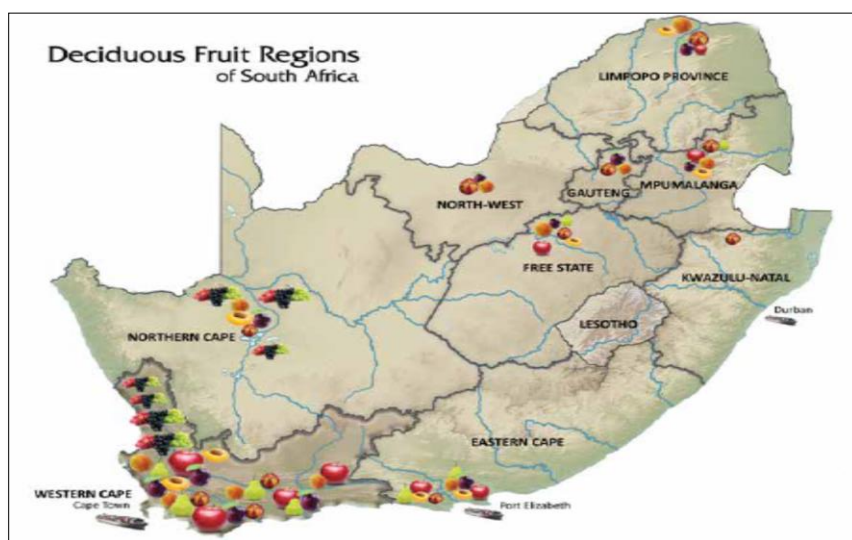
Figure 1-1. The distribution of deciduous fruit growing regions in South Africa (reproduced from Hortgro, 2014)

1.2.   Deciduous fruit supply chain

The supply chain can be described as the pathway fresh fruit embark upon to reach the end-user. The link between the producer (fruit farmer) and the end-user (consumer) is important as it ensures that the fruit quality is maintained throughout the supply chain. A schematic diagram of the different stages of a fruit industry supply chain is illustrated in Figure 1-2.
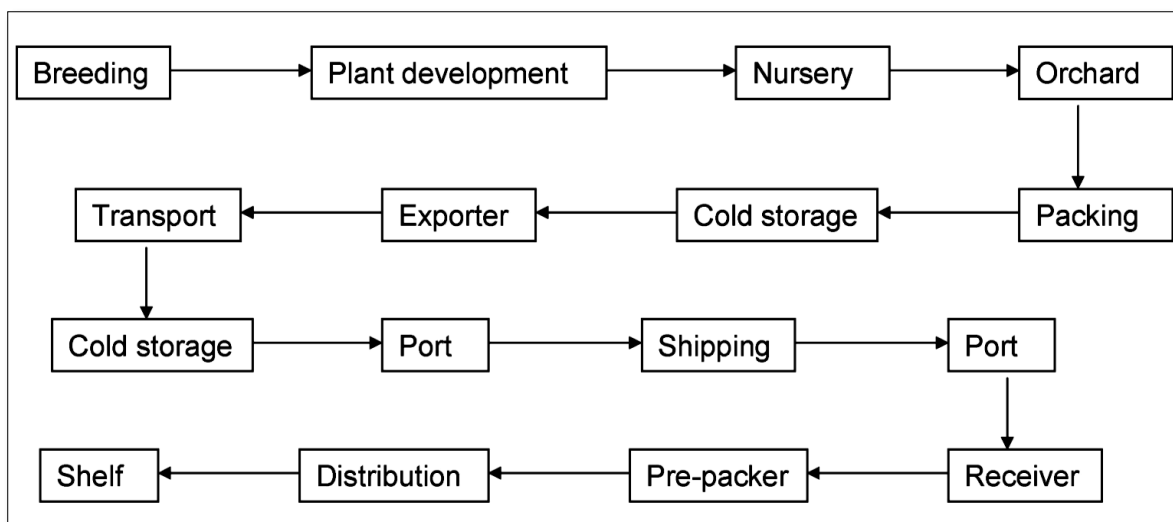
Figure 1-2. The deciduous fruit supply chain (reproduced from Van Dyk and Maspero, 2004)

The quantity and quality of fruit is affected in the supply chain from the production phase to the consumption phase in the form of fruit spoilage (Premanandh, 2011). Fruit spoilage occurs as a result of infection and diseases which can occur in the field (preharvest), during harvesting and after harvesting (postharvest) (Coates and Johnson, 1997). Rodents, insect pests and phytopathogenic microorganisms are responsible for causing preharvest disease in fruit, while ineffective harvesting techniques, handling of fruit, packaging and inefficient storage technologies during postharvest enable microorganisms (Premanandh, 2011), particularly phytopathogens, to cause infection and disease in fruit (Coates and Johnson, 1997).

1.3.   Fungal pathogens in postharvest storage

Microorganisms such as viruses, bacteria, oomycetes, fungi and nematodes (worms) have the potential to cause postharvest diseases in fruit (Strange and Scott, 2005). Fungal pathogens are successful at causing postharvest diseases of fruit in storage because fruit experience physiological changes after harvesting where they become susceptible to pathogens which enable fungal pathogens to establish infection and cause disease (Nunes, 2012). Disease establishment in fruit is mainly due to the abundant spores produced by fungal phytopathogens, from which the spores are easily dispersed in high densities through the air (Strange and Scott, 2005). Some fungal phytopathogens produce

phytotoxic enzymes such as mycotoxins that can penetrate and degrade the fruit tissues and use up nutrients in the fruit which renders the fruit unusable thus contributing to food loss and wastage (Strange and Scott, 2005).

1.4. Fungal species and diseases caused in fruit during postharvest storage

Fungal pathogens that have been reported to cause significant postharvest diseases during storage are species from the *Alternaria*, *Aspergillus*, *Fusarium*, *Geotrichum, Gloeosporium*, *Mucor*, *Monilinia*, *Penicillium*, *Rhizopus* genera, while *Botrytis cinerea* is a prevalent pathogen in postharvest diseases of many fruit in storage (Nunes, 2012; Sonker *et al.*, 2016). Table 1-1 shows the diseases caused by some fungal pathogens in postharvest storage of fruit.

Table 1-1. Postharvest diseases in fruit caused by common fungal pathogens during storage (Redrawn from Coates & Johnson 1997)

Fruit type	Pathogen	Disease caused	Example of disease on fruit
Pome fruit (apples and pears)	*Penicillium* spp.	Blue mould	
	Alternaria spp.	Alternaria rot	
	Mucor piriformis	Mucor rot	
			Blue mould on pears (reproduced from Louw and Korsten, 2014)
Stone fruit (plums, nectarines, peaches & apricot)	*Monilia* spp.	Brown rot	
	Rhizopus spp.	Rhizopus rot	
	Botrytis cinerea	Grey mould	
	Alternaria alternate	Alternaria rot	
			Grey mould on nectarines (reproduced from Fourie, 2013)
Grapes	*Botrytis cinerea*	Grey mould	
	Penicillium spp.	Blue mould	
	Rhizopus spp.	Rhizopus rot	
			Grey mould on grapes (reproduced from Moyer and Grove, 2011)

1.5. Current technologies for managing and controlling fungal postharvest diseases during storage

Fruit are characterised as innately having short shelf-lives and it becomes essential to maintain quality in fruit when the supply chain extends to a global platform where fruit will be stored and transported over large distances (Mahajan *et al.,* 2014). Increasing the shelf life of fruit is dependent upon four factors which are (1) temperature (Prusky, 2011), (2) reducing desiccation (drying out), (3) reducing the senescence (aging) process and (4) preventing and delaying microbial growth (Dhall, 2013). All these factors are important in managing and controlling postharvest diseases in fruit during storage.

The three major control strategies that are currently used to prevent and delay fungal growth in fruit include: (1) physical treatments, (2) chemical treatments and (3) biocontrol agents (Mahajan *et al.,* 2014; Sonker *et al.,* 2016). The constraints in using physical treatments such as heating (which includes "hot water dipping, saturated water heat vapour, hot dry air and hot water rinse with brushing" (Mahajan *et al.,* 2014) are the high-energy demands and cost as well as the heat sensitivities that some fruit have, while the application of chemical fungicides as a chemical treatment is not an environmentally conscious solution as they accumulate to toxic levels in the environment, they are non-specific and lead to the selection of resistant fungal pathogenic strains (Nunes, 2012).

In recent times, there has been a growing shift from using chemical fungicides to using environmentally friendly treatments such as biocontrol agents as alternatives to physical and chemical treatments for postharvest storage of fruit. Biocontrol agents are antagonistic microorganisms that have the ability to control fungal postharvest pathogens and the diseases they cause in fruit (Sonker *et al.*, 2016). Antagonists such as filamentous fungi, yeast and bacteria have been isolated from fruit, vegetable and leaf surfaces as well as from fermented food products (Coates and Johnson, 1997). These isolates are mass produced for commercial application through optimising cell biomass and stabilising the microorganism to ensure that it maintains its biocontrol activity (viability) in a process called formulation (Nunes, 2012). Using these formulations (whole cells of microorganism and/or spores) as postharvest biocontrol agents is limited as the viability is dependent on suitable postharvest environmental conditions to maintain their effectiveness against fungal postharvest pathogens (Pretorius *et al.,* 2015; Nunes, 2012).

The effectiveness and consistent management of postharvest diseases of fruit is attained using an integrated approach where the biocontrol agent is used in conjunction with physical and/or chemical treatments (Nunes, 2012). When the biocontrol agent and other treatments are used independently, they are unable to successfully control over 95% of postharvest diseases (Nunes, 2012).

Comprehensive research into the activity of biocontrol agents in postharvest disease management has indicated that these antagonistic microorganisms produce antimicrobial compounds that aid in disease control (Nunes, 2012). A novel approach of applying biocontrol agents in postharvest storage would be to use the antimicrobial compounds produced by the microorganism rather than using the microorganism itself.

It is evident that a market for alternative biocontrol agents exists in the fruit industry, where using the antimicrobial compounds produced by the microorganism (instead of using the microorganism itself) would offer an environmentally friendly and long-term solution to manage fungal phytopathogens. This concept has been illustrated by the work presented in this study which has, in part, led to the publication: Rangarajan V., Herbst W.J., Mazibuko S. and Clarke K.G. (in press) "*Bacillus* lipopeptides for a novel postharvest disease control technology. Acta Horticulturae.

Chapter 2

Literature review

2.1. Surfactants

2.1.1. Overview of surfactants

Surfactants are a broad class of compounds that can be divided into chemical (synthetic) and natural (biological) surfactants (Soberón-Chávez, 2011). Surfactants are described as amphiphilic compounds implying that they contain hydrophilic and hydrophobic domains (Soberón-Chávez, 2011). Due to the amphiphilic nature of surfactants, they are able to exist at interfaces between polar and non-polar substances (Soberón-Chávez, 2011). Surfactants accumulate at: (1) air-liquid interfaces (e.g. air and water/oil), (2) liquid-liquid interfaces (e.g. water and oil), (3) air-solid interfaces and (4) solid-liquid interfaces (Soberón-Chávez, 2011). Surfactants enable the interfaces to interact and mix easily by reducing the repulsive forces that exist at interfaces (Soberón-Chávez, 2011). The effectiveness of a surfactant is measured by its ability to lower the surface tension at different interfaces (Soberón-Chávez, 2011).

When surfactant molecules are added into a solution, they reduce the surface tension until they reach a critical micelle concentration (CMC) (Soberón-Chávez, 2011). At the CMC, the surfactants form structures called micelles which aggregate due to the weak chemical interactions between the hydrophobic (non-polar) and hydrophilic (polar) domains (Soberón-Chávez, 2011). The CMC is dependent on the surfactant type, pH, ionic strength and the temperature of the solution it is added to (Soberón-Chávez, 2011).

When a surfactant is added into an aqueous solution, the hydrophilic (polar) domains which are the head groups of the micelle project outward into the solution, while the hydrophobic (non-polar) domains, which are the tail groups of the micelle, project inward into the centre of the micelle (Soberón-Chávez, 2011). When the same surfactant is added into a non-polar solution such as oil, the opposite phenomena occurs where the polar heads of the micelle project into the centre of the micelle structure while the non-polar tails project outward into the non-polar solution (inverted micelle) (Soberón-Chávez, 2011).

Due to the amphiphilic nature of surfactants and their ability to form micelle structures, they permit solutions of varying polarities that are immiscible in nature to be miscible and thus they act as emulsifying agents (Kosaric and Vardar-Sukan, 2015).

Surfactants have various applications in the manufacturing of useful products such as plastics, paper, personal care products, household cleaners, paints and coatings, food processing and agricultural products (Soberón-Chávez, 2011). Industrial applications of surfactants include the production of cosmetic products, pharmaceuticals, emulsifiers, wetting-agents and the manufacturing of chemicals. Currently, the surfactants used are chemical (synthetic) surfactants which often have negative impacts on the environment (Soberón-Chávez, 2011).

2.1.2. Microbial biosurfactants

Natural (biological) surfactants are called biosurfactants and are derived from animal, plant and microbial sources (Soberón-Chávez, 2011). Biosurfactants produced by microorganisms (microbial biosurfactants) have gained research interest due to the variety of microorganisms that produce the biosurfactants as well as the chemical diversity of the biosurfactant structures that are produced (Soberón-Chávez, 2011). Due to the structural diversity, microbial biosurfactants present myriad attractive biological properties such as immuno-modulators, anti-tumour agents, antiviral, insecticidal and antifungal agents (Soberón-Chávez, 2011). From an agricultural point of view, an alternative to postharvest chemical fungicides is required as these synthetic fungicides have limited usage as they pose environmental risks (Nunes, 2012) and thus microbial biosurfactants can be applied as replacement antifungal agents that can be used to control phytopathogenic fungi affecting fruit during storage.

2.1.3. Microbial biosurfactant classification

Microorganisms produce an assortment of metabolites during their growth cycle (Kosaric and Vardar-Sukan, 2015). The common metabolites produced can be grouped into two classes which are: (1) primary metabolites and (2) secondary metabolites. Primary metabolites are required for primary metabolic processes that are associated with growth while secondary metabolites are associated with growth limiting or stressful conditions such as reduced nutrients, reduced space, moisture level fluctuations, competition or waste accumulation (Kosaric and Vardar-Sukan, 2015).

Some secondary metabolites are secreted into the culture medium to assist the microorganism to absorb hydrophobic substances, to grow on hydrophobic compounds or to withstand unfavourable conditions where the secondary metabolites are integrated into the cell wall (Kosaric and Vardar-Sukan, 2015). The class of secondary metabolites with the aforementioned attributes are known to have amphiphilic structures and are referred to as biosurfactants (Kosaric and Vardar-Sukan, 2015).

Microbial biosurfactants are classified both by their chemical structure and by the microorganism that produces them (Banat *et al.*, 2010; Soberón-Chávez, 2011). The basic structure of a biosurfactant as

7

shown in Figure 2-1, consists of a hydrophilic domain that comprises of an acid, a cationic or anionic peptide or protein and a sugar component that could be a monosaccharide, disaccharide or polysaccharide molecule (Banat *et al.,* 2010). The hydrophobic domain is composed of saturated or unsaturated hydrocarbons or fatty acids (Banat *et al.,* 2010) with a chain length of eight to 18 carbon atoms (Kosaric and Vardar-Sukan, 2015). Microbial biosurfactants are grouped into either low molecular weight (LMW) or high molecular weight (HMW) biosurfactants as shown in Figure 2-2 (Kosaric and Vardar-Sukan, 2015). The biosurfactants are produced as mixtures that can have up to 40 different molecules having similar chemical structures (homologues) (Soberón-Chávez, 2011). The hydrophilic head groups are usually conserved while the hydrophobic tail groups can have significant variations in the chemical structure (Soberón-Chávez, 2011). The focus of the study presented here will be on lipopeptides (LPs) produced by *Bacillus* species.
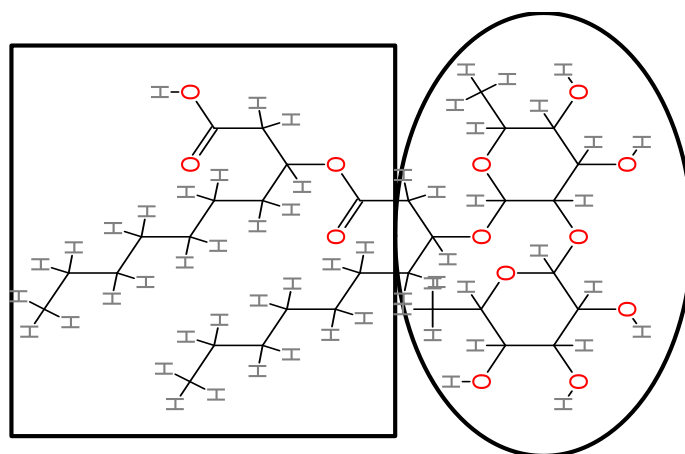
Figure 2-1. Basic chemical structure of a biosurfactant molecule. Boxed structure illustrates the hydrophobic tail groups while the circular structure illustrates the hydrophilic head group (redrawn from Soberón-Chávez, 2011)
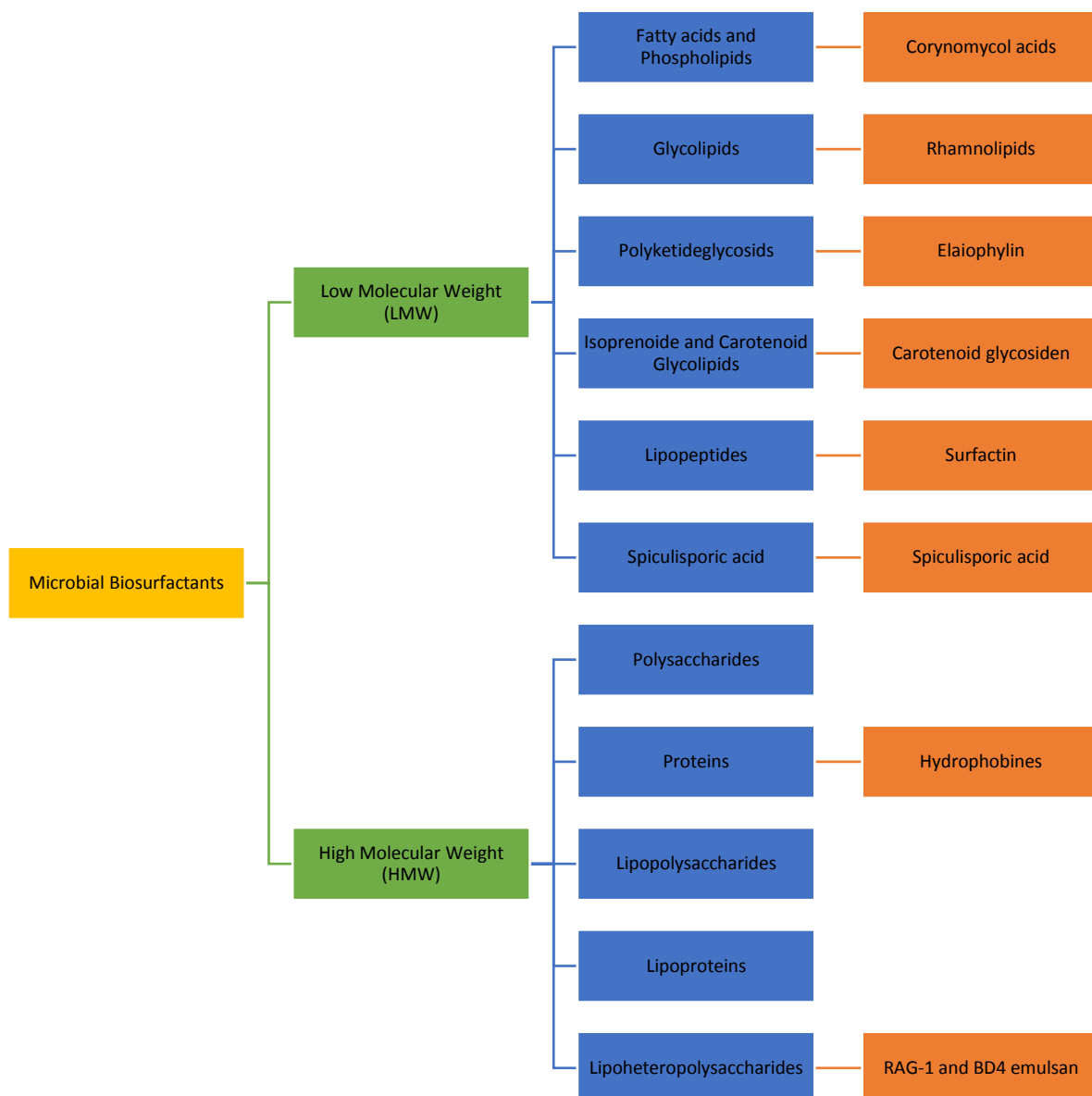
Figure 2-2. Overview of microbial biosurfactant classes and representatives of each class (redrawn from Kosaric & Vardar-Sukan, 2015)

2.2.   Lipopeptides

LPs are produced by certain bacterial genera; however, the focus of this study is specifically directed at the LPs produced by *Bacillus* species.

2.2.1.   *Bacillus* species

Bacillus species are rod-shaped, gram-positive endospore forming microorganisms that are commonly found in the soil. They have also been reported to be found within the tissues of plants, where a symbiotic association exists in which the bacteria obtain nutrients from the plant while the plant is

protected through the production and secretion of anti-pathogenic compounds by the bacteria (Gond *et al.*, 2015).

Bacillus subtilis is a root-colonising (rhizobacterium) microorganism (Gond *et al.,* 2015) that has been isolated from various environmental niches such as air, water and soil where in the latter, the bacteria contributes to mineral cycling of nitrogen and phosphate as well as the chelation of toxic metals (Gond *et al.,* 2015). *B. subtilis* has been extensively used in industry to produce enzymes (such as proteases and amylases) and antibacterial compounds such as difficidin and oxydifficidin that have broad-spectrum activities against aerobic and anaerobic pathogenic bacteria (Zimmerman *et al.*, 1986; Wilson *et al.*, 1987).

Research has been directed at members of the *Bacillus* species as they are well-distinguished producers of LPs (Kosaric and Vardar-Sukan, 2015) since a large fraction (4 - 5%) of their genome is dedicated to the synthesis of LPs (Kosaric and Vardar-Sukan, 2015) and these bacterial species are non-pathogenic to plants, humans and the environment (Kosaric and Vardar-Sukan, 2015) which makes them attractive microorganisms for industrial application.

2.2.2.   Lipopeptide classification

LPs are low molecular weight (as defined above in Figure 2-2) cyclic compounds (Gond *et al.,* 2015; Raaijmakers *et al.,* 2010) that are produced by "large multi-enzymatic proteins" that are classified as non-ribosomal peptide synthetases (NRPSs) (Soberón-Chávez, 2011; Raaijmakers *et al.,* 2010). The NRPSs bring about the structural diversity of LPs which is further enhanced by the culture conditions of the bacteria (Soberón-Chávez, 2011; Ongena & Jacques 2008). Although LPs have been reported to be mainly produced by *Pseudomonas* and *Bacillus* bacterial species (Gond *et al.,* 2015), other microorganisms that produce LPs include species from the fungal genus *Aspergillus* and bacterial species from the *Streptomyces* genus (Raaijmakers *et al.,* 2010).

LPs display diverse biological activities such as cytotoxic, immuno-suppressant and antimicrobial properties (Fernandes *et al.,* 2007; Raaijmakers *et al.,* 2010). Their antimicrobial properties make them attractive as potential biocontrol agents of phytopathogens because they show diverse modes of action in supressing different phytopathogens and the diseases they cause (Romero *et al.,* 2007). The proposed mode of action of LPs is that they disrupt the pathogens cell membrane through ion channel pore formation which leads to leakage of the cell constituents and ultimately to cell death (Raaijmakers *et al.,* 2010). Due to the LP structural diversity, the development of phytopathogen resistance to one type of LP structure may not be a problem since many other LP structures are available indicating, the broad-spectrum applicability for targeting a variety of phytopathogens.

The basic structure of LPs consists of a hydrophobic tail group that is made up of a lipid (fatty acid) component while the hydrophilic head group is made of short oligopeptides (7-10 amino acids) that may be linear or cyclic (Gond *et al.,* 2015; Raaijmakers *et al.,* 2010). Considerable research has been conducted on LPs produced by *Pseudomonas* and *Bacillus* species as the LPs produced by these species show considerable structural diversity (Raaijmakers *et al.,* 2010).

The structural diversity of LPs is due to the type, number and configuration of amino acids making up the hydrophilic oligopeptide as well as the difference in the length and composition of the hydrophobic fatty acid tail (Raaijmakers *et al.,* 2010).

Bacillus species produce three types of cyclic LP families which are surfactins, fengycins and iturins (Fernandes *et al.,* 2007; Raaijmakers *et al.,* 2010). The three families have a common hydrophilic head group that is cyclic and it is attached to a β-amino or β-hydroxy fatty acid tail group that is hydrophobic (Romero *et al.,* 2007). The structural differences among the three families is the oligopeptide sequence and the branching of the fatty acid tail group (Romero *et al.,* 2007). Within each LP family, there are variants that have the same oligopeptide length but differ in the specific position of the amino acid residues in the oligopeptide (Raaijmakers *et al.,* 2010). The characteristics of each *Bacillus* LP family is specified below.

2.2.3.   *Bacillus* lipopeptides

2.2.3.1.   Surfactins

Surfactin is the most well-documented and studied family of LPs as they were the first discovered LPs produced by *B. subtilis* (Zimmerman *et al.*, 1986; Wilson *et al.*, 1987). The surfactin structure consists of 7 α-amino acids linked to one β-hydroxy fatty acid (Gond *et al.,* 2015). The length of the fatty acid molecule varies from C_{13} to C_{16} and the branching of the fatty acid molecule can be linear, iso- or anteiso- (Raaijmakers *et al.,* 2010). There are 20 different LPs within the surfactin family (Fernandes *et al.,* 2007; Soberón-Chávez, 2011; Gond *et al.,* 2015; Kosaric and Vardar-Sukan, 2015) and some representative variants of the surfactin family are esperin, pumilacidin, lichenysin, surfactin and bamylocin (Fernandes *et al.*, 2007; Soberón-Chávez, 2011; Gond *et al.,* 2015)*.* The general chemical structure of surfactin is shown below Figure 2-3.
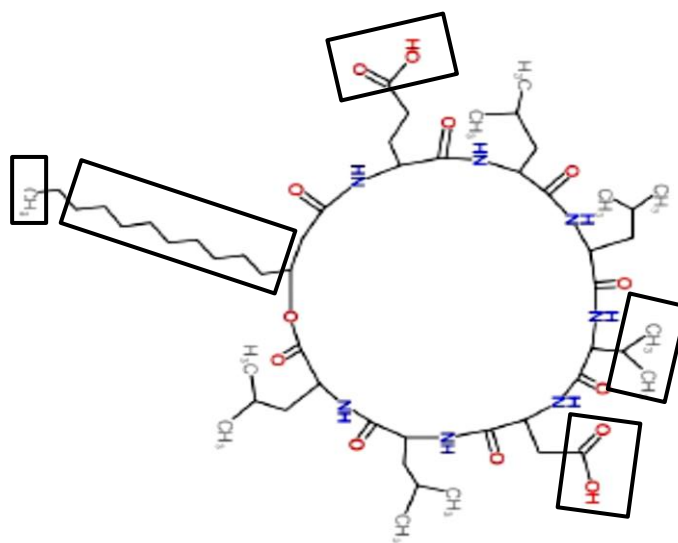
Figure 2-3. Chemical structure of surfactin. Boxed structural groups indicate participation in biological membrane destabilisation in bacteria (redrawn with permission from Herbst, 2017, Originally adapted from Ongena and Jacques, 2008).

B. subtilis produces LPs with a broad spectrum of activities (Fernandes *et al.,* 2007) in which surfactins associate with biological membranes by disrupting and solubilising the membrane integrity. At the critical micelle concentration (CMC), surfactins form mixed micelle structures that completely permeate the biological membrane leading to cell death (Ongena and Jacques 2008). Since research indicates the potent antibiotic properties of surfactin, studying its mode of action has led to the development of new antibiotics (Fernandes *et al.,* 2007).

Most bacteria are susceptible to surfactin destabilizing their cell membrane by forming reverse-micelle structures as shown in Figure 2-4, where the fatty acid chains perforate the cell membrane leading to cell death. Since bacterial cell membranes lack sterols (cholesterol substitute), surfactins are effective at targeting these cell membranes. This enables surfactins to have strong antibacterial activities. Conversely, surfactins have limited antifungal activity as fungal cell membranes contain ergosterols which makes surfactins ineffective against fungal phytopathogens (Gond *et al.,* 2015; Ongena and Jacques, 2008). Apart from the antibacterial activity of surfactins, these LPs also show haemolytic (rupture red blood cells), antiviral and antimycoplasmic properties (Ongena and Jacques, 2008).
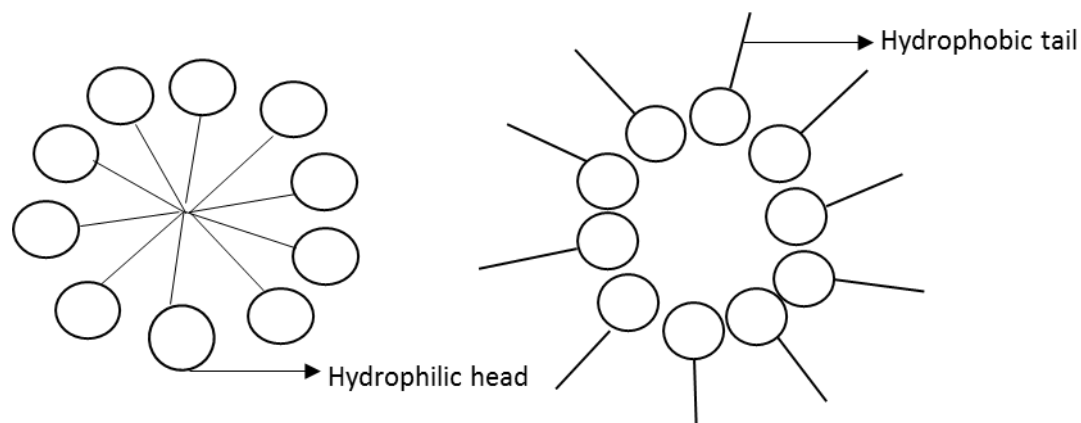
Figure 2-4. The structure of a micelle (left) and a reverse-micelle (right)

2.2.3.2.   Iturins

Iturins are made up of 7 α-amino acids linked to one β-amino fatty acid that has variable lengths from C_{14} to C_{17} (Gond *et al.,* 2015). The six variants of this family are iturin A and C, mycosubtilin, bacillomycin D, F and L (Raaijmakers *et al.,* 2010; Gond *et al.,* 2015) while iturin A is the most well-studied variant of the iturin family (Soberón-Chávez, 2011). Instead of the iturins being produced by NRPSs, they are produced by a hybrid enzyme which is a polyketide synthase fused with a non-ribosomal peptide synthetase (Raaijmakers *et al.,* 2010).

Iturin and surfactin share similar properties in that both LPs show haemolytic activities (Ongena and Jacques, 2008). Also, both iturin and surfactin disrupt the membrane integrity. However, the mode of destabilising the membrane is different as iturin forms ion-conducting pores while surfactin anchors into the membrane to destabilise it (Ongena and Jacques, 2008). Iturins have been reported to show strong *in vitro* antifungal activity against yeast and other fungal species. However they show limited antibacterial activity and no antiviral activity (Ongena and Jacques, 2008). The general structure of iturin is shown below in Figure 2-5.
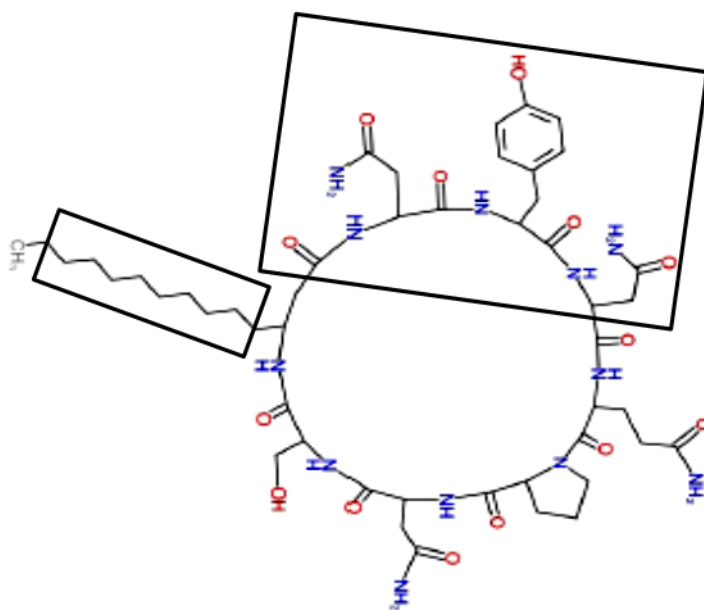
Figure 2-5. Chemical structure of iturin. Boxed structural groups indicate involvement in ion-pore formation of the lipid membrane in fungi (redrawn with permission from Herbst, 2017, Originally adapted from Ongena and Jacques, 2008)

2.2.3.3.   Fengycins

Fengycins display strong antifungal properties specifically towards filamentous fungi while they have limited haemolytic activity, relative to surfactin and iturin (Ongena and Jacques, 2008). The fengycin family is characterised by 10 α-amino acids linked to one β-hydroxy fatty acid (Gond *et al.,* 2015). The length of the fatty acid molecule varies from C_{14} to C_{18} and the branching of the fatty acid molecule can be linear, iso- or anteiso- and it can be saturated or unsaturated (Raaijmakers *et al.,* 2010; Gond *et al.,* 2015). The two variants in this family are the well-studied fengycin A and B which are also called plisplastins A and B (Raaijmakers *et al.,* 2010). The general structure of fengycin is shown below in Figure 2-6. Although fengycins target filamentous fungal pathogens, their mode of action is not well understood, hence it is uncertain which structural groups of the fengycin structure are involved in the interaction with the pathogens membrane (Ongena and Jacques, 2008; Soberón-Chávez, 2011).
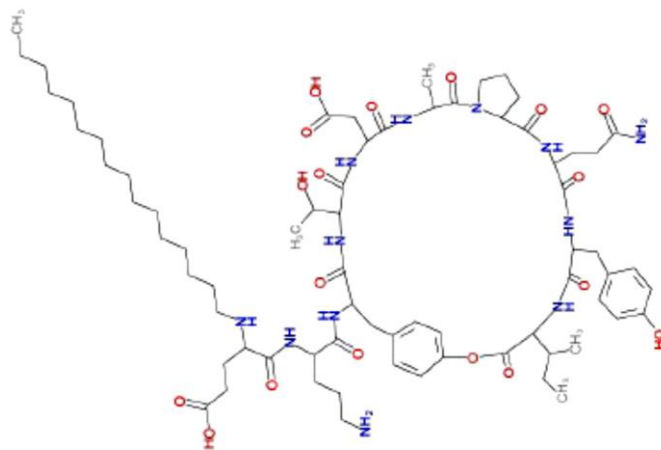
Figure 2-6. Chemical structure of fengycin. (Redrawn with permission from Herbst, 2017, Originally adapted from Ongena and Jacques, 2008)

Similarly to iturins, fengycins show strong antifungal activities, however, fengycins specifically target filamentous fungal pathogens (Romero *et al.,* 2007; Ongena and Jacques 2008) and would be the preferred LP family to be applied as a potential biocontrol agent of filamentous fungal pathogens affecting stone fruit during storage in the supply chain. Although the different LP families have different target specificities, with surfactins being relatively antibacterial while iturins and fengycins relatively antifungal, these LP families function synergistically by complementing each other to control pathogens (Ongena and Jacques 2008; Soberón-Chávez 2010).

Several *Bacillus* species can simultaneously produce a mixture of LP families in different ratios. Although much research has been dedicated towards various *B. subtilis* strains and the surfactins they produce, studies in their application on controlling and managing postharvest diseases caused by fungal pathogens is limited since members of *B. subtilis* are significant producers of surfactins (rather than fengycins and iturins) which show stronger antibacterial properties relative to antifungal properties (Kosaric and Vardar-Sukan 2015). It is therefore important to identify different *Bacillus* species that produce significant amounts of fengycin and iturin LPs relative to surfactin for managing postharvest diseases.

Various *Bacillus* species have been identified as natural producers of LPs and their potential application in managing and controlling postharvest diseases has been realised. In a study conducted by Pretorius *et al.* (2015), a member of the *Bacillus* genus, *Bacillus amyloliquefaciens* DSM 23117 was identified as a strong producer of antifungal lipopeptides. The LPs produced by this bacterial species

could be used as a second-generation biocontrol agent for managing and controlling fungal postharvest diseases of fruit.

2.3. Upstream processing of lipopeptide

For the synthesis of LPs by bacteria to occur, the growth of the bacteria under investigation must be facilitated. The three major components to be considered in the production process of LPs are (1) selection of the appropriate bacterial strain (Rangarajan *et al.,* 2015), (2) correct production medium and nutrient profile and (3) the optimal process conditions (agitation rate, pH and temperature) (Rangarajan and Clarke, 2015). The choice of bacterial strain is dependent upon the type and ratio of LPs required, as determined by the end-application of the LPs. Once the end-application is specified, the appropriate growth medium is used that will promote the bacteria to produce the LPs under the optimal process conditions. Once the appropriate bacterial strain, optimal production medium and process conditions are realised, three types of operating strategies can be employed in the production of LPs: batch, fed-batch and continuous cultures (Clarke, 2013).

2.3.1. Batch culture

Batch culture involves growing the microorganism in a closed system such as a bioreactor or Erlenmeyer flask (Clarke, 2013; Paulová *et al.*, 2013). The nutrients and inoculum are aseptically added to the bioreactor or Erlenmeyer flasks at the beginning of cultivation and no culture is removed during cultivation (Paulová *et al.*, 2013). The characteristic growth phases of the microorganism during batch culture, comprising the lag, exponential, stationary and death phase can be observed and defined throughout the cultivation period (Paulová *et al.*, 2013). The stationary growth phase is particularly important for studies directed at secondary metabolite production as the lengthening of this phase might yield maximum secondary metabolites (Paulová *et al.*, 2013). This operating strategy is also advantageous as the products formed are concentrated, which reduces the procedural steps for downstream processes (Clarke, 2013). However, if the product formed can also be consumed by the organism, or is auto-inhibitory, then this culture strategy may not be optimal.

2.3.2. Fed-batch culture

A fed-batch culture is a partially open operating strategy that involves the gradual addition of one or more nutrient(s) aseptically into the system , without removing culture during operation (Clarke, 2013; Paulová *et al.*, 2013). This means that the volume in the bioreactor increases over time until the maximum volume in the bioreactor is reached and the cultivation process ends (Clarke, 2013; (Paulová *et al.*, 2013). In this time, the product of interest accumulates and is retained inside the system (Paulová *et al.*, 2013). The advantage of using fed-batch cultures is that (1) high cell biomass concentrations can be achieved which can increase the product yield, (2) the gradual addition of

16

nutrients increases the product yield capacity, (3) synthesis of the product is prolonged and (4) a particular phase can be lengthened which can be used to maximise the product yield (Clarke, 2013; Paulová *et al.*, 2013). This production strategy is also useful when the substrate has an inhibitory effect on microbial growth and thus product yield, as the slow addition of nutrients ensures that the inhibitory effect is minimised (Clarke, 2013).

2.3.3. Continuous culture

Continuous cultures are often performed in chemostats (also known as continuous stirred tank reactors, or CSTRs) and they are based on an open system in which there is a continuous addition of nutrients, good reactor mixing and continuous removal of reactor contents (including both product and waste material) (Clarke, 2013; Paulová *et al.*, 2013). The volume in this system is kept constant and thus the specific growth rate of the cells is kept constant as the nutrients are continuously added into the bioreactor while metabolic waste products are removed (Paulová *et al.*, 2013). There are different types of bioreactors that continuous cultures can be maintained in, such as a continuous stirred tank reactor (CSTR) and the continuous bubble column reactor (Clarke, 2013). The advantages of using continuous culture is that the product of interest can be produced continuously over a prolonged time frame with the same quality of the product is maintained. However, two major shortcomings of using this operating strategy on a large scale is: (1) the risk of contamination that occurs during the addition of nutrients and the removal of metabolic waste products and (2) the potential genetic mutation of the microorganism under long-term production of the desired metabolites (Paulová *et al.*, 2013).

2.4. Downstream processing of lipopeptides

Downstream processing in this context, is concerned with the recovery, concentration and purification of LPs from the culture (Clarke, 2013). The type of purification operation used is partly dependent on how the bacterium expresses the product, specifically whether the product is expressed intracellularly or extracellularly as both modes of expression have different and significant implications on the purification of the product. When a product is produced intracellularly, the bacterial cells are lysed and the targeted product is located and separated from other cell constituents using differential centrifugation which separates cell constituents based on the density, mass and size (Wingfield, 2016). For example, in the purification of protein expressed by *Escherichia coli*, the targeted protein would be inside insoluble proteins called inclusion bodies or the periplasm, where proteins in the inclusion bodies would be inactive when isolated, requiring a folding mechanism to restore the activity (Wingfield, 2016). Although the proteins would be mostly pure, which implies simple purification, a trade-off between the purity and the activity of the protein/product needs to be considered when the

17

product of interest is expressed intracellularly (Wingfield, 2016). Conversely, when a product is produced extracellularly, it is dilute as it is contained in the large volume of culture medium making it necessary to reduce the volume of the culture medium to concentrate the product which would be followed by purification steps to yield the desired product purity (Wingfield, 2016). Since LPs are extracellular compounds, they are secreted into the culture medium and can thus be obtained in the supernatant (after the cells are removed) through appropriate downstream unit operations that are dependent on exploiting some property of the LPs which enable their recovery and purification (Kosaric and Vardar-Sukan, 2015).

Currently, the commercial potential of LPs has not been fully realised mainly due to the high costs involved in the overall production of LPs (Banat *et al.,* 2010). It is estimated that 70% (Rangarajan and Clarke, 2016; Kosaric and Vadar-Sukan, 2015) of the total production cost is directed towards the downstream processing of LPs and is dependent on (1) the bacterial strain used, (2) the mixture of LPs produced, (3) the yields of LPs produced and (4) the end-application of the LPs which determine the number and type of downstream unit operations employed (Kosaric and Vardar-Sukan, 2015; Reis *et al.*, 2013).

In developing an ideal downstream recovery and purification programme, the number of unit operations used should be minimised to reduce the overall costs involved in the purification process (Clarke, 2013; Banat *et al.,* 2010). The purity required in the final product is another deciding parameter that determines the number of unit operations to be used, which is dependent on the end-application of the product. Since the end-application of LPs will involve fruit treatment, the LP purity needs to be high indicating the numerous number of unit operations that will be required to achieve the purity requirements.

Several approaches have been implemented in attempts to reduce the recovery and purification costs. These approaches involve the use of genetically modified strains that are engineered to over-produce the desired LPs, using inexpensive substrates such as waste products and optimised culture medium together with the optimal process conditions (Banat *et al.,* 2010).

The common unit operations applied in the downstream processing of LPs include centrifugation, precipitation, solvent extraction, foam fractionation, filtration, adsorption and chromatographic techniques (Clarke 2013; Kosaric and Vadar-Sukan 2015; Shaligram and Singhal, 2010). The unit operation selected uses some property of the LPs such as charge or solubility (Shaligram and Singhal, 2010) to separate the LPs from the undesired components (impurities) to achieve an increased degree of purity. The LP separation techniques are briefly discussed in the following sections.

2.4.1. Centrifugation

Centrifugation is an initial step prior to any selected LP purification technique as it is used to separate the bacterial cells and solid constituents from the culture under a centrifugal force (Mukherjee *et al.,* 2006; Clarke, 2013). The resulting cell-free supernatant contains LPs which can then be purified by applying other unit operations. Centrifugation can be costly, and there are other unit operations which can be used to separate solid from liquid components, such as filtration. However, the focus of this work is on purification of the supernatant liquid.

2.4.2. Precipitation

This recovery and purification technique is important in the initial recovery of LPs from the cell-free supernatant as it concentrates as well as achieving some degree of increased purity (Rangarajan and Clarke, 2016). The LPs are recovered from the cell-free supernatant by exploiting the pH and solubility properties of the LPs in the cell-free supernatant (Mukherjee *et al.,* 2006; Clarke, 2013).

Precipitation is achieved when the LP solubility in the cell-free supernatant decreases due to a change in pH (acid precipitation) (Clarke, 2013). A decrease in the pH decreases the solubility of LPs in the cell-free supernatant which results in the LPs precipitating along with other macromolecular impurities such as proteins (Mukherjee *et al.,* 2006; Clarke, 2013). During acid precipitation, concentrated hydrochloric acid (HCl) is added to the cell-free supernatant containing LPs until the solution reaches pH 2 (Dhanarajan *et al.,* 2015; Wang *et al.*, 2010). Acid precipitation is the preferred method for LPs over salt precipitation as the co-precipitation of macromolecules such as proteins, polysaccharides and peptides from the cell-free supernatant is minimised, which prevents further downstream unit operations that would be required to remove the salt from the LPs (Rangarajan and Clarke, 2016).

The cell-free supernatant is commonly acidified to pH 2 (Dhanarajan *et al.,* 2015; Wang *et al.,* 2010) while Chen and Juang (2008) and Chen *et al.* (2008) have reported acidification of the cell-free supernatant to pH 4 to obtain a surfactin recovery of > 97% with a purity of 55%. Although pH 2 is commonly reported as the desired pH value for acidification of the cell-free supernatant, little or no information regarding the recovery and purity of LPs, particularly fengycin and iturin, at this pH value is available. The preferred pH value for precipitation of the cell-free supernatant of 2, suggests that pH 2 lies at or below the pKa of the LPs, making them protonated and thus less soluble in water.

2.4.3. Solvent extraction

Extraction is a separation technique involving two immiscible liquid phases, usually between an aqueous phase and an organic phase, where the product of interest is partitioned between the two phases (Wells, 2003; Clarke, 2013). The liquid phases are selected so that one phase selectively

extracts the product of interest while providing a high recovery of the product as well (Wells, 2003). The separation technique is discussed in detail below.

Solvent extraction is also referred to as liquid-liquid extraction (LLE). In this type of extraction procedure, the desired solutes and impurities are present in an aqueous phase, called a feed solution (Kislik, 2012). The feed solution is brought into contact with a second immiscible phase which is usually an organic solvent. However, the second phase can be a solid, gas or supercritical fluid, depending on the properties of the solute being extracted (Wells, 2003). If the second phase is chosen well, then the compound of interest is recovered preferentially in the second phase, while the impurities remain in the aqueous phase (Wells, 2003).The solute in the second phase is called the extract while the aqueous phase with minimal solute remaining is called the raffinate (Kislik, 2012). The LLE method relies upon the solute being relatively more soluble in the extraction phase than the aqueous phase (Wells, 2003). Often, in order to increase recovery of the desired solute from a mixture, repeated cycles of the extraction procedure are used (Kislik, 2012).

A solvent miscibility table is used to determine the appropriate solvents and their combinations for LLE application (Wells, 2003). Once the solvent(s) have been selected, the LLE procedure is performed in a separating funnel (at lab scale) with mechanical mixing to maximise mass transfer, after which the two phases are allowed to separate to obtain the extract and the raffinate (Wells, 2003). The extract is then concentrated by removing the solvent using a sample concentrator or rotary evaporator. The recovered solvent can then be recycled and reused (Wells, 2003). For industrial applications, extraction is performed in extraction columns containing mixer-settler tanks which allow mixing and separation of the two phases to occur. The mixer-settler allows the two phases to be separated after mixing. The solvent can be evaporated using a rotary evaporator, condensed and recycled for further extraction procedures.

Most solvents are immiscible with water and two distinct phases will be formed. However, the degree of solubility of the selected solvent in water and the degree of water solubility in the solvent should be examined as saturation may occur. The challenge with saturation is that the recovery of the extract will contain some water molecules while the raffinate will contain some organic solvent molecules which then becomes a challenge in the disposal of the raffinate (Wells, 2003).

The major limitations of using LLE include limited selectivity where impurities along with the product of interest are contained in the extract, necessitating further purification. Large volumes of solvents will be wasted if an appropriate solvent regeneration strategy is not in place which presents additional costs to the downstream purification programme. Another major challenge to solvent extraction is

the potential formation of emulsions if the product of interest is an amphiphilic molecules such as a surfactant/biosurfactant, which prevents the complete separation of the two phases and thus the recovery of the product (Wells, 2003).

In LP purification, the cell-free supernatant can either be extracted directly with an organic solvent (Romero *et al.*, 2007; Gordillo and Maldonado, 2009; Kosaric and Vardar-Sukan, 2015) or first acid precipitated and the acid precipitate then extracted with an organic solvent (Kim *et al.,* 2004; Fernandes *et al.,* 2007; Gond *et al.,* 2015). It is reported that although acid precipitation of the cell-free supernatant is not required prior to solvent extraction, extraction of the acid precipitate improves the extraction yield of LPs because in their protonated form they are more soluble in an organic solvent than in an aqueous solvent (Soberón-Chávez, 2011).

Extraction of LPs from the cell-free supernatant using an organic solvent is not frequently described in literature, potentially due to the process complexity arising from the emulsification properties of LPs. A variety of LP purification publications report the more common procedure involving acidification of the cell-free supernatant to pH 2, after which the acid precipitate is lyophilised and then extracted with an organic solvent (Fernandes *et al.,* 2007; Chen and Juang, 2008; Lee *et al.,* 2010).

A wide variety of organic solvents are commonly used for LP extraction. These solvents include ethyl acetate, chloroform, methanol, n-hexane, diethyl ether, acetone, ethanol, butanol and mixtures of ethyl acetate and methanol as well as chloroform and methanol (Soberón-Chávez 2010; Gordillo and Maldonado 2009; Kosaric and Vardar-Sukan 2015; Chen and Juang 2008) while Romero *et al.* (2007) and Lee *et al.* (2010) reported n-butanol and methanol respectively, for the extraction of LPs.

Although there are a range of organic solvents that can be used for solvent extraction, these solvents have primarily been investigated for the extraction of surfactin, while a limited number of studies on the extraction of antifungal LPs have been performed. Although a variety of organic solvents can be used for the extraction of fengycin and iturin, the organic solvent selection, in addition to the recovery and purity of antifungal LPs extracted, has not been previously reported.

2.4.4.   Adsorption

2.4.4.1.   The adsorption process

Adsorption can be described as a surface phenomenon that occurs at the interface of two phases where there is a change in concentration in the interface compared to that in the two phases (Dabrowski, 2001). The phases involved in the adsorption process include liquid-solid phases (Dabrowski, 2001). In a typical adsorption process, the molecules in one phase accumulate at the interface between the two phases. For instance, in a liquid-solid phase, the molecules in the liquid

phase accumulate at the interface between the liquid and solid phase (Dabrowski, 2001). The molecule of interest in the liquid is called the adsorbate, while the solid surface is known as the adsorbent (Dabrowski, 2001). In large-scale industrial processes, liquid-solid and gas-solid interfaces are commonly used (Dabrowski, 2001) while the liquid-solid interface is the preferred adsorption system (Snyder, 1968), particularly for recovery of a biomolecule from the culture broth.

The accumulation of the adsorbate molecules on the adsorbent surface can occur through physical interactions, called physisorption, or through chemical interactions, called chemisorption (Snyder, 1968). Physisorption involves the formation of weak intermolecular forces (Van de Waals forces) between the adsorbent surface and adsorbate molecules (Snyder, 1968). The adsorption and desorption (removal of adsorbate molecules from the adsorbent surface) process in physisorption is rapid as it is relatively easy to break down the Van de Waals forces and thus the adsorption energy required to break the bonds is relatively small (Snyder, 1968). Chemisorption involves the formation of strong covalent or ionic bond formation between the adsorbate molecules and adsorbent surface (Snyder, 1968). Due to the strong bonds formed between the adsorbate molecules and adsorbent surface, adsorption and desorption is a slow process, requiring relatively large adsorption energies to form or break down the bonds (Snyder, 1968).

2.4.4.2.   Parameters influencing adsorption

2.4.4.2.1.   Adsorbent characteristics

One of the most important factors that contribute to the adsorption process is the selection of an appropriate type of adsorbent, often in the form of a resin, with particular chemical and physical characteristics. There are diverse adsorbents available, owing to the range of industrial applications that the adsorbents are used in (Dabrowski, 2001). The different industrial applications include water purification, the removal of impurities from liquid and gas solutions and the purification of liquid and gas mixtures (Dabrowski, 2001). The types of industrial adsorbents used can generally be grouped into three classes: (1) carbon adsorbents such as activated carbons that are non-polar in nature, (2) mineral adsorbents such as silica gels and zeolite that are polar and (3) polymer-based adsorbents that can be polar or non-polar (Dabrowski, 2001).

One significant feature of the adsorbent is the porosity, which includes the pore volume, distribution of the pores on the adsorbent surface as well as the pore diameter, all of which determine the surface area available for adsorbance (Dabrowski, 2001). Adsorbents have varying pore sizes which are arranged in complex networks within the adsorbent, giving rise to three types of pores of varying diameters; macropores that are > 50 nm, mesopores that are 2 – 50 nm and micropores that are < 2

nm (Dabrowski, 2001; Wells, 2003). The difference in the adsorbent pore size allows for adsorbate molecule selectivity based on size which means that small molecules can access adsorption sites of microporous resins while large molecules can access adsorption sites of macroporous resins.

Physical adsorption in porous adsorbents is a multi-step process that consists of: (1) film diffusion where the adsorbate molecules in the liquid (called the bulk phase) diffuse onto the adsorbent surface which is followed by (2) pore diffusion where the adsorbate molecules in the liquid pass through the adsorbent pores and lastly (3) adsorptive reaction where the adsorbate molecules bind at appropriate binding sites on the adsorbent surface (Dabrowski, 2001; Wells, 2003).

Activated carbon, which is classified as a microporous adsorbent, has been used by Liu *et al.* (2007) to study the adsorption rate of surfactin from the cell-free supernatant onto activated carbon, while a follow-up study by Montastruc *et al.* (2008) studied the adsorption of surfactin directly from the *Bacillus* culture. It was reported that the surfactin recovery obtained directly from the culture was 26% lower than the recovery of surfactin obtained from the cell-free supernatant. This suggests that activated carbon adsorbed other culture components such as protein in addition to the LPs (Montastruc *et al.*, 2008). Although activated carbon may be a suitable adsorbent for the recovery of LPs, it is generally added into the *Bacillus* culture to promote growth and LP production (Rangarajan and Clarke, 2015).

Macroporous adsorbents have been found to be suitable for the recovery and purification of high value biological molecules such as antibiotics (Tucker, 1989), anthocyanins (antioxidants) (Chen *et al.*, 2015) and anti-cancer agents such as chaetominine (Liu *et al.*, 2016) and sulforaphane (Yuanfeng *et al.*, 2016). These adsorbents are suitable for large-scale application due their easy regeneration, procedural simplicity and low-cost relative to solvent extraction (Liu *et al.*, 2016; Yuanfeng *et al.*, 2016). The attractive properties of macroporous adsorbents is (1) their high adsorption specificities which are due to the surface properties of the adsorbents, (2) high surface areas to increase the adsorption capacity, (3) strong mechanical strength and (4) appropriate pore diameter and pore sizes to allow rapid diffusion, providing a high purity product (Chen *et al.*, 2008; Wang *et al.*, 2010; Dhanarajan *et al.*, 2015; Yuanfeng *et al.*, 2016).

The adsorbate affinity for a macroporous resin is based on the surface area, pore size and diameter as well as the polarity of the resin (Wang *et al.*, 2010). The polarity of the adsorbent is an important parameter when selecting an appropriate adsorbent as it determines the molecules that will be adsorbed (molecule of interest or impurities) and the degree of adsorption, suggesting that the appropriate resin, under optimal adsorption conditions will recover the adsorbate with a high purity.

Macroporous resins are available in different polarities that range from polar, moderately polar, weakly polar to non-polar (Wang *et al.*, 2010; Dhanarajan *et al.*, 2015). Several studies have investigated a range of macroporous resins for the adsorption of LPs (Dhanarajan *et al.,* 2015; Wang *et al.,* 2010; Chen *et al.,* 2008) and it was found that non-polar macroporous adsorbents were superior. This suggests that separation and purification of LPs is based on the hydrophobic interaction with the non-polar resin. Although polar resins could recover LPs, the hydrophilic interaction between the LPs and the resin was weaker relative to the hydrophobic interaction between the LPs and the resin, which makes non-polar resins successful at LP adsorption over their polar counterparts.

Among the macroporous adsorbents investigated, the non-polar resin HP-20 was found to be suitable for the adsorption of *Bacillus megaterium* LPs after the screening of four macroporous resins (XAD-4, XAD-7, HP-20 and HP-2MG), each having unique physical characteristics and different adsorption and desorption capacities (Dhanarajan *et al.*, 2015). Dhanarajan *et al.* (2015) indicated that HP-20 displayed the highest adsorption capacity of the four resins screened in batch adsorption experiments accompanied with optimal adsorption conditions such as the temperature, pH, resin and LP concentration.

Although HP-20 resin displayed the highest adsorption capacity, it was selected based on the total LP recovery yield, with no adsorption data of the individual LP families in batch studies, under optimal conditions (Dhanarajan *et al.*, 2015). The optimal recovery and adsorption conditions for the individual LP families produced by *B. amyloliquefaciens* remain to be investigated for batch adsorption studies.

2.4.4.2.2. Adsorbent operating conditions

Two adsorption operating systems exist, namely static (batch) adsorption and dynamic (column) adsorption. Static adsorption refers to the continuous mixing of a specific volume of adsorbate solution and adsorbent mass in order to obtain adsorption parameters such as the adsorption and desorption capacities, adsorption kinetics as well as adsorption isotherms (Dhanarajan *et al.*, 2015).

In contrast to static adsorption, dynamic adsorption is performed in columns that are packed with an adsorbent and the adsorbate solution is continuously in contact with the adsorbent throughout the adsorption process. Adsorption parameters such as the adsorbate solution flow rate and the break through curve can be determined (Dhanarajan *et al.*, 2015). Although static adsorption studies may be ideal for laboratory scale, it is the dynamic adsorption studies that are applicable for large-scale industrial operations as large quantities of the adsorbate solution can be used while the information obtained from the break though curve can be used to inform on (1) the regeneration time of the adsorbent, from which the adsorbate can be recovered and (2) the life-span of the adsorbent to

determine the frequency of adsorbent reuse (Dabrowski, 2001) where organic solvents are used to wash the column and the adsorption-desorption studies conducted to evaluate how reusable the adsorbent is after a defined number of adsorption-desorption cycles have been performed (Liu *et al.*, 2016).

To obtain maximum adsorption of the adsorbate on the surface, the appropriate conditions such as the temperature, solution pH, agitation as well as the resin and adsorbate concentrations must be considered. Table 2-1 illustrates these adsorption parameters and the corresponding ranges that have been investigated for LP adsorption in batch experiments prior to column studies. It is evident in the studies that the initial LP concentration, adsorbent concentration, temperature and pH are the dominant parameters that drive the adsorption process and as such, these parameters need to be optimised for an adsorption system.

The optimal LP concentration, resin concentration, temperature and pH of an adsorption system has been commonly obtained through one factor at a time experiments where one factor (e.g. LP concentration) is varied while maintaining the other factors (e.g. adsorbent concentration, temperature and pH) constant. Once the optimum for one variable has been obtained, the next variable (e.g. adsorbent concentration) can then be varied while maintaining the other variables constant. The procedure is repeated until optimal conditions for all variables are obtained (Chen *et al.,* 2008; Wang *et al.,* 2010; Dhanarajan *et al.*, 2015).

Although limited studies on LP purification on macroporous resins have been performed using one factor at a time experiments, they would be appropriate if the factors were independent. However, they are not independent. Consequently, the disadvantages of using this method is that firstly, the interaction and degree of interaction between the factors cannot be determined and secondly, the individual effect that each variable contributes to the adsorption of LPs cannot be estimated (Czitrom, 1999), thus the optimal conditions would not be accurately defined. This suggests that an effective method such as a response surface methodology (RSM) design would be suitable to identify and estimate the interactions of the factors on LP adsorption from which optimal LP adsorption conditions would be obtained.

25

Table 2-1. Adsorption parameters and ranges for optimal lipopeptide adsorption in batch experiments

Adsorption parameters

Adsorbent	Adsorbent concentration (g/L)	Initial LP concentration (g/L)	Temperature (°C)	pH	LP solution volume (mL)	Bacterium	Agitation (rpm)	Reference
HP-20	5 - 20	0.5 - 3	25 - 45	6.7	20	*Bacillus megaterium*	150	Dhanarajan *et al.* (2015)
X-5	10 - 50	0.3752	25	7	20	*Bacillus amyloliquefaciens ES-2*	100	Wang *et al.* (2010)
XAD-7	2	0.2 - 0.4	25	6.5 - 11	200	*Bacillus subtilis* ATCC 21332	NS*	Chen *et al.* (2008)
Activated carbon	1.25 - 5	0.0075 - 0.038	20 - 40	6.5 - 8.5	20	*Bacillus subtilis* ATCC 21332	80 - 180	Liu *et al.* (2007)

*NS = not stated

In addition to the factors that influence adsorption, the mechanism of adsorption is important as the adsorption behaviour of a system can be characterised through two important parameters: (1) adsorption kinetics and (2) adsorption isotherms, which give information on how long the system takes to reach equilibrium and the maximum amount of adsorbate molecules that can be adsorbed at equilibrium. These two parameters are discussed below.

2.4.4.2.3.   Adsorption kinetics

Adsorption kinetics is concerned with the rate at which adsorbate molecules are adsorbed as well as the quantity of adsorbate on the resin surface. The rate at which adsorption occurs will depend on the adsorption conditions used, which will in turn determine the completion of the adsorption process when equilibrium is reached (Qiu *et al.,* 2009).

Adsorption Kinetic parameters are important to investigate as the information obtained can be used to determine the performance of the adsorption system in dynamic adsorption or flow-through systems such as when using a column instead of a batch system, which can then be related to pilot and up-scale studies (Qiu *et al.,* 2009). Obtaining appropriate adsorption kinetic data through experiments will enable the use of batch adsorption kinetic models to describe the adsorption process (Qiu *et al.,* 2009).

The two commonly used models for batch kinetic studies include the adsorption reaction models and adsorption diffusion models, which are used to assess the performance of an adsorbent under defined conditions (Qiu *et al.*, 2009). The models are also used to explain the basic mechanism of adsorption (Qiu *et al.*, 2009). Adsorption reaction models consist of the pseudo first-order rate equation and the pseudo second-order rate equation. The pseudo first-order rate equation was the earliest model used to describe solid-liquid adsorption systems and is based on the adsorption capacity (Q_e). The model is used to explain physical adsorption while the pseudo second-order rate equation is derived from the kinetics of chemical reactions (Qiu *et al.,* 2009). If the modelled data is best described by the pseudo-second order model, the rate limiting step may be chemisorption. However, if the modelled data is best described by the pseudo-first order model, the rate limiting step may be diffusion which is explained by the adsorption diffusion models (Qiu *et al.*, 2009).

Adsorption diffusion models describe how adsorbate molecules diffuse from the liquid phase onto the adsorbent surface (Qiu *et al.,* 2009). The diffusion models consist of the liquid film diffusion model and the intraparticle diffusion model, both of which describe the mass transfer in physical adsorption (Qiu *et al.*, 2009). Although both types of adsorption models describe the kinetics of adsorption, the reaction models derived from the kinetics of chemical reactions (pseudo-second order rate model)

provide a holistic approach of the adsorption process while the adsorption diffusion models provide specific mechanisms of adsorption.

2.4.4.2.4.   Adsorption isotherms

When the adsorbate and adsorbent are in contact for a sufficient amount of time at a constant temperature, an equilibrium is established where the adsorption sites on the adsorbent are filled and no more adsorbate molecules can be further adsorbed onto the surface of the adsorbent (Snyder, 1968). The equilibrium relationship between the amount (mg or g) of adsorbed molecules (known as the adsorption capacity, Q_e) and the concentration (mg/L or g/L) of the non-adsorbed molecules in the liquid phase (C_e), at a constant temperature, can be described by correlations known as adsorption isotherms (Snyder, 1968).

Giles *et al.* (1960) described four types of adsorption isotherms for liquid-solid adsorption which are referred to as the C, L, H and S isotherms respectively. The four types of isotherms describe the initial slope of adsorption. As the contact time between the adsorbate and adsorbent is increased, the isotherms plateau. The plateau indicates that all the adsorption sites have been occupied, and a complete monolayer on the surface of the adsorbent has been formed (Snyder, 1968; Limousin *et al.*, 2007). The different isotherms are shown in Figure 2-7.
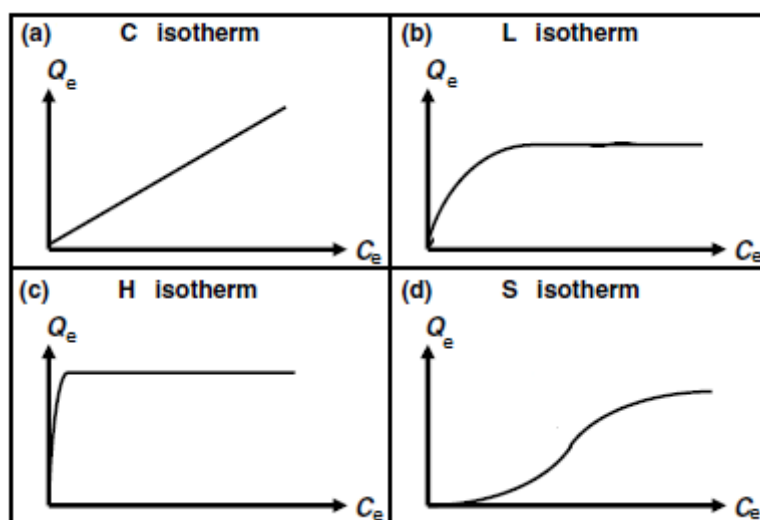
Figure 2-7. Adsorption isotherm types (Redrawn from Limousin *et al.* (2007), originally adapted from Giles *et al.* (1960) and Snyder (1968)). Q_e is the adsorption capacity while C_e is the non-adsorbed molecules in the liquid phase.

Adsorption isotherms are obtained through experiments. Once the experimental data has been obtained, adsorption isotherm model equations can then be fitted to correctly interpret the

28

experimental data. Modelling of the experimental data can then be used to determine the model that best describes the adsorption process, thus elucidating the behaviour of the adsorbate molecules in the system (Dabrowski, 2001).

The Langmuir isotherm model is described as the simplest theoretical model that is used to describe some adsorption systems that have been conducted experimentally (Snyder, 1968). The model was derived from adsorption kinetic studies (Dabrowski, 2001) and is mainly based on four assumptions: (1) The adsorbent surface is homogenous with a defined number of adsorption sites on the adsorbent surface with each adsorption site having the same amount of energy , (2) one molecule can bind per adsorption site with no interaction between adjacent molecules which (3) gives rise to a monolayer and lastly (4) the binding of molecules to the adsorption site may be through chemical or physical interactions without disrupting molecules that are already on the adsorption sites (Dabrowski, 2001; Limousin *et al.,* 2007).

Snyder (1968) explains that monolayer formation in solid-liquid adsorption systems is a common phenomenon which fulfils one of the Langmuir assumptions. This assumption holds true for adsorbents that have a homogeneous surface, i.e. there are distinct adsorption sites that are evenly distributed on the adsorbent surface. However, the adsorption surface of some adsorbents is heterogeneous, suggesting an uneven distribution of adsorption sites, with adsorbate molecules favouring certain adsorption sites over others. The adsorbent heterogeneity explains why certain solid-liquid systems cannot be explained by the Langmuir isotherm model and, since interactions between adjacent adsorbate molecules occurs in most adsorption systems, the Langmuir isotherm model does not hold (Snyder, 1968).

If an adsorption system fails to hold any of the Langmuir assumptions, the Langmuir isotherm model will not be able to interpret the adsorption system. However, the system may be explained by the Freundlich model (Snyder, 1968). The Freundlich model is an empirical model that can incorporate both monolayer and multilayer formation of the adsorbate molecules on the adsorbent surface (Limousin *et al.,* 2007; Dhanarajan *et al.,* 2015). The model assumptions are that (1) the adsorbent surface is heterogenous with an infinite number of adsorption sites, (2) each adsorption site has a different amount of energy and (3) adsorbate molecules interact by competing for adsorption sites (Limousin *et al.,* 2007)

2.5.   Conclusions

The deciduous fruit industry of South Africa is an important industry as it the largest exporter of deciduous fruits in the southern hemisphere (Forum, 2016). Enhancing the competitiveness of the fruit industry will ensure that the increasing demand for fruit consumption from a global perspective can be met. This need can be met, provided that the fruit quality is maintained throughout the global supply chain through the minimisation of fruit wastage and spoilage caused by fungal phytopathogens during postharvest storage.

A proposed innovative approach to replacing chemical fungicides as a postharvest disease management treatment is to use LPs produced by *Bacillus* species. A study conducted by Pretorius *et al.* (2015) identified *B. amyloliquefaciens* DSM 23117 as a potential biocontrol agent effective against fungal phytopathogens as the *Bacillus* species was identified as a strong producer of antifungal LPs.

Although *B. amyloliquefaciens* produces fengycin, iturin and surfactin in different ratios, the ultimate goal is to obtain a pure fengycin product without iturin and surfactin as the two LPs have haemolytic properties and would not be suitable for fruit application. Before a pure fengycin product can be obtained, several grey areas that exist in the purification programme of LPs have been highlighted in the literature review. These areas have led to research questions that motivated hypothesis formulation and ultimately hypothesis testing which motivated the research study.

Chapter 3

Research questions, hypotheses and objectives

The overall aim of the research study which was to develop an appropriate downstream concentration and purification programme for antifungal lipopeptides produced by *B. amyloliquefaciens* for application in postharvest disease management of fruit during storage. Through a thorough literature investigation several key questions have arisen, which when answered, provide information needed to achieve this aim.

3.1.   Research questions

The major concerns arising in the literature review led to these key questions that need to be addressed.

1.   When does *B. amyloliquefaciens* produce maximum antifungal LP (fengycin and iturin) concentration and selectivity (the ratio of antifungals to surfactin)?

2.   Which analytical techniques are suitable for the quantification of the LPs in each unit operation used?

3.   Is there a specific order in which unit operations need to be applied in the purification programme of antifungal LPs?

4.   What is the pH required for the complete precipitation of fengycin and iturin from the acidified cell-free supernatant?

5.   Which organic solvent(s) are best for the extraction of antifungal LPs and how are these solvents selected?

6.   What are the appropriate adsorption parameters for antifungal LP adsorption?
    6.1. What are the factors that affect LP adsorption?
    6.2. How will the optimal process conditions for LP adsorption be determined?
    6.3. Are there interactions and what type (if any) exist between the factors?
    6.4. What type of adsorption model will best describe the adsorption data obtained?

7. How effective will the partially purified and purified LP mixtures be on inhibiting filamentous fungal phytopathogens growth in *in vitro* studies and how will efficacy be quantified?

3.2.   Hypotheses

The following hypotheses have been put forward with regards to each of the key questions, and will be addressed in this study.

1. Optimal antifungal LP production by *B. amyloliquefaciens* is achieved during the stationary phase of growth.

2. High performance liquid chromatography (HPLC) is suitable for rigorous antifungal LP quantification while thin layer chromatography (TLC) is suitable for semi-quantitative antifungal LP quantification.

3. An efficient purification programme for *B. amyloliquefaciens* antifungal LPs involves unit operations that progressively increase the purity of the LPs.

4. Acidification of the cell-free supernatant to pH 2 is optimal for the precipitation of fengycin and iturin.

5. Polar organic solvents will extract maximum antifungal LPs due to the interaction with polar and/or charged amino acids in the LP cyclic peptide which determines the degree of LP solubility in the solvents.

6. The lipopeptide to resin ratio (LP/R), temperature and pH for optimal antifungal LP adsorption on HP-20 resin can be determined and the mechanism of fengycin and iturin adsorption elucidated.

7. Purified LP mixtures (from solvent extraction) have an enhanced effect on fungal phytopathogen growth inhibition compared to partially purified LP mixtures (from acid precipitation).

3.3.   Objectives

To test the hypotheses, the following objectives were pursued:

1. Set-up batch culture experiments in shake flasks to study the antifungal LP production kinetics which will be used to determine the optimal production and harvesting time of the LPs from the culture broth.

2. Quantify antifungal LPs in aqueous solutions via HPLC and antifungal LPs in organic solvents via TLC

3. Explore classical downstream unit operations including acid precipitation, solvent extraction and adsorption for improvement in the purity of antifungal LPs

4. Evaluate the effect of acidification of the cell-free supernatant to various pH values that are below 6.

5. Investigate the effect of organic solvent polarity on the extraction efficiency and purity of antifungal LPs as well as the effect of multiple extractions on the purity of antifungal LPs.

6. Optimise the main factors affecting adsorption (LP/Resin ratio, pH and temperature) using statistically designed experiments (central composite design), followed by adsorption kinetics and isotherms to explain the adsorption behaviour of antifungal LPs.

7. Conduct *in vitro* efficacy tests of the antifungal LPs of different purities (obtained from the different unit operations) on *Alternaria brassicicola*, *Aspergillus sclerotiorum*, *Botrytis cinerea*, *Monilinia fructigena*, *Penicillium expansum* and *Rhizopus stolonifera*, as the common fungal pathogens that affect deciduous fruit.

Chapter 4

Materials and Methods

4.1. Microorganism maintenance

4.1.1. Test organism

A lyophilized sample of *B. amyloliquefaciens* DSM 23117 was obtained from the Deutsche SammLung von Mikroorganismen und Zellkulturen (DSMZ) culture collection. The bacterium was isolated in Germany from soil that contained plant growth-associated microorganisms. The bacteria revival procedure involved adding 1 mL of nutrient broth that was sterilised (Speedy Autoclave HL-340, Gemmy Industrial Corp & Cannic, Inc.) for 15 min at 121°C to the freeze-dried sample, which was then incubated (Labcon Orbital Shaker Incubator) at 30°C for 30 min. Following the revival procedure, the revived bacteria in the nutrient broth solution were aseptically streaked onto nutrient agar plates using an inoculating loop. The streaked plates were incubated at 30°C for 16 h. After incubation, the streak plates were removed from the incubator and allowed to cool down to room temperature for 30 min before they were sealed with Parafilm and stored (upside down) at 4°C for further experiments. Streak plates were routinely prepared through sub-culturing every two months and were used for the short-term maintenance of the microorganism while 20% (v/v) glycerol stocks were prepared and stored at -18°C for the long-term maintenance of the microorganism.

4.1.2. Phytopathogenic fungi

Active cultures of the fungal pathogens, in the form of agar slants, were obtained from the DSMZ culture collection. The fungal species were common pathogens of fruit and plants and their characteristics are summarised in Table 4-1. From the agar slants, a small block of the agar containing mycelia was cut with a sterile bent inoculating loop and aseptically transferred onto potato dextrose agar (PDA) plates with the side containing the mycelium placed onto the centre of the PDA plate. The PDA plates were incubated for 4 – 5 days at 25°C. Following incubation, the PDA plates were removed from the incubator and allowed to cool down to room temperature for 30 min before they were sealed with Parafilm and stored (upside down) at 4°C for further experiments. The fungal pathogens were maintained on PDA plates at 4°C and were sub-cultured every six months to prolong the lifespan of the fungi which enabled the long-term storage of the pathogens.

Table 4-1. Phytopathogen characteristics

Strain	DSM no.	Source	Geographic origin
Alternaria brassicicola	62008	Plant	N/A
Aspergillus sclerotiorum	870, Type strain	Rotting fruit	United States of America (USA)
Botrytis cinerea	51451	Grape vine	Italy
Monilinia fructigena	2678	Pome fruit	United Kingdom (UK)
Penicillium expansum	62841	Rotting fruit	Germany
Rhizopus stolonifera	63011	Bread mould	Germany

4.2. Microorganism culture conditions

4.2.1. Inoculum preparation

The initial phase of growing *B. amyloliquefaciens* involved preparing an inoculum. The inoculum was prepared through the aseptic transfer of two loopfuls of the bacteria from the nutrient agar plate and into a sterile 500 mL unbaffled Erlenmeyer flask that contained 100 mL nutrient broth. The inoculated flask was incubated for 20 h at 30°C with agitation at 150 rpm.

4.2.2. Growth medium preparation

The growth medium used for *B. amyloliquefaciens*, shown in Table 4-2, was previously described by Pretorius *et al.* (2015) for LP production. The glucose was prepared and autoclaved separately from the other medium components to prevent chemical modification of the growth medium components through the formation of Maillard reaction products at high temperatures (autoclaving at 121°C for 15 min). The Maillard products have been reported to be produced when the free carbonyl (aldehyde) group of glucose reacts with amino acids (in the yeast extract) and salts in the medium resulting in a dark-brown coloured culture medium (Kim and Lee, 2003) which would result in a reduced initial glucose concentration which would impede the growth of the bacteria due to substrate and nutrient deprivation (Kim and Lee, 2003).

Table 4-2. Growth medium composition for lipopeptide production by *B. amyloliquefaciens*

Constituent	Concentration (g/L)
Glucose (anhydrous)	40
NH_4NO_3	4
Na_2HPO_4	7.098
KH_2PO_4	6.805
$MgSO_4.7H_2O$	0.322
$MnSO_4.H_2O$	0.0017
$FeSO_4.7H_2O$	0.002
$CaCl_2.2H_2O$	0.001
Yeast extract	0.05

To prepare 900 mL of growth medium; the nitrate, phosphate and magnesium salts were added into a 1 L Schott bottle. The yeast extract was added into the Schott bottle mixture followed by the addition of 900 mL of demineralised H_2O. The mixture was heated and stirred (ARE heating magnetic stirrer, VELP Scientifica®) at 70°C for 30 min. While the heating and stirring was taking place, the manganese, iron and calcium salts were made into 10 mL solutions containing 170 mg, 200 mg and 100 mg of each salt respectively. 0.1 mL of each solution was then added into the 900 mL solution which was further stirred until the components were completely mixed and the solution was a clear pale yellow colour (due to the yeast extract). 120 mL aliquots of this solution was distributed into 500 mL baffled Erlenmeyer flasks which were plugged with non-adsorbent cotton wool covered with aluminium foil.

In 50 mL conical centrifuge tubes (Falcon™), 6 g of glucose was added followed by 15 mL of demineralised H_2O. The Falcon tubes were plugged with non-adsorbent cotton wool and the mixture was heated (by microwave for approximately 2 min) which ensured that the glucose was completely dissolved. The Falcon tubes were then covered with aluminium foil. The plugged Falcon tubes and shake flasks were autoclaved for 15 min at 121°C. At room temperature, the glucose (15 mL) was aseptically transferred into a shake flask (containing 120 mL of nutrients) to make up the final growth medium with a volume of 135 mL.

4.2.3.   Test flask preparation

10% v/v (15 mL) of the inoculum was aseptically transferred into a sterile 500 mL baffled Erlenmeyer flask that contained 135 mL of growth medium. This flask was referred to as the test flask and it was used for further experimental studies.

4.3.   Experimental procedures

4.3.1.   Experimental design

A schematic representation of the experimental procedure is outlined in Figure 4-1. The study was composed of four sections. The first section focused on the production of LPs while the remaining three sections focused on the downstream purification of LPs which included acid precipitation, solvent extraction and adsorption. After the LPs were produced, the cell free supernatant was obtained from the culture broth. The culture broth was precipitated to obtain precipitate containing LPs. The LP acid precipitate was then subjected to solvent extraction and adsorption experiments respectively. Lipid and protein analysis was conducted on the LPs obtained after each unit operation application, and the same LPs were subjected to *in vitro* antifungal efficacy studies.
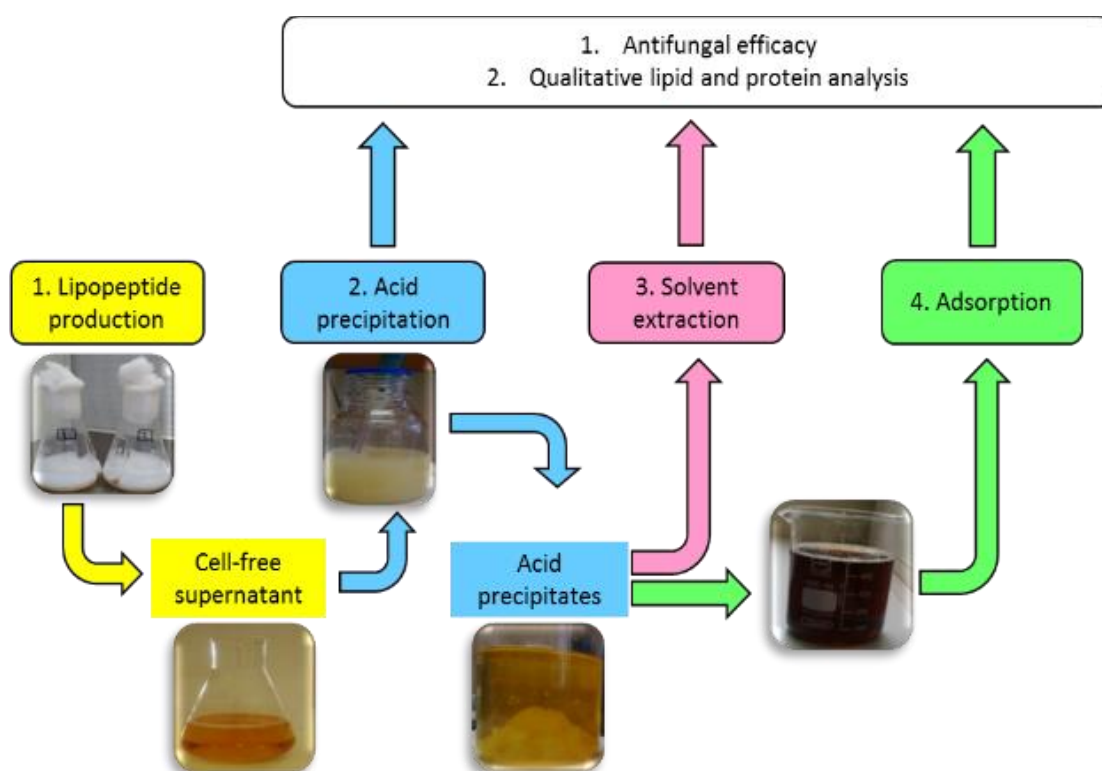
Figure 4-1. Experimental design flow diagram

4.3.2. Lipopeptide production and harvesting

To study the effect of predetermined downstream unit operations on the recovery and purity of antifungal LPs, a sufficient quantity of LPs was required to conduct the experiments. To produce sufficient LPs, the following experiments were performed.

Eight prepared test flasks were incubated at 30°C for 28 h with agitation at 150 rpm. Test flasks were prepared in triplicate and incubated with agitation at 150 rpm for 72 h at 30°C. To determine the time at which optimal fengycin and iturin (antifungal) LPs were produced, the cell, glucose, ammonium (NH_4^+) and nitrate (NO_3^-) concentrations were measured over time to establish the growth of the bacterium, the amount of LPs produced and the amount of glucose, NH_4^+ and NO_3^- used during the production of LPs. At defined time intervals during the incubation period, 2 mL samples of the culture were aseptically taken from the test flasks and transferred into 2 mL Eppendorf tubes. The samples were taken during times when the lag, early-exponential, mid-exponential, early-stationary and late-stationary phases of growth were observed. From the collected samples, the cell, glucose, NH_4^+, NO_3^- and LPs concentration was determined (section 4.4.1 - 4.4.4).

Following incubation, the culture broth was harvested at the optimum time and transferred to 50 mL Falcon tubes and centrifuged (model mrc CN-1860) for 25 min at 3 980 x g (6 000 rpm) which ensured that it was free of cells. LP production and harvesting was conducted continuously twice a week, concurrently with other downstream experiments.

4.3.3. Acid precipitation

To investigate the influence, if any, of different pH values on acid precipitation, it was necessary prepare precipitates at different pH values and then to characterise the precipitates in terms of LP recovery and purity, as well as the presence of residual impurities. The preparation of the precipitates and determination of the LP recovery and purity is detailed below.

4.3.3.1.   Preparation of acid precipitates

The cell-free culture supernatant was acidified to pH 2 (Metrohm 744 pH meter) through the drop-wise addition of 16% w/w HCl and the solution stored for 16 h at 4°C for complete precipitation. The off-yellow coloured acid precipitate (containing LPs with some impurities) was concentrated and recovered by centrifugation (Eppendorf 5702 R) at 2 900 x g (4 400 rpm) for 15 min. The supernatant was discarded while the acid precipitate (in the pellet) was stored in 50 mL Falcon tubes at -18°C until further experimental use.

Approximately 15 mL of the acid precipitates collected from production and harvesting (section 4.3.2) was oven-dried at 37°C for 2 days (Chen and Juang, 2008) until all the moisture was removed. The resulting dry acid precipitate was crushed into powder (using a pestle and mortar), weighed and stored in a 50 mL Falcon tube at -18°C.

4.3.3.2.   Characterisation of acid precipitates

Test flasks were prepared in triplicate and were incubated at 30°C for 28 h at 150 rpm. After incubation, the culture was transferred into 50 mL Falcon tubes and was centrifuged at 3 980 x g (6 000 rpm) for 20 min. The supernatant was separated from the biomass and was re-centrifuged in Eppendorf tubes for 5 min at 14 000 x g (14 500 rpm) to obtain a cell-free supernatant. 1.8 mL of the cell-free supernatant was individually transferred into three 2 mL Eppendorf tubes, from which samples were prepared for LP analysis by reverse-phase high performance liquid chromatography (RP-HPLC) to determine the initial LP concentration prior to acid precipitation (section 4.4.4.1).

From the remaining cell-free supernatant, 30 mL aliquots were distributed into 50 mL Falcon tubes that were oven-dried (Memmert) (24 h at 37°C), cooled in a desiccator and weighed to four decimal places. Duplicate experiments were conducted where the pH of the cell-free supernatant was adjusted to pH values 1, 2, 3 and 4 respectively, by adding drops of 16% w/w HCl. The Falcon tubes were then stored at 4°C for 16 h and the acid precipitate formed was collected by centrifugation at 2 900 x g (4 400 rpm) for 15 min. The supernatant after this centrifugation was discarded and the Falcon tube with the pellet was oven-dried at 37°C for 24 - 48 h. The Falcon tube with the pellet was weighed to four decimal places after 24 and 48 h of oven-drying to ensure that the mass obtained was constant. The mass of the dried acid precipitate pellet was obtained by subtracting the mass of the empty Falcon tube from the mass of the Falcon tube with the pellet.

10 mL alkaline demineralised H_2O (adjusted to pH 11 by the drop-wise addition of 2N NaOH) was used to dissolve the dried pellet. As the pellet was dissolving, the pH decreased, thus additional drops of 2N NaOH were added to maintain the solution at pH 8. The solution was incubated at 30°C with agitation at 150 rpm for two days until the pellet was re-dissolved. Following the two-day incubation, the solution was centrifuged for 15 min at 2 900 x g (4 400 rpm) to remove insoluble components (biomass, proteins, polysaccharides etc.). 1.8 mL of the supernatant from each pH value was individually transferred into three 2 mL Eppendorf tubes and samples prepared for LP analysis by RP-HPLC to determine the final LP concentration after acid precipitation (section 4.4.4.1).

To calculate the recovery of the LPs in the acid precipitates at the different pH values (appendix A, equation (1)), the mass of the LPs in the resolubilised acid precipitate in alkaline water [determined

from the LP concentration (by RP-HPLC) in the resolubilised acid precipitate and the volume of alkaline water used to resolubilse the acid precipitate] was divided by the mass of LPs in the cell-free supernatant prior to acid precipitation [determined from the concentration (by RP-HPLC) of LPs in the cell-free supernatant prior to acid precipitation and the volume of the cell-free supernatant]. The ratio of the fractional recovery thus calculated was multiplied by 100 to obtain the percentage recovery.

To calculate the purity of the LPs in the acid precipitates at the different pH values (appendix A, equation (2)), the mass of the LPs in the resolubilised acid precipitate in alkaline water [determined from the LP concentration (by RP-HPLC) in the resolubilised acid precipitate and the volume of alkaline water used to resolubilse the acid precipitate] was divided by the dry mass of the acid precipitate pellet. The fractional purity thus obtained was multiplied by 100 to obtain the percentage purity.

To determine the presence of residual impurities, qualitative protein and lipid analysis on all the samples was conducted in duplicate using TLC (section 4.4.5).

4.3.4.   Solvent extraction
To determine the efficiency of organic solvents in extracting maximum fengycin and iturin LPs, with relatively high recovery and purity percentages, several organic solvents of varying polarity indices were investigated.

4.3.4.1.   Preparation of solvent extracts
Solid extraction was carried out as previously described by Chen and Juang (2008) with modifications. In these experiments the acid precipitates, pre-dried in an oven at 37°C for 24 h and cooled in a desiccator to remove excess moisture, were used. All the experiments outlined were carried out in triplicate.

4.3.4.2.   Characterisation of solvent extracts

4.3.4.2.1.   One-stage extraction
To determine the LP concentration in the acid precipitate that was to be used for solvent extraction, 0.1 g dried precipitate was dissolved in 10 mL of alkaline demineralised H_2O adjusted to pH 8 by the drop-wise addition of 2N NaOH. The solution was agitated and incubated until the acid precipitate was completely dissolved. 1.5 mL of the dissolved acid precipitate was individually transferred into three 2 mL Eppendorf tubes and samples were prepared for LP analysis by thin layer chromatography (TLC) to determine the LP concentration (section 4.4.4.2).

To determine the LP concentration in the solvent extract, 0.1 g acid precipitate was added into 50 mL Falcon tubes and 20 mL of organic solvents of varying polarity indices (2.8 – 5.8), as shown in Table

4-3, were individually added into the Falcon tubes. The Falcon tubes were then tightly capped and incubated for 24 h with agitation at 150 rpm, after which the solution was centrifuged for 15 min at 2 900 x g (4 400 rpm) to separate the solvent extract from the solids that settled out. 1.5 mL of the solvent extract from each replicate was individually transferred into 2 mL Eppendorf tubes and the samples analysed by thin layer chromatography (TLC) (section 4.4.4.2) to determine the LP concentration.

To determine the mass of precipitate in the solvent extract, the remaining solvent extract was transferred into new 50 mL Falcon tubes and it was stored at -18°C, while the solids that settled out were oven-dried at 37°C for 48 h and weighed to four decimal places after 24 and 48 h to ensure that the mass obtained was constant. The difference in mass between the empty Falcon tube and the Falcon tube containing the solids that settled out was calculated which provided the mass of the solids that settled out. The mass of the solids that settled out was then subtracted from the mass of the acid precipitate initially added (0.1 g) to give the mass of acid precipitate that was in the solvent extract.

Table 4-3. Organic solvents used for antifungal lipopeptide extraction

No.	Solvent	Polarity index	Boiling point (°C)
1	Acetonitrile	5.8	81.6
2	Ethanol	5.2	78.5
3	Methanol	5.1	64.6
4	Acetone	5.1	56.2
5	Ethyl acetate-methanol (2:1, v/v)	4.8*	70.8*
6	Chloroform-methanol (2:1, v/v)	4.6*	69.4*
7	Ethyl acetate	4.4	77
8	Chloroform	4.1	61.7
9	Isopropanol	3.9	82.4
10	1-Octanol	3.2	195
11	Diethyl ether	2.8	34.6

Polarity indices based on Snyders' polarity index. * Average polarity indices and boiling points

It was discovered that methanol extracted all the LPs in the acid precipitate as the concentration of LPs in the methanol extract was similar to the concentration of LPs in alkaline demineralised H_2O,

therefore the concentration of LPs in the methanol extract represented the total LPs extracted from the acid precipitate. Thus, to calculate the recovery of LPs in the solvent extract (appendix A, equation (3)), the mass of LPs in the solvent extract [determined from the product of the LP concentration (by TLC) in the solvent extract and the volume of organic solvent used to dissolve the acid precipitate] was divided by the mass of LPs in the methanol extract [determined from the product of the LP concentration (by TLC) in the methanol extract and the volume of methanol used to dissolve the acid precipitate]. The fractional recovery thus calculated was multiplied by 100 to obtain the percentage recovery.

To calculate the purity of LPs in the solvent extract (appendix A, equation (4)), the mass of LPs in the solvent extract [determined from the product of the LP concentration (by TLC) in the solvent extract and the volume of organic solvent used to dissolve the acid precipitate] was divided by the mass of acid precipitate in the solvent extract [determined by subtracting the mass of the solids that settled out from the mass of the acid precipitate initially added (0.1 g)]. The fractional purity thus obtained was multiplied by 100 to obtain the percentage purity.

To determine the presence of residual impurities, qualitative protein and lipid analysis on all the samples was conducted in duplicate using TLC (section 4.4.5).

4.3.4.2.2.   Three-stage extraction

To improve the purity of LPs, a three-stage solvent extraction procedure was conducted, using methanol and diethyl ether separately. Two extraction strategies that were used are described as outlined below.

4.3.4.2.2.1.   Three-stage methanol extraction

The experimental design of the three-stage methanol extraction procedure is shown below in Figure 4-2.
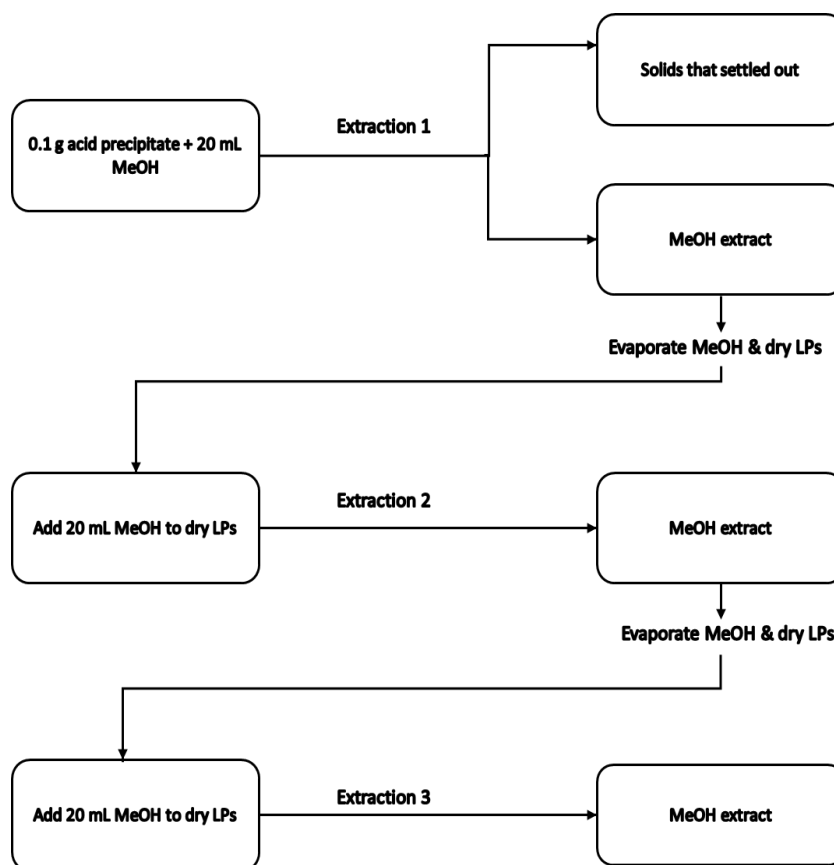
Figure 4-2. Three-stage lipopeptide extraction procedure using methanol

0.1 g acid precipitate was added into Falcon tubes after which 20 mL of methanol was then added. The Falcon tubes were then tightly capped and incubated for 24 h at 150 rpm agitation, after which, the solution was centrifuged for 15 min at 2 900 x g (4 400 rpm) to separate the solids that settled out from the solvent extract. 1.5 mL of the methanol extract from each replicate was transferred into 2 mL Eppendorf tubes and the concentration of LPs in the methanol extract determined by TLC analysis (section 4.4.4.2).

The remaining methanol extract was transferred into new Falcon tubes and the methanol evaporated in a 100°C water bath for approximately 10 min, so that the LPs in the methanol extract remained in the Falcon tube. The methanol was evaporated in preparation for the next extraction step. The Falcon tubes were oven-dried at 37°C for 48 h and weighed to four decimal places after 24 and 48 h to ensure that the mass obtained was constant.

The solids that settled out were oven-dried at 37°C for 48 h and weighed to four decimal places after 24 and 48 h to ensure that the mass obtained was constant. The difference in mass between the empty Falcon tube and the Falcon tube containing the solids that settled out was calculated which provided

the mass of the solids that settled out. The mass of the solids that settled out was then subtracted from the mass of the acid precipitate initially added (0.1 g) to give the mass of acid precipitate that was in the solvent extract. This represented the first stage extraction step (as in section 4.3.4.2.1) from which the recovery and purity percentage was then determined as in section 4.3.4.2.1 (appendix A, equation (3) and (4) respectively).

In Falcon tubes containing the dried LP extracts obtained from the first extraction, 20 mL methanol was added. The Falcon tubes were tightly capped and incubated for 24 h at 150 rpm agitation. Since there were no solids that settled out, 1.5 mL of the methanol extract from each replicate was transferred into 2 mL Eppendorf tubes and the concentration of LPs in the methanol extract was determined by TLC analysis. The methanol in the methanol extract was evaporated in a 100°C water bath so that the LPs in the methanol extract remained in the Falcon tube. The Falcon tubes were oven-dried at 37°C for 48 h and weighed to four decimal places after 24 and 48 h to ensure that the mass obtained was constant. This represented the second extraction step and the recovery and purity percentage was then determined as in section 4.3.4.2.1 (appendix A, equation (3) and (4) respectively).

In the Falcon tubes containing the dried LP extracts obtained from the second extraction, 20 mL methanol was added. The Falcon tubes were tightly capped and incubated for 24 h at 150 rpm agitation after which 1.5 mL of the methanol extract from each replicate was transferred into 2 mL Eppendorf tubes and the concentration of LPs in the methanol extract determined by TLC analysis. The methanol in the methanol extract was evaporated in a 100°C water bath so that the LPs in the methanol extract remained in the Falcon tube. The Falcon tubes were oven-dried at 37°C for 48 h and weighed to four decimal places after 24 and 48 h to ensure that the mass obtained was constant. This represented the third extraction step and recovery and purity percentage was then determined as in section 4.3.4.2.1 (appendix A, equation (3) and (4) respectively).

4.3.4.2.2.2.   Three-stage diethyl ether-methanol extraction

The experimental design of the three-stage diethyl ether-methanol extraction procedure is shown below in Figure 4-3.
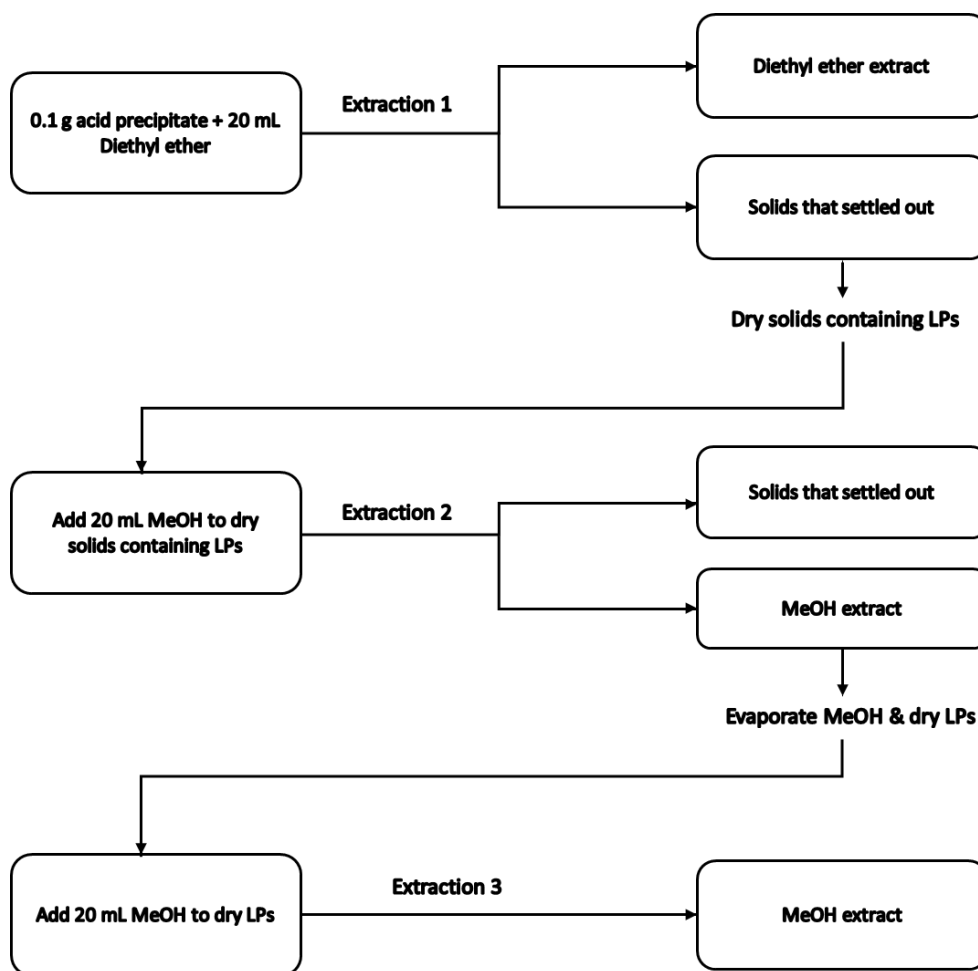
Figure 4-3. Three-stage lipopeptide extraction procedure using diethyl ether-methanol.

The dried acid precipitate was added into Falcon tubes after which 20 mL of diethyl ether was then added. The Falcon tubes were tightly capped and incubated or 24 h at 150 rpm agitation after which, the solution was centrifuged for 15 min at 2 900 x g (4 400 rpm) to separate the solids that settled out from the solvent extract. 1.5 mL of the diethyl ether extract from each replicate was transferred into 2 mL Eppendorf tubes and the concentration of LPs in the diethyl ether extract determined by TLC analysis (section 4.4.4.2). The remaining diethyl ether extract was transferred into new 50 mL Falcon tubes and it was stored at -18°C. The diethyl ether extract contained surfactin (as determined from section 4.3.4.2.1), while the solids that settled out contained fengycin, thus the solids that settled out were oven-dried at 37°C for 48 h and weighed to four decimal places after 24 and 48 h to ensure that the mass obtained was constant.

The difference in mass between the empty Falcon tube and the Falcon tube containing the solids that settled out was calculated which provided the mass of the solids that settled out. The mass of the solids that settled out was then subtracted from the mass of the acid precipitate initially added (0.1 g)

to give the mass of acid precipitate that was in the diethyl ether extract. This represented the first stage extraction step (as in section 4.3.4.2.1) from which the recovery and purity percentage was then determined as in section 4.3.4.2.1 (appendix A, equation (3) and (4) respectively).

In the Falcon tubes containing the solids that settled out (obtained from the first extraction), 20 mL methanol was added. The Falcon tubes were tightly capped and incubated for 24 h at 150 rpm agitation, after which the solution was centrifuged for 15 min at 2 900 x g (4 400 rpm) to separate the solids that settled out from the solvent extract. 1.5 mL of the methanol extract from each replicate was transferred into 2 mL Eppendorf tubes and the concentration of LPs in the methanol extract determined by TLC analysis. The remaining methanol extract was transferred into new Falcon tubes and the methanol evaporated in a 100°C water bath so that the LPs in the methanol extract remained in the Falcon tube. The Falcon tubes were oven-dried at 37°C for 48 h and weighed to four decimal places after 24 and 48 h to ensure that the mass obtained was constant.

The difference in mass between the empty Falcon tube and the Falcon tube containing the solids that settled out was calculated which provided the mass of the solids that settled out. The mass of the solids that settled out was then subtracted from the mass of the acid precipitate initially added (0.1 g) to give the mass of acid precipitate that was in the methanol extract. This represented the second extraction step from which the recovery and purity percentage was then determined as in section 4.3.4.2.1 (appendix A, equation (3) and (4) respectively).

In the Falcon tubes containing the dried LP extracts obtained from the second extraction, 20 mL methanol was added. The Falcon tubes were tightly capped and incubated after which 1.5 mL of the methanol extract from each replicate was transferred into 2 mL Eppendorf tubes and the concentration of LPs in the methanol extract determined by TLC analysis. The methanol in the methanol extract was evaporated in a 100°C water bath so that the LPs in the methanol extract remained in the Falcon tube. The Falcon tubes were oven-dried at 37°C for 48 h and weighed to four decimal places after 24 and 48 h to ensure that the mass obtained was constant. This represented the third stage extraction step from which the recovery and purity percentage was then determined as in section 4.3.4.2.1 (appendix A, equation (3) and (4) respectively).

In the Falcon tubes containing the dried LP extracts obtained from the third extraction, 20 mL of demineralised alkaline water adjusted to pH 8 was added to resolubilise the methanol and diethyl ether-methanol extracts. The Falcon tubes were tightly capped and incubated at 30°C for 24 h after which they were stored at -18°C for use in antifungal efficacy studies (section 4.3.6).

4.3.5. Adsorption

To further improve the recovery and purity of fengycin and iturin, the optimal adsorption conditions of these LPs on a macroporous resin was investigated.

4.3.5.1.   Preparation of batch adsorption equilibrium experiments

4.3.5.1.1.   Preparation of resolubilised acid precipitates

In a 1 L beaker, acid precipitate ($\sim$ 20 mL) collected after acid precipitation after production and harvesting (section 4.3.2), was re-dissolved in 400 mL demineralised alkaline H_2O (pH was adjusted to 8) and the solution was stirred for 40 min while maintaining the pH of the solution at pH 8. As the precipitate re-dissolved in the alkaline water, the pH reduced and thus an additional 108 mL of 2N NaOH was added dropwise to maintain the pH at 8 (final volume of solution 508 mL). When the pH remained constant at pH 8 after 40 min, the solution was centrifuged at 14 000 x g (14 500 rpm) for 5 min to remove un-dissolved components such as biomass, to obtain resolubilised acid precipitate. 1.8 mL of the resolubilised acid precipitate was transferred into 2 mL Eppendorf tubes and the initial LP concentration was analysed by RP-HPLC (section 4.4.4.1). The remaining resolubilised acid precipitate was transferred into 50 mL Falcon tubes and stored at -18°C until batch adsorption experiments were conducted.

4.3.5.1.2.   Macroporous resin preparation

The polymeric Diaion HP-20 macroporous resin (Supelco, M & M Industries, Inc.) was used for adsorption experiments. The physical characteristics of the resin are shown in Table 4-4. Prior to use, the resin was pre-treated to remove impurities that may have been trapped inside the pores during the manufacturing process of the resin. 50 g of the resin was placed into a 1 L unbaffled Erlenmeyer flask and 280 mL of 95% (v/v) ethanol was added to the resin. The flask was plugged with cotton wool and sealed with Parafilm to ensure that the ethanol did not evaporate. The flask was then incubated at 30°C with shaking at 150 rpm for 24 h. The ethanol was decanted and the residual ethanol was evaporated from the resin by placing the flask in a 100°C water bath. The resin was then transferred into a 500 mL beaker and dried in an oven at 45°C for 2 days. Subsequent to the 2 day drying process, the beaker containing the resin was sealed with aluminium foil and placed in a desiccator until experimental use.

Table 4-4. HP-20 resin specifications

Resin properties	
Matrix	Styrene-divinylbenzene
Polarity	Non-polar
Pore size volume	$\sim$ 1.3 mL/g
Particle size	250 – 850 μm
Surface area	$\sim$ 500 m^2/g
Maximum operating temperature	130°C

4.3.5.1.3.   Statistical design of batch adsorption experiments

The pH, temperature and lipopeptide to resin (LP/R) ratio were identified, from literature, as three main factors that affected adsorption and as such, the optimal conditions for maximum LP adsorption on HP-20 macroporous resin were investigated through the optimisation of these factors using a response surface methodology (RSM) design. Since RSM designs consisted of three types of central composite designs (CCDs), a rotatable design with five levels (-1.682, -1, 0, 1, 1.682) was used as each factor had five levels and the limits of each factor were specified. The levels of each factor were selected based on values reported in literature (Chen *et al.*, 2008; Wang *et al.,* 2010; Dhanarajan *et al.,* 2015). The selected pH values ranged from pH 7 – 11 while the temperature ranged from 27 – 43°C. The ratio of LP/R range was selected to be 0.05 – 0.6 as the optimal LP/R ratio was calculated to be 0.3 ($\frac{3\ g/L}{10\ g/L}$) for LPs adsorbed on HP-20 resin (Dhanarajan *et al.,* 2015), thus 0.3 was the basis for the LP/R ratio range.

The experiments were designed with STATISTICA 13.2 with the fengycin design matrix illustrated in Table 4-5. The design enabled combinations of the different levels of each factor to be tested. The experimental runs were conducted randomly in triplicate with a total of 48 experimental runs including six centre point runs. Similar design matrices for iturin and surfactin were also determined with variation in the LP/R ratio.

Table 4-5. Design matrix of a rotatable central composite design (CCD) for fengycin

Standard run	Factors			Response	
	LP/R (g/g)	Temperature (°C)	pH	% Adsorption	Q_e
1	0.2	30	8		
2	0.2	30	10		
3	0.2	40	8		
4	0.2	40	10		
5	0.5	30	8		
6	0.5	30	10		
7	0.5	40	8		
8	0.5	40	10		
9	0.05[*]	35	9		
10	0.6[*]	35	9		
11	0.3	27[*]	9		
12	0.3	43[*]	9		
13	0.3	35	7[*]		
14	0.3	35	11[*]		
15	0.3[#]	35[#]	9[#]		
16	0.3[#]	35[#]	9[#]		

LP/R: lipopeptide to resin ratio, Q_e: adsorption capacity, *: The extremes of each level called star-points and #: median of each factor called the centre-points

To obtain the various LP/R ratios, the LP concentration was varied while the resin concentration was kept constant at 5 g/L (0.1 g) as shown in Table 4-6 – Table 4-8. The total LP concentration was determined by RP-HPLC to be 5.7 g/L, from which the initial concentration of each LP was determined assuming a constant ratio of 0.7, 0.2 and 0.1 for fengycin, iturin and surfactin respectively.

Table 4-6. Fengycin to resin (LP/R) concentration ratio CCD specifications

Resin concentration: 5 (g/L)			Total fengycin concentration: 4 g/L		
$\frac{LP\ (g)}{R\ (g)}$	$\frac{0.005}{0.1}$	$\frac{0.02}{0.1}$	$\frac{0.03}{0.1}$	$\frac{0.05}{0.1}$	$\frac{0.06}{0.1}$
Ratio	0.05	0.2	0.3	0.4	0.6
LP (g/L)	0.25	1	1.5	2.5	3
LP stock (mL)	1.25	5	7.5	12.5	15
Buffer	18.75	15	12.5	7.5	5
Dilution	16x	4x	2.6x	1.6x	1.3x

Table 4-7. Iturin to resin (LP/R) concentration ratio CCD specifications

Resin concentration: 5 (g/L)			Total iturin concentration: 1 g/L		
$\frac{LP\ (g)}{R\ (g)}$	$\frac{0.00126}{0.1}$	$\frac{0.005}{0.1}$	$\frac{0.008}{0.1}$	$\frac{0.0126}{0.1}$	$\frac{0.016}{0.1}$
Ratio	0.0126	0.05	0.08	0.126	0.16
LP (g/L)	0.063	0.25	0.4	0.63	0.8
LP stock (mL)	1.25	5	7.5	12.5	15
Buffer	18.75	15	12.5	7.5	5
Dilution	16x	4x	2.6x	1.6x	1.3x

Table 4-8. Surfactin to resin (LP/R) concentration ratio CCD specifications

Resin concentration: 5 (g/L)		Total surfactin concentration: 0.7 g/L			
LP (g)	0.0008	0.0035	0.00538	0.00875	0.01076
R (g)	0.1	0.1	0.1	0.1	0.1
Ratio	0.008	0.035	0.0538	0.0875	0.1076
LP (g/L)	0.044	0.2	0.3	0.44	0.54
LP stock (mL)	1.25	5	7.5	12.5	15
Buffer	18.75	15	12.5	7.5	5
Dilution	16x	4x	2.6x	1.6x	1.3x

4.3.5.1.4. Preliminary batch adsorption equilibrium tests

Prior to commencement of the statistically designed experiments, preliminary tests were conducted where 20 mL of the resolubilised acid precipitate (0.4 - 2 g/L at ± pH 8) was added into 100 mL unbaffled Erlenmeyer flasks which contained 0.1 g resin. The flasks were plugged with cotton wool and incubated at 35°C and 45°C respectively for 26 h, a time which was assumed to be sufficient for equilibrium to be reached by, based on literature. It was observed that on the onset of 18 h of incubation, the LP resolubilised acid precipitate changed from clear to murky due to contamination by gram positive bacteria which was confirmed by the gram stain, endospore test and nutrient agar spread plates (methodologies detailed in appendix C, no. 1 - 3). To prevent further contamination of experiments, all equipment used was sterilised for 15 min at 121°C and flasks were prepared aseptically. The preliminary tests also revealed that even when the experiments were free from bacterial contamination, the pH of the solution declined by 0.3 – 1 pH units, particularly at 45°C, which necessitated the use of a 0.1M phosphate buffer or a 0.1M bicarbonate-carbonate buffer solution (preparation of buffers detailed in appendix C, no. 4, Table 0-3 and Table 0-4) to maintain the solution at the desired pH.

To ensure that the adsorption system had reached equilibrium and that the non-adsorbed LPs in the liquid phase (C_e) collected at 24 h were at equilibrium with the resin, preliminary adsorption kinetic tests were also investigated (see section 4.3.5.2.3). All adsorption experiments were conducted in triplicate.

4.3.5.2.   Characterisation of batch adsorption equilibrium experiments

4.3.5.2.1.   Batch adsorption optimisation

In a 100 mL unbaffled sterile Erlenmeyer flask, 0.1 g resin of HP-20 resin was aseptically added into the flask. In a separate beaker, an aliquot of the resolubilised acid precipitate was diluted with a buffer of the desired pH, to make up a final volume of 20 mL of the desired initial LP concentration. The resolubilised acid precipitate was then aseptically filter sterilised (using a 0.22 µm syringe filter) into the flask containing the resin. The flask was plugged with sterile non-adsorbent cotton wool, sealed with Parafilm and incubated at the desired temperature for 24 h with shaking at 150 rpm. The incubation period ensured that equilibrium was reached within 24 h (data shown in appendix C, no. 5). 1.8 mL of the non-adsorbed LPs in the liquid phase at 24 h, from each replicate, was aseptically transferred into 2 mL Eppendorf tubes and the concentration of LPs was determined by RP-HPLC (section 4.4.4.1).

The adsorption capacity (Q_e) and percentage adsorption was calculated for each experimental condition (appendix A, equations (5) and (6) respectively) with the LP concentration determined by RP-HPLC in all batch adsorption and desorption experiments.

Q_e represented the mass of LPs adsorbed per mass of the resin at equilibrium. To calculate Q_e, the concentration of non-adsorbed LPs in the liquid phase (C_e in g/L) was subtracted from the initial LP concentration (C_o in g/L), to obtain the concentration (g/L) of the LPs adsorbed on the resin. The concentration of LPs adsorbed was multiplied by the volume (V in L) of resolubilised acid precipitate used to obtain the mass of LPs adsorbed on the resin. The mass of adsorbed LPs was then divided by the mass of resin (M in g) added to obtain Q_e.

The percentage of LPs adsorbed at equilibrium, at the various experimental conditions, was calculated by subtracting the non-adsorbed LPs in the liquid phase (C_e) from the initial LP concentration (C_o in g/L) to obtain the concentration of adsorbed LPs. The concentration of adsorbed LPs was divided by the initial LP concentration (C_o in g/L), to give the fractional concentration of adsorbed LPs. The fractional concentration of adsorbed LPs was multiplied by 100 to obtain the percentage adsorption.

The design matrix, with the calculated response variables (Q_e) and percentage adsorption), was then entered into STATISTICA 13.2, after which the design was analysed, and the optimal pH, temperature and LP/R ratio obtained through ANOVA, effect estimates, pareto chart and surface plot analysis.

4.3.5.2.2. Lipopeptide purity at optimal batch adsorption conditions

Once the optimal batch adsorption conditions were determined, the purity of the adsorbed LPs was also determined. 20 mL of the optimal LP concentration was placed into a 50 mL pre-dried (in an oven for 24 h at 40°C and cooled in a desiccator) and pre-weighed (to four decimal places) Falcon tube. The alkaline demineralised H_2O and buffer solution making up the resolubilised acid precipitate was evaporated in a 100°C water bath, leaving LPs in the Falcon tubes. The remaining LPs in the Falcon tubes were oven-dried at 37°C for 48 h and weighed to four decimal places after 24 and 48 h to ensure that the mass obtained was constant. The mass obtained represented the initial LP mass prior to adsorption.

In a 100 mL unbaffled sterile Erlenmeyer flask, 0.1 g resin of HP-20 resin was aseptically added into the flask. In a separate flask, an aliquot of the resolubilised acid precipitate was diluted with an appropriate buffer at the optimal pH to make up a final volume of 20 mL of the optimal LP concentration. The flask was plugged with sterile non-adsorbent cotton wool and sealed with Parafilm after which it was incubated at the appropriate temperature with shaking at 150 rpm. After a 24 h incubation, the non-adsorbed LPs in the liquid phase were transferred into new pre-dried (in an oven for 24 h at 40°C and cooled in a desiccator) and pre-weighed (to four decimal places) 50 mL Falcon tubes. The alkaline demineralised H_2O and buffer solution making up the resolubilised acid precipitate was evaporated in a 100°C water bath after which the LPs in the Falcon tube were oven-dried at 37°C for 48 h and weighed to four decimal places after 24 and 48 h to ensure that the mass obtained was constant. The mass obtained represented the final LP mass after adsorption.

The final LP mass after adsorption was subtracted from the initial LP mass before adsorption to obtain the total mass of adsorbed LPs. To calculate the purity of adsorbed LPs (appendix A, equation (7)), the concentration of non-adsorbed LPs in the liquid phase at equilibrium (determined by RP-HPLC) was subtracted from the initial LP concentration (determined by RP-HPLC) to obtain the concentration of adsorbed LPs. The concentration of adsorbed LPs was multiplied by the volume of resolubilised acid precipitate used, to obtain the mass of adsorbed LPs. The mass of adsorbed LPs was divided by the total mass of adsorbed LPs, to give the fractional mass of adsorbed LPs. The fractional mass was multiplied by 100 to obtain a percentage purity.

4.3.5.2.3. Adsorption kinetics

It was essential to describe the adsorption kinetics of LPs adsorbed onto the HP-20 resin as this would give insight into the rate limiting mechanism of fengycin and iturin (Qiu *et al.*, 2009). Preliminary adsorption kinetic tests were conducted to ensure that within the 24 h incubation period, equilibrium had been reached (data shown in appendix C, no. 5).

In a 100 mL unbaffled sterile Erlenmeyer flask, 0.1 g of HP-20 resin was aseptically added into the flask. In a separate flask, an aliquot of the resolubilised acid precipitate was diluted with an appropriate buffer at pH 9 to make up a final volume of 20 mL of the desired initial LP concentration. The flask was plugged with sterile non-adsorbent cotton wool and sealed with Parafilm and was incubated at 30°C with shaking at 150 rpm. At 2 h time intervals, 200 µl of non-adsorbed LPs in the liquid phase were aseptically pipetted and transferred into 1.5 mL Eppendorf tubes and the concentration of LPs at time t determined by RP-HPLC (section 4.4.4.1). Throughout the sampling duration, no more than a total of 10% of the liquid phase was taken to ensure that the remaining solution in the flask was representative of the adsorption system. When the optimal LP/R ratio, temperature and pH were obtained (CCD and isotherm experiments), adsorption kinetic experiments were conducted under the optimal conditions obtained.

The adsorption capacity (Q_t) at time t and adsorption percentage at each time interval was calculated using equations 9 and 6 in appendix A respectively. Q_t represented the mass of LPs adsorbed per mass of resin at time t. To calculate Q_t at a given time interval, the concentration of non-adsorbed LPs in the liquid phase (C_e in g/L) at time t was subtracted from the initial LP concentration (C_o in g/L) to obtain the concentration (g/L) of the LPs adsorbed on the resin. The concentration of LPs adsorbed was multiplied by the volume (V in L) of the resolubilised acid precipitate used, to obtain the mass of LPs adsorbed onto the resin. The mass of adsorbed LPs was then divided by the mass of resin (M in g) initially added to obtain Q_t.

The % adsorption at time t was calculated by subtracting the non-adsorbed LPs in the liquid phase (C_t) from the initial LP concentration (C_o in g/L) to obtain the concentration of adsorbed LPs. The concentration of adsorbed LPs was divided by the initial LP concentration (C_o in g/L), to give the fractional concentration of adsorbed LPs. The fractional concentration of adsorbed LPs was multiplied by 100 to obtain the percentage adsorption.

To better understand the adsorption kinetics of LPs adsorbed onto the HP-20 resin, pseudo-first-order and pseudo-second-order models (appendix A, equation (10) and (11) respectively) were used to determine the kinetic model that best represented the adsorption process and behaviour of LPs on HP-20 resin.

4.3.5.2.4. Adsorption isotherms

To study the process of adsorption, graphs that are known as adsorption isotherms were used to evaluate the amount of LPs adsorbed on HP-20 macroporous resin at equilibrium. The adsorption isotherm graphs described the relationship between the adsorption capacity (Q_e) and the

concentration of non-adsorbed LPs in the liquid phase (C_e) at equilibrium at a constant temperature and pH.

The LP concentration was varied while the resin concentration was kept constant at 0.1 g. In a 100 mL sterile unbaffled Erlenmeyer flask, 0.1 g of HP-20 resin was aseptically added into the flask. In a separate flask, an aliquot of the resolubilised acid precipitate was diluted with a buffer at the optimal pH (from CCD experiments) to make up a final volume of 20 mL of the desired initial LP concentration. The LP concentrations investigated ranged between 1 – 5 g/L fengycin, 0.25 – 1.25 g/L iturin and 0.2 – 0.88 g/L for surfactin which resulted in LP/R ratio ranges of 0.2 – 1, 0.05 – 0.25 and 0.02 – 0.18 for fengycin, iturin and surfactin respectively. The LP solution was aseptically filter sterilised (using a 0.22 μm syringe filter) into the flask containing the resin. The flask, plugged with sterile non-adsorbent cotton wool and sealed with Parafilm) was incubated at the optimal temperature (determined from CCD experiments) for 24 h with shaking at 150 rpm. 1.5 mL of the non-adsorbed LPs in the liquid phase at 24 h was aseptically transferred into 2 mL Eppendorf tubes and the concentration of LPs was determined by RP-HPLC (section 4.4.4.1). The adsorption capacity at equilibrium (Q_e) and percentage adsorption was calculated for each isotherm experiment as described in section 4.3.5.2.1 with equations (5) and (6) (appendix A).

The experimental data obtained were then fitted to Langmuir and Freundlich isotherm models (appendix A, equation (12) and (13) respectively) to determine which model best represented the adsorption process and behaviour of LPs on the HP-20 resin. The models were first linearized to obtain the adsorption parameters and the correlation coefficient (R^2) value which indicated how well the model fitted the data.

4.3.5.3.   Characterisation of batch desorption equilibrium experiments

To study LP desorption, 0.1 g of HP-20 resin was aseptically added into a sterile 100 mL unbaffled Erlenmeyer flask. In a separate flask, an aliquot of the resolubilised acid precipitate was diluted with a buffer at the optimal pH to make up a final volume of 20 mL of the optimal LP concentration determined from CCD experiments. The LP solution was aseptically filter sterilised (using a 0.22 μm syringe filter) into the flask containing the resin. The flask, plugged with sterile non-adsorbent cotton wool and sealed with Parafilm, was incubated at the optimal temperature (determined from CCD experiments) for 24 h with shaking at 150 rpm. After 24 h, the resin beads and the liquid phase was separated through filtering and the saturated resin beads oven dried at 37°C for 48 h. The resin beads were added into 100 mL unbaffled Erlenmeyer flasks that contained 20 mL of methanol that was adjusted through the dropwise addition of 2N NaOH to pH values 8, 9 and 10 respectively. Desorption was then carried out at the optimal temperature with shaking at 150 rpm for 24 h after which the LPs

in the desorption solution was analysed by RP-HPLC (section 4.4.4.1). The percentage desorption was then calculated (appendix A, equation (8)). The concentration of LPs in methanol was multiplied by the volume of methanol used to give the mass of LPs in methanol. The mass of LPs in methanol was then divided by the mass of LPs adsorbed on the resin to give the fractional mass of LPs desorbed. The fractional mass of LPs desorbed was multiplied by 100 to obtain the percentage desorption.

4.3.6. *In vitro* antifungal efficacy

Antifungal efficacy tests were based on the method adapted from Chen *et al.* (2016) with modification. Prior to antifungal efficacy experiments, preliminary tests were conducted to determine the temperature at which all the phytopathogens grew optimally. All phytopathogens were grown on PDA plates and were incubated at room temperature (20°C ± 3°C) and 30°C separately for 5 days. The growth of the phytopathogens at both temperatures was compared after 5 days and it was determined that *A. brassicicola*, *A. sclerotiorum* and *M. fructigena* grew well at 30°C while *B. cinerea*, *P. expansum* and *R. stolonifera* grew well at room temperature (20°C ± 3°C).

4.3.6.1. Control plate preparation

The six phytopathogens were individually sub-cultured on freshly prepared PDA plates. The back end of a sterile 1 mL pipette tip (10 mm) was used to cut an actively growing fungal plug (towards the border of the plate) from a previously cultured PDA plate. The side of the fungal plug containing the fungus was placed on the centre of a new PDA plate. The plate was incubated for 5 days at the optimal temperature. At the end of the 5-day incubation period; the diameter of fungal growth was measured. The diameter of the fungal plug (10 mm) was subtracted from the diameter of fungal growth and this represented the extent of fungal growth in the control plate (D_c). For fungal phytopathogens that did not grow radially (*M. fructigena, P. expansum* and *R. stolonifera)*, instead of using the diameter as a measure of growth, the area of fungal growth was used instead where the area was measured by scanning the plate and the resulting image edited with ImageJ software (appendix C) to determine the area (mm^2) of the fungal plug and area of fungal growth that covered the PDA plate. The area of the 10 mm fungal plug was subtracted from the area of fungal growth and this represented the area of fungal growth in the control plate (D_c). Plates were prepared in triplicate for each fungal species.

4.3.6.2. Test plate preparation

The cell-free supernatant (prior to acid precipitation), resolubilised acid precipitate, methanol extract in water and diethyl ether-methanol extract in water (from third-stage extraction step) were used in

the preparation of the test plates. Prior to use, the solutions were separately aseptically filter sterilised with a 0.22 μm membrane into sterile 2 mL Eppendorf tubes.

Working with one solution at a time, 100 μl aliquot was aseptically spread (with a sterile glass rod) on a prepared PDA plate. The plate was incubated at 25°C for 2 h to allow the solution to diffuse throughout the plate, after which a 10 mm actively growing fungal plug was placed on the centre of the PDA plate with the side containing the fungus placed on the agar surface. The plate was incubated again at the optimal phytopathogen temperature for 5 days and at the end of the five-day incubation period, the diameter of fungal growth was measured with a ruler. The diameter of the fungal plug (10 mm) was subtracted from the diameter of fungal growth and this represented the diameter of growth in the test plate (D_t). For fungal phytopathogens that did not grow radially (*M. fructigena, P. expansum* and *R. stolonifera)*, instead of using the diameter as a measure of growth, the area of fungal growth was used instead where the area was measured by scanning the plate and the resulting image edited with ImageJ software to determine the area (mm^2) of the fungal plug and area of fungal growth that covered the PDA plate. The area of the 10 mm diameter fungal plug was subtracted from the area of fungal growth and this represented the area of fungal growth in the test plate (D_t). Triplicate plates for each fungal species were prepared for each LP solution.

The % fungal growth inhibition (appendix A, equation (14)) was then estimated as follows. The diameter or area of growth in the test plate containing the antifungal LPs (D_t) was subtracted from the diameter or area of fungal growth in the control plate (D_c) to obtain the total fungal inhibition (in mm or mm^2). Fungal inhibition was then divided by the total fungal growth (D_c) to obtain the fractional fungal growth. The fractional fungal growth was multiplied by 100 to obtain the percentage fungal growth inhibition.

4.4.   Analytical techniques

4.4.1.   Cell concentration

The cell concentration was a measurement used to quantify the growth of *B. amyloliquefaciens*. Two methods were used: an indirect method (optical density) and a direct method (cell dry weight).

4.4.1.1.   Optical density

To determine the cell concentration at any given time interval, a 2 mL sample of the culture was aseptically taken from the test flasks and transferred into a 2 mL Eppendorf tube. A dilution of the culture sample was prepared in a 1.5 mL Eppendorf tube to a total volume of 1 mL using demineralised H_2O as the diluent. The diluted sample was centrifuged (Eppendorf® Minispin Plus) for 5 min at 14 000 x g (14 500 rpm). The supernatant was discarded, and the pellet re-suspended with 1 mL demineralised H_2O and vortexed until the pellet was homogenised. Optical density (OD) values were taken at 620 nm wavelength (UV/Vis spectrophotometer, Varian®) with demineralised H_2O used as the blank. When the measured OD value exceeded 0.6, it was diluted again to ensure that value remained within the linear region of measurement.

To express the OD values (indirect measure) as the cell dry weight (CDW) (direct measure), a CDW calibration curve was prepared as outlined below.

4.4.1.2.   Cell dry weight

From a 24 h culture, a dilution series ranging from 300-fold to 20-fold was prepared in triplicate using demineralised H_2O as the diluent. 1 mL from each dilution series was then transferred into a 1.5 mL Eppendorf tube and the OD values were taken at 620 nm ensuring that they remained within the linear region of measurement (i.e. OD ≤ 0.6). To obtain the corresponding CDW measurements of the OD values from the dilution series, 15 MS® Nylon membrane filters of 0.22 μm pore size were used for filtering. Before use, the membrane filters were labelled, dried in an oven (Memmert) for 24 h at 60°C, cooled in a desiccator and weighed to four decimal places (OHAUS adventurer®). The remaining dilution (from dilution series) was filtered using a Buchner vacuum filter (Millipore) and the wet filter paper was dried in an oven at 60°C for 24 h. After drying and cooling in a desiccator, the filter paper was weighed to four decimal places again.

To obtain the dry weight of the bacteria, the mass of the membrane filter before filtration (without cells) was subtracted from the mass of filter membrane containing the dried cells. The resultant mass of the bacteria was then divided by the volume of the dilution that was filtered (appendix A, equation (15)).

A CDW calibration curve was constructed as shown in Figure 4-4 and the equation obtained was $y = 2.1171x$ with a correlation coefficient (R^2) of 0.9812. The gradient of the equation was then used to express the OD values as CDW which allowed the CDW to be obtained directly from the OD values without having to conduct CDW experiments at each sampling time interval.
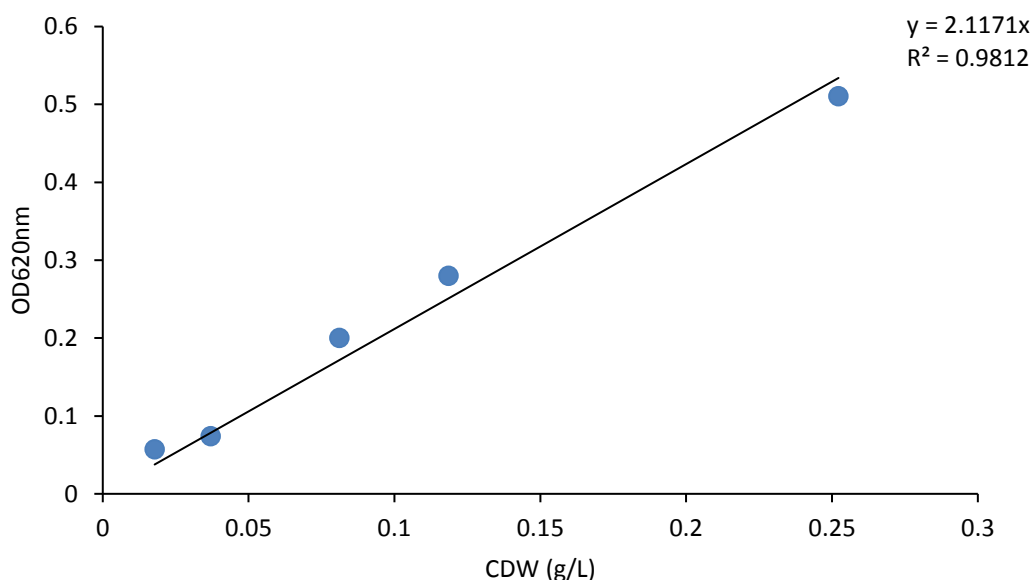
Figure 4-4. Calibration curve relating the OD to CDW. *The data points represent the mean values calculated from triplicates at each time point with the standard deviation of the mean represented by the error bars.*

4.4.2. Glucose concentration

The concentration of glucose was assayed spectrophotometrically using the dinitrosalicylic acid (DNS) method. This method was based on the reduction of 3,5-dinitrosalicylic acid to 3-amino-5nitrosalicylic acid in the presence of reducing sugars in the sample, with the colour orange being an indicator of the reaction. The more reducing sugars were present in the sample, the more intense the colour of the sample was, which indicated that more glucose was present in a sample.

To determine the glucose concentration at any given time interval, a 2 mL sample of the culture was aseptically taken from the test flasks and transferred into a 2 mL Eppendorf tube. The Eppendorf tube was centrifuged at 14 000 x g (14 500 rpm) for 5 min to obtain a cell-free supernatant which was transferred to a new 2 mL Eppendorf tube. The cell-fee supernatant was diluted appropriately to ensure the OD value did not exceed 0.6 and remained within the linear region of measurement. Demineralised H_2O was used as the diluent. 1 mL of the diluted cell-fee supernatant and 1 mL of the prepared DNS reagent (appendix C) was added into a test tube. The sample was placed in a water bath

for five min at 100°C. After removal from the water bath, 0.33 mL of 40% (w/v) sodium potassium tartrate ($KNaC_4H_4O_6.4H_2O$) was added to the test tube, which was then placed in ice-cold water for two min. OD measurements were taken at 540 nm wavelength, with the blank containing 1 mL of demineralised H_2O, 1 mL DNS reagent and 0.33 mL of 40% (w/v) $KNaC_4H_4O_6.4H_2O$.

To express the OD values as the glucose concentration, a glucose calibration curve was prepared as outlined. A glucose resolubilised acid precipitate of 1 g/L was made, from which standard solutions ranging from 50 mg/L to 900 mg/L concentrations were prepared in test tubes. Demineralised H_2O was used as the diluent and the standard solutions had a final volume of 1 mL. 1 mL of the prepared DNS reagent was added to each standard solution. The same procedure for the culture samples was then followed for the standard solutions.

A glucose calibration curve was constructed as shown in Figure 4-5 and the equation obtained was $y = 0.0028x$ with a correlation coefficient (R^2) of 0.984. The gradient of the equation was then used to express the OD values as the glucose concentration.
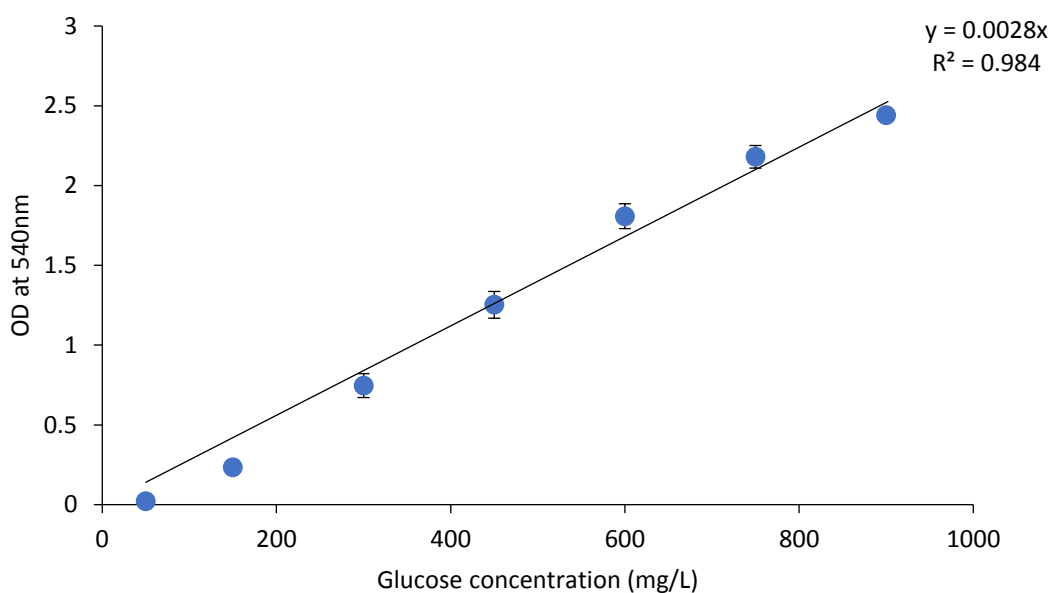
Figure 4-5. Calibration curve relating the OD to the glucose concentration, determined by DNS. *The data points represent the mean values calculated from triplicates at each time point with the standard deviation of the mean represented by the error bars.*

4.4.3. Ammonium and nitrate concentration during growth

The ammonium and nitrate concentration were determined semi-quantitatively using the MQuant™ ammonium (NH_4^+) test and the MQuant™ nitrate (NO_3^-) test respectively. Prior to the tests being

conducted, the initial concentration of NH_4^+ and NO_3^- was determined from the concentration of 4 g/L ammonium nitrate (NH_4NO_3) that was initially added into the growth medium.

4.4.3.1. NH_4^+ concentration

The initial NH_4^+ concentration was calculated to be 901.51 mg/L from the 4 g/L NH_4NO_3 initially added to the culture medium. The test required a maximum concentration of 400 mg/L; therefore, the cell-fee supernatant (prepared as in section 4.4.2) was diluted with demineralised H_2O so that it was within a measurable range. Dilutions were made to a final volume of 1 mL. Working with one diluted sample at a time, one drop of the NH_4-1 solution was added to the sample and the solution was mixed by vortexing. The test strip was immersed for 3 seconds in the solution and after 10 seconds, the colour on the test strip that matched precisely with the colour on the colour scale represented the concentration of the NH_4^+ in mg/L.

4.4.3.2. NO_3^- concentration

The initial NO_3^- concentration was calculated to be 3098.49 mg/L from the 4 g/L NH_4NO_3 initially added to the culture medium. The test required a maximum concentration of 500 mg/L; therefore, the cell-fee supernatant (prepared as in section 4.4.2) was diluted with demineralised H_2O so that it was within a measurable range. Dilutions were made to a final volume of 1 mL. Working with one diluted sample at a time, the test strip containing two reaction zones was immersed for a second in the solution and after a minute from removing the test strip from the solution, the colour on the test strip that matched exactly with the colour on the colour scale represented the concentration of the NO_3^- in mg/L.

4.4.4.   Lipopeptide concentration

The LP concentration was determined by reverse phase high performance liquid chromatography (RP-HPLC) and thin layer chromatography (TLC) analysis.

4.4.4.1.   RP-HPLC procedure for lipopeptide analysis

LPs were analysed by RP-HPLC which made use of the specifications outlined in Table 4-9. The sample preparation procedure for RP-HPLC analysis comprised a 10-fold dilution of the cell-free supernatant (prepared as in section 4.4.2) with acetonitrile containing 0.05% trifluoroacetic acid (TFA). In a 2 mL Eppendorf tube, 100 µl of the supernatant was mixed with 900 µl of the acetonitrile (containing TFA). The acetonitrile (containing TFA) caused precipitation which was immediately observed. Subsequent to the dilution, the samples were aseptically filter-sterilised with a 0.22 µm syringe filter into sterile HPLC vials before RP-HPLC analysis. If samples needed to await HPLC analysis, the diluted samples were stored at -18°C and filter sterilised just before analysis.

Table 4-9. Lipopeptide analysis specifications by RP-HPLC

RP-HPLC specifications	
Column	Phenomenex Luna 3µm C18 column (250 x 4.6 mm)
Detector	Dionex Ultimate 3000 Diode-array detector
Mobile phase A	0.05% (v/v) Trifluoroacetic acid (Fluka®) in water
Mobile phase B	0.05% (v/v) Trifluoroacetic acid in acetonitrile (high purity UV grade, Burdick & Jackson)
Mobile phase gradient	Start at 35% B, increase to 40% B during the next 2 minutes, isocratic at 40% B for the next 5 minutes, increase to 63% B during the next 43 minutes, increase to 80% B during the next 10 minutes, increase to 87% B during the next 35 minutes, return to 35% B during the next 10 minutes and isocratic stabilisation at 35% B for the next 5 minutes.
Flow rate	0.9 mL/min
Absorbance	210 nm

Prior to LP analysis, standards of fengycin (≥ 90%), iturin A (≥ 95%) and surfactin (≥98%), all obtained from Sigma-Aldrich, were used to prepare calibration curves. The calibration curves were constructed from the area of the peaks plotted against the concentration of the LPs so that the area of the LP peaks can be converted to concentrations in g/L. To prepare the fengycin calibration curve, four fengycin standard solutions of 100, 200, 300 and 500 mg/L concentration were prepared in methanol and run through the RP-HPLC column. From the fengycin chromatogram (appendix B, Figure 0-1), the fengycin homologues were grouped into one combined group and the area of the grouped peaks was plotted against the concentrations to obtain the fengycin calibration curve shown in Figure 4-6.

$$y = 0.7489x$$
$$R^2 = 0.9991$$
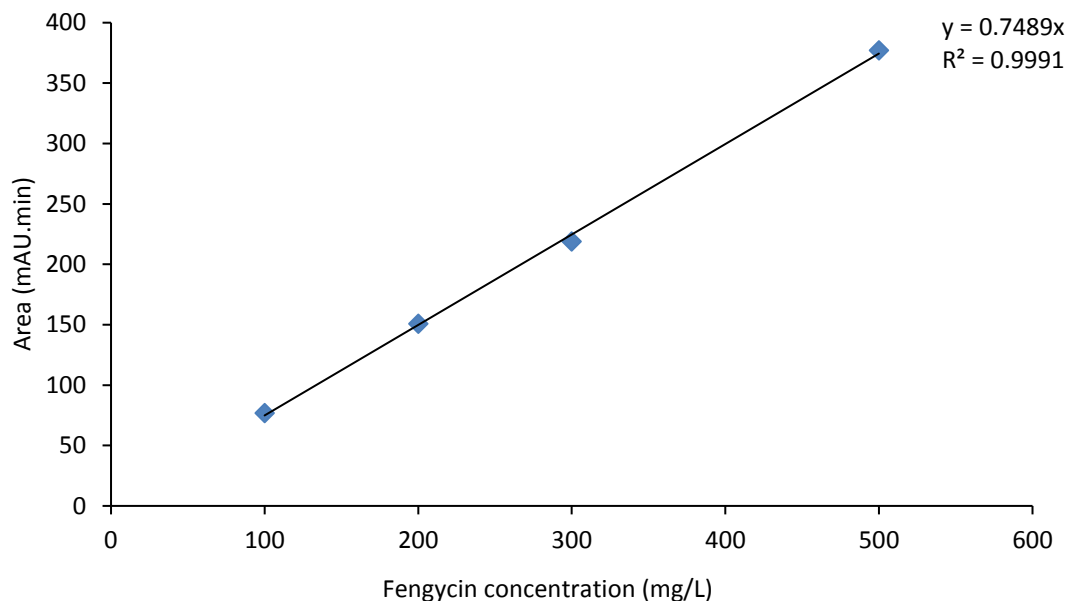
Figure 4-6. Fengycin calibration curve relating the peak area to the concentration

To prepare the iturin A calibration curve, three iturin standard solutions of 50, 100 and 200 mg/L concentration were prepared in methanol and run through the RP-HPLC column. From the iturin chromatogram (appendix B, Figure 0-2), seven iturin homologues were observed and the area of peak 1 – 5 was added and the combined peak area plotted against the concentrations to obtain the iturin A calibration curve shown in Figure 4-7. Peak 6 and 7 of the iturin homologues was not included in the combined area of the peaks as these peaks overlapped with the fengycin homologues.

To prepare the surfactin calibration curve, concentrations ranging from 0.2 g/L to 2.5 g/L were prepared in demineralised water and run through the RP-HPLC column. Six surfactin homologues were observed and the combined areas of the peaks for each standard was plotted against its concentration to obtain the calibration curve in Figure 4-8.
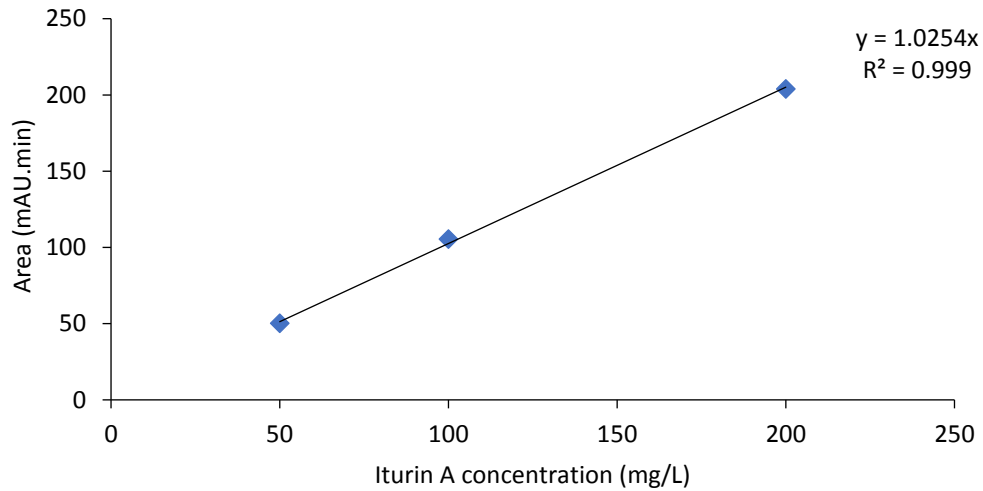
Figure 4-7. Iturin A calibration curve relating the combined peak areas to the concentration
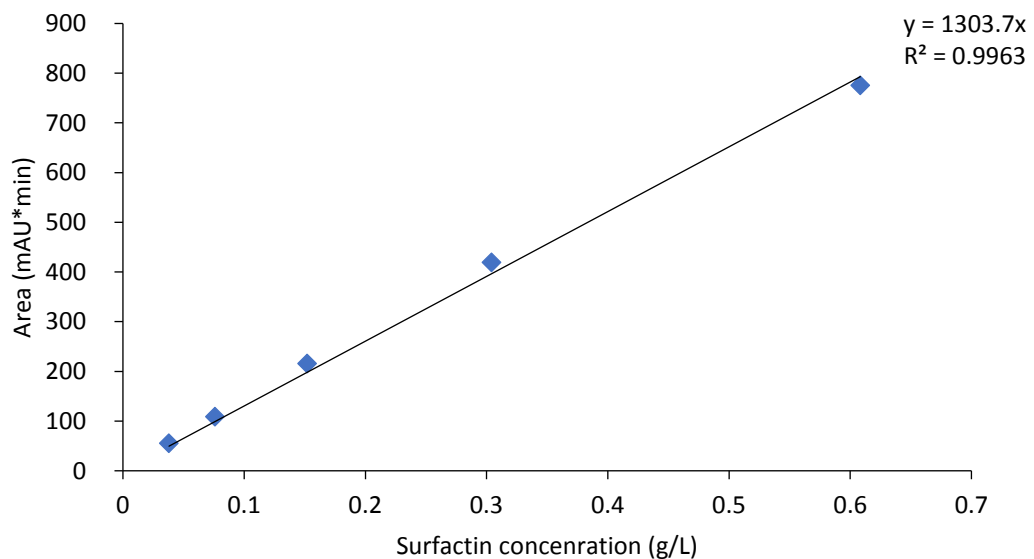
Figure 4-8. Surfactin calibration curve relating the combined peak areas to the concentration

4.4.4.2. TLC procedure for lipopeptide analysis

A latch-lid Chromatank TLC unit chamber (General Glassblowing Company, Inc) was equilibrated for at least 30 min with 60 mL of the mobile phase which was a solution of chloroform: methanol: water (65: 25: 4, v/v). A 20 x 20 cm TLC Silica gel 60 F_{254} aluminium plate (Merck Millipore) was sectioned into four 10 x 10 cm TLC plates. On each plate, a height of 1.5 cm was marked (by pencil) from the base of the plate and then 8 cm above the 1.5 cm mark, with 0.5 cm remaining from the top of the

TLC plate, as displayed in diagram Figure 4-9. At the 1.5 cm mark, 1 cm spots were marked where samples were to be placed with a capillary tube (Sigma-Aldrich capillary tube).

1 μl of demineralised H_2O was pipetted and transferred into the capillary tube. The point where the H_2O reached in the capillary tube was marked with a permanent marker. This marked point was used as a reference point for all the samples to be analysed by TLC, so that exactly 1 μl of sample was pipetted at a time.

The TLC plate was dried with a hair dryer after each sample was spotted, while the capillary tube was cleaned thoroughly with methanol when different samples were spotted on the TLC plate. After sample spotting, the TLC plate was placed in the TLC chamber (two TLC plates were incubated at a time). The TLC plate was kept perpendicular to the chamber through the use chamber holders. The TLC plate was developed for ~ 30 min until the mobile phase reached 0.5 cm from the top of the TLC plate. After ~ 30 min, the TLC plate was removed from the chamber and allowed to air dry in the fume cupboard and dried with a hair dryer.
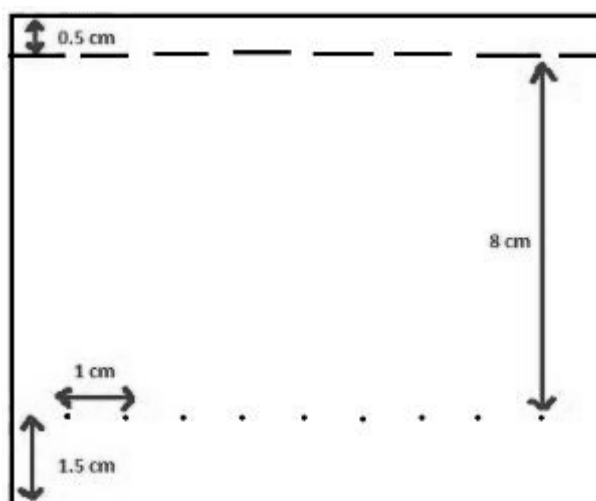
Figure 4-9. TLC plate dimensions for lipopeptide analysis

On each TLC plate used for analysis, 2 μl of each standard (fengycin, iturin and surfactin) solution obtained from Sigma-Aldrich® was made into concentrations of 1 g/L each. Each standard solution was individually spotted onto the TLC plate by pipetting 1 μl of a standard solution at a time into the capillary tube with which it was then spotted onto the TLC plate.

5 μl of the solution to be analysed was spotted. 1 μl of each solution was spotted at a time and after each 1 μl application, the TLC plate was dried with a hair dryer. This procedure was repeated five times

for each solution that was spotted. The capillary tube was washed 2-3 times with methanol between different solution spotting applications on the TLC plate. Subsequent to developing and drying the TLC plate, it was sprayed (with the TLC plate held at approximately 10 cm from the spray) until saturation with 0.005% primuline reagent (acetone: demineralised H_2O, 80:20 v/v).

Excess primuline reagent underneath the TLC plate was wiped off with a paper towel and the TLC plate was scanned (Canon Canoscan LIDE 220) for a total of 15 min at different time intervals (e.g. 5min, 7min, 9min, 11min and 15min). From the scanned images, the image in which the area of the bands closely matched the area of the LP bands on the standard graphs at a particular time was edited using ImageJ software (appendix C). Using the TLC standard graphs developed for fengycin and surfactin (appendix B, Figure 0-4 and Figure 0-5 respectively), the area of the bands (in mm^2) was converted into concentration (in g/L) using equation (16) (appendix A) which enabled the quantification of fengycin and surfactin present in a sample. The recovery and purity percentages of LPs from the various supernatants (from acid precipitation) and solvent extracts (from solvent extraction) was calculated using the equations (1) - (4) respectively (appendix A).

4.4.5. Lipid and protein analysis

Qualitative lipid and protein analysis was carried out using TLC. Lipid analysis involved spraying the same developed TLC plate (as outlined in section 4.4.4.2) with 0.005% primuline and determining the relative quantity of lipid impurities present in different samples. Protein analysis involved the same procedure except that, after the TLC plate was dried, 0.2% ninhydrin reagent was poured onto cotton wool and dabbed onto the TLC plate until saturation. The TLC plates were developed for 45 min and images of the TLC plate were taken by scanning and the resulting images were edited with Image J software.

4.4.6. Antifungal homologue characterisation

Antifungal homologue characterisation was carried out by liquid chromatography electrospray ionisation mass spectroscopy (LC-ESI-MS). Fengycin and iturin homologues produced by *B. amyloliquefaciens* were identified by LC-ESI-MS.

1 mL samples of the LP standards, cell-free supernatant, resolubilised acid precipitate and solvent extracts were submitted for LC-ESI-MS analysis. The organic solvent extracts that recovered fengycin were spotted on a TLC plate from which the plate was developed and stained with primuline. The two bands that were assumed to be fengycin bands were each individually scrapped from the TLC plate and placed into separate 1.5 mL Eppendorf tubes and 1 mL of the organic solvent that was used to

extract the LPs was added into the Eppendorf tube to separate the LPs from the silica material of the TLC plate. The Eppendorf tubes were centrifuged at 14 000 x g (14 500 rpm) for 5 min and the supernatant transferred into new 1.5 mL Eppendorf tubes. The separated fengycin bands in the respective organic solvent were submitted for LC-ESI-MS analysis, together with the LP standards, cell-free supernatant and resolubilised acid precipitate.

The liquid chromatography used was ultraperformance liquid chromatography (UPLC). LP homologues were separated on the Waters UPLC Bridged Ethylene Hybrid (BEH) C18 column (2.1 x 100 mm, 1.7 µm particle size) that was fitted to an Acquity photodiode Array (PDA) detector. 5 µl of each LP sample was injected and separated by UPLC at a flow rate of 0.300 mL/min using a gradient elution (shown in Table 4-10) of mobile phase A which consisted of 0.1% (v/v) formic acid in water and mobile phase B which consisted of 0.1% (v/v) formic acid in acetonitrile.

Table 4-10. UPLC gradient specifications

Time (min)	Mobile A (%)	Mobile B (%)
0	60	40
0.5	60	40
11	5	95
15	5	95
16	60	40
18	60	40

The LP homologues separated were charged due to the mobile phase used in the UPLC gradient elution. The charged homologues needed to be separated from the mobile phase solvent before their masses could be determined by mass spectroscopy and this was achieved through electrospray ionisation (ESI) which occurred in three steps: (1) formation of charged droplets, (2) solvent evaporation from charged droplets (desolvation) and (3) highly charged ion production in the gas phase (Ho *et al.*, 2003).

Firstly, the UPLC eluents (containing charged LP homologues) were passed through a capillary tube (2.5 kV) with a cone voltage of 15 V to produce a mist of charged droplets. The charged droplets at the tip of the capillary tube were subjected to a temperature of 275°C and a gas setting of 650 L/h which allowed the charged droplets to reduce in size as the solvent evaporated. As the solvent continued to decrease, the surface charge density of the droplet became highly charged as the droplet

reduced in size resulting in highly charged droplets. Lastly, the ions at the surface of the highly charged droplet entered the gas phase from which the ion masses in the mass to charge ratio (m/z) were determined by the Waters (Milford, MA, USA) Synapt G2 quadrupole time of flight mass spectrometer. ESI was applied in the positive mode with the data scanned over the 400 – 2000 m/z range and processed using Waters MassLynx Mass Spectrometry Software (version 4.1)

Chapter 5

Results and Discussion

5.1.   Lipopeptide production kinetics

Prior to downstream process optimisation studies, it was necessary to investigate when *B. amyloliquefaciens* DSM 23177 produced optimal antimicrobial LPs. To study the LP production kinetics, shake flasks were used and the time (h) when optimal LPs were produced was determined from the data in Figure 5-1. During the first 8 h of incubation, bacterial growth was initiated as oxygen and other nutrients were non-limiting. From 8 – 24 h, rapid bacterial growth was observed, which was coupled with the rapid consumption of glucose, ammonium and nitrate ions. This rapid growth signified the exponential growth phase.

During the exponential growth phase, both nitrogen sources in the form of ammonium and nitrate ions were used for growth and LP production, where a maximum cell concentration of 6.73±0.33 g/L and maximum fengycin and surfactin concentrations of 0.447±0.003 g/L and 0.287±0.004 g/L respectively, were obtained at 24 h of incubation, a time which related to the end of the exponential phase and start of the stationary phase. Iturin was produced maximally at 48 h with a concentration of 0.37±0.003 g/L, a time relating to the end of the stationary phase and start of the decline phase. Although nitrate ions and residual ammonium was available at 48 h, the carbon source became limiting thus the cells and LP production declined.

It can be deduced that fengycin and surfactin production is growth associated as maximum fengycin and surfactin concentrations were obtained at a maximum cell concentration at 24 h, while iturin production was associated with the stationary phase of growth where sporulation occurred, which maximized the production of iturin. It can also be deduced that from 8 h onwards, oxygen became limiting, which coincided with the rapid cell growth and LP production, implying that both nitrogen sources were used for growth and LP production.

In the presence of both ammonium and nitrate ions as nitrogen sources, a diauxic pattern was expected where the bacterium would first use ammonium ions in the non-oxygen limiting state, which would then be followed by the consumption of nitrate ions in the oxygen-limiting state (Rangarajan and Clarke, 2015;

Rangarajan *et al.*, 2015). The nitrate ions in the oxygen-limited state would act as a nitrogen source and a final electron acceptor, while the ammonium ions would not be used despite their availability. Contrary to literature, *B. amyloliquefaciens* used both nitrogen sources in the oxygen-limited state, implying that the nitrate ions, in addition to being used for growth and LP production, acted as the final electron acceptor when oxygen was depleted.
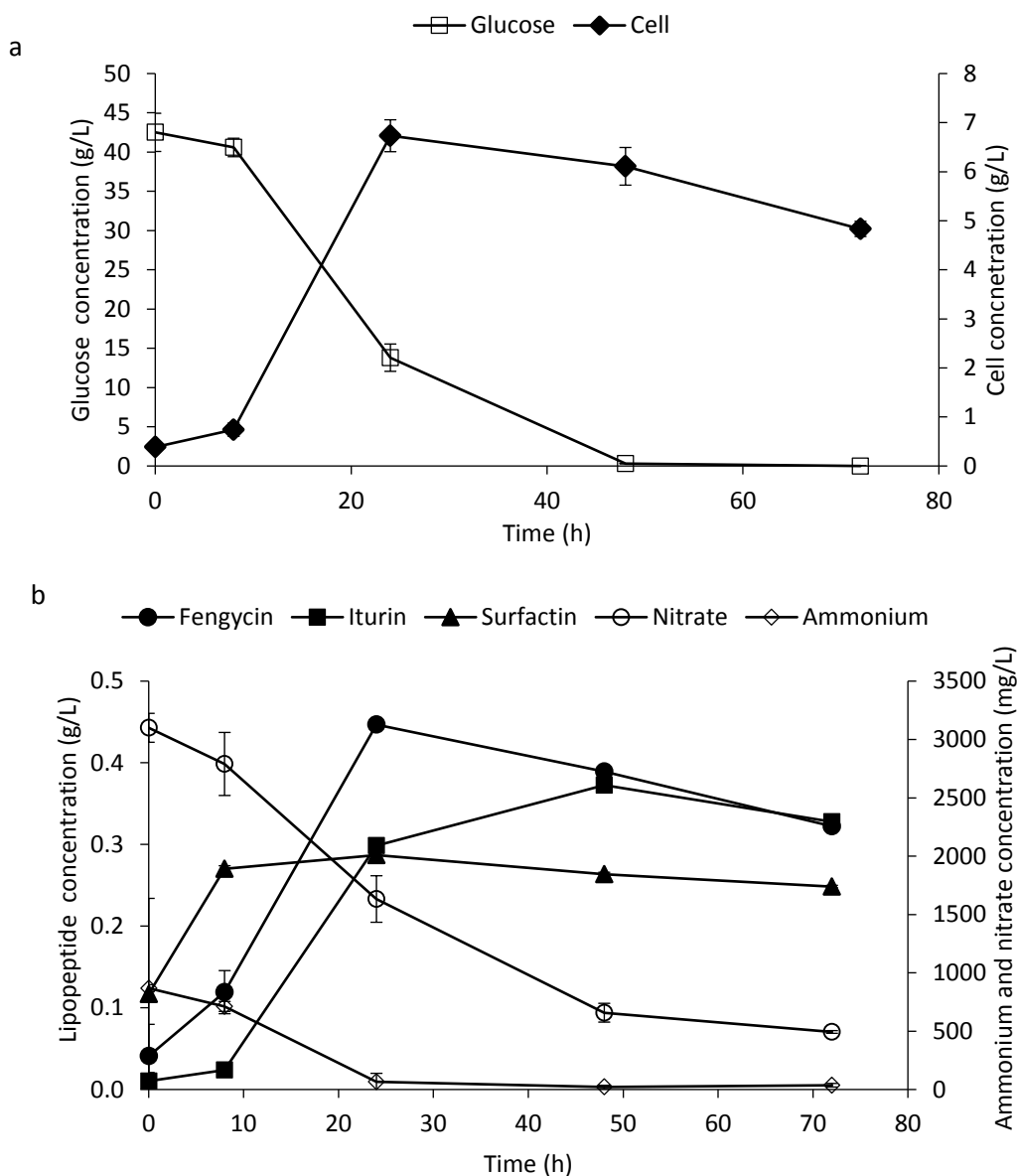
Figure 5-1. Kinetic profiles of (a) glucose and cell concentration and (b) lipopeptide, ammonium and nitrate concentrations over a 72 h incubation time. *The data points represent the mean values calculated from triplicates at each time point with the standard deviation of the mean represented by the error bars.*

To determine the optimal harvesting time, the maximum antifungal concentration and the maximum antifungal selectivity was considered. The antifungal selectivity was described as the amount of antifungals (fengycin and iturin) to the amount of surfactin. Maximum antifungal selectivities of 2.60, 2.88 and 2.62 were obtained at 24 h, 48 h and 72 h respectively. This suggested that maximum antifungal selectivity was at 48 h, which coincided with the maximum concentration of iturin produced. However, the fengycin concentration was maximum at 24 h. The harvesting time was determined to be between 24 - 48 h. Thus, the optimal harvesting time of LPs from the culture broth was selected to be 28 h as the iturin concentration was slightly increased, while the fengycin concentration was close to the maximum concentration.

Once the kinetics of optimal antifungal LP production was determined, the next phase involved the purification of the LPs from the cell-free supernatant. Purification is achieved by using a multi-step procedure involving various downstream unit operations that concentrate and purify the LPs is preferred (Chen *et al.* 2008). In this study, the effect of acid precipitation, solvent extraction and adsorption on the recovery and purification of fengycin and iturin was investigated.

5.2. Acid precipitation

Acid precipitation is regarded as the initial step for LP recovery from the culture broth and for the removal of low molecular weight impurities such as acids, amino acids and alcohols which are products of the *Bacillus* species metabolic pathway (Chen *et al.*, 2007; Rangarajan and Clarke, 2016). The concentration of LPs by acid precipitation is achieved by the drop-wise addition of the acid (HCl) in the cell-free supernatant. The decrease in pH of the cell-free supernatant enables protonation of the LPs, which causes them to form an insoluble mustard-coloured precipitate as the micelle structure of the LPs is destabilised (Soberón-Chávez, 2011; Rangarajan and Clarke, 2016). To collect the precipitate, the solution is centrifuged which separates the supernatant from the precipitate which contain LPs and macromolecular impurities such as protein, peptides, polysaccharides and lipids (Rangarajan and Clarke, 2016). It has been a common phenomenon in literature for the cell-free supernatant to be acidified to pH 2 (Sen and Swaminathan, 2005; Chen *et al.,* 2008; Rangarajan and Clarke, 2016) and pH 4 for surfactin (Chen *et al.*, 2007). This observation suggested that the LP amino acids were at or below their pKa's at pH values between 1 – 4, which enabled their precipitation in the cell-free supernatant. The objectives of these experiments were to determine the effect of varying the cell-free supernatant pH on the recovery and purity of fengycin and iturin, in order to determine the optimum pH for acid precipitation of the antifungal LPs.

In the cell-free supernatant, the amino acids in the LP peptide structure existed in a deprotonated state, making them soluble as the pH of the cell-free supernatant was above the pKa of the amino acids. When HCl was added to the cell-free supernatant, the change in pH caused the state of the amino acids to change from deprotonated to protonated. It was in the protonated state that the LPs were insoluble as the pH of the cell-free supernatant was at or below the pKa of the amino acids.

The percentage of LPs recovered after acid precipitation is shown in Figure 5-2. Maximum recovery percentages were obtained at pH 1 and 2 for all the LPs with surfactin having the highest recovery of 92% followed by fengycin with 78% and iturin 62%. Single-factor ANOVA followed by the T-test as an ad hoc analysis indicated that there was no significant difference (with α = 0.05) in the LP percentage recovery at pH 1 and 2, implying that either of the pH values can be used for the maximum recovery of the three LP families. Although LP precipitation occurred at all the pH values investigated, the LPs were highly protonated at pH 1 or 2. The highly protonated state suggested that hydrogen bonding between the amino acids and the aqueous solution (of cell-free supernatant) was the weakest at pH 1 or 2, which enabled the high percentage recoveries at these pH values.
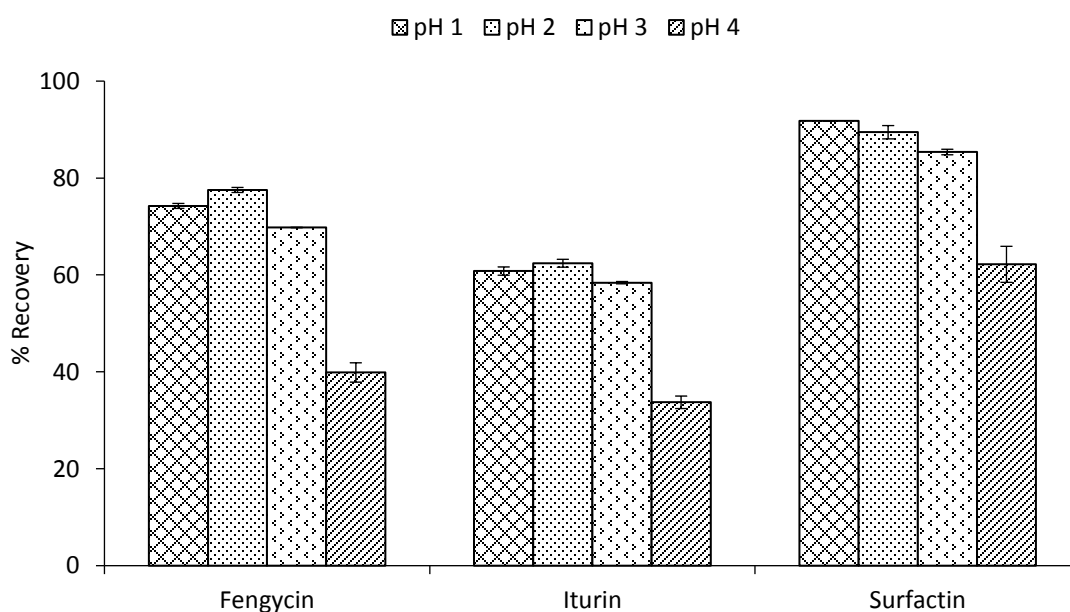
Figure 5-2. Lipopeptide recovery after acid precipitation of the cell-free supernatant determined by RP-HPLC. *The bars represent the mean recovery values calculated from duplicates at each pH value with the standard deviation of the mean represented by the error bars.*

The overall percent recovery of the LPs can be ranked as surfactin > fengycin > iturin across all the pH values. This can be explained by the amino acid composition of the peptide structure of each LP. The higher the composition of non-polar amino acids, the less soluble the LP is in aqueous solutions, as there are stronger interactions that occur between the amino acids than between the amino acids and the aqueous medium they are in. However, the higher the composition of polar and charged amino acids, the stronger the interactions between the amino acids and the aqueous medium they are in; thus, they are more soluble.

Most surfactin was recovered from the cell-free supernatant because of its high composition (71%) of non-polar amino acids relative to fengycin and iturin, which made it the least soluble and thus the most precipitated. On the other hand, fengycin has 20% non-polar amino acids implying that strong interactions occur between fengycin and the cell-free supernatant. Due to the strong interactions between fengycin and the cell-free supernatant, the decrease in pH slightly decreased the solubility of fengycin (due to non-polar amino acids), which made fengycin precipitate. that even with the decrease in pH, the interactions were decreased to some degree which made fengycin slightly insoluble thus precipitating to some degree. Iturin has a non-polar amino acid composition of 14%, implying very strong interactions between iturin and the cell-free supernatant which made iturin weakly insoluble and thus precipitated slightly. This explained the observed trend in the recovery percentages.

Literature reported that the total LP recovery obtained after acid precipitation as the initial downstream step ranged between 90 – 95% (Rangarajan and Clarke, 2016) while the surfactin recovery was reported to be ≥ 95% for *B. subtilis* ATCC 21332 (Chen *et al.,* 2007; Chen and Juang, 2008). The total LPs recovered in the study, as shown in Table 5-1 indicate that the recovery percentages were below the reported values. The percentage recoveries obtained in literature were predominantly for *Bacillus* species that significantly produced surfactin over fengycin and iturin. However, the surfactin recovery of 92% obtained in this study, lies slightly below the reported percentage recovery values which can also be attributed to the *Bacillu*s species as *B. amyloliquefaciens* is a predominant antifungal producer.

Table 5-1. Total lipopeptides recovered by acid precipitation

Treatment	Total lipopeptide recovery (%)
pH 4	39
pH 3	68
pH 2	75
pH 1	72

Although pH 3 did not recover maximum LPs, maximum purities of 64 ± 0.04 % for fengycin followed by iturin and surfactin at 17 ± 0.07% and 5 ± 0.02% respectively were obtained as shown in Figure 5-3. The purity value of 64 ± 0.04%, obtained in this study was 9% higher than the purity of surfactin as previously reported by Chen *et al.* (2007) and Chen and Juang (2008). Similar statistical analysis used for the percentage recoveries at the four pH values indicated that there was no significant difference (with α = 0.05) in the LP purity at pH 1 and 2 while there was a significant difference in the purity obtained at pH 3 and 4 with 95% confidence. This suggested that pH 3 was the best pH for the maximum purity of all the LP families.
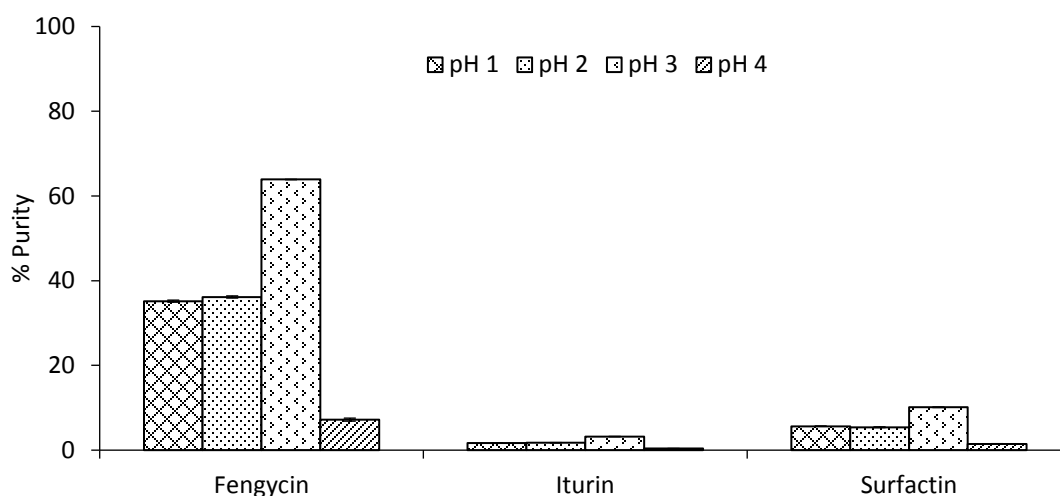
Figure 5-3. Lipopeptide purity after acid precipitation of the cell-free supernatant determined by RP-HPLC analysis. *The bars represent the mean purity values calculated from duplicates of each pH value with the standard deviation of the mean represented by the error bars.*

The expected trend was that an appropriate pH value would be obtained in which the antifungal selectivity would be improved in comparison to the selectivity obtained in the cell-free supernatant. The selectivities illustrated in Table 5-2 show that maximum antifungal selectivity was obtained at pH 2, implying that less surfactin was obtained at this pH value in contrast to pH 4, where the least antifungal selectivity was observed. To determine the optimal pH for acid precipitation of the antifungal LPs, the percentage recovery and purity as well as the antifungal selectivity was considered. It can be deduced from the data that high recovery percentages were obtained pH 1 or 2, with a maximum antifungal selectivity obtained at pH 2. However, high purity percentages were obtained at pH 3, thus pH 3 was considered as the optimal pH for antifungal LP precipitation.

Table 5-2. Effect of acid precipitation on antifungal selectivity

Treatment	Antifungal selectivity ($g_{antifungals}/g_{surfactin}$)
Cell-free supernatant	20
pH 4	13
pH 3	16
pH 2	17
pH 1	16

The relatively low percentage recoveries and purities recorded at pH 4 was attributed to the presence of protein impurities that were visualised and identified by qualitative TLC analysis of the cell-free supernatant (before acid precipitation) and resolubilised acid precipitate after acid precipitation, using the ninhydrin reagent as shown in Figure 5-4. This suggested that more protein than LPs were recovered at pH 4, while more LPs than protein were recovered between pH values 1 – 3.

Ninhydrin is known to react with free primary and secondary amines in peptides and protein to produce a purple colour. Fengycin contained free primary and secondary amines which reacted with the ninhydrin reagent which explains the stained fengycin bands in the TLC plate, while surfactin and iturin lack free primary and secondary amines and hence no reaction occurred with the ninhydrin reagent.
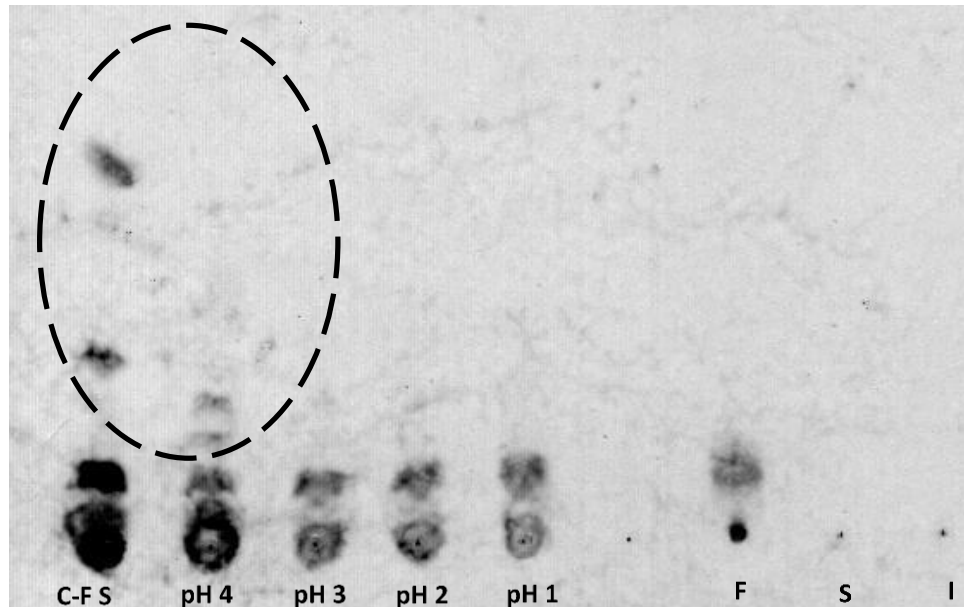
Figure 5-4. Protein impurity analysis stained by 0.2% ninhydrin reagent on a TLC plate. *C-F S: cell -free supernatant, F: fengycin standard, S: surfactin standard and I: iturin standard. The circular band shows protein and peptide impurities.*

Since acid precipitation was the initial downstream unit operation in the purification programme, it set a benchmark upon which subsequent downstream procedures relied upon to improve the purity of the LPs (Rangarajan and Clarke, 2016). The main aim of acid precipitation was to concentrate and recover maximum LPs while increasing the purity to some degree by separating the LPs from the culture broth (Rangarajan and Clarke, 2016). From the results attained in this study, pH 1 or 2 was suitable for the maximum recovery of fengycin and iturin while maximum antifungal LP purities were obtained at pH 3.

Considering the optimal pH for antifungal LP precipitation, acid precipitation of the cell-free supernatant to pH 3 would be suitable as the initial concentration step, which takes into consideration the percentage recovery and purity, as well as the antifungal selectivity. Based on the percentage purities of fengycin and iturin, acid precipitation at pH 3 would minimise the number of downstream unit operations used further in the purification programme, depending on the degree of purity required, which is dependent on the application. Since the antifungal LPs would be applied to fruit during storage, they need to be in their purest form with surfactin separated from iturin and fengycin which necessitates the use of further downstream unit operations such as solvent extraction for further improvement in fengycin and iturin purity.

5.3.   Solvent extraction

Solvent extraction was the next unit operation used in the purification programme, following acid precipitation. After the acid precipitate was collected by centrifugation and dried, a variety of organic solvents were investigated for their efficiency in extracting antifungal LPs. Following the percentage purities of 64% and 17% for fengycin and iturin respectively, obtained by acid precipitation, an improvement in the purity was required.

Organic solvents that have been reported in literature for the extraction of surfactin include alkanes (hexane, pentane), alcohols (butanol, ethanol, methanol), ethers (diethyl ether), esters (ethyl acetate), alkyl halides (chloroform, dichloromethane) and ketones (acetone) (Chen and Juang, 2008), while various mixtures of chloroform and methanol have been reported as suitable solvents for the efficient extraction of surfactin (Chen and Juang, 2008). Although there is a variety of organic solvents to choose from, the recovery and purity of antifungal LPs extracted by the various organic solvents has not been previously investigated.

The organic solvents used in this study were chosen based on polarity, using the Snyders polarity index, which defines the polarity of an organic solvent based on a combination of parameters such as the dipole moment, acidity, basicity and dispersion forces (Katritzky *et al.*, 2004). The advantage of using the Snyders polarity index was that the polarity index of mixed solvents could be obtained.

5.3.1.   Screening of suitable organic solvents

A range of polar and non-polar organic solvents were used in this study to compare the extraction efficiency of fengycin and iturin by the different solvents. The dried acid precipitate was added into a volume of organic solvent and the mixture allowed to mix, after which the percentage recovery and purity of fengycin and iturin obtained from the various solvents was compared to determine the best solvent for antifungal LP extraction.

From the three LP families, only two LP families (fengycin and surfactin) were detected by TLC analysis from the solvent extracts as illustrated in Figure 5-5. Iturin could not be detected as its concentration may have been below the detection limit for the TLC method used and thus only fengycin and surfactin were able to be quantified. It is also evident that the band intensity of the iturin standard is relatively less intense than the band intensity observed in the fengycin and surfactin standard although the concentration of the standards was equal at 1 g/L. The area of the bands for each LP family was converted

to a concentration in g/L using a calibration curve appendix B (Figure 0-4 and Figure 0-5) which related the area of the bands to the concentration from which the % recovery and purity was calculated.

The solvent extracts showed two bands with retardation factor (R_f) values $RF_1 = 0.096$ and $RF_2 = 0.036$ respectively, while the fengycin standard showed only one band (with $R_f = 0.063$) therefore the area of the two bands from the solvent extracts were assumed to be fengycin bands and thus were combined and then converted to a concentration to obtain a total fengycin concentration from which the recovery and purity percentage was calculated.
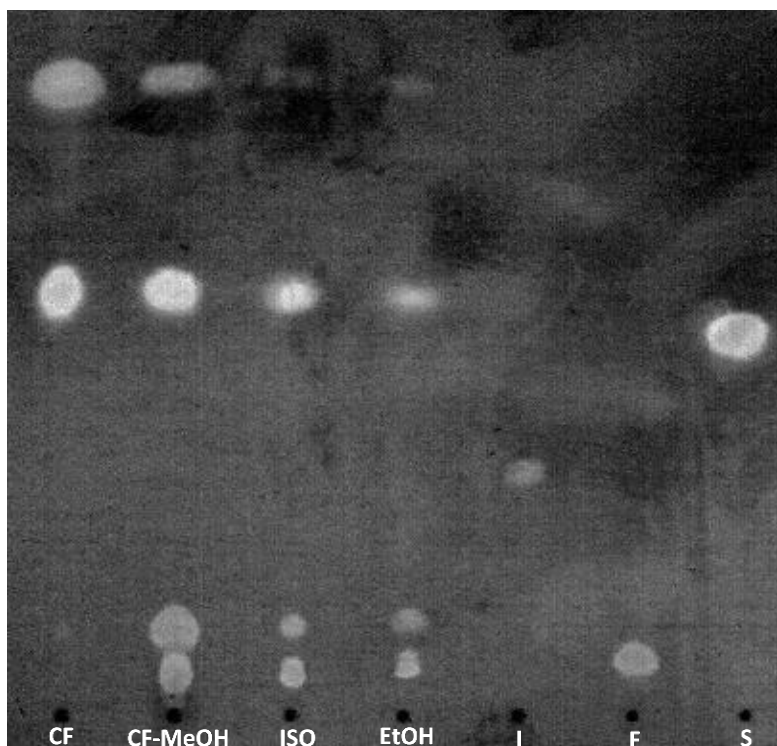
Figure 5-5. Lipopeptide solvent extracts stained with 0.005% primuline reagent on a TLC plate. *CF: Chloroform, CF-MeOH: Chloroform-Methanol (2:1, v/v), ISO: Isopropanol, EtOH: Ethanol, I: Iturin standard, F: Fengycin standard and S: Surfactin standard. 5 µl of each solvent extract and 2 µl of each standard was spotted onto the TLC plate. The TLC plate was scanned and the image edited with ImageJ version 1.4.3.67.*

The trend observed in Figure 5-6 is that alcohols and mixtures containing alcohols extracted maximum LPs relative to other organic solvents used in the study. All the organic solvents extracted surfactin to varying degrees with isopropanol, methanol, ethyl acetate – methanol the best solvent for surfactin extraction as an average recovery of ≥ 98 ± 7.62% was obtained. Acetone, alcohols and their mixtures, were efficient in the recovery of fengycin. Methanol and isopropanol were the overall superior solvents for the recovery

78

of LPs, however, methanol was the best solvent for fengycin as a 100 ± 0.00% recovery of fengycin was obtained. From the alcohols that extracted fengycin, 1-octanol extracted the least amount of fengycin (16 ± 0.58%) as only one fengycin band, instead of two was observed on the TLC plate.
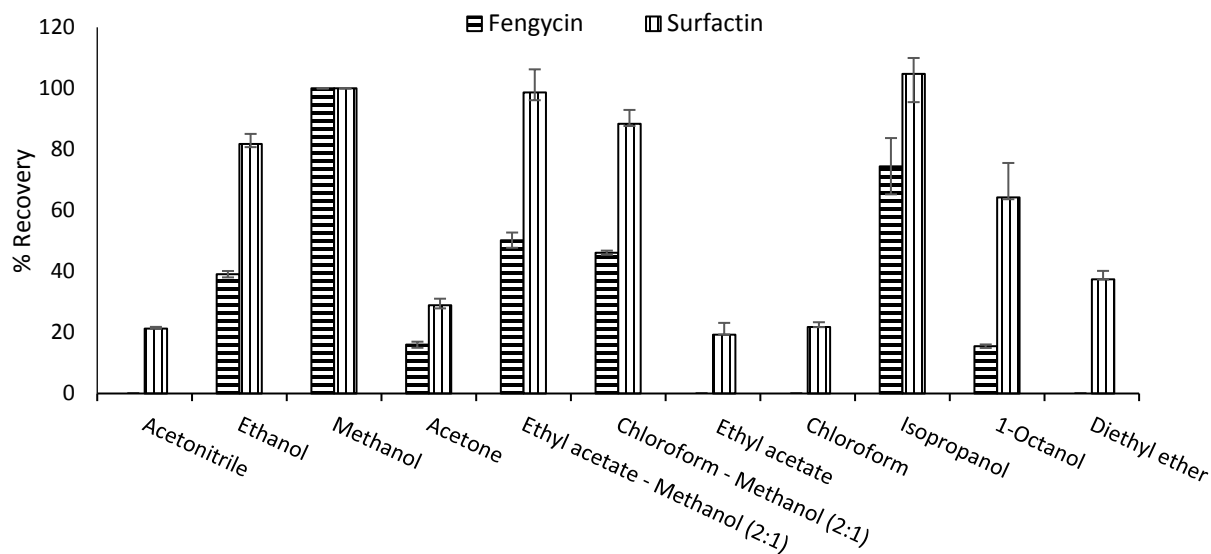
Figure 5-6.Recovery of lipopeptides extracted into organic solvents determined by TLC analysis. *The bars represent the mean recovery values calculated from triplicates of each organic solvent with the standard deviation of the mean represented by error bars. The organic solvents are presented in order of decreasing polarity indices (from left to right)*

Isopropanol and 1-octanol are considered non-polar (based on the polarity index) solvents compared to methanol and ethanol as they have longer carbon chains relative to the hydroxyl (OH⁻) group making them relatively non-polar and are considered as higher alcohols. Although these solvents are considered non-polar, they extracted fengycin while a polar organic solvent such as acetonitrile was expected to extract fengycin but was unable to recover fengycin from the dried acid precipitate. This implies that the functional group of alcohols (OH) and ketones (carbonyl C=O) interact with the LPs to enable extraction. Strong hydrogen bonding interactions occurred between fengycin and the functional groups of these organic solvents, which made fengycin more soluble in alcohols and ketones than in other organic solvents and thus was extracted by these organic solvents.

The principle of peptide solubility in organic solvents is determined by the nature of amino acids (Needham, 1970). The degree of amino acid solubility in polar solvents can be ranked as follows: charged

> polar uncharged > non-polar, where amino acids with charged side chains are highly soluble in polar solvents, polar uncharged amino acids are soluble in polar solvents and non-polar amino acids are weakly soluble in polar solvents. (Needham, 1970; Nick Pace *et al.*, 2004). The peptide moiety of surfactin contains both types of charged amino acids (glutamic acid and aspartic acid), while fengycin consists of two glutamic acid amino acids in the peptide structure. The presence of both types of charged amino acids increased the solubility of surfactin in polar solvents in comparison to the presence of one type of charged amino acid as in fengycin may explain the high surfactin recovery percentages obtained in organic solvents that also extracted fengycin, except for methanol. In methanol, the presence of any charged amino acid, irrespective of the type of charged amino acid (either glutamic acid or aspartic acid,) appears to be highly efficient in the recovery of the LPs.

Surfactin recovery in non-polar solvents was also efficient, to varying degrees, due to the presence of non-polar amino acids. Since 71% of the surfactin peptide is composed of non-polar amino acids, varying degrees of solubility in non-polar solvents, and thus recovery, was obtained. However, only 20% of fengycin is made up of non-polar amino acids therefore the repulsive forces between the peptide moiety and the non-polar solvents was large which prevented their solubility and thus fengycin was not recovered in non-polar solvents.

The nature of LP amino acid composition may also partially explain why fengycin and surfactin were able to be visualised on the TLC plate, while iturin could not. Ranking the LPs based on hydrophilicity shows that iturin > fengycin > surfactin. Since the stationary phase of the TLC plate is made of silica, which is polar, stronger interactions existed between iturin and silica, which retarded the movement of iturin on the TLC plate, while stronger interactions between fengycin and surfactin existed between these LPs and the mobile phase, which enabled their movement with the solvent front.

Literature studies such as Juang *et al.* (2012) reported a surfactin recovery of 21% when n-hexane was used as the non-polar extracting solvent, while a 95% recovery of surfactin was reported when ethyl acetate was used as the polar extracting solvent (Juang *et al.*, 2012). This observation would have implied that polar solvents were efficient at extracting surfactin. However, as seen in this study, extraction is dependent of the functional groups of solvents, instead of solely on polarity.

It is hypothesised that fengycin extraction efficiency is not solely dependent on the polarity of the organic solvent but that the functional groups of the solvents interact with the LPs, effecting solubility. This is borne out by the data, where higher alcohols (which are considered non-polar) can extract fengycin but

non-polar solvents such as diethyl ether cannot extract fengycin. It can be concluded that the OH group in the solvent is therefore important in fengycin extraction.

The purity percentages illustrated in Figure 5-7 showed trends similar to the percentage recoveries, where alcohols and mixtures containing alcohols showed relatively high purity percentages for both fengycin and surfactin, with methanol being optimal for the purity of fengycin (74 ± 0.00%) while 1-octanol was optimal for the surfactin purity (40 ± 6.87%). Although all the solvents extracted surfactin, the percentage purities obtained were all below the reported values in literature, which is not surprising considering that in the literature, the LPs were recovered from *B. subtilis* which predominantly produces surfactin, in contrast to the *B. amyloliquefaciens* used in this study which produced all three types of LPs.
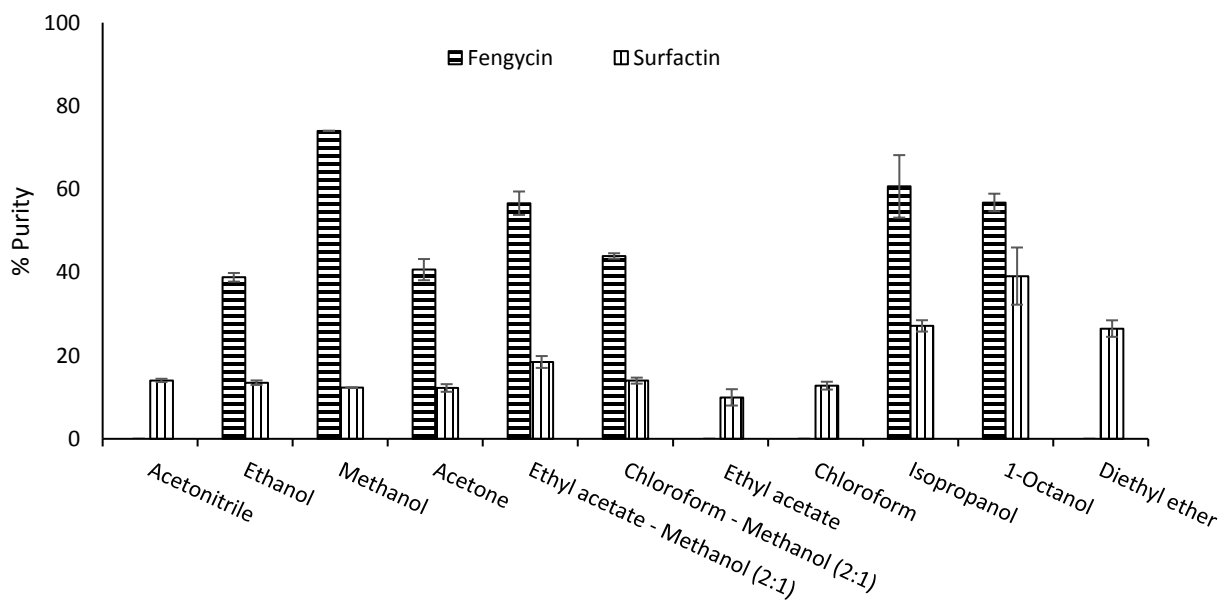
Figure 5-7. Purity of lipopeptides extracted into organic solvents determined by TLC analysis. *The bars represent the mean purity values calculated from triplicates of each organic solvent with the standard deviation from the mean represented by error bars. The organic solvents are presented in order of decreasing polarity indices (from left to right)*

Since the LPs are purified for their application on fruit, the complete removal of the organic solvents as contaminants from the LP extract is mandatory as trace amounts may pose as health hazards (such as allergies). This separation is easily accomplished by evaporating the solvent using, for example, a rotary

evaporator. However, this does not ensure that all of the solvent is completely removed, and there may remain trace amounts. For this reason, purity and recovery of LPs is not the only consideration, but a suitable food grade solvent should be used as an additional requirement.

The solvents used in this study were evaporated by using a water bath set to 100°C as most of the solvents used had boiling points that were below that of water, thus they were easily evaporated., However, it was difficult and time-consuming to completely evaporate 1-octanol as it had a boiling point of 195°C, which in this case, a rotary evaporator or vacuum based evaporator would be required.

In addition to the extraction of LPs, lipid impurities shown in Figure 5-8 and protein impurities shown in Figure 5-9 were co-extracted by the various organic solvents. The lipids co-extracted with the LPs were hydrophobic lipids as they had strong interactions with the solvent front, thus they were carried the furthest to the top of the TLC plate.
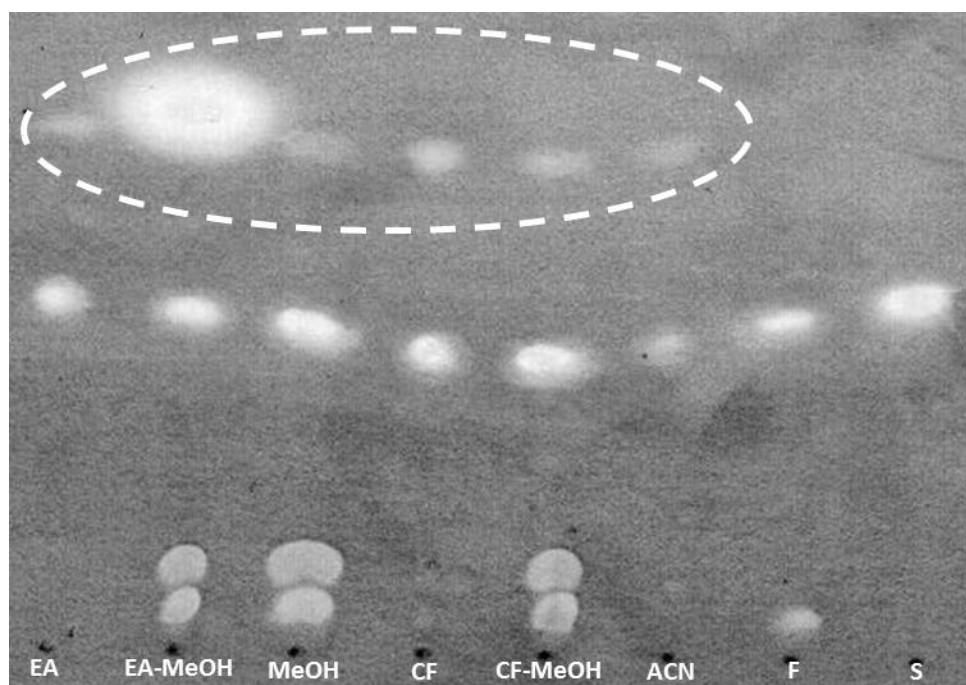
Figure 5-8. Co-extraction of lipopeptides and hydrophobic lipids by organic solvents determined by TLC analysis. *EA: Ethyl acetate, EA-MeOH: Ethyl acetate–Methanol (2:1, v/v), MeOH: Methanol, CF: Chloroform, CF–MeOH: Chloroform-Methanol (2:1, v/v), ACN: Acetonitrile, F: Fengycin standard and S: Surfactin standard. Circular structure shows the hydrophobic lipid impurities. 5 µl of each solvent extract and 2 µl of each standard was spotted onto the TLC plate, which was stained with 0.2% ninhydrin reagent after development. The TLC plate was scanned and the image edited with ImageJ version 1.4.3.67.*
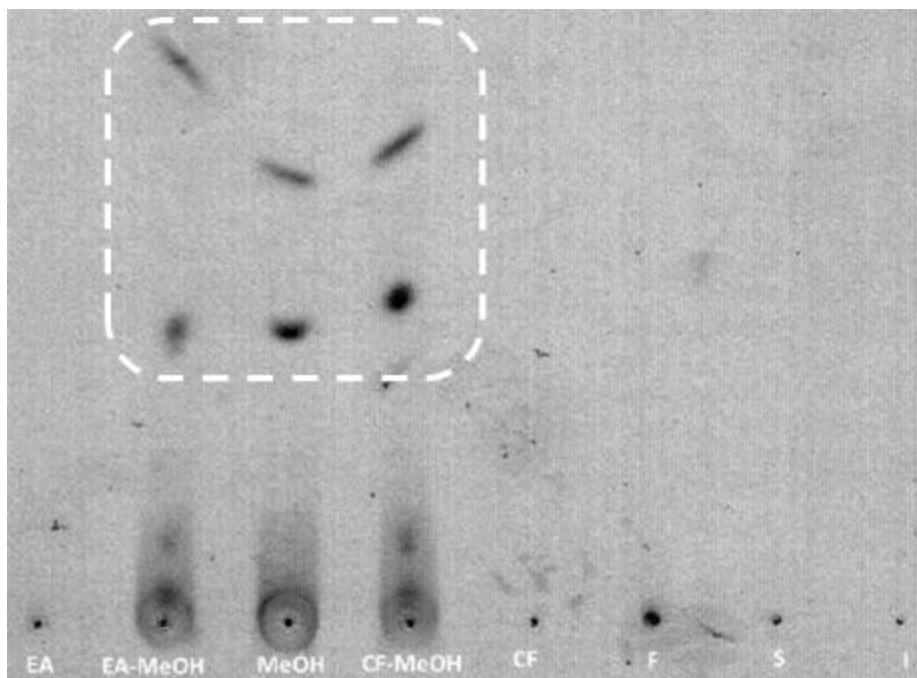
Figure 5-9. Co-extraction of protein impurities by organic solvents on a TLC plate. *EA: Ethyl acetate, EA-MeOH: Ethyl acetate–Methanol (2:1, v/v), MeOH: Methanol, CF–MeOH: Chloroform-Methanol (2:1, v/v), CF: Chloroform, F: Fengycin standard and S: Surfactin standard. Boxed structure represents protein impurities. 5 µl of each solvent extract and 2 µl of each standard was spotted onto the TLC plate, which was stained with 0.2% ninhydrin reagent after development. The TLC plate was scanned and the image edited with ImageJ version 1.4.3.67.*

5.3.2. Three-stage solvent extraction

With the appropriate organic solvents identified for optimal fengycin extraction, the effect of the number of extractions on the purity percentage was investigated. A three-stage extraction procedure was conducted to improve the purity of LPs. Two extraction approaches were investigated: (1) three-stage methanol extraction and (2) three-stage diethyl ether-methanol extraction. In the first extraction approach, the dried precipitate was extracted three times with while the second extraction approach involved the extraction of the acid precipitate with diethyl ether and twice with methanol. Since diethyl ether extracted surfactin, selectivity could be achieved as fengycin would remain in the undissolved acid precipitate which would then be recovered by extraction with methanol, preferably with a higher purity.

The recovery and purity percentages of LPs obtained after the three-stage extraction using methanol and diethyl ether-methanol are shown in Table 5-3 and Table 5-4. An inverse proportion trend was observed between the number of extractions and the recovery percentages of both fengycin and surfactin, while an increase in the purity percentages was observed. Increasing the number of extractions decreased the

percentage of LPs recovered while an increase in the purity percentage was obtained. Although the diethyl ether–methanol extraction recovered 90% of fengycin, methanol would be the suitable solvent as a final purity of 89% was obtained which was close to the fengycin standard from Sigma-Aldrich that is ≥ 90%.

Table 5-3. Lipopeptide recovery percentage following a three-stage extraction using methanol and diethyl ether–methanol

	% Recovery			
Extraction	**3-stage Methanol**		**Diethyl ether-methanol**	
	Fengycin	**Surfactin**	**Fengycin**	**Surfactin**
1	100 ± 0	100 ± 0	-	42 ± 9
2	99 ± 3	99 ± 4	100 ± 4	98 ± 7
3	89 ± 4	97 ± 9	90 ± 16	98 ± 5

Table 5-4. Lipopeptide purity percentage following a three-stage extraction using methanol and diethyl ether–methanol

	% Purity			
Extraction	**3-stage Methanol**		**Diethyl ether-methanol**	
	Fengycin	**Surfactin**	**Fengycin**	**Surfactin**
1	75 ± 2	12 ± 3	-	-
2	88 ± 2	14 ± 1	-	-
3	89 ± 4	16 ± 2	74 ± 13	13 ± 1

The results obtained suggests that methanol is the superior solvent for fengycin extraction with a significant improvement in the purity after the 3-stage extraction procedure was employed. To date, this is one of a limited number of studies that has investigated the LP extraction efficiency of various organic solvents in a logical and ordered manner. Although the 3-stage extraction procedure provided insight into the degree of purity that can be obtained, a better systematic approach involving an extraction with a polar solvent (determined in the study to be methanol) followed by an extraction with a non-polar solvent would be ideal as the extraction would be aimed at removing impurities to improve the purity.

5.4.   Adsorption

The adsorption principle of LPs on a polymeric macroporous resin was based on the hydrophobic interactions that occur between the LPs and the resin. With the factors affecting adsorption of LPs identified, several experiments were conducted to highlight and shed some light on the adsorption behaviour of fengycin and iturin.

5.4.1.   Batch equilibrium adsorption experiments

The factors affecting adsorption were identified to be the temperature, pH, LP to resin ratio. RSM was used to design batch adsorption experiments to optimise the adsorption of LPs on a macroporous resin, HP-20, by optimisation of the three main factors: (1) LP to resin ratio (LP/R), (2) temperature and (3) pH. To date, a limited number of studies have investigated the purification of surfactin (and fewer studies for fengycin) by adsorption of the LPs onto macroporous resins. However, no study has investigated the optimal batch adsorption conditions for fengycin and iturin. Further, the interactive effects of the three variables on adsorption of the antifungal LPs on HP-20 resin have not previously been elucidated.

The three variables were optimised through a rotatable design, with the percentage adsorption selected as the response variable. Optimal adsorption conditions were determined using the percentage adsorption as it was the desired response variable for optimisation due to the following principle. At low adsorbate concentrations, all the adsorbate molecules are adsorbed as there are many adsorption sites available on the adsorbent surface. However, as the adsorbate concentration is increased, less adsorption sites become available thus fewer adsorbate molecules are adsorbed at high adsorbate concentrations, therefore, the optimal adsorbate to adsorbent ratio can be determined.

5.4.1.1.   Fengycin adsorption parameters on HP-20 macroporous resin

ANOVA analysis and the estimate of the effect of each variable on fengycin adsorption showed that the LP/R ratio and the pH were significant factors that influenced the adsorption of fengycin. More specifically, the model in which the significance of the variables was obtained indicated that the quadratic term of the LP/R ratio and the linear term of the pH was significant in the adsorption of fengycin on HP-20 resin as shown in Figure 5-10.

A quadratic effect indicates that the optimum level of a variable is within the experimental ranges studied and its effect on the response is dependent on the interaction(s) with other variables studies. The linear effect indicates that the variable itself has a significant effect (positive or negative) on the response with no interaction with other variables studied. This implied that the LP/R ratio interaction with pH was

necessary to obtain the optimal percentage of fengycin adsorbed while pH on its' own was sufficient in having a significant effect on the adsorption of fengycin.

The Pareto chart in Figure 5-10 indicated in descending order the contribution of each variable in determining the optimum conditions for fengycin adsorption. The pH followed by the LP/R ratio were found to influence fengycin adsorption on HP-20 significantly. The two-way interactions between the variables and the effect on the percentage adsorption is shown Figure 5-11 - Figure 5-13 from which optimal conditions were deduced to be 0.5 and 10 for the LP/R ratio and pH respectively. The negative values shown in the figure keys are a result of the model artefact which are meaningless. The optimal temperature was found to be 40°C, however, since temperature had no effect on the adsorption of fengycin, the maximum temperature used in the experimental design (43°C) was selected for further experimental studies on adsorption isotherms and kinetics since temperatures ≥ 40°C resulted in relatively increased percentage adsorption values across any LP/R ratio and pH value above 9.
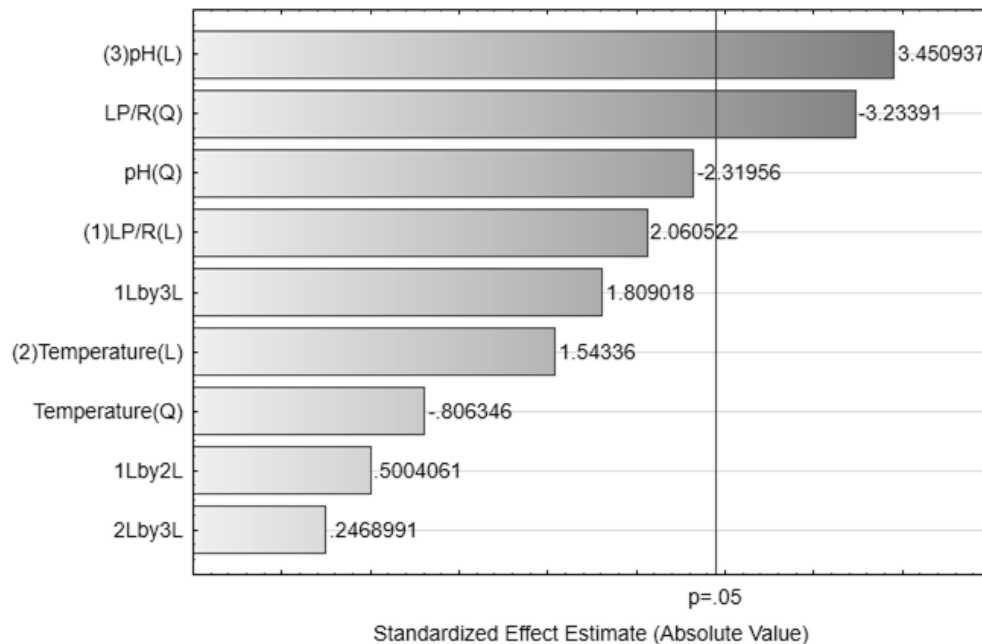
Figure 5-10. Degree of variable contribution on the adsorption of fengycin on HP-20 resin. *L refers to the linear terms and Q to the quadratic terms of the model. The Pareto chart was generated in STATISTICA 13.2*
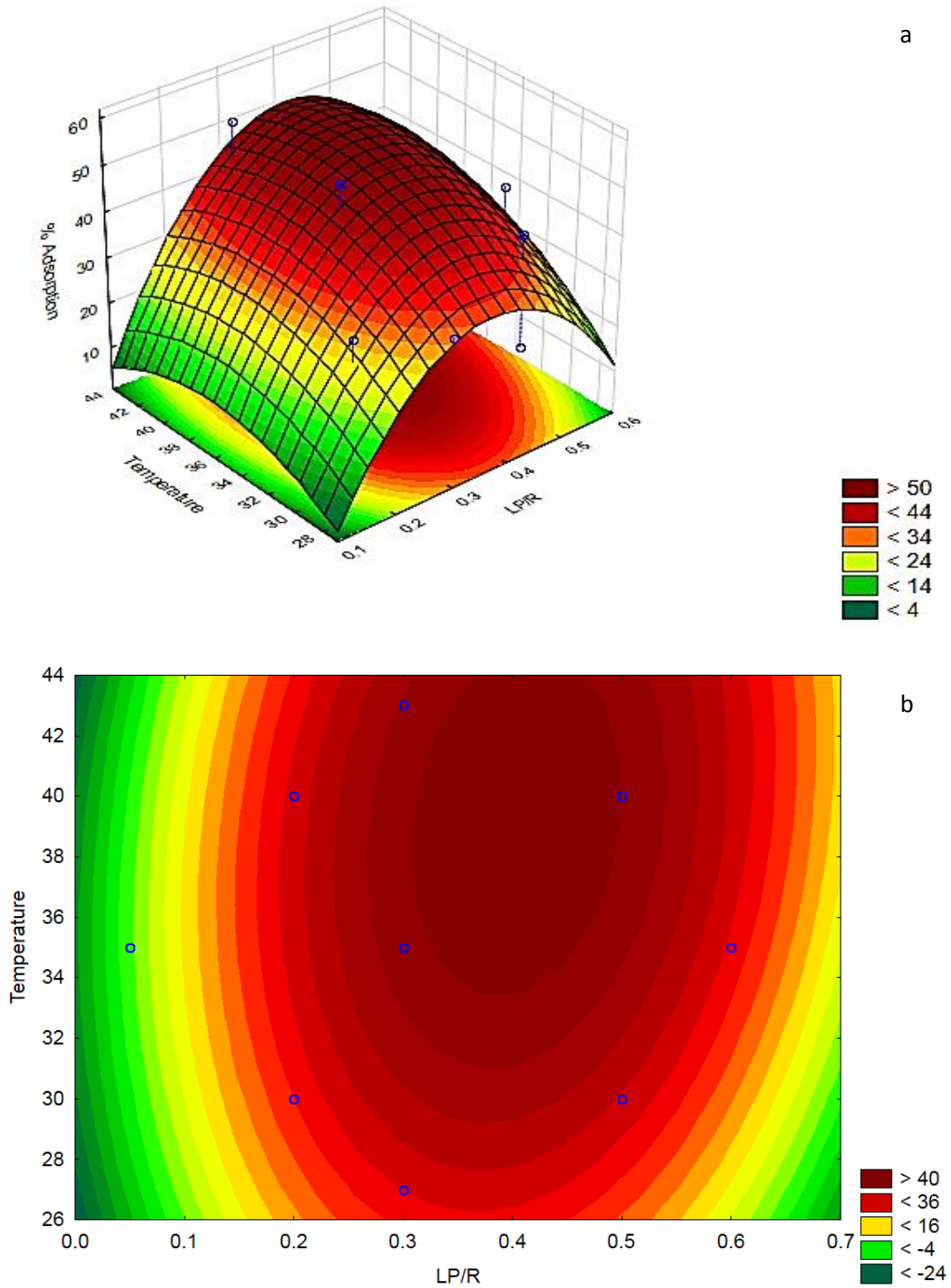
Figure 5-11. Effect of temperature and lipopeptide/resin ratio on the percentage fengycin adsorbed on HP-20 resin shown as (a) 3D surface plot and (b) contour surface plot. *LP/R refers to the lipopeptide to resin ratio. The surface plots were generated in STATISTICA 13.2*
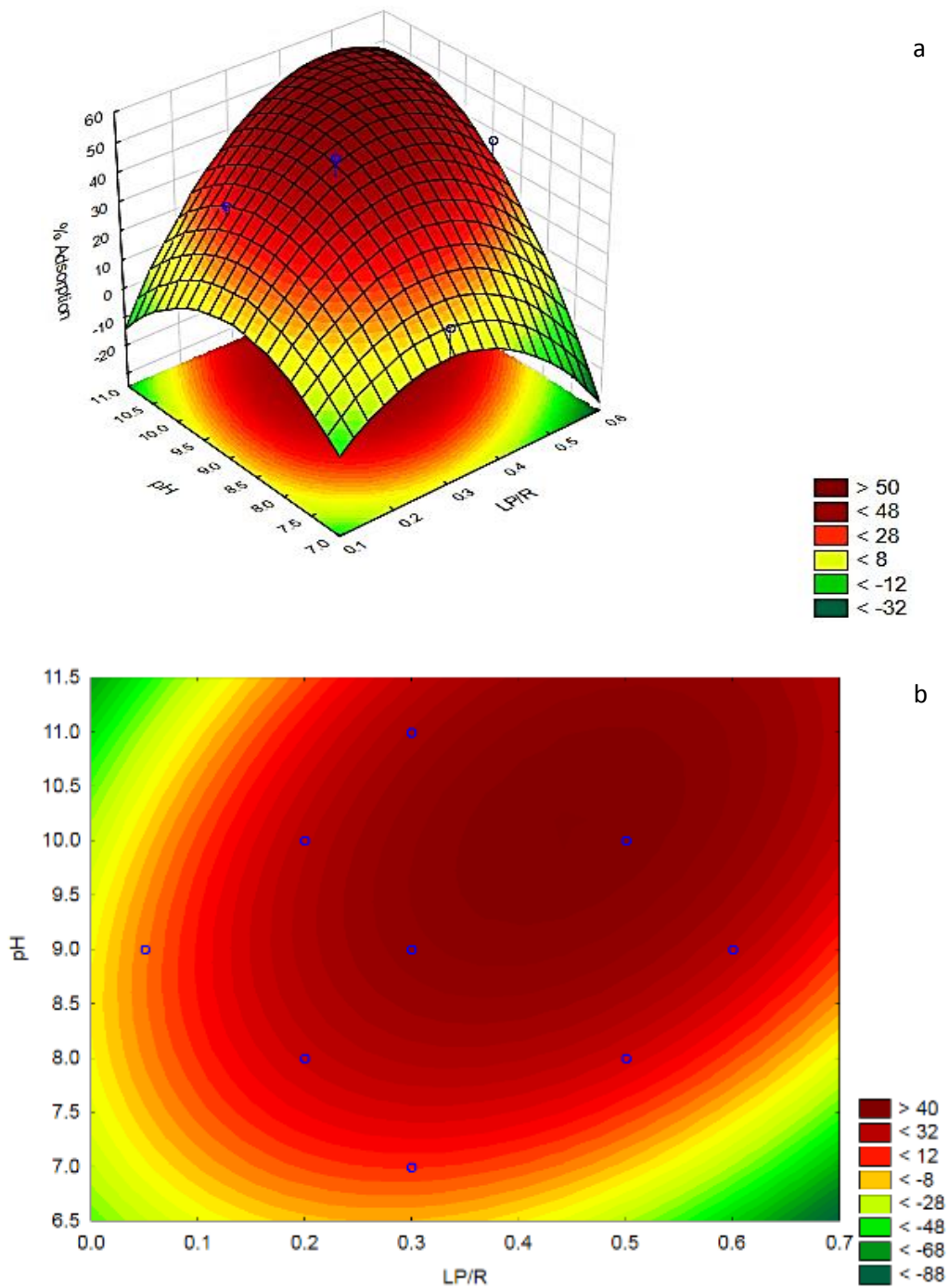
Figure 5-12. Effect of pH and lipopeptide/resin ratio on the percentage fengycin adsorbed on HP-20 resin shown as (a) 3D surface plot and (b) contour surface plot. *LP/R refers to the lipopeptide to resin ratio. The surface plots were generated in STATISTICA 13.2*
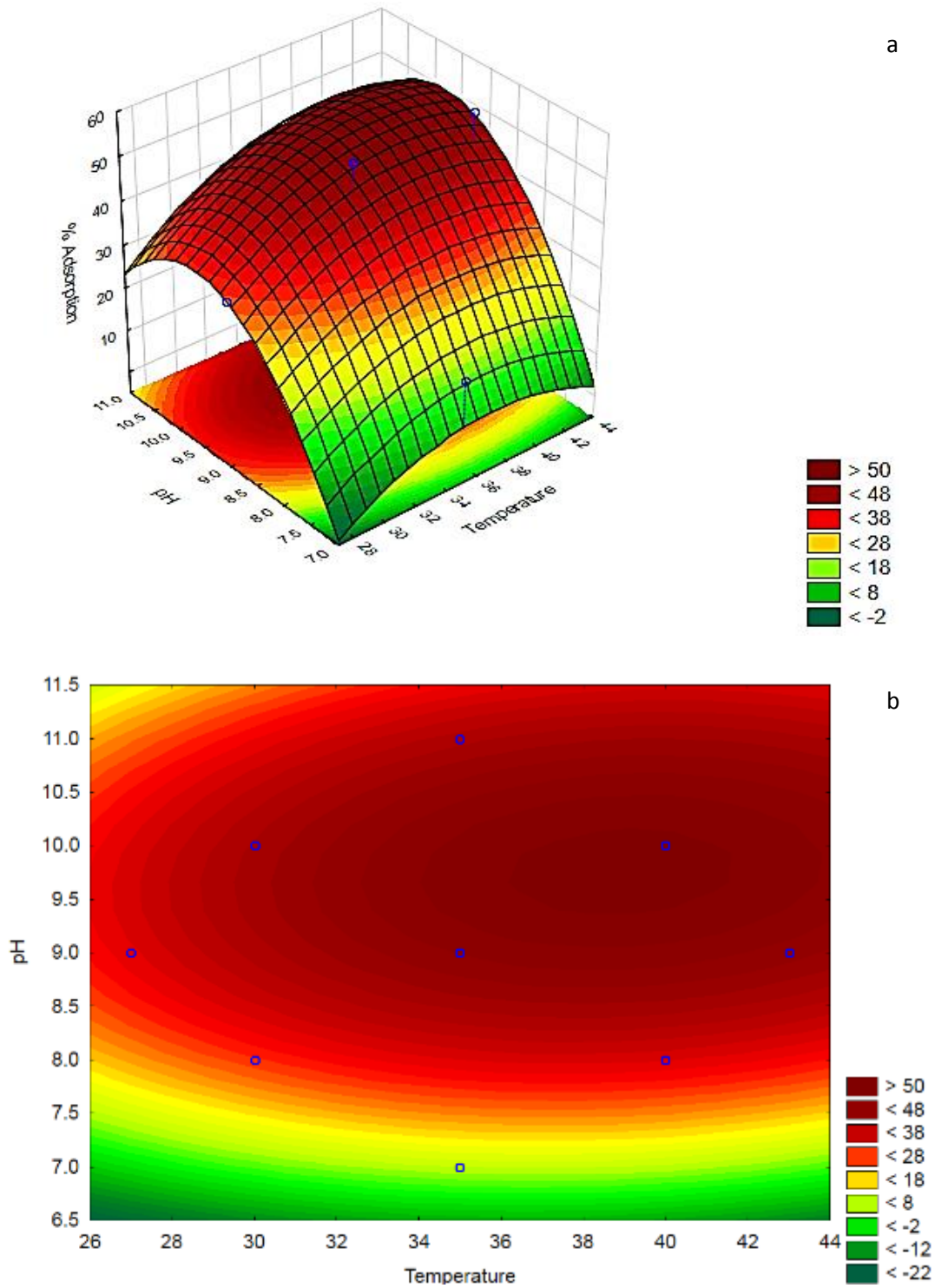
Figure 5-13. Effect of pH and temperature on the percentage fengycin adsorbed on HP-20 resin shown as (a) 3D surface plot and (b) contour surface plot. *The surface plots were generated in STATISTICA 13.2*

Since *B. amyloliquefaciens* was a co-producer of the three LP families with 70% of the total LPs produced being fengycin, CCD experiments were designed based on the fengycin concentration. Since it was determined that iturin and surfactin account for 20% and 10% respectively of the total LPs produced, the LP/R ratio could be determined separately for iturin and surfactin. Once the LP/R ratio was determined, the same temperature and pH values used for fengycin were inputted into STATISTICA to obtain response surface plots for iturin and surfactin respectively.

5.4.1.2. Iturin adsorption parameters on HP-20 macroporous resin

Data analysis of the adsorption behaviour of iturin on the HP-20 resin illustrated that the temperature and LP/R ratio were equally significant variables that influence the adsorption of iturin as shown in Figure 5-14, in contrast to pH that was found to be significant in the adsorption of fengycin. The linear term of temperature and the quadratic term of the LP/R ratio significantly influenced the adsorption of iturin on HP-20 resin. This implied that the effect of temperature, without any interaction(s) with the other two variables was significant in the adsorption of iturin while the LP/R ratio dependent on the interaction with temperature to influence the adsorption of iturin.

Since iturin responded differently (from fengycin) to the tested variables, this allowed for selective adsorption of the LPs under different LP/R ratios, pH and temperature. Based on the data from the surface plots shown in Figure 5-15 - Figure 5-17, no optimal conditions could be determined as the LP/R ratio ranges may exist outside the experimental region investigated. This suggested that the range of iturin concentrations used was narrow and thus further optimisation studies for iturin are required. However, based on the experimental region for iturin, the minimum conditions for further investigation on the adsorption of iturin was determined to be 0.01, 40°C and 9 for the LP/R ratio, temperature and pH respectively.
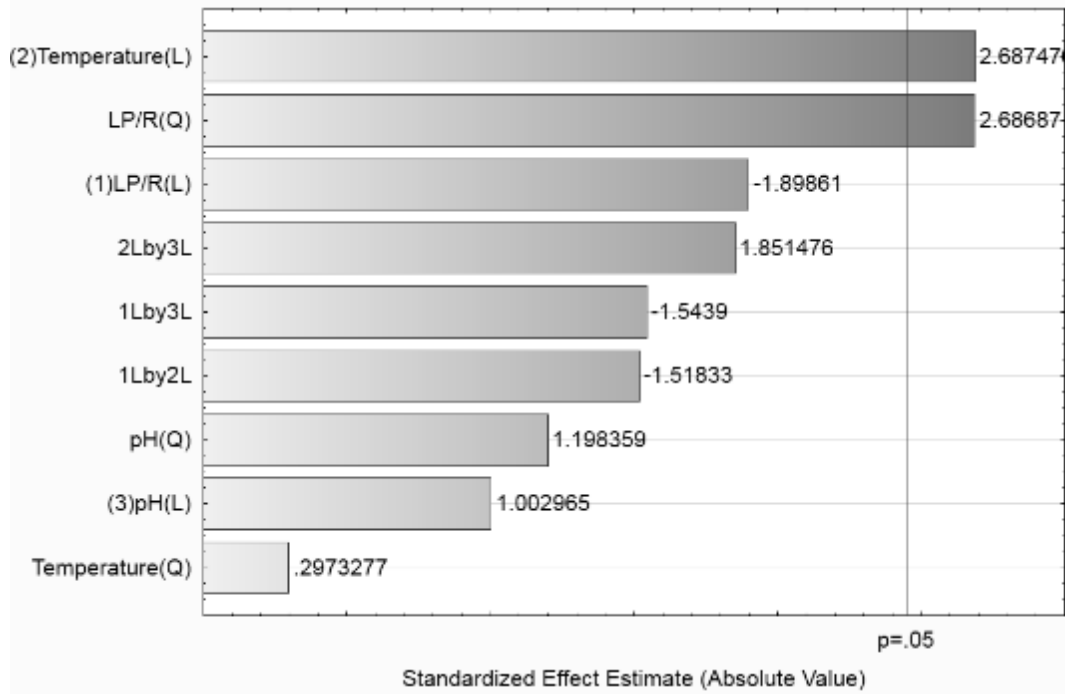
Figure 5-14. Degree of variable contribution on the adsorption of iturin on HP-20 resin. *L refers to the linear terms and Q to the quadratic terms of the model. The Pareto chart was generated in STATISTICA 13.2*
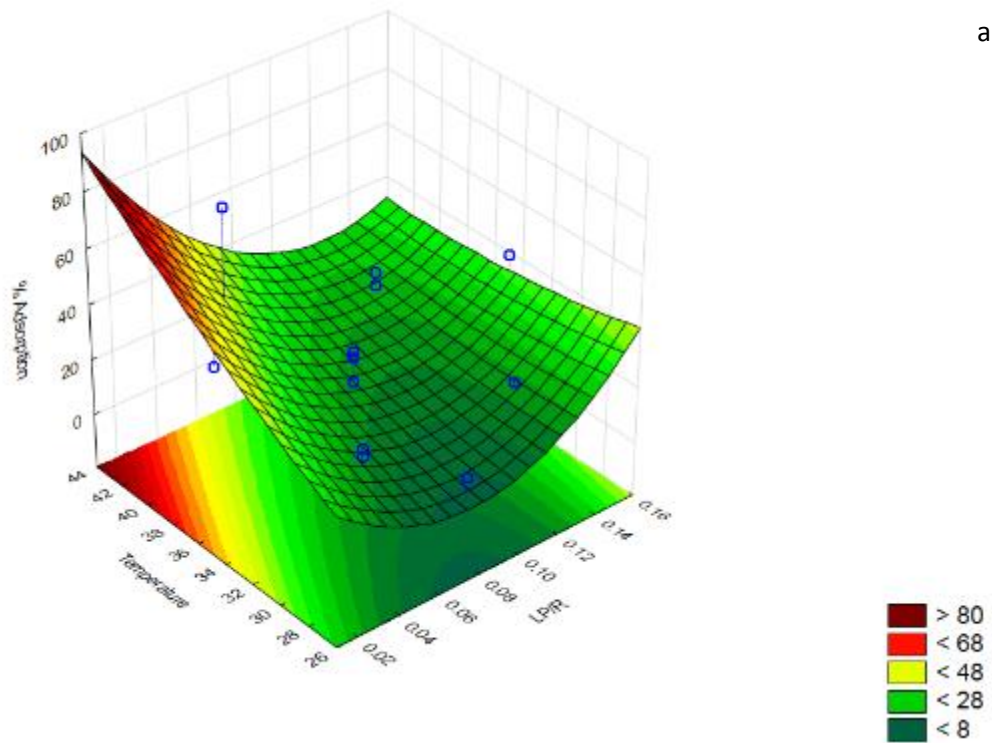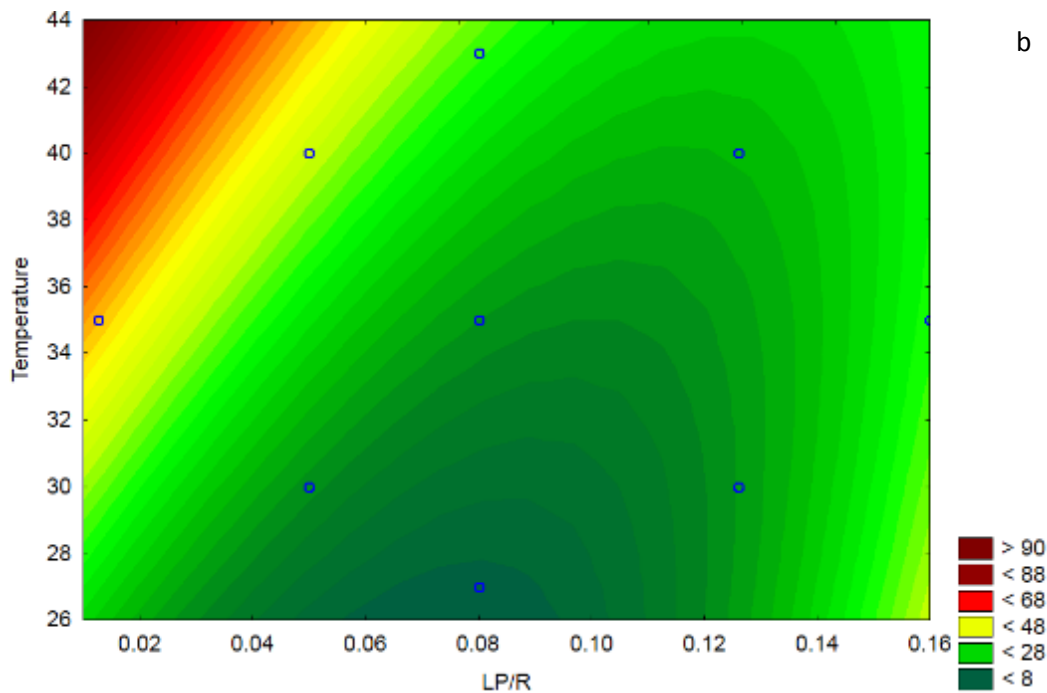
Figure 5-15. Effect of temperature and lipopeptide/resin ratio on the percentage iturin adsorbed on HP-20 resin shown as (a) 3D surface plot and (b) contour surface plot. *LP/R refers to the lipopeptide to resin ratio. The surface plots were generated in STATISTICA 13.2*

92
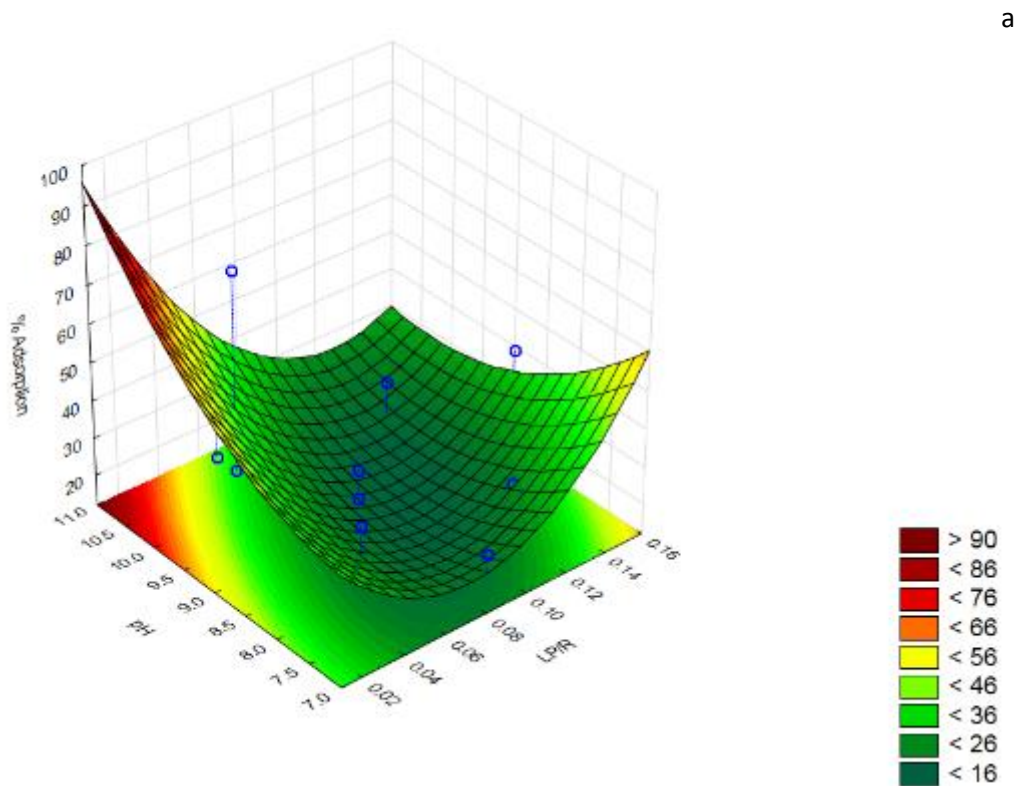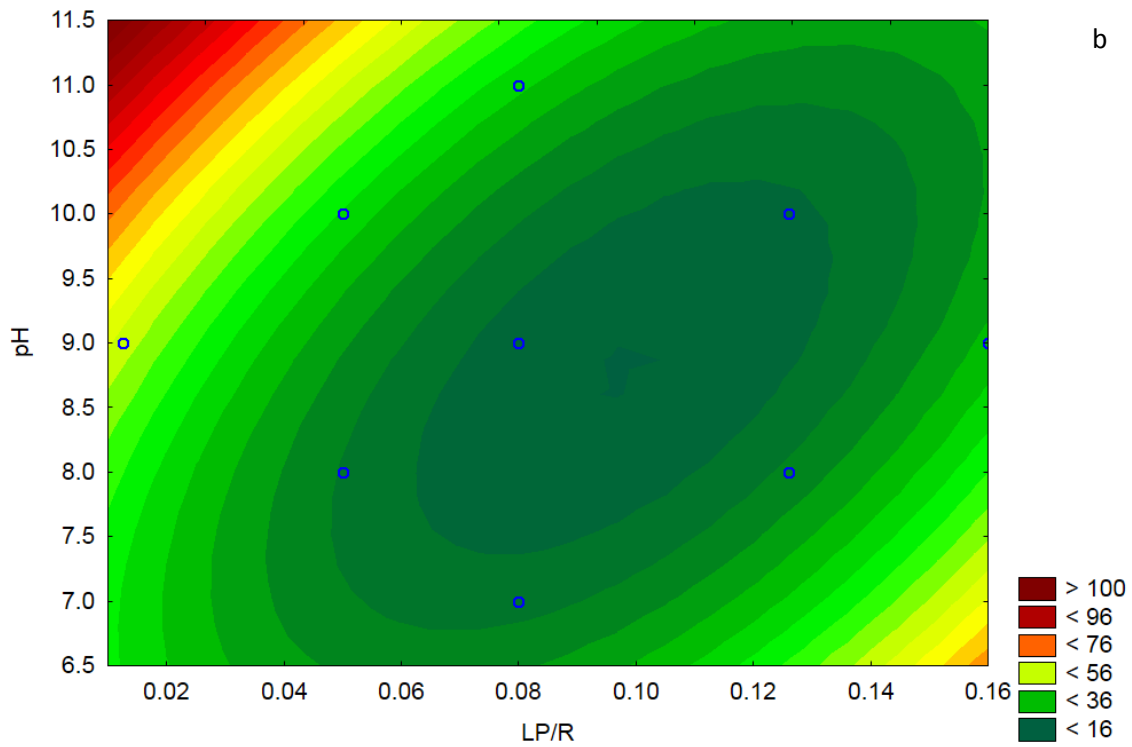
Figure 5-16. Effect of pH and lipopeptide/resin ratio on the percentage Iturin adsorbed on HP-20 resin shown as (a) 3D surface plot and (b) contour surface plot. *LP/R refers to the lipopeptide to resin ratio. The surface plots were generated in STATISTICA 13.2*

93
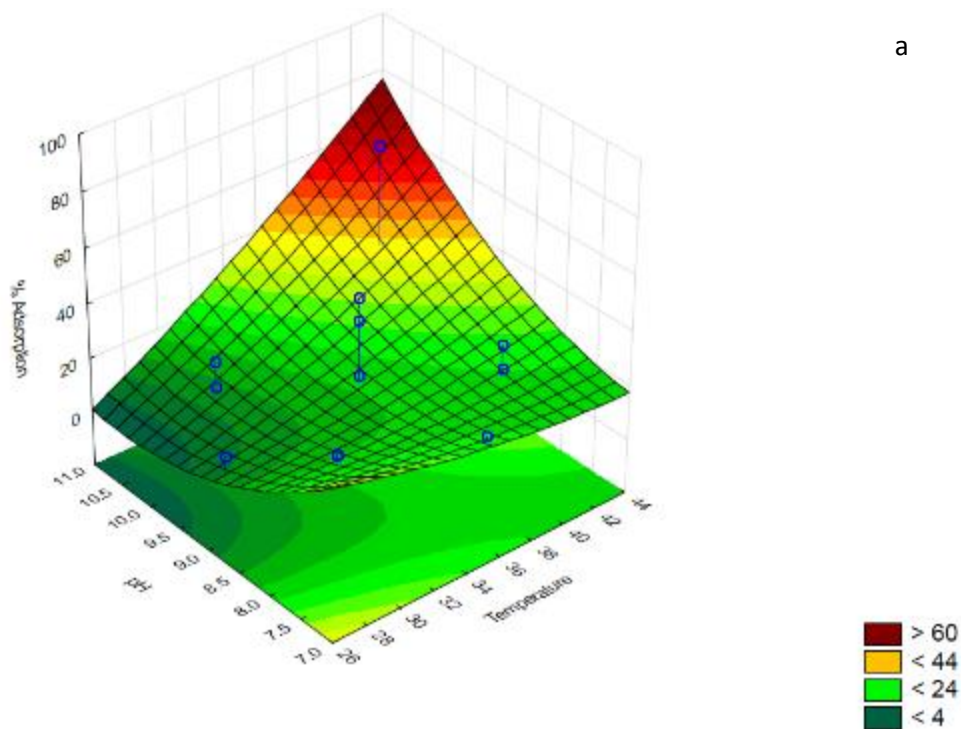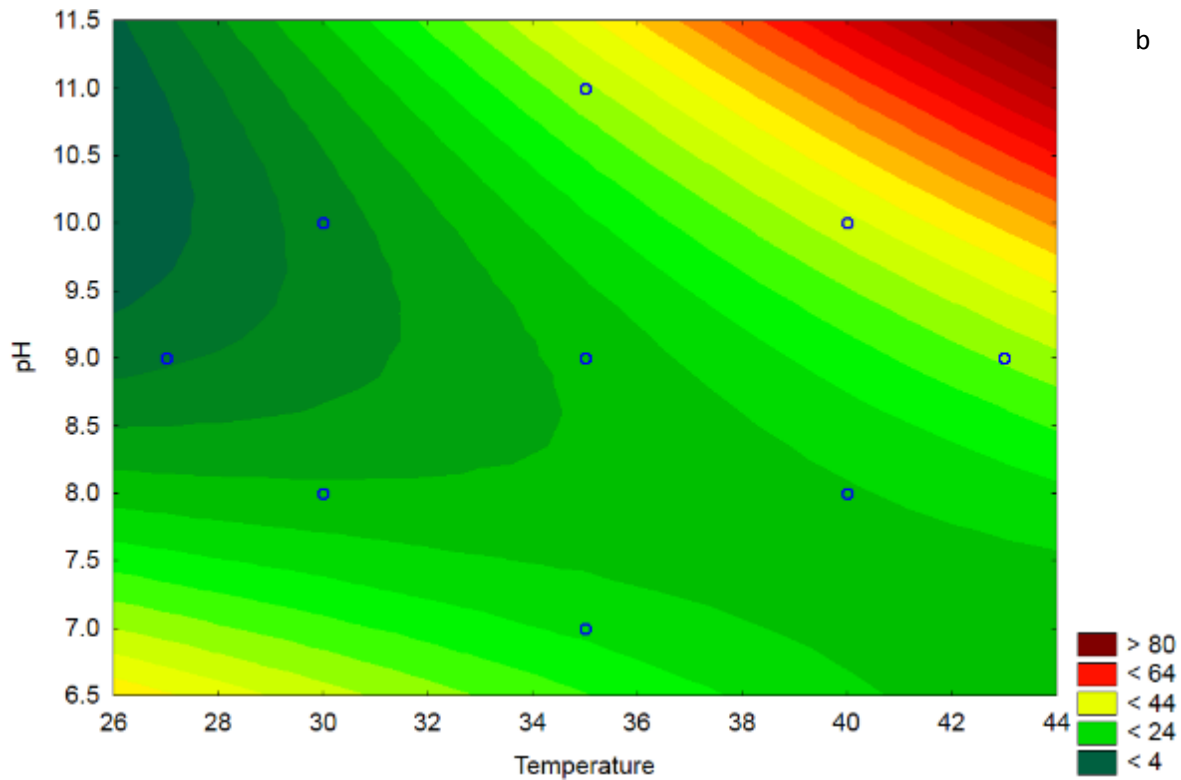
Figure 5-17. Effect of pH and temperature on the percentage iturin adsorbed on HP-20 resin shown as (a) 3D surface plot and (b) contour surface plot. *The surface plots were generated in STATISTICA 13.2*

5.4.1.3.   Surfactin adsorption parameters on HP-20 macroporous resin

Interestingly, none of the tested variables had any significant effect (at α =0.05) on the adsorption of surfactin on HP-20 resin as can be seen in Figure 5-18. The data from the surface plots shown in Figure 5-19 - Figure 5-21. One reason for the insensitivity of the surfactin adsorption to the tested variables may have been the initial surfactin concentration. Since the LP mixture used was low in surfactin (as a function of the organism's LP productivity), this resulted in the narrow range of the LP/R ratio, which could have resulted in the insignificance of all the variables including the LP/R ratio.
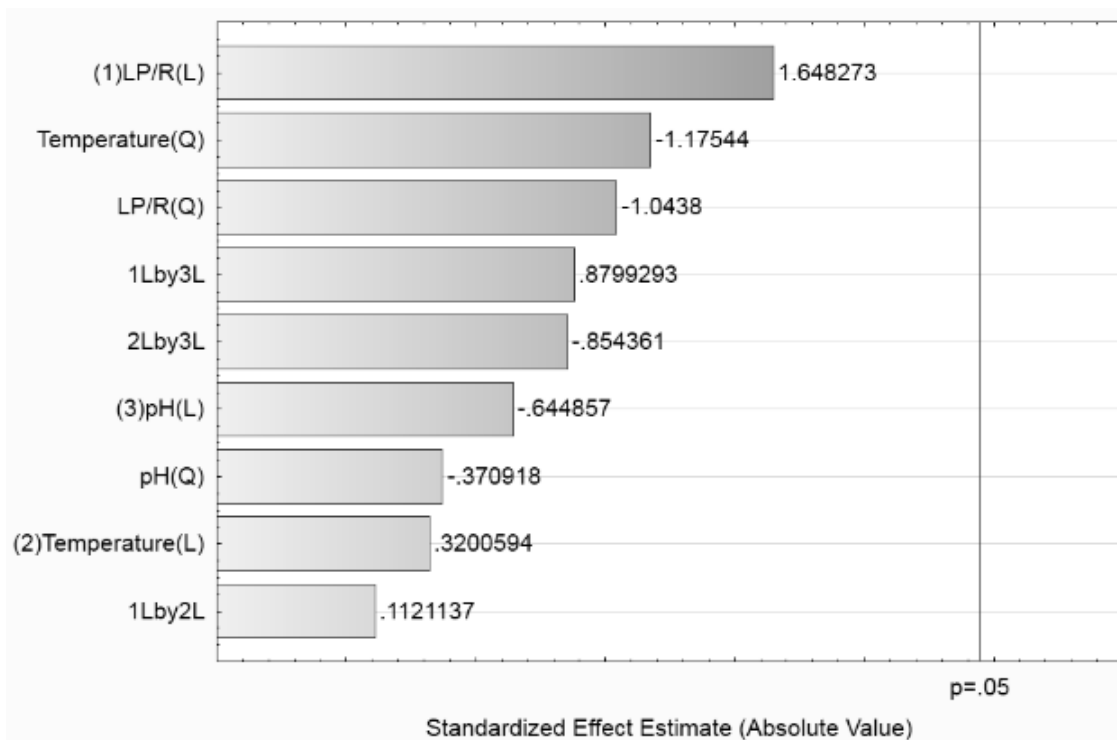
Figure 5-18. Degree of variable contribution on the adsorption of surfactin on HP-20 resin. *L refers to the linear terms and Q to the quadratic terms of the model. The Pareto chart was generated in STATISTICA 13.2*

a
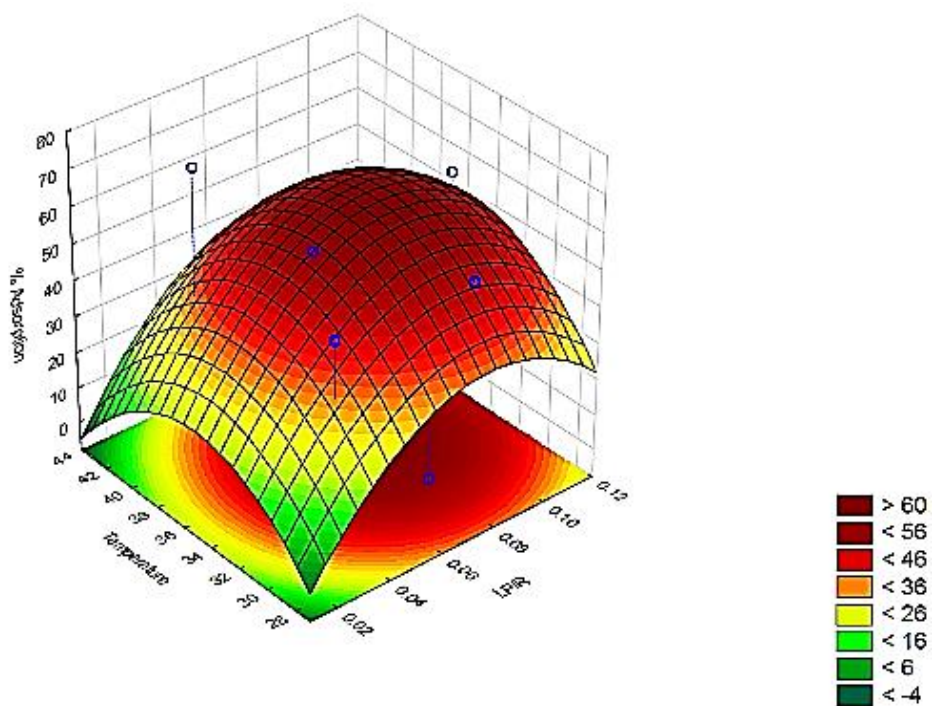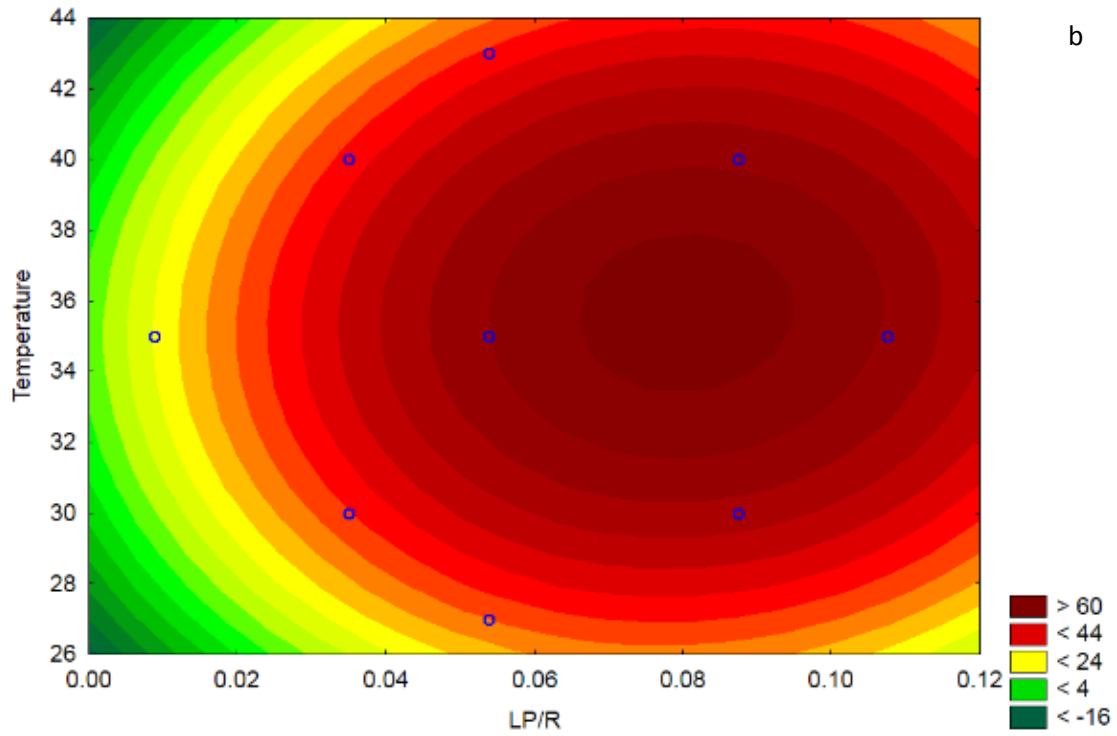
Figure 5-19. Effect of temperature and lipopeptide/resin ratio on the percentage surfactin adsorbed on HP-20 resin shown as (a) 3D surface plot and (b) contour surface plot. *LP/R refers to the lipopeptide to resin ratio. The surface plots were generated in STATISTICA 13.2*

96
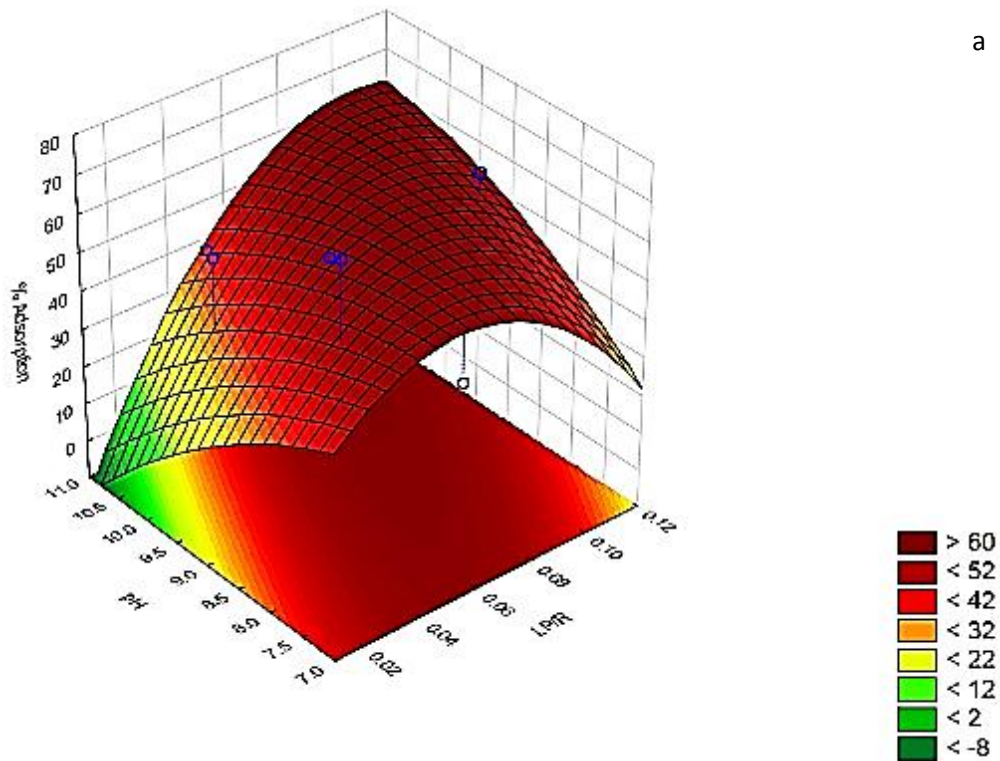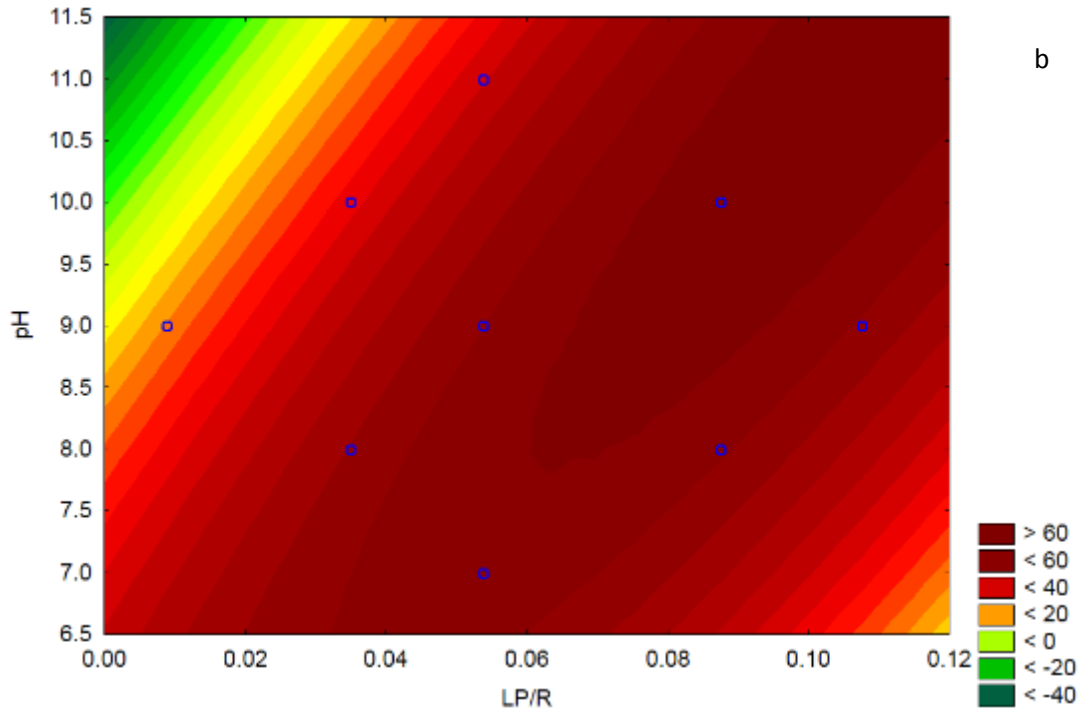
Figure 5-20. Effect of pH and lipopeptide/resin ratio on the percentage surfactin adsorbed on HP-20 resin shown as (a) 3D surface plot and (b) contour surface plot. *LP/R refers to the lipopeptide to resin ratio. The surface plots were generated in STATISTICA 13.2*

97
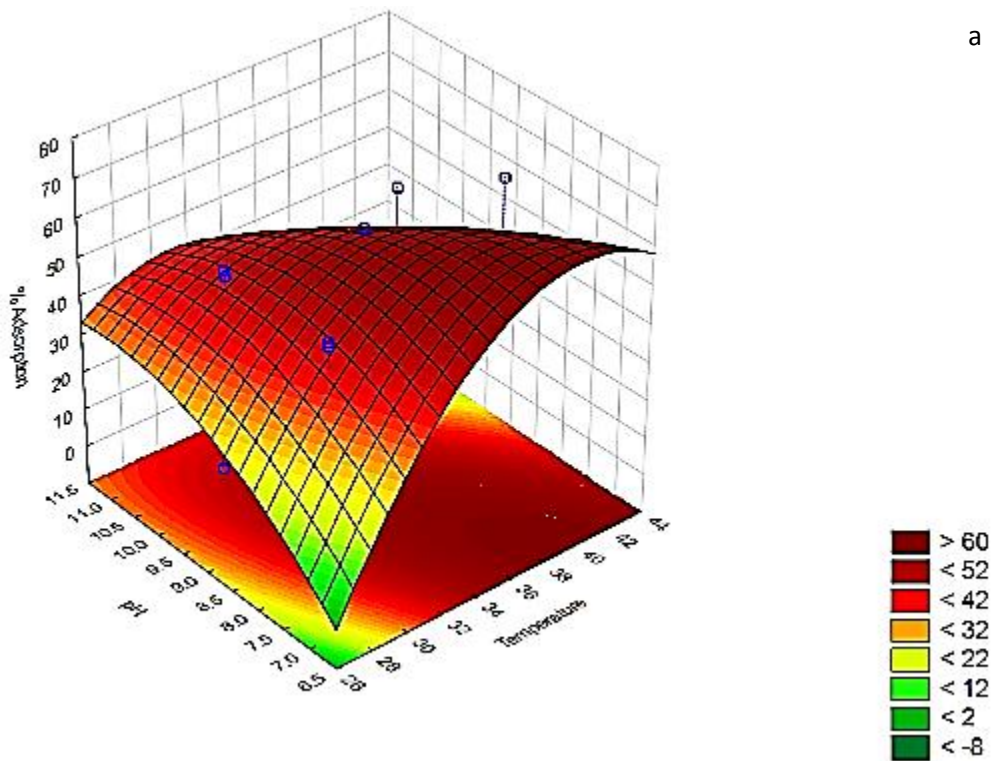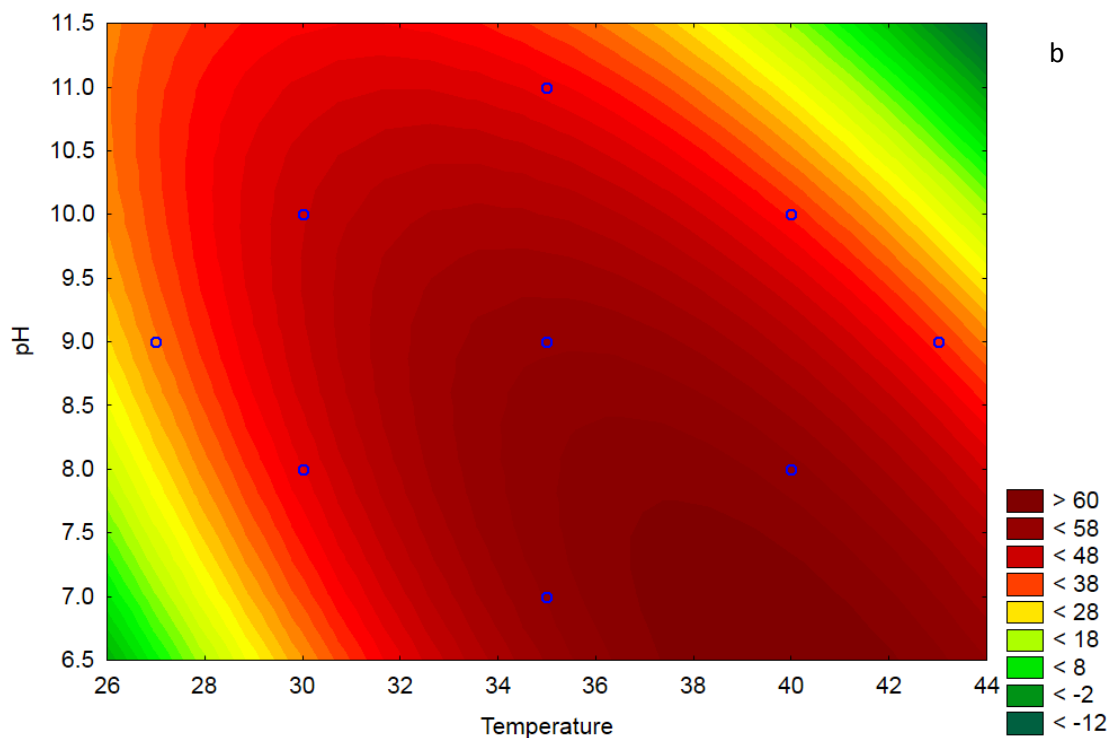
Figure 5-21. Effect of pH and temperature on the percentage surfactin adsorbed on HP-20 resin shown as (a) 3D surface plot and (b) contour surface plot. *The surface plots were generated in STATISTICA 13.2*

The optimal fengycin adsorption conditions were used for adsorption isotherms and kinetic studies and as such, the resulting iturin and surfactin conditions were determined, although these conditions were not specifically optimum for the latter two LP families. Since the three LP families have different optimal adsorption conditions, selectivity of adsorption towards individual LPs can be achieved.

It can be concluded that the common thread observed in the surface plots of the adsorption conditions of fengycin and iturin is that the LP/R ratio was found to be a significant variable that influenced the adsorption of the LPs on HP-20 resin in comparison to the other two variables, namely temperature and pH. Nonetheless, the temperature and pH may aid in the selectivity among the three LP families which can be further used to optimise iturin and surfactin produced by *B. amyloliquefaciens*.

5.4.2. Adsorption Kinetics
The rate at which maximum LPs are adsorbed onto HP-20 was investigated through adsorption kinetics studies. The kinetics of fengycin and iturin adsorption on HP-20 was studied under the optimal LP/R ratio, temperature and pH obtained for fengycin, from the CCD experiments. From the kinetic parameters of

fengycin and iturin adsorption, the behaviour of the antifungal LPs would then be explained and predicted through modelling of the experimental data through pseudo-first order and pseudo-second-order models.

The optimal adsorption conditions for fengycin, determined from the CCD experiments, was 2.5 g/L of fengycin at 5 g/L of resin (0.5 LP/R ratio), 43°C and a pH value of 10. The adsorption conditions were optimal for fengycin, as a result the corresponding LP/R ratio for iturin and surfactin was 0.13 (0.63 g/L at 5 g/L resin) and 0.088 (0.44 g/L at 5 g/L resin) respectively.

The percentage adsorption and the adsorption capacity at time t (Q_t) were both used as response variables to illuminate on the kinetics of adsorption. The percentage adsorption and Q_t, which was the mass of LPs adsorbed on the resin at any given time throughout the incubation period, was used to quantify LP adsorption. Preliminary batch kinetic experiments indicated that the adsorption equilibrium of fengycin was reached at 18 h of incubation (appendix C, Figure 0-8) thus validating that sampling of the liquid phase at 24 h in the CCD and isotherm experiments was a sufficient incubation time frame to achieve equilibrium, which those experiments needed to reach.

Under optimal adsorption kinetics, maximum Q_t of total LPs was achieved at 22 h with 0.44 ± 0.006 g of LPs adsorbed per g of resin with an adsorption percentage of 65 ± 0.91% as shown in Figure 5-22. In-depth analysis of the kinetic data indicated that an optimal Q_t of 0.34 ± 0.007 g, 0.0638 ± 0.006 g and 0.0370 ± 0.003 g for fengycin, iturin and surfactin respectively was adsorbed per g of resin at 22 h, 24 h and 18 h respectively. The corresponding percentage adsorption values for the LPs was 71.65 ± 1.45%, 53.44 ± 5.14% and 48.75 ± 3.813% for fengycin, iturin and surfactin respectively. The purity percentages of the adsorbed LPs were determined to be 74.58 ± 1.51%, 14.02 ± 1.35% and 9.78 ± 0.64% for fengycin, iturin and surfactin respectively.

The initial slope of the curve is meant to show the diffusion of adsorbate molecules from the liquid phase and onto the surface of the adsorbent (Du *et al.*, 2008). The kinetic curves shown in Figure 5-22 do not strongly indicate any diffusion trend of the LPs from the liquid phase and onto HP-20 resin surface. This may suggest that diffusion occurs rapidly and cannot be observed from the recorded data. The time of sampling may have prevented observation of the initial slope as the sampling times were too far apart (2 h intervals). It is recommended that this experiment be repeated with more frequent sampling times, to more clearly elucidate the mechanism of adsorption. As a positive of this, it appears from this data that almost complete adsorption occurs very quickly, which has implications for process scale up – fast adsorption means that low residence times, and therefore small adsorption columns, would be required.

It is evident that the surfactin kinetic parameters (Q_t and percentage adsorption) are relatively lower than those obtained for fengycin and iturin. This may be a result of the low concentration that surfactin accounts for in the total LPs produced by *B. amyloliquefaciens,* where surfactin accounts for only 10% of the total LPs produced.
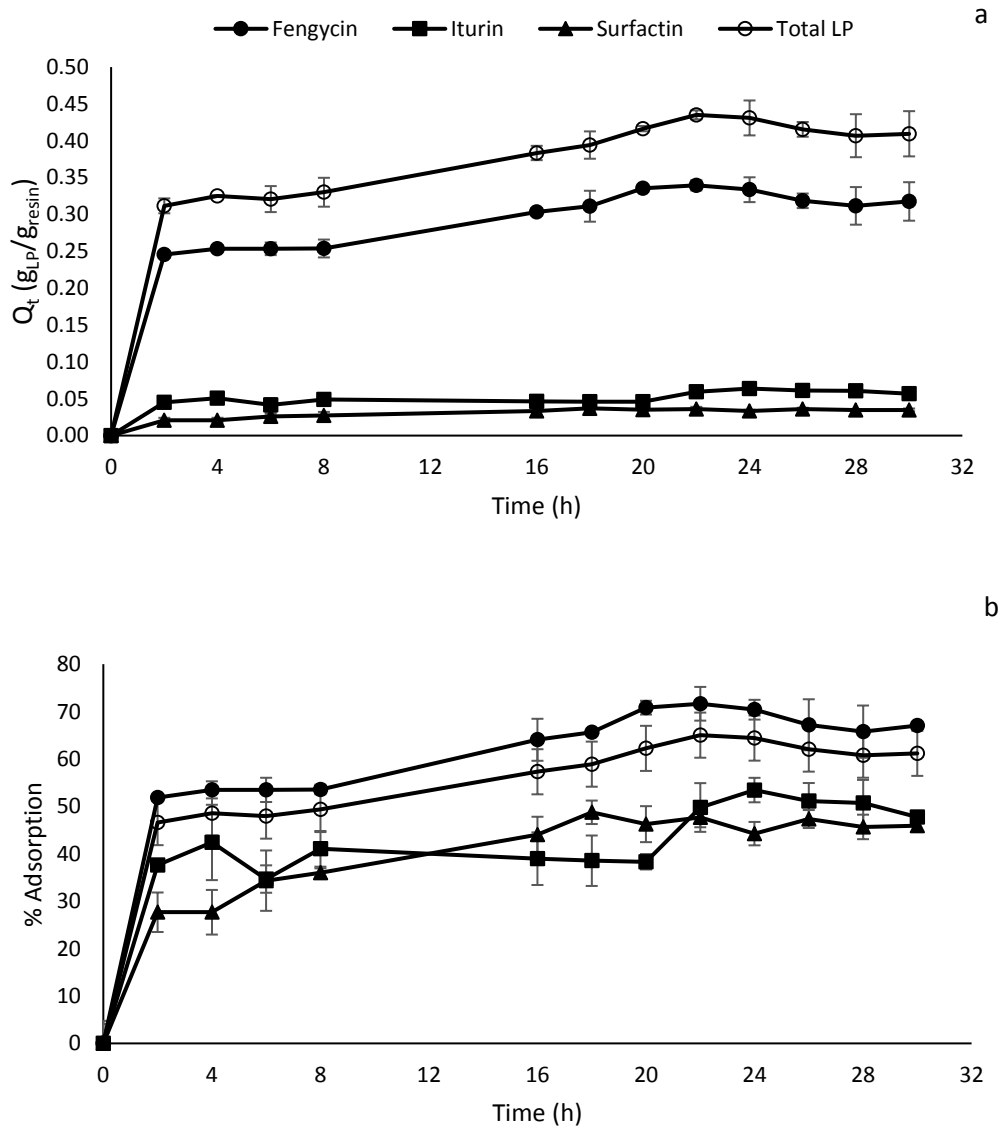
Figure 5-22. Adsorption kinetic response (a) Q_t and (b) percentage adsorption of lipopeptides on HP-20 resin at optimal fengycin adsorption conditions. *Optimal conditions were obtained from a central composite design (CCD). The data points represent the mean values calculated from triplicates at each time point with the standard deviation of the mean represented by the error bars.*

Since adsorption kinetics informed about the rate at which maximum LP adsorption was achieved on HP-20 resin in batch adsorption equilibrium studies, pseudo-rate-order models were used to investigate the rate limiting step of LP adsorption.

A pseudo-rate-order reaction is used to determine the order of reactants in a system involving multiple reactants, whose concentrations change over time. Pseudo-rate-order reactions are second-order reactions, where the rate of the reaction is dependent on the concentration of two first order reactants (reaction rate dependent on concentration of two reactants) or one second order reactant (reaction rate dependent on the product concentration of a single reactant).

To determine the mechanism of antifungal LP adsorption on HP-20 resin, two models were used, namely the pseudo-first-order rate model (appendix A, equation (10)) and the pseudo-second-order rate model (appendix A, equation (11)), to investigate the possible rate limiting step which is known to be mass transfer (diffusion) or chemical interactions. Both pseudo-kinetic models explain solid-liquid adsorption (Qiu *et al.*, 2009). The rate limiting step in the pseudo-first-order rate model is diffusion and thus explains physisorption while the rate limiting step in the pseudo-second-order rate model is the chemical reaction and thus explains chemisorption (Qiu *et al.*, 2009).

When non-linear models were linearized to estimate the theoretical parameters (K_1 and K_2), large differences between the experimental and theoretical Q_e were obtained. Lin and Wang (2015) reported this problem to be a result of the linearization of non-linear models, which misrepresented the data and thus the error obtained between the theoretical and experimental Q_e. Therefore, to circumvent the linearization error, a method to determine the parameters directly from the non-linear model derivation was used.

In this method, the solver function in Microsoft Excel, which uses non-linear regression, was used to minimise the difference between the experimental and theoretical Q_e through minimising the sum of squared error (SSE). When the error was minimised, the theoretical Q_e values obtained from the pseudo-kinetic models were compared to the experimental Q_e values obtained, while the pseudo-rate constants, K_1 and K_2 changed due to the change in the theoretical Q_e values, as shown in Table 5-5 and Table 5-6.

The theoretical Q_e values obtained from the pseudo-first-order model were lower than the experimental Q_e values, while the Q_e values obtained from the pseudo-second-order model were close to the experimental Q_e values which may have implied that the rate limiting step was chemisorption. However, fitting of the experimental data to the non-linear models showed that both models poorly fit the initial

101

experimental data points, while the equilibrium data points have a good fit for fengycin and surfactin as illustrated in Figure 5-23 and Figure 5-24. Generally, K_1 is dependent on the initial concentration of adsorbate. At low adsorbate to adsorbent ratios, the initial contact time of the adsorbate and resin would be explained by the pseudo-first-order model (Yuanfeng *et al.*, 2016). K_2, like K_1, can explain low adsorbate to adsorbent ratios and high adsorbate to adsorbent ratios, which suggests that the pseudo-second-order model might describe the entire adsorption process. However, the limited data points at the start of the run mean that it is difficult to conclude which model most accurately describes the physical system. It is recommended that the experiment be repeated with more frequent sampling, especially in the first few minutes.

Table 5-5. Pseudo-first-order kinetic model parameters

Lipopeptide family	Minimised error through sum of square error (SSE)		Experimental
	K_1 (h^{-1})	Q_e (g$_{LP}$/g$_{resin}$)	Q_e (g$_{LP}$/g$_{resin}$)
Fengycin	0.558339	0.309983	0.339556215
Iturin	0.846888	0.053163	0.063825283
Surfactin	0.266839	0.0348322	0.03614534
Total	0.540298	0.397612	0.435138461

Table 5-6. Pseudo-second-order kinetic model parameters

Lipopeptide family	Minimised error through sum of square error (SSE)		Experimental
	K_2 (g$_{resin}$/g$_{LP}$ h^{-1})	Q_e (g$_{LP}$/g$_{resin}$)	Q_e (g$_{LP}$/g$_{resin}$)
Fengycin	2.838476	0.330902	0.339556215
Iturin	24.05397	0.056284	0.063825283
Surfactin	10.34336	0.03861735	0.03614534
Total	1.88598	0.426203	0.435138461

It can be concluded that the pseudo-second order kinetic model might explain the adsorption of the LPs on HP-20, in which the rate limiting step may be attributed to chemisorption. Nevertheless, further experimental studies are required to determine the mechanism of antifungal LP adsorption kinetics, as the data obtained in this study is inconclusive and therefore cannot clearly inform on the adsorption of fengycin and iturin. The inadequate fit of the data on the model may be due to experimental error such as sampling times that were too far apart, or too infrequent in the initial few minutes of the experiment. Thus, it is possible that equilibrium was rapidly reached and therefore the important part of the curve was not seen.
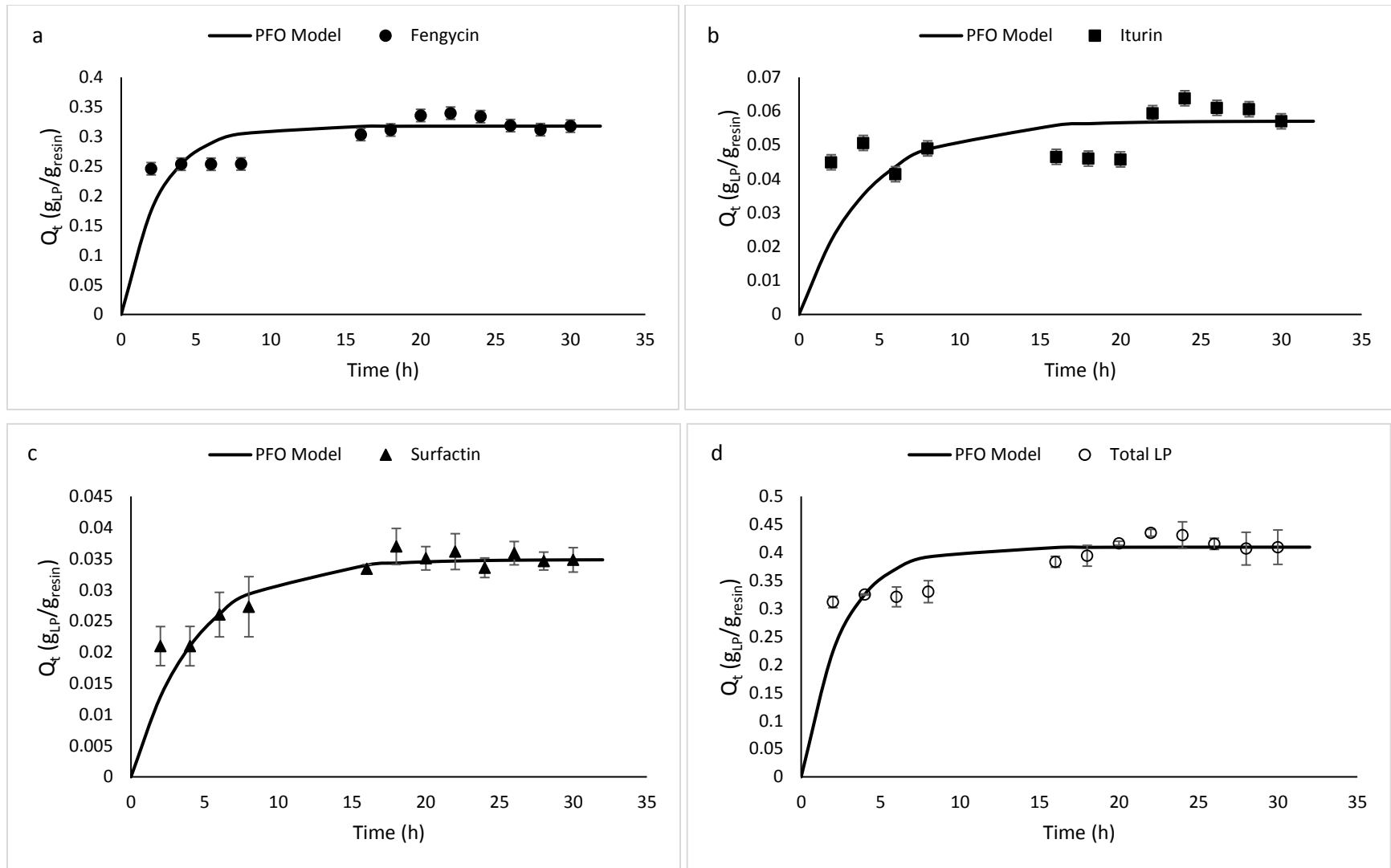
Figure 5-23. Pseudo-first-order kinetic curves of (a) fengycin, (b) iturin, (c) surfactin and (d) total LPs adsorbed on HP-20 resin. *PFO indicates the pseudo-first-order kinetic model fitted onto experimental data. The data points represent the mean experimental values calculated from triplicates at each time point with the standard deviation of the mean represented by the error bars.*
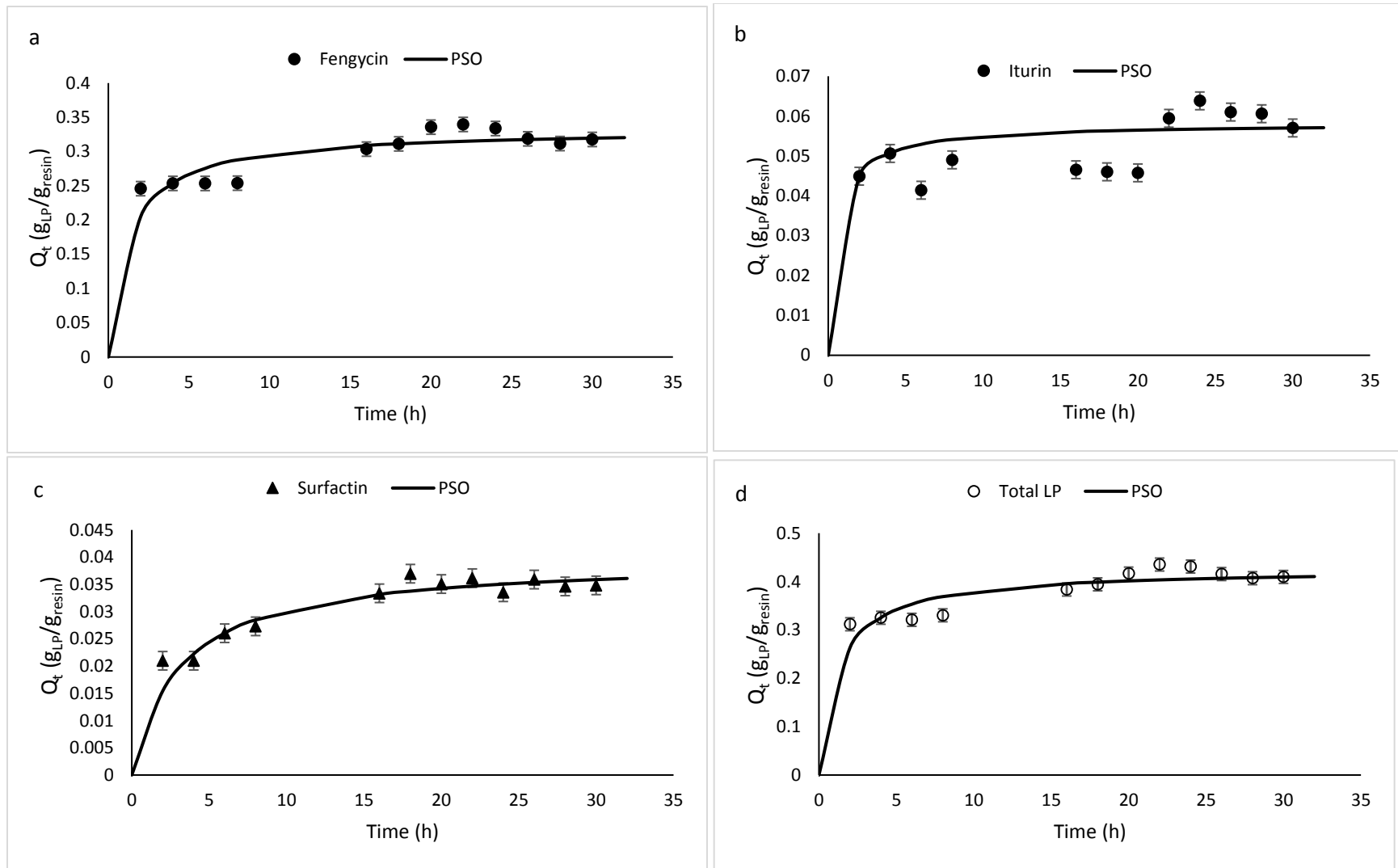
Figure 5-24. Pseudo-second-order kinetic curves of (a) fengycin, (b) iturin, (c) surfactin and (d) total LPs adsorbed on HP-20 resin. *PSO indicates the pseudo-second-order model fitted onto experimental data. The data points represent the mean experimental values calculated from triplicates at each time point with the standard deviation of the mean represented by the error bars.*

5.4.3. Adsorption isotherms

The second mechanism in which the adsorption behaviour of the antifungal LPs was studied was through adsorption isotherms. When the LP concentration is increased, the adsorption capacity (Q_e) increases until all the adsorption sites on the surface of the resin are filled and the resin is said to be saturated, thus equilibrium has been reached. To determine the LP concentration that will saturate the resin to yield the maximum Q_e, adsorption isotherm studies were conducted at a constant pH and temperature.

Adsorption isotherm studies were conducted through varying the LP/R ratio which ranged between 0.2 – 1, 0.05 – 0.25 and 0.02 – 0.18 for fengycin, iturin and surfactin respectively, at a constant pH value of 10 and temperature of 43°C which were determined to be optimal for fengycin from CCD experiments (section 5.4.1). As the LP concentration was increased, maximum Q_e values of 0.44 ± 0.002 g, 0.08 ± 0.006 g and 0.07 ± 0.01 g LPs of fengycin, iturin and surfactin respectively were adsorbed per g of resin at equilibrium, as shown in Figure 5-25. The LP concentrations used to achieve maximum Q_e values were 3 g/L fengycin, 0.8 g/L iturin and 0.88 g/L surfactin, while the corresponding maximum Q_e value of 0.57 ± 0.01 g total LP per g resin was obtained at a concentration of 4.34 g/L total LPs.

The percentage adsorption, together with the Q_e, was used to determine the LP concentration that would yield maximum LP adsorbed on HP-20 resin. A fengycin concentration of 3 g/L was determined to be the concentration required to saturate the resin as 76.5 ± 0.37% of fengycin molecules were adsorbed onto the resin as illustrated in Figure 5-26. The fengycin concentration required to saturate the resin, as established from the CCD experiments (Section 5.4.1.1), was determined to be 2.5 g/L (0.5 LP/R ratio) with 70.4 ± 3.55% of fengycin adsorbed onto the resin as illustrated in Figure 5-22.

Although the fengycin concentration that was required to saturate the resin, determined from both CCD experiments and isotherm experiments was found to be close, the percentage adsorption values indicate that the Q_e obtained using 0.5 LP/R ratio at optimal adsorption conditions (pH 10 and 43°C) was not the optimal Q_e, implying that the resin was not saturated at this ratio. Furthermore, it was observed that when the fengycin concentration was increased beyond 3 g/L, Q_e did not plateau, instead Q_e decreased with an increase in the fengycin concentration (Figure 5-25) which is a contrary observation to what was expected according to literature (Dhanarajan *et al*., 2015). This observation suggested that: (1) at high fengycin concentrations, the micelle structure conformation may change which inhibits the adsorption of fengycin onto the resin surface and (2) chemical interactions start occurring between the resin and the fengycin molecules which may prevent the adsorption of fengycin molecules at high fengycin concentrations.

The Iturin and surfactin Q_e values followed the expected plateau trend, except for the Q_e values obtained at the iturin and surfactin concentrations of 0.9 g/L and 0.61 g/L respectively. This suggested that the sample may have been contaminated with microbial contaminants, despite all attempts to remain sterile, resulting in decreased LPs available for adsorption.

When comparing the Q_e values with the percentage adsorption values for iturin and surfactin, the iturin concentration required to saturate the resin was determined to be 0.5 g/L with a percentage adsorption of 54.5 ± 3.99%, indicating that the maximum Q_e was 0.05 ± 0.011 g iturin per g resin instead of 0.08 ± 0.006 g iturin per g resin as previously suggested (based only on the Q_e value) as shown in Figure 5-25. The surfactin concentration required to saturate the resin was determined to be 0.54 g/L with 58.6 ± 4.18% of surfactin molecules adsorbed per g of resin, therefore the maximum Q_e was 0.06 ± 0.004 g surfactin per g resin instead of 0.07 ± 0.01 g surfactin per g resin as previously suggested (based only on the Q_e value, Figure 5-25).

Since the adsorption kinetic data was performed at 0.63 g/L and 0.44 g/L iturin and surfactin concentrations respectively (corresponding to the 2.5 g/L fengycin concentration), none of the LP kinetics were conducted at the optimal concentration. This implied that selectivity could be achieved through the selection of an appropriate LP concentration.
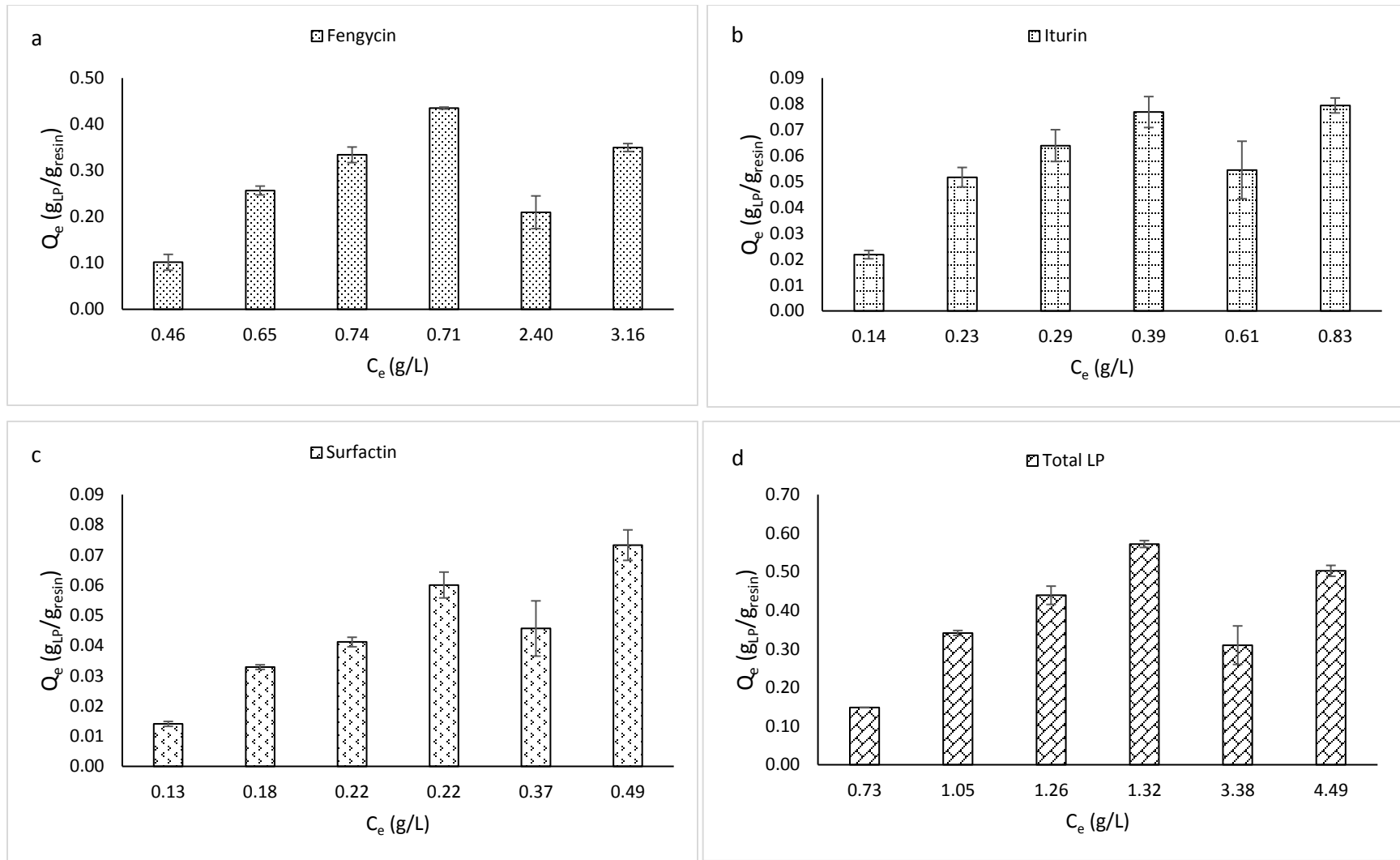
Figure 5-25. Adsorption isotherms of (a) fengycin, (b) iturin, (c) surfactin and (d) total LP on HP-20 resin at a constant temperature of 43°C and pH of 10. *The data points represent the mean experimental values calculated from triplicates at each equilibrium concentration (C_e) with the standard deviation of the mean represented by the error bars.*
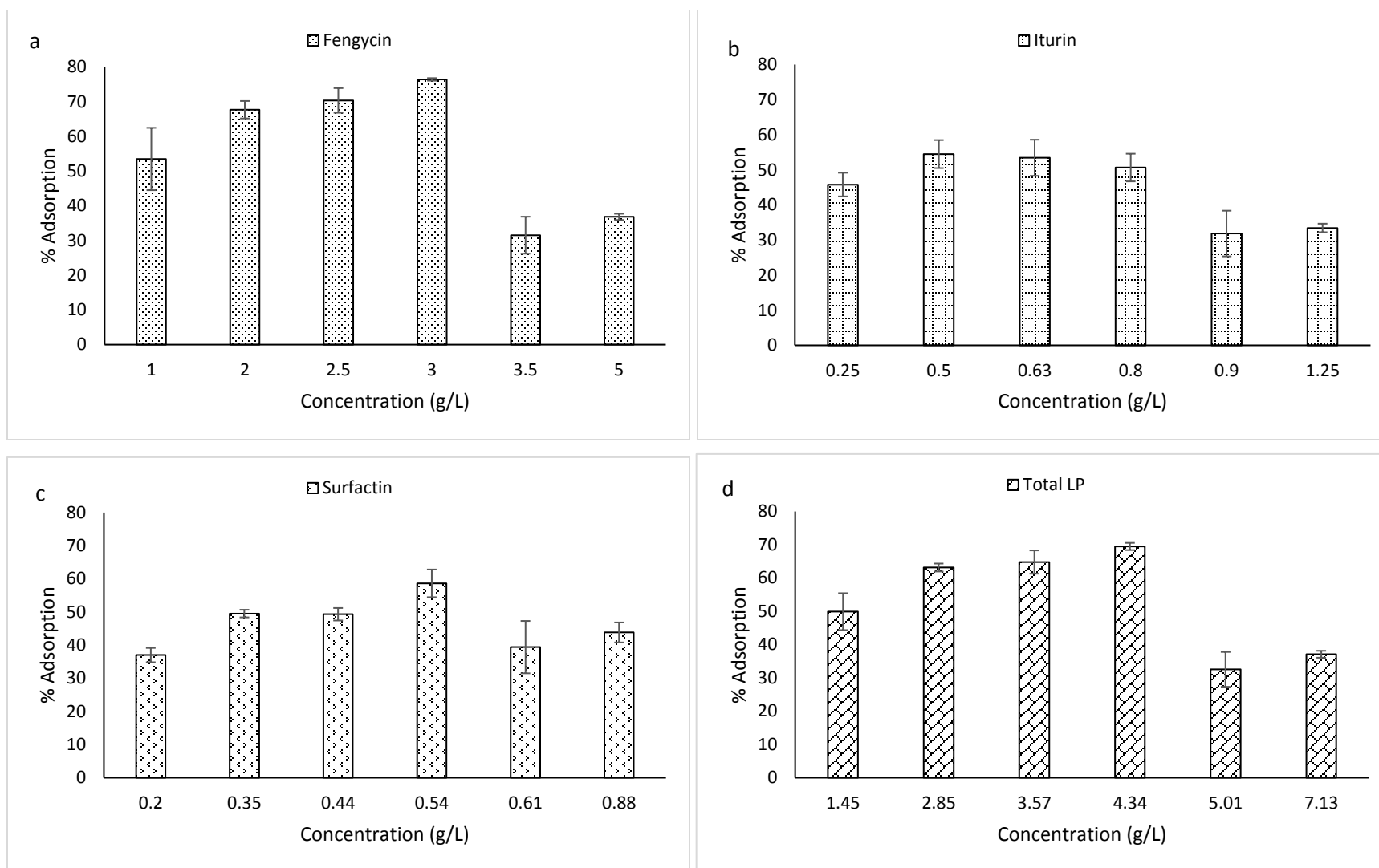
Figure 5-26. Percentage of (a) fengycin, (b) iturin, (c) surfactin and (d) total LPs adsorbed at equilibrium. *The data points represent the mean experimental values calculated from triplicates at each initial LP concentration with the standard deviation of the mean represented by the error bars.*

To attempt to understand the adsorption behaviour of the LPs on HP-20 resin, experimental data was individually fitted to the Langmuir and Freundlich isotherm models to determine which model best represented the data and thus characterised the adsorption behaviour of the LPs. The Langmuir model assumes that the surface of the resin is homogenous with a finite number of adsorption sites. When the adsorption sites are filled, a monolayer of the adsorbate molecules forms on the surface of the resin indicating that equilibrium had been reached (Dhanarajan *et al.*, 2015; Yuanfeng *et al.*, 2016). In contrast to the Langmuir model, the Freundlich model assumes that the surface of the resin is heterogeneous with an infinite number of adsorption sites which enables multi-layer formation on the resin surface (Dhanarajan *et al.*, 2015; Yuanfeng *et al.*, 2016).

When non-linear models were linearized in order to estimate the isotherm parameters (Q_m , K_L, K_F and n), large differences between the experimental and theoretical Q_e were obtained, thus the solver function in Microsoft Excel (as in section 5.4.2) was used to minimise the difference between the experimental and theoretical Q_e through minimising the sum of squared error (SSE) to obtain the theoretical parameters (Q_m , K_L, K_F and n) directly from the non-linear model.

The Langmuir and Freundlich parameters are shown in Table 5-7. The Q_m of the Langmuir model (appendix A, equation (12)) and the and K_F of the Freundlich model (appendix A, equation (13)) informed on the amount of LPs adsorbed on the resin, therefore these parameters were compared to the experimental Q_e.

Table 5-7. Langmuir and Freundlich isotherm model parameters

Lipopeptide family	Langmuir parameters		Freundlich parameters		Experimental
	Q_m (g$_{LP}$/g$_{resin}$)	K_L (L/g$_{LP}$)	K_F (g$_{LP}$/g$_{resin}$*(L/g$_{LP}$)$^{1/n}$)	n	Q_e (g$_{LP}$/g$_{resin}$)
Fengycin	0.272498	11.72713	0.363733431	2.705412	0.339556215
Iturin	0.43555	0.80121	0.135645337	2.91537	0.063825283
Surfactin	0.659994	0.416293	0.169418	1.634208799	0.03614534
Total	0.496541	10.58209	0.457901254	2.820904	0.435138461

It is evident from Table 5-7 that the Q_m and K_F differ from the experimental Q_e suggesting a lack of fit from both models. The experimental data individually fitted on the models, as shown in Figure 5-27 and Figure 5-28 further suggests the lack of fit. The lack of fit may be due to the data not following the expected plateau trend, which impacted on the fitting of the data to the models. Further isotherm experiments need to be conducted to obtain conclusive isotherm data as well as other models such as the Redlich–Peterson model, in addition to the Langmuir and Freundlich model can be used to determine the adsorption behaviour of the LPs. The Redlich–Peterson isotherm model has been reported to provide a higher accuracy in estimating the isotherm parameters than both the Langmuir and Freundlich isotherm models, thus fitting of the experimental data to this model may provide a better fit (Wu *et al.*, 2010).
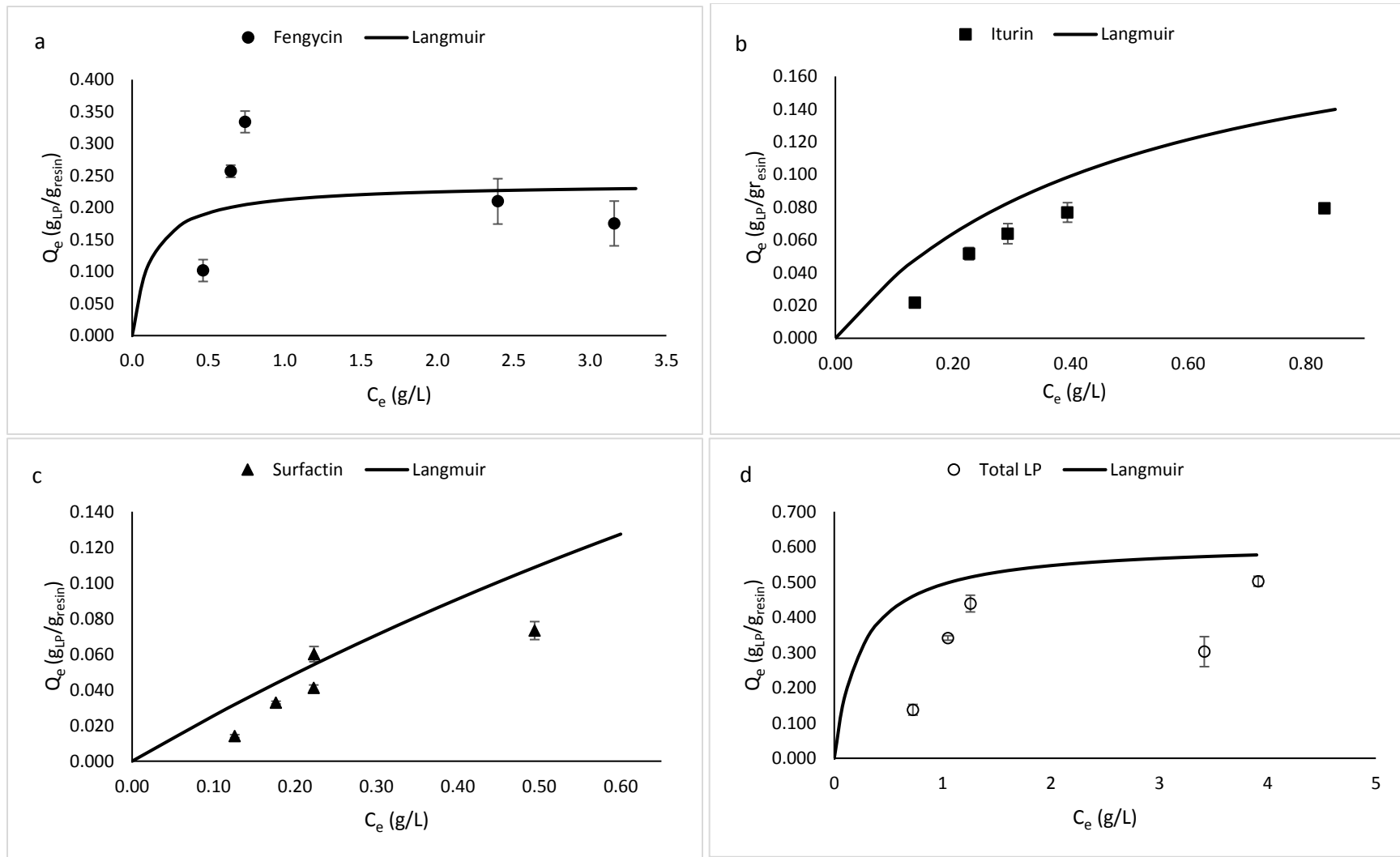
Figure 5-27. Langmuir equilibrium models of (a) fengycin, (b) iturin, (c) surfactin and (d) total LPs adsorbed on HP-20 resin. *The data points represent the mean experimental values calculated from triplicates at equilibrium concentration with the standard deviation of the mean represented by the error bars.*
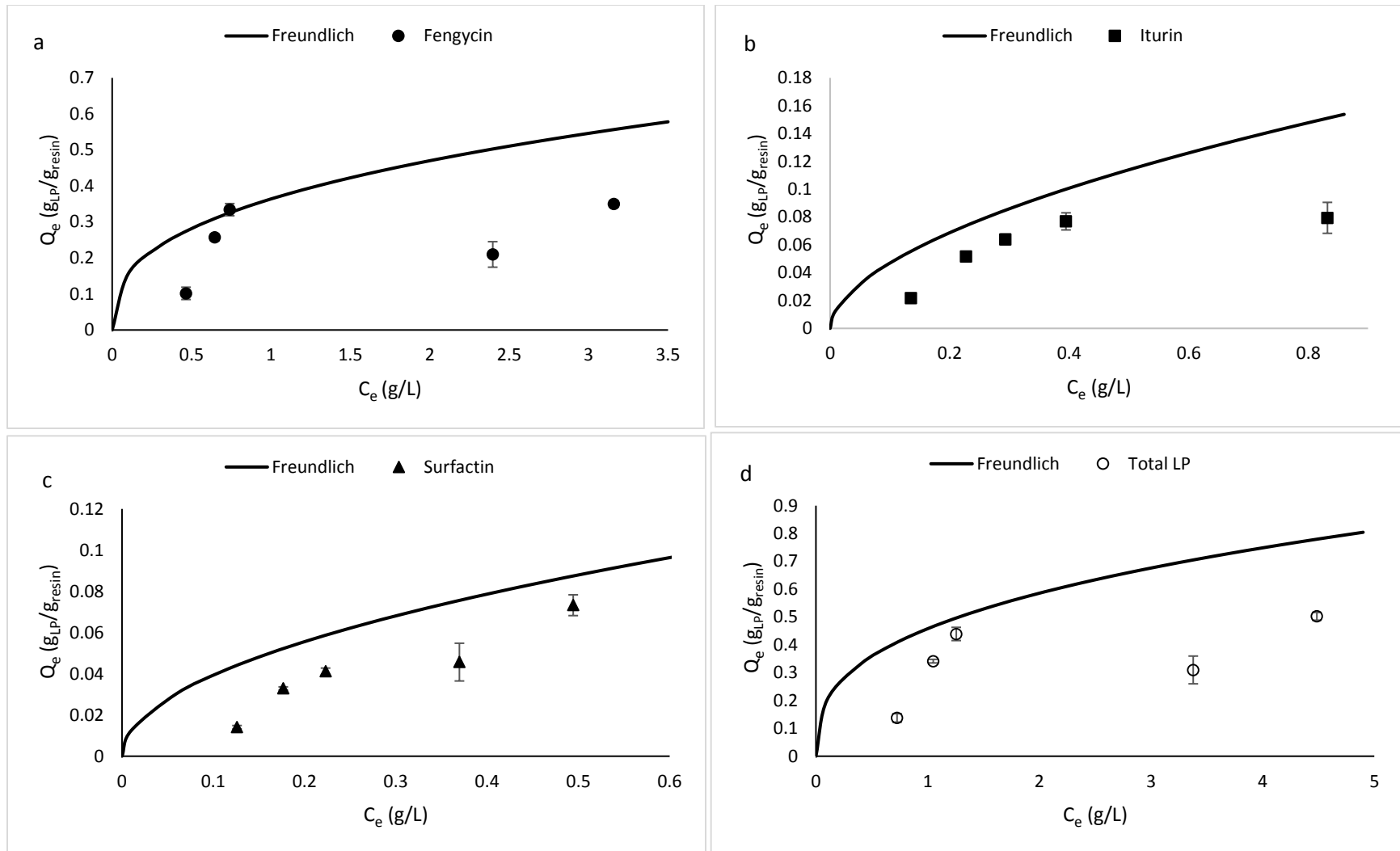
Figure 5-28. Freundlich equilibrium models of (a) fengycin, (b) iturin, (c) surfactin and (d) total LPs adsorbed on HP-20 resin. *The data points represent the mean experimental values calculated from triplicates at equilibrium concentration with the standard deviation of the mean represented by the error bars*

5.5.   Desorption

As conditions for optimal antifungal LP adsorption were determined, the quantity of antifungal LPs that could be removed from the resin was investigated through desorption studies. Desorption is described as the reverse process of adsorption and it is concerned with the removal of LPs that are adsorbed on the resin surface. Desorption experiments are commonly carried out with organic solvents of varying concentrations such as acetone (Dhanarajan *et al.,* 2015) or ethanol (Wang *et al.,* 2010).

pH has been identified in literature as an important paramater in adsorption studies as it determines the solubility of LPs in solvents of varying polarities. Therefore, the effect of methanol adjusted to different pH values on LP desorption from HP-20 resin was investigated. Methanol was individually adjsuted to 3 different pH values (pH 8, 9 and 10) and the dried resin beads recovered from adsorption at the optimal adsorption operating conditions of 43°C, 0.5 LP/R ratio and pH 10 were desorbed for 24 h at 150 rpm agitation.

It is evident from Figure 5-29 that pH has an effect on LP selectivity where methanol at pH 8 recovered a maximum of 8.62 ± 2.43% and 47.00 ± 11.52% iturin and surfactin respectively with a maximum 39.68 ± 3.32% of fengycin recovered at pH 9. This suggests that the change in pH changed the polarity of methanol, which influenced the protonated state of the amino acids in the cyclic peptide structure. Stronger interactions existed between fengycin and methanol at pH 9 implying that the deprotonated state of fengycin at this pH value was the most efficient at overcoming interactions between fengycin and the resin, thus desorption was efficient at pH 9. Methanol at pH 8 was efficient for the desorption of iturin and surfactin as stonger interactions between these LPs and methanol were possible at this pH value. Although desorption was possible, the desorption percentages were relatively lower than adsorption percentages obtained for all the LPs. A study conducted by Dhanarajan *et al.* (2015) also found the desorption percentage of LPs adsorbed on HP-20 to be lower than the adsorption percentage. The low desorption percentages may suggest that strong interactions such as covalent bonding of the LPs to the resin may exist thus inhibiting their complete desorption from the resin, however further studies are required to further explore the parameters affecting desorption, in addition to pH.
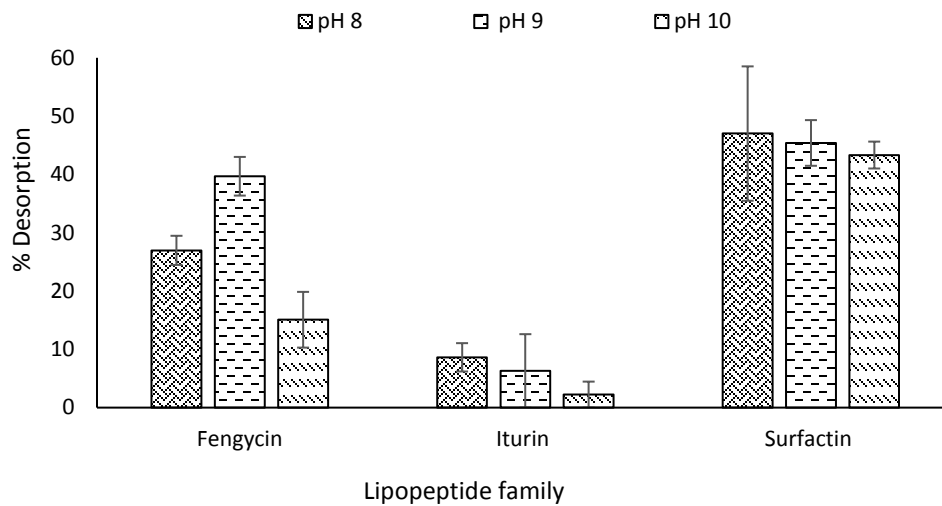
Figure 5-29. Percentage of lipopeptides desorbed from HP-20 resin with methanol at varying pH values determined by RP-HPLC. *The data points represent the mean experimental values calculated from duplicates with the standard deviation of the mean represented by the error bars*

5.6.   Antifungal homologue characterisation by LC-ESI-MS

RP-HPLC was an appropriate analytical technique to use for the differentiation and quantification of the three LP families. However, RP-HPLC was inadequate in the characterisation of fengycin homologues which can be seen in the chromatogram of the fengycin standard (appendix B, Figure 0-1). The chromatogram showed that the fengycin peaks were grouped as a large overlapping peak that could not be separated into individual peaks, which related to different fengycin homologues. This challenge made it difficult to determine which fengycin homologues were produced by *B. amyloliquefaciens,* more specifically, which homologues were expressed after concentration and purification downstream unit operations were applied. Although the focus of the research was not to study the effect of downstream unit operations on the quantity of individual fengycin (and iturin) homologues expressed, it was necessary to know which fengycin homologues were expressed by *B. amyloliquefaciens* after TLC plates spotted with LPs resolubilised in water and different solvent extracts, illustrated in Figure 5-30, showed two bands with R_f values corresponding more closely to the fengycin standard and were assumed to be fengycin (fengycin homologues). Therefore, a sensitive method such as mass spectroscopy was required to confirm whether these two bands were indeed fengycin and additionally which fengycin homologues the two bands represented.
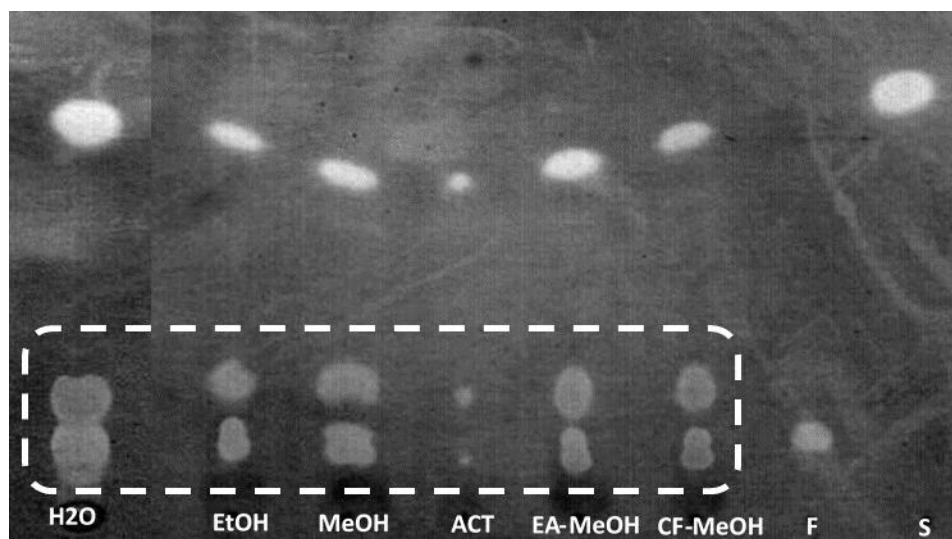
Figure 5-30. Lipopeptide organic solvent extracts separated on a TLC plate. *H_2O: Water, EtOH: Ethanol, MeOH: Methanol, ACT: Acetone, EA-MeOH: Ethyl acetate-Methanol (2:1, v/v), CF-MeOH: Chloroform-methanol (2:1, v/v), F: Fengycin standard and S: Surfactin standard. Boxed structure represents the two fengycin bands. The TLC plate was stained with 0.005% primuline reagent, scanned and the image edited with ImageJ version 1.4.3.67.*

Liquid chromatography electrospray ionisation mass spectroscopy (LC-ESI-MS) was used to determine and confirm the identity of the two LP bands obtained from TLC analysis of LP fractions from the various downstream unit operations. Since RP-HPLC analysis was unable to distinguish among the fengycin homologues, although this is not the aim of the study, the sensitive technique LC-ESI-MS was used to determine if indeed both the bands were fengycin.

Ultraperformance liquid chromatography (UPLC) was used to separate the LP homologues after which ESI was applied in the positive mode to give LP masses as mass to charge ratio (*m/z*). The *m/z* peak values were given as singly charged homologue ions ([M+H]) while some homologues contained both singly charged ions and doubly charged LP homologue ions ([M+2H]^2) whose *m/z* peak values were compared to the *m/z* peak values obtained in literature to determine the homologue identity.

The fengycin standard LC-ESI-MS chromatogram showed eight clustered peaks (appendix B, Figure 0-6) while the iturin A standard LC-ESI-MS chromatogram only showed four clustered peaks (appendix B, Figure 0-7) while both standards also showed the presence of impurities (appendix B, Figure 0-6 and Figure 0-7). The *m/z* peak values were obtained through processing of the data using the Waters MassLynx Mass Spectrometry Software (version 4.1). The four clustered iturin standard *m/z* values shown in Table 5-8 and the eight clustered iturin *m/z* values shown in Table 5-9 were compared to *m/z* values available in literature to characterise and identify the LP homologues in the standard which could then be used to identify the LP homologues present in the LP fractions.

Fragmentation of the fengycin mass peaks (in *m/z*) 1491.83 and 1506.86 showed mass peaks that had fingerprint signatures of fengycin B (i.e. 1108 and 944) and therefore they could be further identified to the specific fengycin homologues which were fengycin B (C$_{16}$) and fengycin B (C$_{17}$) respectively. Fragmentation of the remaining six fengycin peaks did not show any fingerprint signatures of either fengycin A or B thus the [M+H] and [M+2H]^2 *m/z* values were used to find the corresponding values in literature to identify the homologues. Two mass peaks (811.311 and 1187.03 *m/z*) could not be identified as these peak values did not appear in literature. However, since comparatively little work has been done on fengycin, these may simply be unidentified homologues. Nonetheless, they could not be positively identified as such without significant further research, which is beyond the scope of this study.

Only two mass peaks of the iturin A standard were identified as the remaining two mass peaks could not be identified from literature. The mass peak 811.30 (in *m/z*) appeared in both the fengycin and iturin standards which makes it difficult to characterise the type of LP with this particular mass peak. This also

117

explains the purity of the standards which shows that the fengycin standard has some iturin in it and vice versa which is also supported by the insufficient separation of iturin and fengycin by RP-HPLC where there is an overlap where iturin ends (Iturin 7 at 29.831 min) and where fengycin begins (28 min) (appendix B, Figure 0-1 and Figure 0-2).

The cell-free supernatant, resolubilised acid precipitate and solvent extracts were individually analysed by LC-ESI-MS to determine the antifungal homologues present (appendix D, Table 0-6 and Table 0-7). Of interest was the identity of the two bands that appeared on the TLC plate, that were assumed to be fengycin. LC-ESI-MS of the individually separated bands shown in Table 5-10 revealed that the mass peaks obtained for the top band contained iturin homologues while the bottom band contained a mixture of fengycin and iturin homologues apart from EA-MeOH$_2$ and CF-MeOH$_2$ which contained iturin homologues. In addition, two mass peaks that could not be identified 1184.77 (from ISO$_1$) and 1116.01 (from CF-MeOH$_2$) could be LP homologues that have never been identified prior to this study.

Table 5-8. Iturin A standard homologues determined by LC-ESI-MS

Peak no.	UPLC retention time (min)	Mass peak (*m/z*) obtained in this study		Mass peak (*m/z*) reported in literature		Homologue identity
		Doubly charged [M+2H]^2	Singly charged [M+H]	Doubly charged [M+2H]^2	Singly charged [M+H]	
1	2.323	522.27	1043.56	-	1044.5	Iturin A2 (C$_{14}$)
2	2.773	529.29	1057.56		1057.5	Iturin A3/A4/A5 (C$_{15}$)
3	**3.265**	**-**	**811.30**	**-**	**-**	**Unidentified**
4	**4.209**	**-**	**867.36**	**-**	**-**	**Unidentified**

Table 5-9. Fengycin standard homologues determined by LC-ESI-MS

Peak no.	UPLC retention time (min)	Mass peak (*m/z*) obtained in this study		Mass peak (*m/z*) reported in literature		Homologue identity
		Doubly charged $[M+2H]^2$	Singly charged $[M+H]$	Doubly charged $[M+2H]^2$	Singly charged $[M+H]$	
1	**3.381**	**-**	**811.31**	**-**	**-**	**Unidentified**
2	4.105	762.43	1524.83	-	1520.2	Fengycin B (C_{18})
3	4.518	746.92	1491.85	747.0, 747.1, 747.0	1491.8*	Fengycin B (C_{16})
4	4.931	753.43	1506.80	753.9, 754.2	1505.8*	Fengycin B (C_{17})
5	5.203	738.42	1476.86	-	1477.9	Fengycin A (C_{17})
6	**5.203**	**738.92**	**1506.62**	**-**	**-**	**Unidentified**
7	6.2	745.43	1490.84	747.0, 747.1, 747.0	1491.8*	Fengycin A (C_{18})/ B (C_{16})/ C (C_{17})
8	**6.662**	**579.29**	**1187.03**	-	-	**Unidentified**

* Contained fingerprint signatures 1108.57 (994.49) and 1109.53 (994.5) in fragmentation of [M+H] mass peak

Table 5-10. LC-ESI-MS analysis of lipopeptide organic solvent extracts separated on a TLC plate

Sample	Peak no.	UPLC retention time (min)	Mass peak (*m/z*) obtained in this study		Homologue identity
			Doubly charged $[M+2H]^2$	Singly charged $[M+H]$	
ISO_1	1	2.86	535.24	1031.55	Bacillomycin D (Iturin)
	2	3.389		1045.55	Iturin A2 (C_{14})
	3	**4.375**		**1184.77**	**unidentified**
ISO_2	1	3.389		811.31	Iturin/Fengycin
	2	4.381		867.38	Iturin
$MeOH_1$	1	2.839	543.24	1031.54	Bacillomycin D (Iturin)
	2	3.339		1045.56	Iturin A2 (C_{14})
	3	4.306		867.37	Iturin
$MeOH_2$	1	3.332		811.31	Iturin/Fengycin
	2	4.307		867.36	Iturin
	3	4.696	732.41	1464.77	Fengycin A (C_{16})
$EA-MeOH_1$	1	2.843	520.33	1031.54	Bacillomycin D (Iturin)
	2	3.343		1045.56	Iturin A2 (C_{14})
	3	4.31		867.36	Iturin
$EA-MeOH_2$	1	3.323		1034.91	Iturin
	2	4.311		867.37	Iturin
$CF-MeOH_1$	1	2.496	550.25	1031.54	Bacillomycin D (Iturin)
	2	3.289		1036.29	Iturin
	3	4.252		867.40	Iturin
$CF-MeOH_2$	**1**	**3.31**		**1116.01**	**unidentified**
	2	4.277		867.37	Iturin

Subscripts $_1$ and $_2$ refer to the top and bottom fengycin bands respectively, separated on a TLC plate. ISO: Isopropanol, MeOH: Methanol, EA-MeOH: Ethyl Acetate-Methanol and CF-MeOH: Chloroform-Methanol organic solvent extract

5.7.   *In vitro* antifungal efficacy

Antifungal efficacy studies were conducted to determine the effectiveness of the partially purified LPs and purified LP mixtures on inhibiting the growth of six common fungal phytopathogens that cause diseases of fruit during postharvest storage. Figure 5-31 - Figure 5-36 shows the growth of the phytopathogens prior to treatment with LPs.

a

b
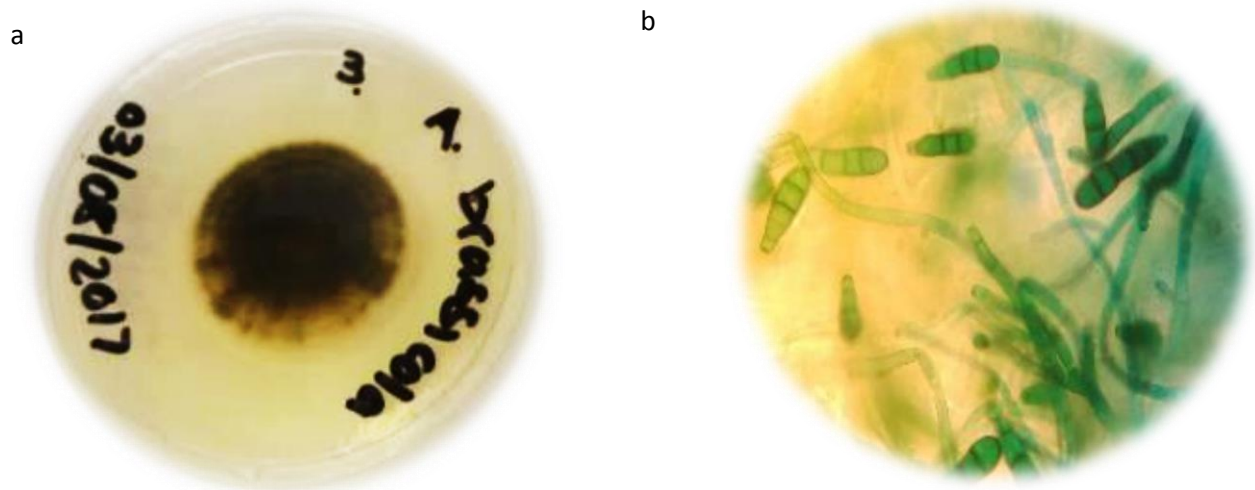
Figure 5-31. *A. brassicicola* (a) PDA plate and (b) hyphal structures with conidia**.** *Fungus grown on a PDA pate for 5 days at 30°C and wet mount slides of hyphae and conidia stained with methylene blue and viewed under 1000x magnification (Zeiss Axiostar Plus Microscope). Images captured with a digital camera.*

121

a

b
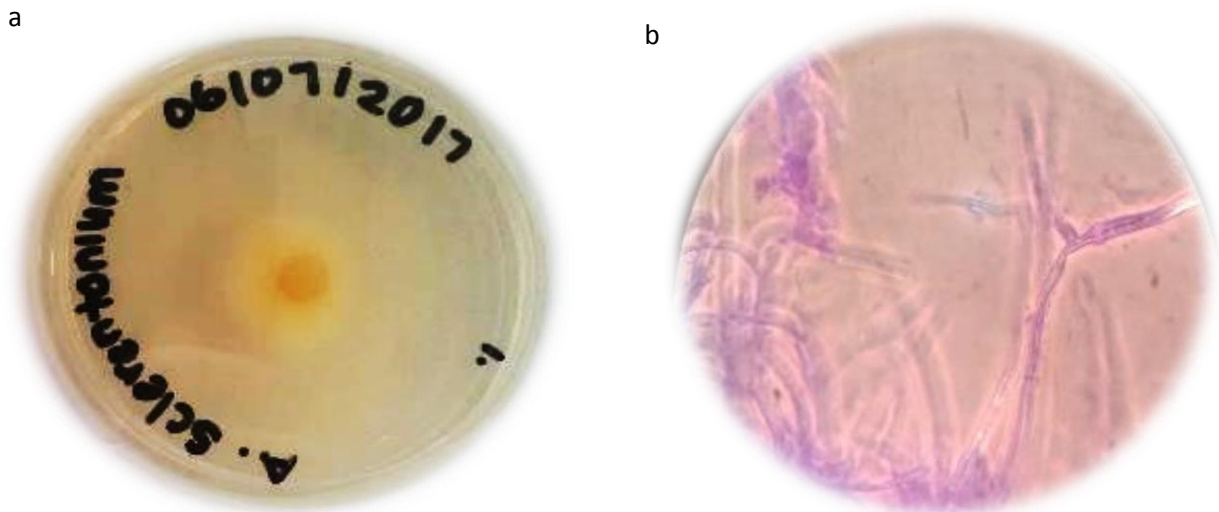
Figure 5-32. *A. sclerotiorum* (a) PDA plate and (b) hyphal structures with conidia. *Fungus grown on a PDA pate for 5 days at 30°C and wet mount slides of hyphae and conidia stained with methylene blue and viewed under 1000x magnification (Zeiss Axiostar Plus Microscope). Images captured with a digital camera.*

a

b
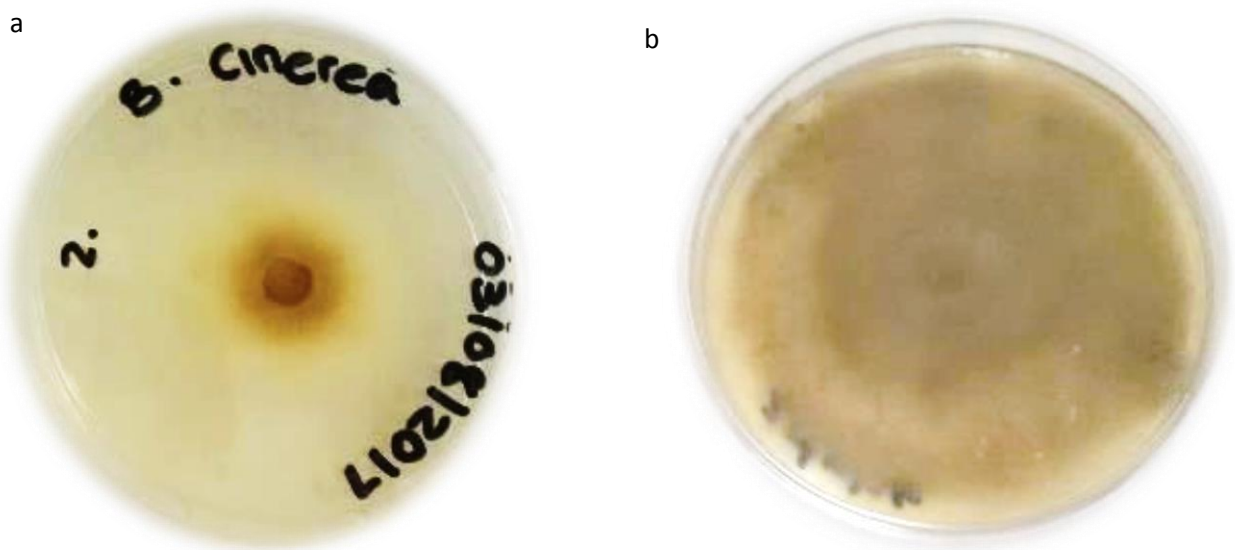
Figure 5-33. *B. cinerea* (a) bottom view and (b) top view on a PDA plate. *Fungus on (a) was grown for 5 days and (b) 2 weeks at room temperature (20 ± 3°C). images captured with a digital camera.*

a
b
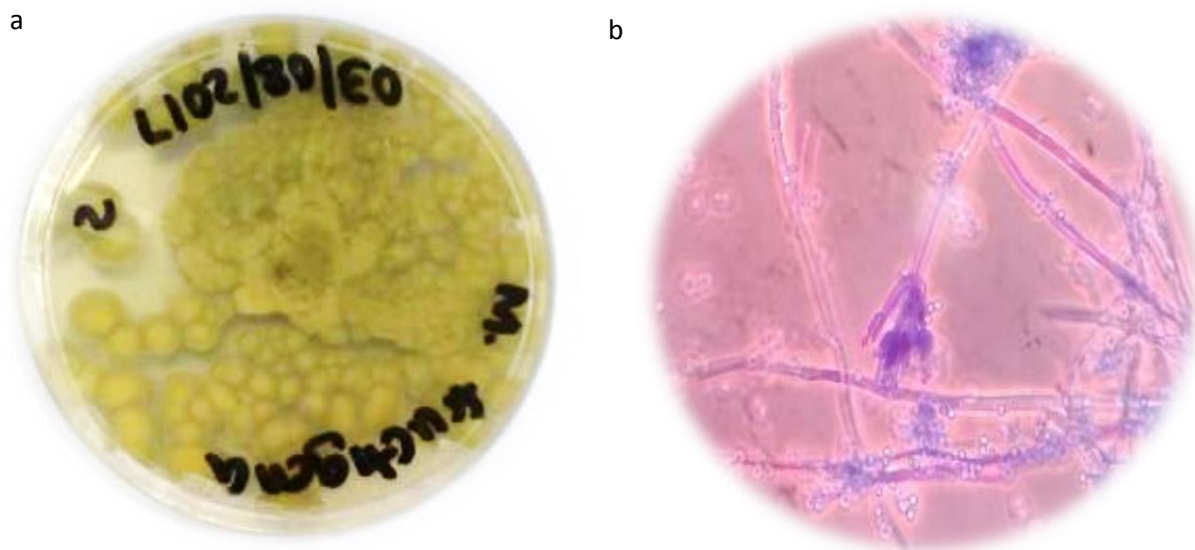
Figure 5-34. *M. fructigena* (a) PDA plate and (b) hyphal structures with conidia. *Fungus grown on a PDA pate for 5 days at 30°C and wet mount slides of hyphae and conidia stained with methylene blue and viewed under 1000x magnification (Zeiss Axiostar Plus Microscope). Images captured with a digital camera*

a
b
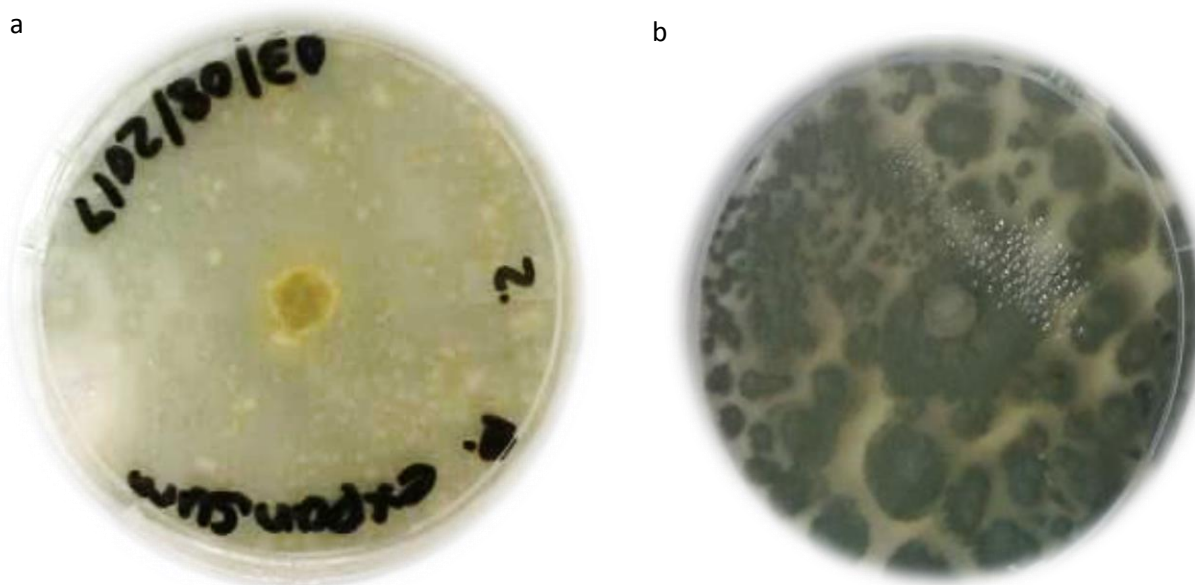
Figure 5-35. *P. expansum* (a) bottom view and (b) top view on a PDA plate. *Fungus was grown on a PDA pate for 5 days at room temperature (20 ± 3°C). Images captured with a digital camera.*

a
b
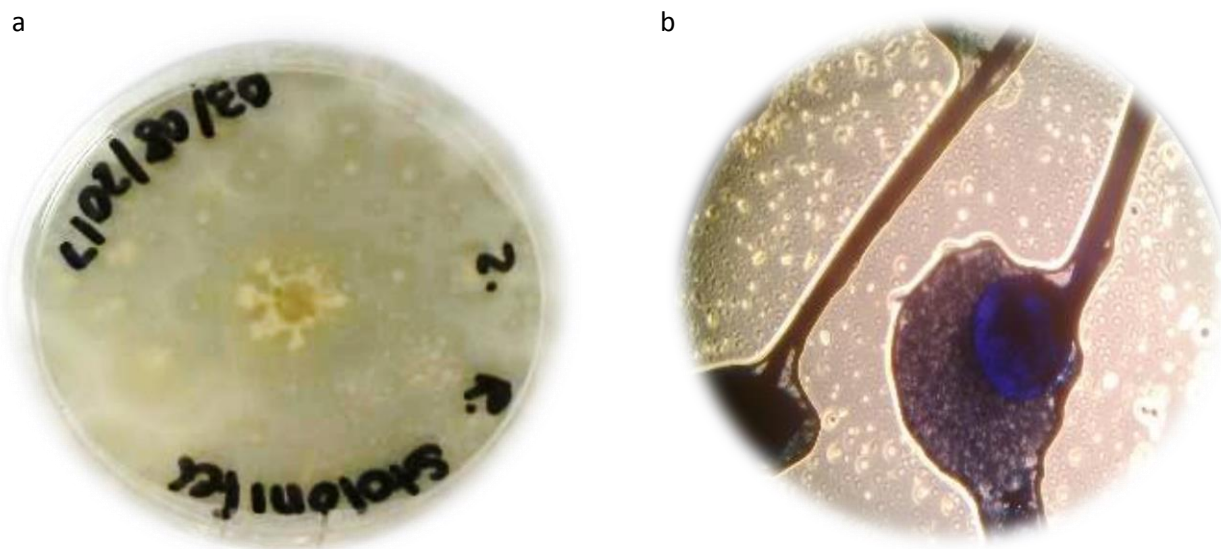
Figure 5-36. *R. stolonifera* (a) PDA plate and (b) intact sporangium on a sporangiophore. *Fungus grown on a PDA pate for 5 days at room temperature (20 ± 3°C) and wet mount slides of sporangium stained with methylene blue and viewed under 400x magnification (Zeiss Axiostar Plus Microscope). Images captured with a digital camera.*

Efficacy studies were performed using a semi-quantitative *in vitro* antimicrobial activity method which involved spreading of the individual LP fractions on PDA plates which were then inoculated with fungal plugs of the individual phytopathogens. The plates were incubated at an optimal temperature for 5 days after which the effect of the LP fractions on fungal growth was determined as the percentage growth inhibition.

The *in vitro* antifungal efficacy tests indicated the order of LP fraction effectiveness to be 12 g/L fengycin resolubilised acid precipitate 2 (RAP2) > 4 g/L fengycin resolubilised acid precipitate 1 (RAP1) > 2.15 g/L fengycin in diethyl ether-methanol extract (DiethylE-MeOH) = 2.13 g/L fengycin in methanol extract (MeOH) > 0.6 g/L fengycin in cell-free supernatant (CFS). The concentrated treatment of 12 g/L fengycin from RAP2 was found to be the overall most effective treatment with fungal growth inhibition ranging between 30 – 100% as shown in Figure 5-37 and Figure 5-38 - Figure 5-43. The CFS fraction was the least effective treatment as the concentration was 20-fold less than the 12 g/L LP fraction. Surprisingly, although the CFS was the LP fraction with the least phytopathogen inhibition effect, it had the same selectivity as RAP1 and RAP2, as shown in Table 5-11. It is evident from Figure 5-37 that *A. brassicicola* was the most susceptible phytopathogen to the LP fractions while *A. sclerotiorum* was the most resistant phytopathogen of the six pathogens studied with the order of phytopathogen susceptibility determined as: *A. brassicicola > B. cinerea > R. stolonifera > P. expansum > M. fructigena > A. sclerotiorum.*

124

It can be deduced that the LP fractions have an effect on fungal growth inhibition and the effect on fungal growth can be characterised, through further experimental studies, as either fungistatic where fungal growth is temporarily inhibited, or fungicidal, implying that the treatment disrupts hyphal structures leading to cell death. To confirm the fungistatic-fungicidal effect of LPs on the pathogen, further experiments involving the transfer of the fungal plug onto non-treated PDA plates will need to be conducted to determine if the pathogen will grow and if it does, it may imply that the LPs have a fungistatic effect which temporarily inhibited the growth of the pathogen. Further tests are required to determine the effect of the LP treatments on the hyphal and spore morphology through scanning electron microscopy (SEM), more specifically, how the fungal phytopathogens grow after treatment with the various LP fractions and the impact of phytopathogen growth defects due to prolonged exposure with LP treatments (Mnif *et al.*, 2016).

Since the method used was a semi-quantitative method, a quantitative method is required to determine the minimum inhibitory concentration (MIC) of LPs required to inhibit all six phytopathogens and how the hyphal structure and conidia are affected by the LP dosage.

It can be concluded from the data obtained in the study, as shown in Table 5-11, that the inhibition effect of fengycin is concentration dependent rather than purity dependent.
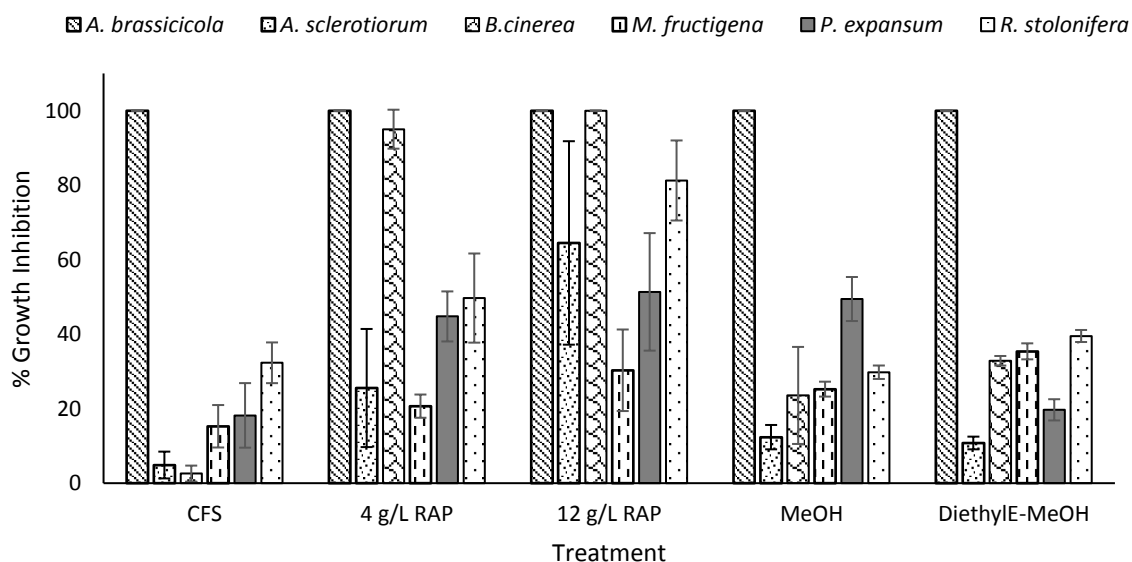
Figure 5-37. Effect of lipopeptide treatment on fungal phytopathogen growth inhibition. *CFS: Cell-free-supernatant, RAP: Resolubilised acid precipitate, MeOH: Methanol extract and DiethylE-MeOH: Diethyl ether–Methanol extract. The data points represent the mean experimental values calculated from triplicates with the standard deviation of the mean represented by the error bars.*
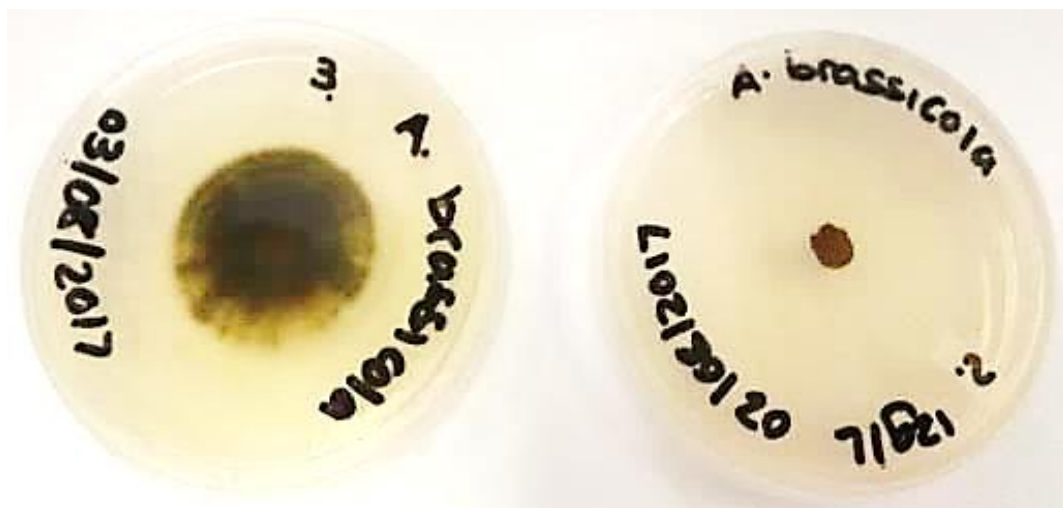
Figure 5-38. *A. brassicicola* (left) control plate and (right) 12 g/L fengycin treatment. Images captured with a digital camera.

Figure 5-39. *A. sclerotiorum* (left) control plate and (right) 12 g/L fengycin treatment. Images captured with a digital camera.

Figure 5-40. *B. cinerea* (left) control plate and (right) 12 g/L fengycin treatment. Images captured with a digital camera.

126

Figure 5-41. *M. fructigena* (left) control plate and (right) 12 g/L fengycin treatment. Images captured with a digital camera.

Figure 5-42. *P. expansum* (left) control plate and (right) 12 g/L fengycin treatment. Images captured with a digital camera.

Figure 5-43. *R. stolonifera* (left) control plate and (right) 12 g/L fengycin treatment. Images captured with a digital camera.

Table 5-11. Fengycin parameters in lipopeptide fractions used for antifungal efficacy studies

Lipopeptide fraction	Concentration (g/L)	% Purity	Antifungal selectivity ($g_{antifungals}/g_{surfactin}$)	Average % growth inhibition
CFS	0.6	-	8	29
RAP1	4	-	8	56
RAP2	12	-	8	71
MeOH extract	2.13	89	5.54	40
DiethylE-MeOH extract	2.15	74	5.5	40

CFS: Cell-free supernatant, RAP: Resolubilised acid precipitate, MeOH: Methanol and DiethylE-meOH; Diethyl ether-methanol. Antifungal selectivity calculated based on the fengycin and iturin to surfactin

5.8.   Summary of results

The percentage recoveries and purities of the LPs obtained after acid precipitation, solvent extraction and adsorption are shown in Table 5-12 and Table 5-13. It is apparent that solvent extraction was the superior unit operation employed for the purification of fengycin due to the high recoveries and purities obtained. More specifically, the three-stage extraction with methanol yielded a fengycin purity of 89 ± 4% which is close to that of the Sigma-Aldrich fengycin standard that is ≥ 90%.

Table 5-12. Lipopeptide recoveries after concentration and purification

Downstream unit operation	Lipopeptide family % recovery		
	Fengycin	Iturin	Surfactin
Acid precipitation	78 ± 0.5	62 ± 0.8	92 ± 0
1-stage methanol extraction	100 ± 0	-	100 ± 0
3-stage methanol extraction	89 ± 4	-	97 ± 9
3-stage diethyl ether–methanol extraction	90 ± 16	-	98 ± 5
Macroporous adsorption	72 ± 2	53 ± 5	49 ± 4

Table 5-13. Lipopeptide purity improvement after concentration and purification

Downstream unit operation	Lipopeptide family % purity		
	Fengycin	Iturin	Surfactin
Sigma-Aldrich standard	≥ 90	≥ 95	≥ 98
Acid precipitation	64 ± 0	17 ± 0	5 ± 0
1-stage methanol extraction	74 ± 0	-	39 ± 7
3-stage methanol extraction	89 ± 4	-	16 ± 2
3-stage diethyl ether–methanol extraction	74 ± 13	-	13 ± 1
Macroporous adsorption	75 ± 2	14 ± 1	10 ± 1

Chapter 6

Conclusions

The aim of the study was to develop an appropriate downstream concentration and purification programme for the *B. amyloliquefaciens* LPs, fengycin and iturin, for application as biocontrol agents of fungal phytopathogens that cause diseases of fruit during postharvest storage. The commonly used unit operations in LP purification processes involve acid precipitation, solvent extraction and macroporous adsorption and as such, optimisation studies of these unit operations for antifungal concentration and purification were necessary which would aid in the selection of optimal process parameters. It is through the knowledge gaps that exist in literature regarding the downstream processing of fengycin and iturin that the basis of the research study was formed.

To date, no study has systematically investigated existing downstream unit operations for the development of an appropriate concentration and purification programme for fengycin and iturin LPs produced by *B. amyloliquefaciens.* Acid precipitation studies, followed by solvent extraction and adsorption studies, were conducted on the LPs produced from this organism and optimal conditions successfully obtained, with the effectiveness of the LPs on fungal growth inhibition demonstrated against specific target fungal organisms. The conclusions of this study indicate the economic viability of antifungal LPs as second-generation biocontrol agents of fungal phytopathogens. Specific conclusions relating to the hypotheses proposed are detailed below.

1. **Optimal antifungal LP production by *B. amyloliquefaciens* is achieved during the stationary phase of growth.**

It was hypothesized that optimal fengycin and iturin production was associated with the stationary phase of growth. Antifungal LP production kinetics were evaluated to determine the time at which maximum fengycin and iturin were optimally produced which enabled the appropriate harvesting time of the LPs from the culture broth. Maximum fengycin and surfactin were produced at 24 h while maximum iturin production was obtained at 48 h. This implied that maximum fengycin and surfactin were produced towards the end of the exponential growth phase and beginning of the stationary phase.

The associated antifungal selectivities at 24 h, 48 h and 72 h were 2.60, 2.88 and 2.62 respectively. This indicated that a maximum antifungal selectivity of 2.88 was obtained at 48 h. However, the concentration of fengycin at 48 h was 1.15-fold lower than the maximum fengycin concentration

obtained at 24 h. Since the optimal production of the antifungal LPs is based on both the maximum concentration produced and the maximum selectivity, the optimum harvesting time was determined to be between 24 h and 48 h, which was the stationary phase of growth. Optimal antifungal LPs are produced in the stationary phase of growth which proved the hypothesis. The kinetics of LP production showed that selectively among the LP families can be achieved by selecting an appropriate harvesting time during production, which is an important parameter particularly for scale-up application.

2. **High performance liquid chromatography (HPLC) is suitable for rigorous antifungal LP quantification while thin layer chromatography (TLC) is suitable for semi-quantitative antifungal LP quantification.**

Although both HPLC and TLC could be successfully used for LP quantification, the quantification by TLC is semi-quantitative while HPLC is a more sensitive technique. This observation was made as iturin could not be detected by TLC at the concentrations produced, while RP-HPLC was able to successfully detect and quantify iturin in all LP fractions analysed by RP-HPLC. This suggests that RP-HPLC is a sensitive technique as it is well-established in contrast to the TLC technique that was recently developed. Thus, the hypothesis put forward is proved.

3. **An efficient purification programme for *B. amyloliquefaciens* antifungal LPs involves unit operations that progressively increase the purity of the LPs.**

A downstream purification programme consists of successive unit operations that gradually increase the purity. In this study, the order of the unit operations was applied to ensure that the LPs were first concentrated by acid precipitation to reduce the volume for the following purification procedures, as well to effect some degree of purification, which was then followed by solvent extraction and adsorption on a macroporous resin respectively. Solvent extraction proved to be the superior purification method, achieving a maximum fengycin purity of 89% after a 3-stage extraction using methanol, while a maximum fengycin purity of 75% and 14% iturin was obtained by adsorption at optimal adsorption conditions. Interestingly, the purity of iturin obtained by adsorption was less in comparison to the percentage purity obtained by precipitation. For postharvest biocontrol, a 3-stage extraction using methanol may be sufficient as the purity obtained is close to that of the Sigma-Aldrich fengycin standard that is ≥ 90%, thus proving the hypothesis.

4. **Acidification of the cell-free supernatant to pH 2 is optimal for the precipitation of fengycin and iturin.**

Acid precipitation is regarded as the appropriate initial unit operation in the recovery of LPs from the culture broth, which is aimed at the concentration and recovery of the LPs. It has been a common

phenomenon in literature for the cell-free supernatant to be acidified to pH 2 and pH 4 (reported for surfactin). This suggested that the LP amino acids were at or below their pKa's at pH values between 1 – 4, which enabled their precipitation in the cell-free supernatant. In this study, the optimal pH for acid precipitation of fengycin and iturin was investigated.

Maximum recovery percentages for all the LPs was obtained at pH 1 and 2 (no significant difference with α = 0.05), with surfactin having the highest recovery of 92%, followed by fengycin with 78% and iturin with 62%. Although pH 3 did not recover maximum LPs, optimal purities of 64% for fengycin followed by iturin and surfactin at 17 % and 5 % respectively were obtained. The associated antifungal selectivity showed that pH 2 had a maximum antifungal selectivity of 17 while pH 4 had the least antifungal selectivity of 13, indicating that pH 4 would be suitable for surfactin, but nor antifungal LP, recovery.

Since the optimal pH for antifungal LP precipitation is based on the maximum recovery and purity percentages as well as the maximum selectivity, the optimum pH was determined to be pH 3, which disproves the hypothesis.

5. **Polar organic solvents will extract maximum antifungal LPs due to the interaction with polar and/or charged amino acids in the LP cyclic peptide which determines the degree of LP solubility in the solvents.**

Although a variety of organic solvents can be used for the extraction of LPs, many of the organic solvents that have been used for the extraction of surfactin provide limited information on the extraction efficiency of the organic solvents for antifungal LPs. In this study, screening for organic solvents that recovered antifungal LPs showed that alcohols and mixtures containing alcohols extracted more LPs relative to other organic solvents tested, which proved the hypothesis. Methanol and mixtures containing methanol, extracted 100% of fengycin and surfactin respectively. Although iturin could not detected by TLC analysis in the extract, a fengycin purity of 74% and a surfactin purity of 12% was achieved in the methanol extract.

A three-stage extraction procedure using two independent approaches (three-stage methanol extraction and diethyl ether-methanol extraction) further improved the LP purity. Final purities of 89% and 16% for fengycin and surfactin respectively were obtained after the three extractions with methanol, while purities of 74% and 13% were obtained for fengycin and surfactin extraction respectively with the diethyl ether-methanol. Consequently, methanol proved to be the superior solvent for fengycin extraction as the purity obtained was close to the purity of the fengycin standard from Sigma-Aldrich of ≥ 90%. Although methanol was identified as the superior solvent for fengycin

extraction, trace amounts of this solvent should be removed from the extract to ensure acceptable safety standards for postharvest application.

6. **The lipopeptide to resin ratio (LP/R), temperature and pH for optimal antifungal LP adsorption on HP-20 resin can be determined and the mechanism of fengycin and iturin adsorption elucidated.**

A response surface methodology design (CCD) of batch adsorption experiments revealed the effect of the LP/R ratio and pH as significant parameters ($\alpha = 0.05$) in the adsorption of fengycin, with an optimal LP/R ratio of 0.5, pH of 10 and temperature of 43°C obtained. Although the effect of the LP/R ratio and temperature were found to be equally significant parameters ($\alpha = 0.05$) in the adsorption of iturin, no optimal conditions could be deduced. Further optimisation studies for iturin adsorption are required as the optimal LP/R ratios for iturin may exist outside the LP/R ratios used in this study.

Adsorption kinetic studies indicated equilibrium times of 22 h, 24 h and 18 h respectively, for fengycin, iturin and surfactin at the optimal fengycin adsorption conditions. Maximum adsorption percentages of 71.65 ± 1.45%, 53.44 ± 5.14% and 48.75 ± 3.813% for fengycin, iturin and surfactin respectively were obtained for the corresponding equilibrium times. To determine the rate limiting step of adsorption, kinetic data was individually fitted to the pseudo-first-order and pseudo-second-order kinetic models. Comparison of the experimental and theoretical Q_e suggested that the data may be explained by the pseudo-second-order kinetic model. However, both pseudo-kinetic models fit the initial experimental data points poorly which suggested that equilibrium was reached rapidly and thus the initial part of the curve was not observed.

To further elucidate the adsorption behaviour of the antifungal LPs on HP-20 resin, adsorption isotherm studies were conducted to determine the concentration of fengycin and iturin required to saturate the resin. 3 g/L fengycin and 0.8 g/L iturin were determined to be the concentrations of the LPs required to saturate the resin, which yielded adsorption percentages of 76.5 ± 0.37% and 54.5 ± 3.99% for fengycin and iturin separately. Individual fitting of the data to the Langmuir and Freundlich isotherm models indicated a lack of fit for both models. Thus, the adsorption behaviour of the antifungal LPs could not be explained by the isotherm models.

Although the mechanism of antifungal adsorption on HP-20 was not fully elucidated by pseudo-kinetic rate models and adsorption isotherm models, optimal fengycin adsorption conditions were determined, thus proving the hypothesis.

7. Purified LP mixtures (from solvent extraction) have an enhanced effect on fungal phytopathogen growth inhibition compared to partially purified LP mixtures (from acid precipitation).

To determine the effectiveness of the partially purified LPs and purified LP mixtures on inhibiting the growth of *Alternaria brassicicola*, *Aspergillus sclerotiorum*, *Botrytis cinerea*, *Monilinia fructigena*, *Penicillium expansum* and *Rhizopus stolonifera*, as the common fungal phytopathogens that affect deciduous fruit during postharvest storage, efficacy studies were performed using a semi-quantitative *in vitro* antimicrobial activity technique. The resolubilised acid precipitate treatment of 12 g/L fengycin was found to be the most effective treatment with fungal growth inhibition ranging between 30 – 100%. It was discovered that *A. brassicicola* was the most susceptible phytopathogen of the six pathogens studied since application of the cell-free supernatant caused 100% growth inhibition, while *A. sclerotiorum* was the most resistant phytopathogen as application of the cell-free supernatant (least concentrated fengycin fraction) inhibited 5% of fungal growth. The hypothesis is thus disproved as the effectiveness of the LP treatments was dependent on the concentration and not the purity.

Recommendations

1. Lipopeptide production

With the production kinetics of fengycin and iturin obtained, LP production needs to be conducted in an instrumented bioreactor under controlled conditions, preferably, with the strain genetically modified to over-produce fengycin and iturin to overcome the low yields.

2. Acid precipitation

Although an optimal pH for acid precipitation was established, the complete precipitation of the LPs from the cell-free supernatant did not occur. This resulted in fengycin and iturin recovery percentages that were ≤ 78% and ≤ 67% respectively. Investigation into the LP precipitation mechanism may be required to understand the factors that influence the incomplete precipitation of the LPs from the cell-free supernatant.

3. Solvent extraction

Solvent extraction could also be aimed at improving the purity of LPs by using organic solvents that will select for the impurities instead of the LPs. Since fengycin and iturin were the LPs of interests, surfactin would be considered as an impurity in this case, thus solvents that will select for impurities (lipids and protein) as well as for surfactin could be considered. Since polar solvents extract LPs and hydrophobic impurities, while non-polar solvents extract hydrophobic impurities only, a systematic multistep approach involving both polar and nonpolar organic solvents could be investigated.

A three-stage extraction procedure involving diethyl ether as the non-polar solvent and methanol as the polar solvent was used in this study. Repeat experiments using these organic solvents need to be conducted to obtain accurate data as there were inconsistencies in the initial LP concentration, due to the variation in LP concentration in the acid precipitate used, which affected the purity percentage. Using a combination of other polar and non-polar solvent pairs that were screened in this study for LP extraction needs to be further explored and investigated to identify the appropriate solvent extraction pair for antifungal LP extraction.

Although the aqueous two-phase extraction system (ATP) has been used for surfactin purification, no data for fengycin and iturin has been reported. Instead of using dextran as the lower phase of the ATP system, different salts such as phosphate and citrate salts can be used, and the appropriate salt concentration determined. A recovery programme for LPs in the PEG phase and recycling of the PEG for further LP purification would also need to be investigated.

4. Adsorption

Investigation into the adsorptive behaviour of fengycin and iturin, through adsorption kinetic and isotherm studies, needs to be rigorously conducted through repeated experiments. Adsorption isotherm studies involving fengycin concentrations that are above 3 g/L is essential to elucidate why the adsorption capacity (Q_e) decreased instead of the plateau trend that was reported and expected from literature. This suggests that there may be structural conformation changes that occur at high fengycin concentrations which inhibit optimal adsorption of fengycin, and thus need to be further examined.

5. *In vitro* antifungal efficacy studies

The *in vitro* antifungal efficacy technique used was semi-quantitative. A quantitative method is required to determine the minimum inhibitory concentration (MIC) of LPs required to inhibit the growth of all six phytopathogens. Once the MIC has been determined, the effect of the LP dosage on the hyphal structures and conidia can be conducted through scanning electron microscopy (SEM). From this work, the LP effect on inhibiting fungal phytopathogen growth can be characterised as either fungistatic or fungicidal.

The experiments should be conducted through normalising to a single concentration to more easily facilitate comparison between treatments.

Studying the mode of fengycin action and the functional groups of fengycin involved in pathogen growth inhibition is necessary.

6. LP analysis by TLC

Fengycin validation studies on TLC analysis are required to ensure the accuracy of the analytical technique in the quantification of fengycin. The two bands that were assumed to be fengycin were further analysed by LC-ESI-MS to confirm whether both bands were indeed fengycin. However, it could not be confirmed with certainty that both bands were fengycin. Further analysis with LC-ESI-MS is required, particularly the fragmentation of the obtained parent mass peaks through LC-ESI-MS/MS, which will ensure the identity of the two LP bands and inform on the structure of the identified LPs.

If one of the bands turns out to be iturin, investigation into why it has a significantly different R_f value to the standard iturin needs to be determined, and if both bands are fengycin, investigation into why they form two distinct bands is also required.

References

Banat, I. M., Franzetti, A., Gandolfi, I., Bestetti, G., Martinotti, M. G., Fracchia, L., Smyth, T. J. and Marchant, R. (2010) 'Microbial biosurfactants production, applications and future potential', *Applied Microbiology and Biotechnology*, 87(2), pp. 427–444. doi: 10.1007/s00253-010-2589-0.

Bond, W. J., Midgley, G. F. and Woodward, F. I. (2003) 'What controls South African vegetation — climate or fire?', *South African Journal of Botany*, 69(1), pp. 79–91. doi: 10.1175/2008JCLI2390.1.

Chen, H. L., Chen, Y. S. and Juang, R. S. (2007) 'Separation of surfactin from fermentation broths by acid precipitation and two-stage dead-end ultrafiltration processes', *Journal of Membrane Science*, 299(1–2), pp. 114–121. doi: 10.1016/j.memsci.2007.04.031.

Chen, H. L. and Juang, R. S. (2008) 'Recovery and separation of surfactin from pretreated fermentation broths by physical and chemical extraction', *Biochemical Engineering Journal*, 38(1), pp. 39–46. doi: 10.1016/j.bej.2007.06.003.

Chen, H. L., Lee, Y. S., Wei, Y. H. and Juang, R. S. (2008) 'Purification of surfactin in pretreated fermentation broths by adsorptive removal of impurities', *Biochemical Engineering Journal*, 40(3), pp. 452–459. doi: 10.1016/j.bej.2008.01.020.

Chen, Y., Zhang, W., Zhao, T., Li, F., Zhang, M., Li, J., Zou, Y., Wang, W., Cobbina, S. J., Wu, X. and Yang, L. (2015) 'Adsorption properties of macroporous adsorbent resins for separation of anthocyanins from mulberry', *Food Chemistry*. Elsevier Ltd, 194, pp. 712–722. doi: 10.1016/j.foodchem.2015.08.084.

Clarke, K. G. (2013a) 'Downstream processing', in *Bioprocess Engineering*. Elsevier, pp. 209–234. doi: 10.1533/9781782421689.209.

Clarke, K. G. (2013b) 'Microbial kinetics during batch, continuous and fed-batch processes', in *Bioprocess Engineering*. Elsevier, pp. 97–146. doi: 10.1533/9781782421689.97.

Coates, L. and Johnson, G. (1997) 'Postharvest Diseases of Fruit and Vegetables', *Plant Pathogens and Diseases*, pp. 533–547.

Czitrom, V. (1999) 'One-Factor-at a Time Versus Designed Experiments', *The American Statistician*, 53(2), pp. 126–131.

Dabrowski, A. (2001) 'Adsorption - From theory to practice', *Advances in Colloid and Interface Science*, 93(1–3), pp. 135–224. doi: 10.1016/S0001-8686(00)00082-8.

Dhall, R. K. (2013) 'Advances in edible coatings for fresh fruits and vegetables: a review.', *Critical reviews in food science and nutrition*, 53(5), pp. 435–50. doi: 10.1080/10408398.2010.541568.

Dhanarajan, G., Rangarajan, V. and Sen, R. (2015) 'Dual gradient macroporous resin column chromatography for concurrent separation and purification of three families of marine bacterial lipopeptides from cell free broth', *Separation and Purification Technology*. Elsevier B.V., 143, pp. 72–79. doi: 10.1016/j.seppur.2015.01.025.

Du, X., Yuan, Q., Li, Y. and Zhou, H. (2008) 'Preparative purification of solanesol from tobacco leaf extracts by macroporous resins', *Chemical Engineering and Technology*, 31(1), pp. 87–94. doi: 10.1002/ceat.200700347.

Van Dyk, F. and Maspero, E. (2004) 'An analysis of the South African fruit logistics infrastructure', *ORiON*, 20(1), pp. 55–72. doi: 10.5784/20-1-6.

Fernandes, P. A. V., Arruda, I. R. De, Santos, A. F. A. B. dos, Araújo, A. A. De, Maior, A. M. S. and Ximenes, E. A. (2007) 'Antimicrobial activity of surfactants produced by *Bacillus subtilis* R14 against multidrug-resistant bacteria', *Brazilian Journal of Microbiology*, 38(4), pp. 704–709. doi: 10.1590/S1517-83822007000400022.

Forum, F. P. E. (2016) 'Fresh Fruit Export Directory 2016'.

Fourie, J. (2013) 'Postharvest decay on stone fruit . . . what, when and how to reduce', (July), pp. 50–54.

Giles, C. H., MacEwan, T. H., Nakhwa, S. N. and Smith, D. (1960) 'Studies in adsorption. Part XI. A system of classification of solution adsorption isotherms, and its use in diagnosis of adsorption mechanisms and in measurement of specific surface areas of solids', *Journal of the Chemical Society (Resumed)*, 846, pp. 3973–3993. doi: 10.1039/jr9600003973.

Gond, S. K., Bergen, M. S., Torres, M. S. and White, J. F. (2015) 'Endophytic *Bacillus* spp. produce antifungal lipopeptides and induce host defence gene expression in maize', *Microbiological Research*, 172, pp. 79–87. doi: 10.1016/j.micres.2014.11.004.

Gordillo, M. A. and Maldonado, M. C. (2009) 'Purification of Peptides from *Bacillus* Strains with Biological Activity', *Chromatography and Its Applications*, pp. 201–224.

Greef, P., Kotze, M., National, T., Marketing, A., National, T., Marketing, A. and Trust, C. (2007) *Subsector Study: Deciduous Fruit.*

Herbst, W. J. (2017) 'Kinetic evaluation of lipopeptide production by *Bacillus amyloliquefaciens* by', (March).

Ho, C. S., Lam, C. W. K., Chan, M. H. M., Cheung, R. C. K., Law, L. K., Lit, L. C. W., Ng, K. F., Suen, M. W. M. and Tai, H. L. (2003) 'Electrospray ionisation mass spectrometry: principles and clinical applications.', *The Clinical biochemist. Reviews*, 24(1), pp. 3–12. doi: 10.1146/annurev.bi.64.070195.001531.

Hortgro (2014) 'Key Deciduous Fruit Statistics', pp. 1–92.

Juang, R. S., Chen, H. L. and Tsao, S. C. (2012) 'Recovery and separation of surfactin from pretreated *Bacillus subtilis* broth by reverse micellar extraction', *Biochemical Engineering Journal*. Elsevier B.V., 61, pp. 78–83. doi: 10.1016/j.bej.2011.12.008.

Katritzky, A. R., Fara, D. C., Yang, H. F., Tämm, K., Tamm, T., Karelson, M., Tamm, K., Tamm, T., Karelson, M. and Tämm, K. (2004) 'Quantitative Measures of Solvent Polarity', *Chemical Reviews*, 104(1), pp. 175–198. doi: 10.1021/cr020750m.

Kim, K. W. and Lee, S. B. (2003) 'Inhibitory Effect of Maillard Reaction Products on Growth of the Aerobic Marine Hyperthermophilic Archaeon *Aeropyrum pernix*', *Applied and Environmental Microbiology*, 69(7), pp. 4325–4328. doi: 10.1128/AEM.69.7.4325.

Kim, P. I., Bai, H., Bai, D., Chae, H., Chung, S., Kim, Y., Park, R. and Chi, Y. T. (2004) 'Purification and characterization of a lipopeptide produced by *Bacillus thuringiensis* CMB26', *Journal of Applied Microbiology*, 97(5), pp. 942–949. doi: 10.1111/j.1365-2672.2004.02356.x.

Kislik, V. S. (2012) *Modern (Classical) Fundamental Principles of Solvent Extraction*, *Solvent Extraction*. doi: 10.1016/B978-0-444-53778-2.10001-9.

Kosaric, N. and Vardar-Sukan, F. (2015) 'Biosurfactants : production and utilization--processes, technologies, and economics', in *Biosurfactants : production and utilization--processes, technologies, and economics*. CRC Press, p. 389.

Lee, S. C., Kim, S. H., Park, I. H., Chung, S. Y., Subhosh Chandra, M., Choi, Y. L., Sang-cheol, L., Kim, S. H., Park, I. H., Chung, S. Y., Chandra, M. S. and Choi, Y. L. (2010) 'Isolation, purification, and characterization of novel fengycin S from *bacillus amyloliquefaciens* LSC04 degrading-crude oil', *Biotechnology and Bioprocess Engineering*, 15(2), pp. 246–253. doi: 10.1007/s12257-009-0037-8.

Limousin, G., Gaudet, J. P., Charlet, L., Szenknect, S., Barthes, V. and Krimissa, M. (2007) 'Sorption isotherms: A review on physical bases, modeling and measurement', *Applied Geochemistry*, 22(2),

pp. 249–275. doi: 10.1016/j.apgeochem.2006.09.010.

Liu, C., Jiao, R., Yao, L., Zhang, Y., Lu, Y. and Tan, R. (2016) 'Adsorption characteristics and preparative separation of chaetominine from *Aspergillus fumigatus* mycelia by macroporous resin', *Journal of Chromatography B: Analytical Technologies in the Biomedical and Life Sciences*. Elsevier B.V., 1015–1016, pp. 135–141. doi: 10.1016/j.jchromb.2016.02.027.

Louw, J. and Korsten, L. (2014) '*Penicillium* rot of apples and pears', *Tegnologie*, pp. 74–75.

Mahajan, P. V, Caleb, O. J., Singh, Z., Watkins, C. B. and Geyer, M. (2014) 'Postharvest treatments of fresh produce.', *Philosophical transactions. Series A, Mathematical, physical, and engineering sciences*, 372(2017), p. 20130309. doi: 10.1098/rsta.2013.0309.

Mnif, I., Grau-Campistany, A., Coronel-león, J., Hammami, I. I., Triki, M. A., Manresa, A. and Ghribi, D. (2016) 'Purification and identification of *Bacillus subtilis* SPB1 lipopeptide biosurfactant exhibiting antifungal activity against *Rhizoctonia bataticola* and *Rhizoctonia solani*', *Environmental Science and Pollution Research*, 23(7), pp. 6690–6699. doi: 10.1007/s11356-015-5826-3.

Montastruc, L., Liu, T., Gancel, F., Zhao, L. and Nikov, I. (2008) 'Integrated process for production of surfactin. Part 2. Equilibrium and kinetic study of surfactin adsorption onto activated carbon', *Biochemical Engineering Journal*, 38(3), pp. 349–354. doi: 10.1016/j.bej.2007.07.023.

Moyer, M. and Grove, G. (2011) *Botrytis* bunch rot in commercial Washington grape production.

Mukherjee, S., Das, P. and Sen, R. (2006) 'Towards commercial production of microbial surfactants', 24(11). doi: 10.1016/j.tibtech.2006.09.005.

Needham, T. E. (1970) 'The solubility of amino acids in various solvent systems', *Open Access Dissertations*, pp. 1–95. Available at: http://digitalcommons.uri.edu/oa_diss/159/.

Nick Pace, C., Trevino, S., Prabhakaran, E. and Martin Scholtz, J. (2004) 'Protein structure, stability and solubility in water and other solvents', *Philosophical Transactions of the Royal Society B: Biological Sciences*, 359(1448), pp. 1225–1235. doi: 10.1098/rstb.2004.1500.

Nunes, C. A. (2012) 'Biological control of postharvest diseases of fruit', *European Journal of Plant Pathology*, 133(1), pp. 181–196. doi: 10.1007/s10658-011-9919-7.

Ongena, M. and Jacques, P. (2008) '*Bacillus* lipopeptides: versatile weapons for plant disease biocontrol', *Trends in Microbiology*, 16(3), pp. 115–125. doi: 10.1016/j.tim.2007.12.009.

Paulová, L., Patáková, P. and Brányik, T. (2013) 'Advanced Fermentation Processes', in, pp. 89–110.

doi: 10.1201/b15426-6.

Premanandh, J. (2011) 'Factors affecting food security and contribution of modern technologies in food sustainability', *Journal of the Science of Food and Agriculture*, 91(15), pp. 2707–2714. doi: 10.1002/jsfa.4666.

Pretorius, D., Rooyen, J. Van and Clarke, K. G. (2015) 'Enhanced production of antifungal lipopeptides by *Bacillus amyloliquefaciens* for biocontrol of postharvest disease', *New BIOTECHNOLOGY*. Elsevier B.V., 32(2), pp. 243–252. doi: 10.1016/j.nbt.2014.12.003.

Prusky, D. (2011) 'Reduction of the incidence of postharvest quality losses, and future prospects', *Food Security*, 3(4), pp. 463–474. doi: 10.1007/s12571-011-0147-y.

Qiu, H., Lv, L., Pan, B., Zhang, Q. Q., Zhang, W. and Zhang, Q. Q. (2009) 'Critical review in adsorption kinetic models', *Journal of Zhejiang University-SCIENCE A*, 10(5), pp. 716–724. doi: 10.1631/jzus.A0820524.

Raaijmakers, J. M., de Bruijn, I., Nybroe, O. and Ongena, M. (2010) 'Natural functions of lipopeptides from *Bacillus* and *Pseudomonas*: More than surfactants and antibiotics', *FEMS Microbiology Reviews*, pp. 1037–1062. doi: 10.1111/j.1574-6976.2010.00221.x.

Rangarajan, V. and Clarke, K. G. (2015) 'Process development and intensification for enhanced production of *Bacillus* lipopeptides.', *Biotechnology & genetic engineering reviews*, 31(1–2), pp. 46–68. doi: 10.1080/02648725.2016.1166335.

Rangarajan, V. and Clarke, K. G. (2016) 'Towards bacterial lipopeptide products for specific applications — a review of appropriate downstream processing schemes', *Process Biochemistry*. Elsevier Ltd, 51(12), pp. 2176–2185. doi: 10.1016/j.procbio.2016.08.026.

Rangarajan, V., Dhanarajan, G. and Sen, R. (2015) 'Bioprocess design for selective enhancement of fengycin production by a marine isolate *Bacillus megaterium*', *Biochemical Engineering Journal*. Elsevier B.V., 99, pp. 147–155. doi: 10.1016/j.bej.2015.03.016.

Reis, R. S., Pacheco, G. J., Pereira, A. G. and Freire, D. M. G. (2013) 'Biosurfactants: Production and Applications', *Biodegradation - Life of Science*. doi: 10.5772/56144.

Romero, D., Vicente, A. De, Rakotoaly, R. H., Dufour, S. E., Veening, J., Arrebola, E., Cazorla, F. M., Kuipers, O. P., Paquot, M. and Pérez-garcía, A. (2007) 'The Iturin and Fengycin Families of Lipopeptides Are Key Factors in Antagonism of *Bacillus subtilis* Toward Podosphaera fusca', 20(4), pp. 430–440.

Sen, R. and Swaminathan, T. (2005) 'Characterization of concentration and purification parameters and operating conditions for the small-scale recovery of surfactin', *Process Biochemistry*, 40(9), pp. 2953–2958. doi: 10.1016/j.procbio.2005.01.014.

Shaligram, N. S. and Singhal, R. S. (2010) 'Surfactin – A Review on Biosynthesis , Fermentation , Purification and Applications', 48(2), pp. 119–134.

Snyder, L. R. (1968) *Principles of adsorption chromatography: The separation of non-ionic organic compounds*. Edited by J. C. Giddings and R. A. Keller. MARCEL DEKKER, INC., New York. doi: 10.2116/bunsekikagaku.18.937.

Soberón-Chávez, G. (2011) *Biosurfactants: From Genes to Applications*. Edited by A. Steinbu. Springer Berlin Heidelberg. doi: 10.1007/978 3 642 14490 5.

Sonker, N., Pandey, A. K. and Singh, P. (2016) 'Strategies to control post-harvest diseases of table grape: a review', *Journal of Wine Research*, 1264(April), pp. 1–18. doi: 10.1080/09571264.2016.1151407.

Strange, R. N. and Scott, P. R. (2005) 'Plant Disease: A Threat to Global Food Security', *Annual Review of Phytopathology*, 43(1), pp. 83–116. doi: 10.1146/annurev.phyto.43.113004.133839.

Tucker, F. A. (1989) '4,874,843'.

Wang, Y. Y., Lu, Z., Bie, X. and Lv, F. (2010) 'Separation and extraction of antimicrobial lipopeptides produced by *Bacillus amyloliquefaciens* ES-2 with macroporous resin', *European Food Research and Technology*, 231(2), pp. 189–196. doi: 10.1007/s00217-010-1271-1.

Wells, M. J. M. (2003) Principles of Extraction and the Extraction of Semivolatile Organics from Liquids, Sample Preparation Techniques in Analytical Chemistry. doi: 10.1002/0471457817.ch2.

Wilson, K. E., Flor, J. E., Schwartz, R. E., Joshua, H., Smith, J. L., Pelak, B. A., Liesch, J. M. and Hensens, O. D. (1987) 'Difficidin and oxydifficidin: novel broad spectrum antibacterial antibiotics produced by *Bacillus subtilis*. II. Isolation and physico-chemical characterization.', *The Journal of antibiotics*, 40(12), pp. 1682–91. doi: 10.7164/antibiotics.40.1682.

Wingfield, P. T. (2016) Overview of the Purification of Recombinant Proteins, *Curr Protoc Protein Sci*. doi: 10.1002/0471140864.ps0601s80.Overview.

Wu, F.-C., Liu, B.-L., Wu, K.-T. and Tseng, R.-L. (2010) 'A new linear form analysis of Redlich–Peterson isotherm equation for the adsorptions of dyes', *Chemical Engineering Journal*. Elsevier B.V., 162(1),

pp. 21–27. doi: 10.1016/j.cej.2010.03.006.

Yuanfeng, W., Lei, Z., Jianwei, M., Shiwang, L., Jun, H., Yuru, Y. and Lehe, M. (2016) 'Kinetic and thermodynamic studies of sulforaphane adsorption on macroporous resin', *Journal of Chromatography B: Analytical Technologies in the Biomedical and Life Sciences*. Elsevier B.V., 1028, pp. 231–236. doi: 10.1016/j.jchromb.2016.06.035.

Zimmerman, S. B., SCHWARTZ, C. D., MONAGHAN, R. L., PELAK, B. A., WEISSBERGER, B., GILFILLAN, E. C., MOCHALES, S., HERNANDEZ, S., CURRIE, S. A., TEJERA, E. and STAPLEY, E. O. (1986) 'DIFFICIDIN AND OXYDIFFICIDIN: NOVEL BROAD SPECTRUM ANTIBACTERIAL ANTIBIOTICS PRODUCED BY *BACILLUS SUBTILIS* I. PRODUCTION, TAXONOMYAND ANTIBACTERIAL ACTIVITY*', *The Journal of Antibiotics*, 40(12), pp. 1677–1681. doi: 10.7164/antibiotics.40.1682.

Appendices

Appendix A: Equations

Acid precipitation

$$\% \textbf{ Recovery} = \frac{C_f \times V_f}{C_i \times V_i} \text{ x } 100$$

(1)

$$\% \textbf{ Purity} = \frac{C_f \times V_f}{g_t} \text{ x } 100$$

(2)

Where C_f is the concentration of LP in resolubilised acid precipitate in alkaline water (determined by RP-HPLC), V_f is the volume of alkaline water used to resolubilse the acid precipitate, C_i is the concentration of LP in the cell-free supernatant prior to acid precipitation (determined by RP-HPLC), V_i is the volume of cell-free supernatant prior to acid precipitation and g_t is the mass of dry acid precipitate pellet

Solvent extraction

$$\% \textbf{ Recovery} = \frac{C_f \times V_f}{C_i \times V_i} \text{ x } 100$$

(3)

$$\% \textbf{ Purity} = \frac{C_f \times V_f}{g_t} \text{ x } 100$$

(4)

C_f is the concentration of LP in solvent extract (determined by TLC), V_f is the volume of organic solvent used to dissolve the acid precipitate, C_i is the concentration of LP in methanol extract (determined by TLC), V_i is the volume of methanol used to dissolve the acid precipitate and g_t is the mass of acid precipitate dissolved in the organic solvent extract

Batch adsorption equilibrium

$$Q_e = \frac{(C_o - C_e)V}{M} \text{ x } 100$$

(5)

Q_e: Mass of LPs adsorbed per mass of resin at equilibrium

C_o: Initial LP concentration

C_e: Non-adsorbed LP concentration in liquid phase at equilibrium

V: Volume of resolubilised acid precipitate

M: Mass of resin

$$\% \text{ Adsorption } = \frac{(C_o - C_e)}{C_o} \text{ x } 100$$

(6)

C_o: Initial LP concentration

C_e: Concentration of non-adsorbed LP in liquid phase at equilibrium

$$\% \text{ Purity } = \frac{(C_o - C_e)V}{M_t} \text{ x } 100$$

(7)

C_o: Initial LP concentration

C_e: Concentration of non-adsorbed LP in liquid phase at equilibrium

V: Volume of resolubilised acid precipitate

M_t: Total mass of adsorbed LPs: Initial LP mass before adsorption – final LP mass after adsorption

$$\% \textbf{ Desorption } = \frac{(\textbf{C}_\textbf{d}\textbf{V}_\textbf{d})}{(\textbf{C}_\textbf{o} - \textbf{ C}_\textbf{e})\textbf{V}_\textbf{a}} \textbf{ x } \textbf{100} \tag{8}$$

C_d: LP concentration in desorption solution

C_o: Initial LP concentration

C_e: Non-adsorbed LP concentration in liquid phase at equilibrium

V_d: Volume of desorption solution

V_a: Volume of adsorption solution

Adsorption kinetics

$$\textbf{Q}_\textbf{t} = \frac{(\textbf{C}_\textbf{o} - \textbf{ C}_\textbf{t})\textbf{V}}{\textbf{M}} \tag{9}$$

Q_t: Mass of LPs adsorbed per mass (g) of resin at time t

C_o: Initial LP concentration

C_t: Non-adsorbed LP concentration in liquid phase at time t

V: Volume of resolubilised acid precipitate

M: Mass of resin

Pseudo-first order rate model

$$\textbf{Q}_\textbf{t} = \textbf{Q}_\textbf{e}(\textbf{1} - \textbf{ e}^{-\textbf{K}_\textbf{1}\textbf{t}}) \tag{10}$$

Q_t: Mass of LPs adsorbed per mass of resin at time t

Q_e: Mass of LPs adsorbed per mass of resin at equilibrium (Theoretical)

K_1: Pseudo-first-order rate constant

t: Time

Pseudo-second order rate model

$$Q_t = \frac{K_2 Q_e{}^2 t}{1 + K_2 Q_e t}$$

(11)

Q_t: Mass of LPs adsorbed per mass of resin at time *t*

Q_e: Mass of LPs adsorbed per mass of resin at equilibrium (theoretical)

K_2: Pseudo-second-order rate constant

t: Time

Adsorption isotherms

Langmuir isotherm model

$$Q_e = \frac{Q_m K_L C_e}{1 + K_L C_e}$$

(12)

C_e: Concentration of non-adsorbed LP in liquid phase at equilibrium

Q_e: Mass of LPs adsorbed per mass of resin at equilibrium

Q_m: Maximum mass of LPs adsorbed per mass of resin at equilibrium

K_L: Adsorption equilibrium constant

Freundlich isotherm model

$$Q_e = K_F C_e{}^{1/n}$$

(13)

Q_e: Mass of LPs adsorbed per mass of resin at equilibrium

C_e: Concentration of non-adsorbed LP in liquid phase at equilibrium

K_F: Freundlich constant (measures adsorption capacity)

n: Freundlich constant (measures adsorption intensity)

In vitro antifungal efficacy

$$\% \text{ Growth inhibition} = \frac{D_c - D_t}{D_c} \text{ x } 100$$

(14)

D_c: Diameter (or area) of fungal growth in the control plate

D_t: Diameter (or area) of fungal growth in the test plate

Cell dry weight

$$\text{CDW (g/L)} = \frac{W_2 - W_1}{V}$$

(15)

W_1: Mass of membrane filter without bacterial cells

W_2: Mass of membrane filter with dried bacterial cells

V: Volume of dilution filtered

Area to concentration conversion

$$\text{Concentration (g/L)} = \frac{A}{S} \div V$$

(16)

A: Area of LP band on TLC plate

S: Slope of calibration curve for area vs. μg lipopeptides

V: Volume of sample spotted

148

Appendix B: Standard graphs and chromatograms

Lipopeptide standard chromatogram by RP-HPLC
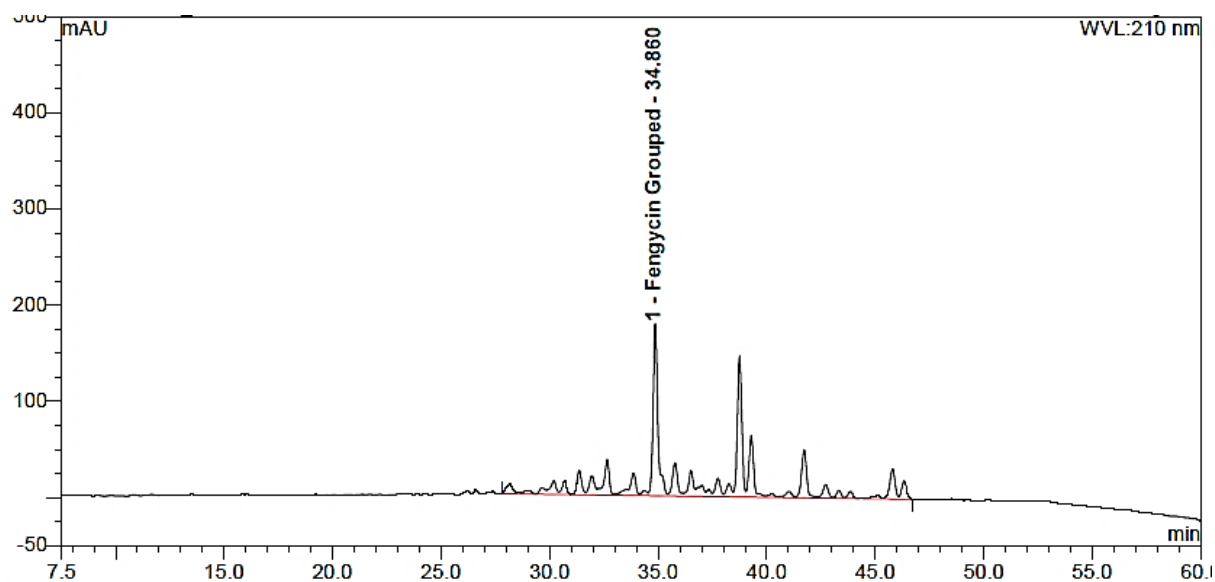
Figure 0-1. Fengycin standard chromatogram determined by RP-HPLC
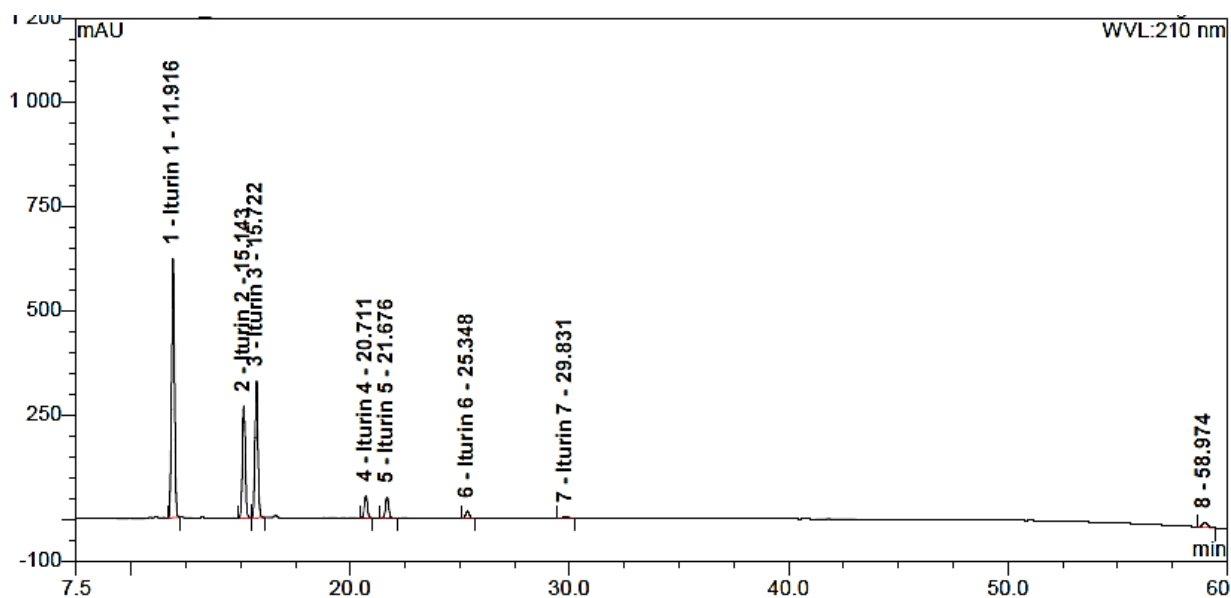
Figure 0-2. Iturin A standard chromatogram determined by RP-HPLC

149
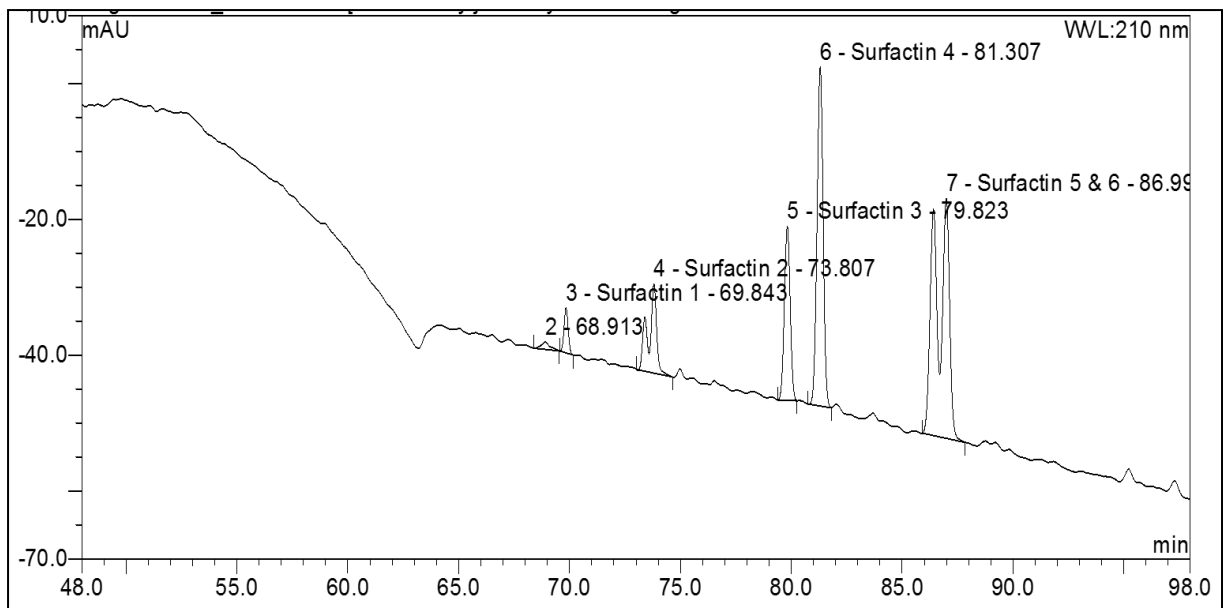
Figure 0-3. Surfactin standard chromatogram by RP-HPLC

Lipopeptide standard curves by TLC
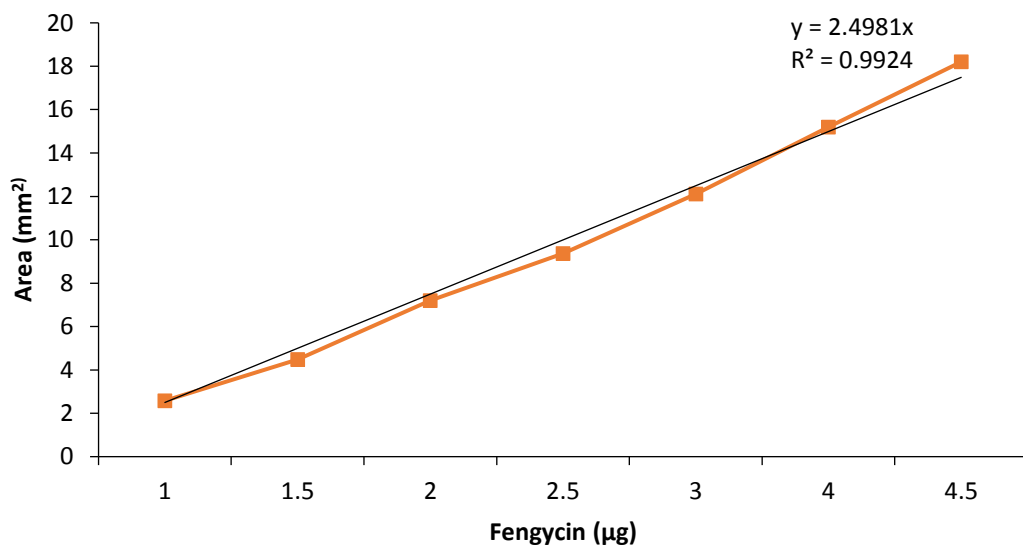
Figure 0-4. Fengycin standard curve determined by TLC
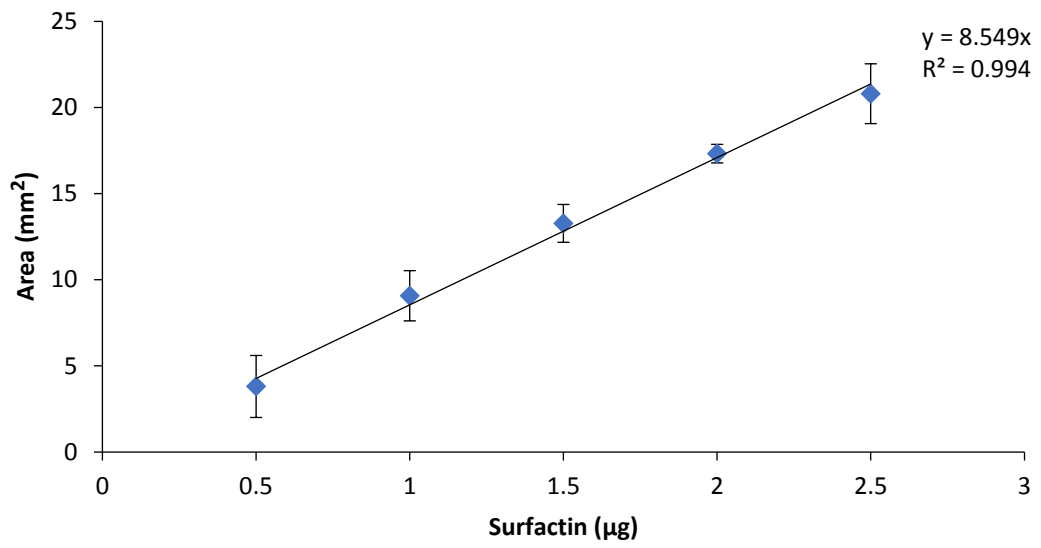
Figure 0-5. Surfactin standard curve determined by TLC

Lipopeptide standard chromatograms by LC-ESI-MS
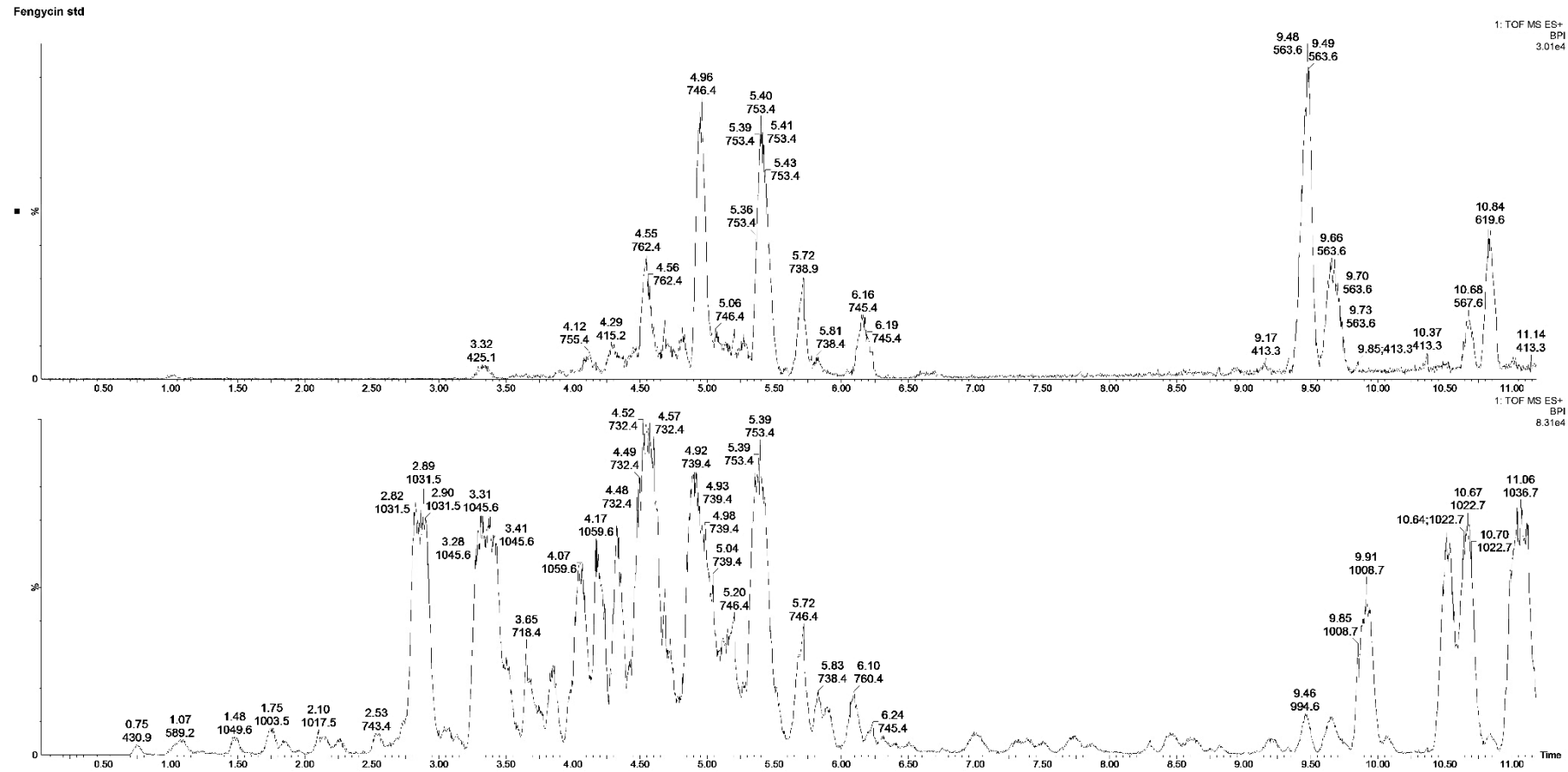
Figure 0-6. Fengycin standard chromatogram determined by LC-ESI-MS. Fengycin mass peaks at high (top) and low (bottom) energy with impurities within the standard indicated by peaks at the far right of the graph
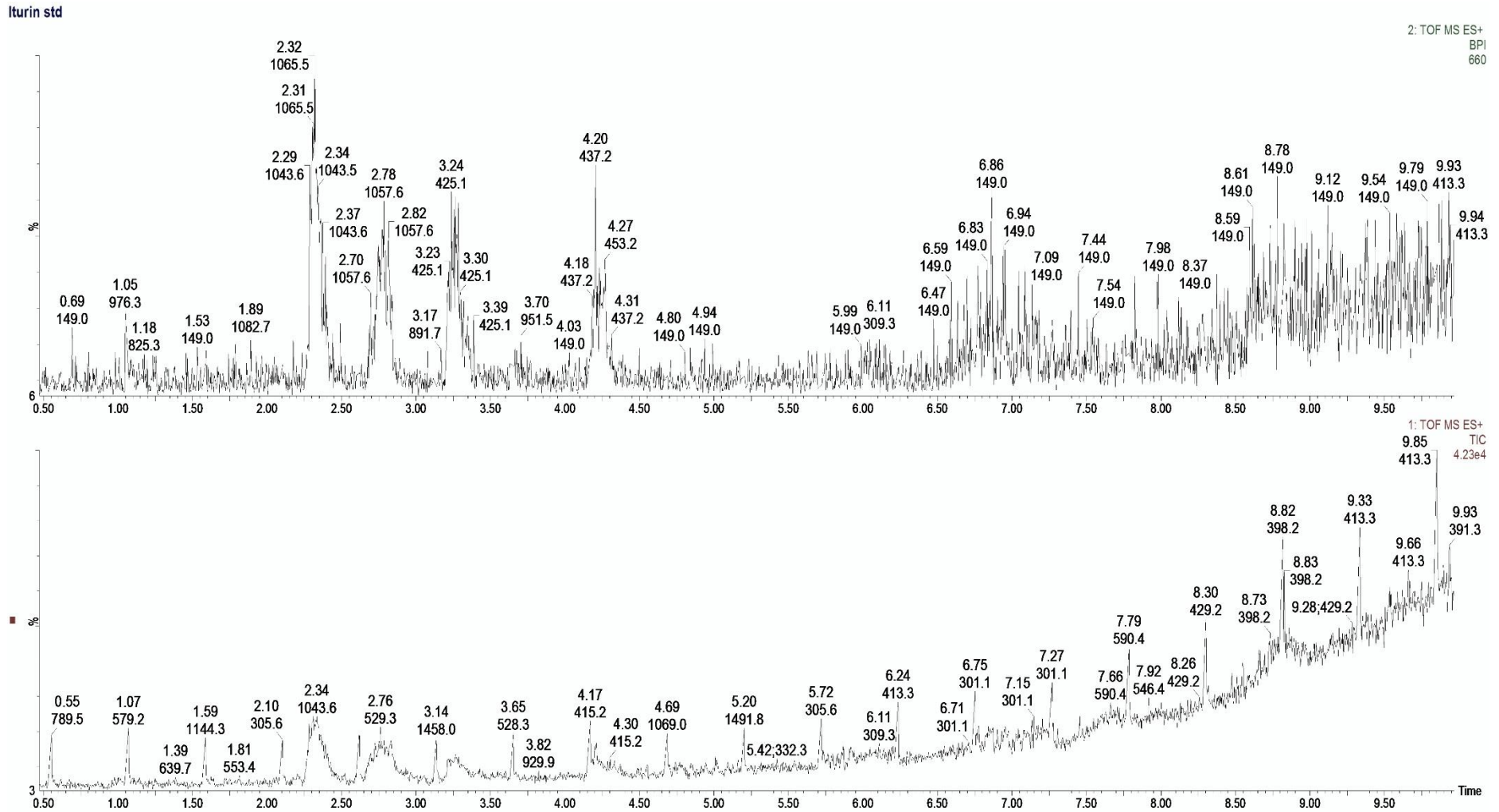
Figure 0-7. Iturin standard chromatogram determined by LC-ESI-MS. Iturin mass peaks at high (top) and low (bottom) energy with impurities within the standard indicated by peaks at the far right of the graph

Appendix C: Reagents, Image analysis and Preliminary experiments

Dinitrosalicylic acid (DNS) reagent preparation

Component	Amount
NaOH	1 g
3,5 dinitrosalicylic acid	1 g
Phenol	200 mg
$Na_2S_2O_5$	50 mg
Distilled water	100 mL

Image analysis by ImageJ software

Prior to analysis, images were scanned in grayscale at 600 dpi. The resultant image was cropped, and the straight-line tool used to measure a known distance on the image. The measured distance was used to set the scale from the analyse drop-down menu. Once the scale was set, the brightness and contrast of the image was adjusted, followed by the threshold adjustment setting which yielded a black and white image, with the region of interest shaded in black. The wand tool was then used to click over the desired region (which was highlighted in yellow) and the measure option selected from the analyse drop-down menu. The desired region was measured in area, which was displayed in a new pop-up window.

Preliminary batch adsorption experiments

Preliminary batch adsorption experiments were carried out to ensure that there were no interferences or deviations in the experimental conditions (pH and temperature) during adsorption, i.e. the pH and temperature of the solution was kept at the desired conditions during the incubation phase of 24 h. The experiments were conducted at 0.04 – 0.2 LP/R ratio at 35°C and 45°C respectively while the pH was kept constant at 7.63 with agitation at 150 rpm (Table 0-1). During adsorption, the LP solution changed from clear to murky thus the experiments were subjected to gram staining, endospore staining and spread plating on nutrient agar plates to determine the contaminants in the batch adsorption experiments.

1.   Gram staining
From the undiluted LP resolubilised acid precipitate and adsorption samples taken at 18, 20, 24 and 26 h, the gram stain procedure was conducted. 50 µl of each sample was placed onto a microscope slide and the specimen was heat-fixed by passing the microscope slide over a Bunsen burner. The

heat-fixed smear was flooded with 100 µl of crystal violet (primary stain) and was allowed to stand for 1 min after which the crystal violet was rinsed off with tap water by holding the slide parallel to the running tap H$_2$O (to prevent loss of smear). The smear was then flooded with 100 µl of Grams iodine for 1 min after which the iodine was rinsed off with tap water. 100 µl of ethanol was used as the decolouriser and was used to flood the smear for 5 sec. After flooding with ethanol, the ethanol was rinsed off and safranin (secondary stain) was used to flood the smear for 30 sec. The safranin was rinsed off after 30 sec and the slide was air-dried and viewed at 1000X total magnification, under oil immersion (Zeiss Axiostar Plus)

2.   Endospore staining

Since spores were resistant to staining dyes, a procedure that relied on steaming the dye was used so that the spores (if any) would retain the dye. From the undiluted LP resolubilised acid precipitate and adsorption samples taken at 18, 20, 24 and 26 h incubation, 50 µl of each sample was placed onto a microscope slide and the specimen was heat-fixed by passing the microscope slide over a Bunsen burner. A small piece of paper towel was cut and placed over the smear which was then flooded with malachite green until the paper towel was saturated with the dye. The slide was passed over a Bunsen burner until the dye produced steam (2 min). The slide was saturated with malachite green again and passed over a Bunsen burner until the dye produced steam (2 min) again. The paper towel was used so that the dye had an increased contact time with the smear before it evaporated. The paper towel was removed and the slide rinsed off with running tap H$_2$O. The slide was viewed at 1000X total magnification, under oil immersion.

3.   Nutrient agar spread plates

To identify the possible source of contamination:

The LP resolubilised acid precipitate (the undiluted and diluted for adsorption preliminary experiments) and all the samples generated from the adsorption preliminary experiments (including samples that were not murky) were subjected to spread plating (Table 0-1). 500 µl of each sample was aseptically transferred onto a nutrient agar plate and was spread with a sterile glass rod (dipped in a petri dish containing 70% ethanol and passed the glass rod over the Bunsen burner until all the ethanol burned off the glass rod). The agar plates were incubated for 16 h at 30°C. The presence of colonies indicated the presence of microbial contamination.

Table 0-1. Identification of potential source of bacterial contamination in lipopeptide resolubilised acid precipitate in preliminary adsorption experiments

Scenario	Condition	Outcome
1	LP resolubilised acid precipitate in non-sterile Falcon tube transferred non-aseptically into 100 mL non-sterile Erlenmeyer flasks	+Ve for bacterial contamination
2.	LP resolubilised acid precipitate in sterile Falcon tube transferred aseptically into 100 mL sterile Erlenmeyer flasks	+Ve for bacterial contamination
3.	LP resolubilised acid precipitate in sterile Falcon tube aseptically filter sterilised (with 0.22 µm syringe filter) into 100 mL non-sterile Erlenmeyer flasks	-Ve for bacterial contamination

From Table 0-1, it was concluded that the source of contamination could have been the LP resolubilised acid precipitate as it might have bacterial cells/spores which are only eliminated by filter sterilisation with a 0.22 µm syringe filter as seen in the third scenario. Another possible source of contamination would be the pH electrode when the initial pH of the LP resolubilised acid precipitate is determined. It was then decided that the pH of the LP resolubilised acid precipitate be adjusted first and then filter sterilised with 0.22 µm syringe filter into a sterile Erlenmeyer flask under aseptic conditions.

4.   Buffer solution preparation

Table 0-2. Preliminary batch adsorption experimental conditions at 35°C and 45°C

LP/R ratio	pH at 24 h	Murkiness
0.04	7.25	None
0.08	6.72	None
0.13	6.94	Observed
0.15	6.92[#]	Observed
0.2	6.66[#]	Observed

- conducted at 45°C

During the 26 h incubation time frame, it was observed that on the onset of 18 h, the solution turned murky, due to bacterial contamination, and the pH decreased by 0.4 – 1 pH unit which necessitated

the use of a buffer solution. Buffer solutions were required to maintain the solution at the desired experimental pH. Since the experimental pH values ranged from pH 7 – 11, buffer solutions at these particular pH ranges were required and are summarised in Table 0.3– 0.5.

Table 0-3. 0.1M Phosphate buffer (Sorensen), pH 5.3 - 8.04

pH	Solution A: $0.1\ M\ KH_2PO_4$	Solution B: $0.1\ M\ Na_2HPO_4.2H_2O$
7	30 mL	70 mL
8	5 mL	95 mL

Table 0-4. 0.1M Bicarbonate-carbonate buffer, pH 9.2 - 10.8

pH	Solution A: $0.1\ M\ NaHCO_3$	Solution B: $0.1\ M\ Na_2CO_3.10H_2O$
9	90 mL	10 mL
10	30 mL	70 mL

Table 0-5. Monosodium phosphate-sodium hydroxide buffer, pH 11.0 - 11.9

pH	Solution A: $0.05\ M\ NaH_2PO_4$	Solution B: $0.1\ M\ NaOH$
11.0	50 mL	6.3 mL

* After mixing solution A with solution B, the solution was diluted 2-fold with demineralised H_2O to a total volume of 100 mL, which was then used in the relevant experiments

**5.**   **Preliminary batch adsorption kinetics**
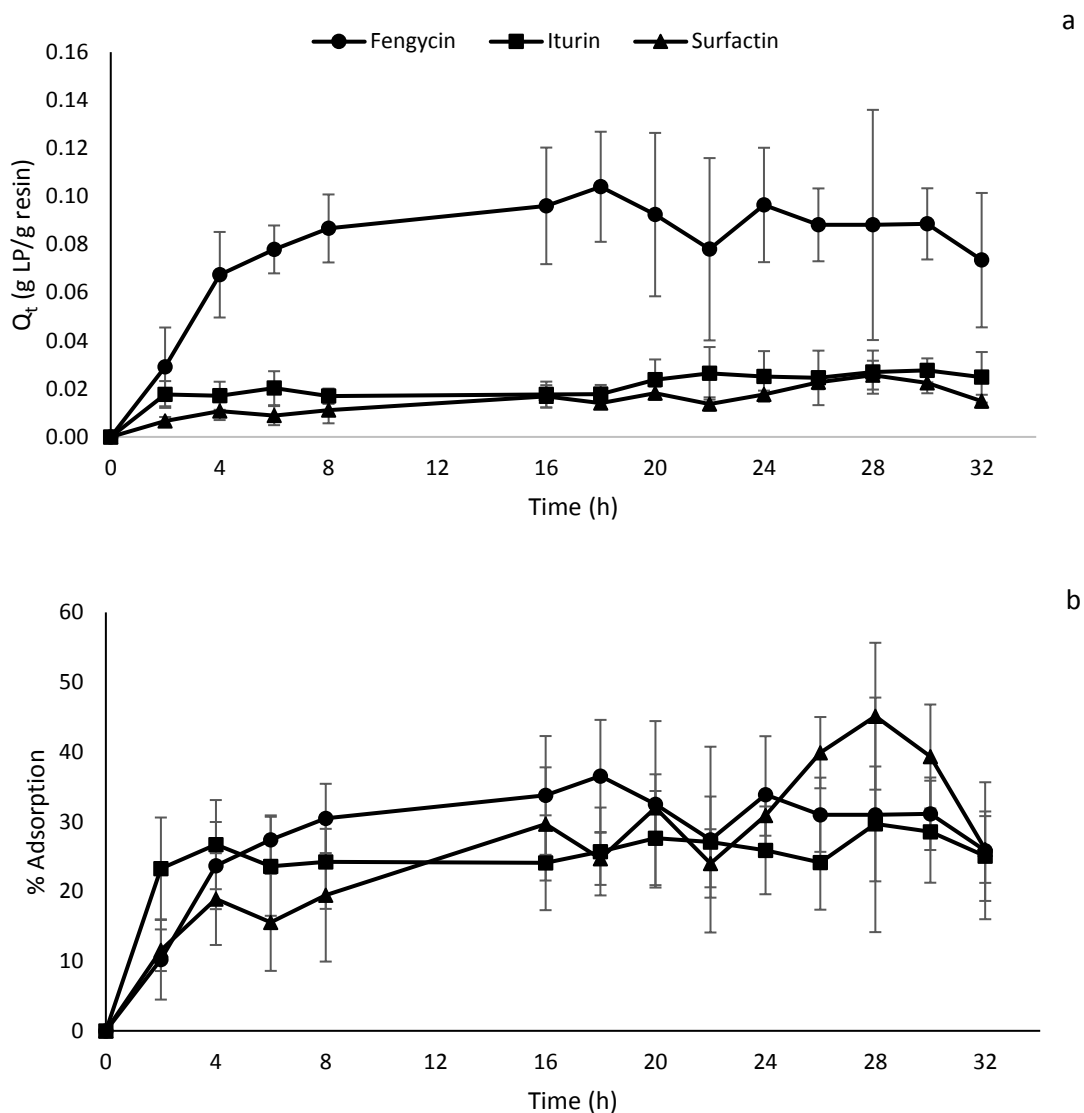
Figure 0-8. Adsorption kinetic response (a) Q_t and (b) percentage adsorption of lipopeptides on HP-20 resin with 0.3 fengycin/resin ratio at 30°C and pH 10. *The data points represent the mean values calculated from triplicates at each time point with the standard deviation of the mean represented by the error bars*

Appendix D: LC-ESI-MS Data

Table 0-6. LC-ESI-MS analysis of lipopeptides in different organic solvent extracts

Sample	Peak no.	UPLC retention time (min)	Mass peak (*m/z*) obtained in this study		Homologue identity
			Doubly charged [M+2H]^2	Singly charged [M+H]	
4 g/L acid precipitate	1	2.86	516.27	1031.54	Bacillomycin D (Iturin)
	2	3.38	523.28	1045.55	Iturin A2 (C$_{14}$)
	3	4.57	732.40	1464.80	Fengycin A (C$_{16}$)
	4	5	739.41	1477.81	Fengycin A (C$_{17}$)
	5	5.44	753.42	1506.84	Fengycin B (C$_{17}$)
	6	5.68	746.42	1491.82	Fengycin A (C$_{18}$)
Cell-free supernatant	1	2.86	516.27	1031.54	Bacillomycin D (Iturin)
	2	3.41	523.27	1045.55	Iturin A2 (C$_{14}$)
	3	4.78	732.40	1463.79	Fengycin A (C$_{16}$)
	4	5.09	739.41	1477.81	Fengycin A (C$_{17}$)
	5	5.13	739.41	1477.81	Fengycin A (C$_{17}$)
pH 3 acid precipitate	1	2.89	516.26	1031.54	Bacillomycin D (Iturin)
	2	3.38	523.77	1045.55	Iturin A2 (C$_{14}$)
	3	4.74	732.40	1464.80	Fengycin A (C$_{16}$)
	4	5.07	739.41	1477.81	Fengycin C (C$_{15}$)
	5	5.48	753.93	1506.83	Fengycin B (C$_{17}$)
MeOH extract	1	2.9	516.27	1031.54	Bacillomycin D (Iturin)
	2	3.38	523.28	1045.56	Iturin A2 (C$_{14}$)
	3	4.68	732.40	1464.80	Fengycin A (C$_{16}$)

	4	5.13	746.42	1477.81	Fengycin A (C_{17})
	5	5.48	753.43	1505.84	Fengycin B (C_{17})
EA-MeOH extract	1	2.85	516.27	1031.54	Bacillomycin D (Iturin)
	2	3.41	523.26	1045.55	Iturin A2 (C_{14})
	3	4.68	732.40	1464.80	Fengycin A (C_{16})
	4	5.08	739.41	1477.81	Fengycin A (C_{17})
	5	5.42	753.43	1506.83	Fengycin B (C_{17})

Acid precipitate resolubilised in alkaline water. ISO: Isopropanol, MeOH: Methanol, EA-MeOH: Ethyl Acetate-Methanol and CF-MeOH: Chloroform-Methanol organic solvent extract

Table 0-7. LC-ESI-MS analysis of lipopeptides in solvent extracts

Sample	Peak no.	UPLC retention time (min)	Mass peak (*m/z*) obtained in this study		Homologue identity
			Doubly charged $[M+2H]^2$	Singly charged [M+H]	
ISO extract	1	2.84	516.27	1031.54	Bacillomycin D (Iturin)
	2	3.32	550.24	1045.55	Iturin A2 (C_{14})
	3	4.69	732.4	1463.79	Fengycin A (C_{16})
	4	5	739.41	1477.81	Fengycin A (C_{17})
	5	5.48	753.42	1447.80	Fengycin A
CF-MeOH extract	1	2.57	599.36	1045.55	Fengycin A (C_{15})
	2	3.36	523.78	1045.55	Iturin A2 (C_{14})
	3	4.43	732.4	1464.81	Fengycin A (C_{16})
	4	4.98	739.41	1478.83	Fengycin A (C_{17})
	5	5.36	753.42	1505.86	Fengycin B (C_{17})

ISO: Isopropanol, MeOH: Methanol, EA-MeOH: Ethyl Acetate-Methanol and CF-MeOH: Chloroform-Methanol organic solvent extract